

INVESTIGATION OF THE COMPLEMENTARY  
USE OF NON-INVASIVE TECHNIQUES FOR  
THE HOLISTIC ANALYSIS OF PAINTINGS  
AND AUTOMATIC ANALYSIS OF LARGE  
SCALE SPECTRAL IMAGING DATA

---

Sotiria Kogou

A thesis submitted in partial fulfilment of the  
requirements of Nottingham Trent University  
for the degree of Doctor of Philosophy

September 2017



## **Declaration**

This work is the intellectual property of the author. You may copy up to 5% of this work for private study, or personal, non-commercial research.

Any re-use of the information contained within this document should be fully referenced, quoting the author, title, university, degree level and pagination.

Queries or requests for any other use, or if a more substantial copy is required, should be directed in the owner(s) of the Intellectual Property Rights.



*To my sister, my Lila*



## Abstract

The analysis of painting materials and methods is acknowledged for providing important information to art history. This study illustrates a detailed examination of the characteristics, advantages and capabilities that the combined application of a variety of non-invasive techniques, ranging from spectral imaging and optical coherence tomography (OCT), to fibre optics reflectance spectroscopy (FORS), X-ray Fluorescence (XRF) and Raman spectroscopy, has to offer. The analysis of painting materials is seen under the prism of a holistic examination of different types of cultural heritage objects. More specifically, the limitations that the individual techniques face and, most importantly, how their complementary use can overcome them are thoroughly investigated through the examination of a large and heterogeneous statistical sample, in a completely novel way. The heterogeneity of the sample is related both to the painting materials (i.e. pigments, binding media and substrates) and the degradation level (i.e. paintings stored in storages of museum and murals of caves that are exposed in the environmental conditions of the desert).

For the extraction of accurate conclusions about the painting materials and methods applied in a specific period, the examination of large number of artworks of this period is required. PRISMS, the spectral imaging system developed by our group enables the time efficient imaging of large painting surfaces, leading to the acquisition of large scale spectral imaging data, which makes such an analysis faster, more cost-effective and less laborious without diminishing the quality of the results. This study proposes methods based on the statistical analysis for the automatic processing of the spectral imaging data in two directions: the revealing of information that is obvious under visual observation and clustering of the spectral information.

With regards to the automatic revealing of hidden information, the potential of principal component analysis (PCA) and independent principal analysis (ICA), two of the most commonly used statistical analysis methods, were examined giving very good results.

In addition, the development of a new method for the automatic clustering of large scale spectral information based on the ‘Self-organised mapping’ (SOM) method is presented. The spectral feature of the analysed areas in the UV-VIS/NIR (400-900 nm) is indicative for its pigment composition, therefore the automatic clustering of the pixel-level spectral information that the PRISMS system provides can classify the areas according to their pigment composition. The application of statistical analysis methods in the preliminary

stage of the analysis of large number of artworks (e.g. large painting collections) of large surface painting areas (e.g. murals) is of significant importance; as they highlight the areas that should be examined in detail.

The multimodal non-invasive approach was applied on the examination of three artworks of significant importance for East Asian art history; the cave 465 of the Mogao complex in China, the export Chinese watercolor paintings from the collections of the Victoria and Albert (V&A) museum and the Royal Horticulture Society (RHS) and the Selden map. The examination of these three works of art, in addition to providing a wide and heterogeneous sample for the detailed examination of the multi-modal approach, has also helped addressing several historical questions.

## Acknowledgments

I would like to express my sincere gratitude to my supervisor Prof Haida Liang for her support during these years and for giving me the opportunity to enrich my research experience. I would also like to express my appreciation to my second supervisor Dr Garth Cave for his help and willingness for discussion during this study.

Besides my supervisory team, I want to express my special appreciation and thanks to Dr Chi Shing Cheung (Sammy) for his friendship and support during the last four years.

I would also like to thank Prof John Wallis for the fruitful conversations that we had, with tea and cookies, about Chemistry.

I would particularly like to thank my family for their inspiring presence in my life and their support in any means (e.g. planting *commelina* and making it blossom in the middle of the winter, so can I extract the dye from its petals).

Many thanks to my friends Elisa, Christina, Marilena, Evi, Penny and Alexandro from back home and the friends that I made here: Giulia, Irini, Edwin, Maria, Natasha, Adam, Abiar, Nada, Alanooud for their love and support during the writing period.

Special thanks to my beloved friends Charalampos Tsoukalas, Artemis Apostolaki, Giulia Furini and Elisa Papadopoulou who, in addition to moral support, helped in proof-reading and editing of this dissertation.

Finally, I would like to thank all the people that helped with the collection of the data in the various projects. More specifically, I would like to thank Andrei Lucian for the collection of PRISMS data and the researchers from the Dunhunang Academy: Shui Biwen, Zhang Wenyuan, Yu Zongren and Prof. Su Bomin for our nice collaboration.



## Table of contents

<b>Chapter 1: Introduction .....</b>	<b>5</b>
<b>Chapter 2: Analytical techniques and methods .....</b>	<b>11</b>
2.1 Spectral Imaging .....	11
2.2 Kubelka-Munk model for the identification of pigments .....	18
2.3 Reflectance Spectroscopy .....	22
2.4 Raman Spectroscopy .....	24
2.5 X-ray Fluorescence (XRF) Spectroscopy .....	25
2.6 Optical Coherent Tomography (OCT) .....	26
2.7 Scanning Electron Microscopy with Energy Dispersive X-ray (SEM-EDX) Spectroscopy .....	28
<b>Chapter 3: Application of statistical methods for automatic post-processing of large-scale data .....</b>	<b>31</b>
3.1 Application of Blind Source Separation (BBS) techniques for the revealing of hidden information .....	32
3.1.1 Introduction .....	32
3.1.2 Spectral Imaging Data & Statistical Analysis methods .....	35
3.1.3 Results .....	36
3.1.3.1 Comparison between the individual spectral images and BSS methods outcome .....	36
3.1.3.2 Comparison between the results obtained by the application of the PCA on the correlation and covariance matrix .....	39
3.1.3.3 Comparison between the result obtained by the application of PCA or ICA method .....	41
3.1.3.4 Examination of the dependence of results on the spectral imaging input .....	43
3.1.3.5 Application of BSS statistical methods on OCT data .....	48
3.1.4 Summary .....	49
3.2 Development of method for the automatic and unsupervised clustering of spectral information obtained by spectral imaging .....	50
3.2.1 Introduction .....	50
3.2.2 Spectral Imaging Data & Developed Clustering Algorithm .....	52
3.2.3 Results .....	59

3.2.4 Summary .....	63
<b>Chapter 4: Holistic approach of the non-invasive analysis of painting materials ..</b>	<b>65</b>
4.1 Multi-modal approach for the identification of pigments .....	66
4.1.1 Introduction .....	66
4.1.2 The use of a multi modal analytical approach in order to overcome limitations that the individual non-invasive analytical techniques face.....	68
4.1.2.1 FORS limitations on the identification of a handful of pigments and dyes .....	68
4.1.2.2 Sensitivity of Raman spectroscopy to fluorescence.....	72
4.1.2.3 Dependence of Raman spectroscopic analysis on spot size.....	73
4.1.2.4 XRF detection limitations and difficulties in the interpretation of the spectra ...	75
4.1.3 Conclusions.....	76
4.2 Non- invasive identification of binding media .....	79
4.2.1 Introduction .....	79
4.2.2 Examination of the potential of reflectance spectroscopy in the near-IR regime for the identification of binding media .....	84
4.2.3 Summary .....	90
4.3 Multimodal approach for the identification of the drawings materials.....	91
4.4 Multimodal approach for the identification of the substrate and the preparation materials.....	94
4.4.1 Introduction .....	94
4.4.2 Complimentary use of OCT scanning and XRF spectroscopy for the classification of paper substrates.....	95
4.4.3 Summary .....	98
<b>Chapter 5: Multi-modal approach for the non-invasive and in situ analysis of Murals of Mogao complex in Dunhuang, China .....</b>	<b>99</b>
5.1 Introduction .....	99
5.2 Materials and Methods.....	101
5.3 Results .....	104
5.3.1 Multimodal approach for the identification of pigments .....	104
5.3.2 Examination of crack formation .....	129
5.3.3Examination of painting techniques and sequence .....	137
5.4 Discussion .....	144

<b>Chapter 6: Multimodal approach for the non-invasive analysis of Chinese export paintings of Victoria and Albert (V&amp;A) and Royal Horticulture Society (RHS) collections .....</b>	<b>146</b>
6.1 Introduction .....	146
6.2 Instruments & materials .....	148
6.3 Results & Discussion .....	152
6.3.1 Identification of pigments .....	152
6.3.2 Examination of the substrate .....	169
6.4 Conclusions .....	171
<b>Chapter 7: Scientific Analysis for the investigation of the origin of Selden map..</b>	<b>175</b>
7.1 Introduction .....	175
7.2 Materials and Methods.....	177
7.3 Results and Discussion.....	181
7.3.1 Identification of the binding medium.....	181
7.3.2 Identification of the pigments .....	183
7.3.3 Examination of painting techniques and signs of alterations.....	189
7.4 Conclusions .....	193
<b>Chapter 8: Conclusions .....</b>	<b>195</b>
<b>Chapter 9: Bibliography.....</b>	<b>202</b>



## **Chapter 1:**

### **Introduction**

The analysis of painting materials and methods is acknowledged for providing important information to both art history and archaeology research, as well as to scientists involved in the conservation of cultural heritage objects. More specifically, scientific analysis of the painting materials and techniques has been proven crucial for the characterization of artworks, as different materials have been used in different periods and different places. Moreover, the analysis of artworks yields very important information about their artistic and technological content, as well as about the technological and cultural exchanges, communication and trade through different historical periods. With regards to the art conservation, the detailed analysis of cultural heritage objects assists in the selection of the optimum methodology for their conservation and restoration.

There is a long history of the application of analytical techniques to the examination of cultural heritage objects. Until recently, the analysis was based mainly on the application of invasive techniques. Invasive techniques, which involve analysis of samples collected from the original artwork, are divided into two categories: the destructive, where the sample is destroyed for the extraction of information and the non-destructive, where the sample remains unaffected during the analysis and thus can be reused for further analysis. In the field of cultural heritage, both destructive (e.g. gas chromatography (GC) [1] [2] and high performance liquid chromatography (HPLC) [3] [4]), and non-destructive (e.g. scanning electron microscopes-energy dispersive x-ray spectroscopy (SEM-EDX) [5] and X-ray diffraction (XRD)) analytical techniques have been widely used. Despite the fact that developments on various invasive analytical techniques have minimized sampling requirements so that the analysis can be performed on micro-samples, sampling still remains undesirable for various reasons. In instances where the paint and/or the substrate are sensitive and fragile (e.g. paper or parchment-based artworks), sampling can be practically impossible without causing significant damage, therefore most institutions do not allow samples to be taken from this kind of objects. Moreover, in cases of well-preserved artworks, sampling can even be considered unethical. However, even in cases where sampling is allowed, invasive

scientific analysis can only be conducted on painting materials of samples collected from damaged or detached areas of the artwork, or areas near its edges. One issue arising from this restriction of the analytical area is that the original location of the sample is often unknown; furthermore, the collected fragments may not be representative of the whole artwork.

The technological advances over the years have enabled the development of non-invasive analytical techniques. The ability to analyse without the need for sampling overcomes the limitations related to ethical restrictions, enabling the examination of even the most fragile objects of art. Moreover, the ability to analyse the whole surface of the examined artworks, results in conclusions that are more representative regarding the applied painting materials and methods. Furthermore, in addition to the development and constant optimization of non-invasive analytical techniques, the advantages of improvements in fibre-optics technology, as well as the minimization of electronic components provide the ability to develop portable instruments with capabilities comparable to the standard bench equipment. The development of portable non-invasive instrumentation allows for *in situ* examination of valuable artworks of which mobility from the place where they are located or stored is undesirable or even impossible, due to their fragility [6] or large size [7–10].

Information provided by the various non-invasive analytical techniques depends on the principles of their operation as well as on the specifications of the instrumentation used. In various disciplines, ranging from biomedical science to art conservation and forensic science, it is realised that no single technique can answer all the questions. In the field of the analysis of artworks, this is becoming particularly true in the study of historical paintings, where the materials involved are extremely wide-ranging and heterogeneous. For this reason, only a multimodal approach can provide holistic information, by combining the strengths and overcoming the limitations of the individual techniques.

The aim of this study follows this approach by investigating in depth the non-invasive, multi-modal approach for the holistic analysis of artworks. More specifically, the limitations that some of the most widely used non-invasive techniques can have and, more importantly, how their complementary use can overcome these problems are examined through the study of a wide range of artworks. The analytical techniques used in this study range from spectral imaging and Optical Coherence Tomography (OCT) to a variety of spectroscopic techniques, from high resolution fibre optics reflectance

spectroscopy (FORS) to Raman and X-ray Fluorescence (XRF) spectroscopy. Given that these techniques are based on different principles of operation, their selection was made in such a way to provide different types/levels of information about the materials analysed. Moreover, the effect of the special features (e.g. spot size) of the instrumentation used was also examined. The characteristics of the painting system under analysis, such as the materials involved and the aging or weathering level, are very crucial factors that may also affect the results of the different analytical techniques. The painting systems analysed in the context of the present study vary with respect to the paint materials (i.e. pigments, substrates and binding media), as well as to their degradation level, extending from watercolour painting stored in museums to murals exposed to environmental conditions in a desert, enabled a more extended examination of the multi-modal analysis. Another significant advantage of this study, compared to other studies that have been conducted on the multi-modal analysis of artworks, is the size of the statistical sample under examination. The majority of the studies conducted on the multi-modal examination of artworks are based on the analysis of either fragments [11], [12] or small collections of artworks, not offering a significant statistical sample for the detailed investigation of the complementarity of the non-invasive analytical techniques. In the present study, a large sample of analytical data was collected from objects of cultural heritage of which non-invasive and in situ analysis is required (i.e. paper-based artworks and murals). This enabled a more detailed examination of analytical advantages and limitations of the individual non-invasive techniques, as well as the benefits of their complementary use.

In order to draw accurate conclusions about the painting traditions of different cultural groups in various periods, the analysis of a large statistical sample of artworks is required. However, the application of point-level analytical examination on the whole surface of large scale collections is extremely time consuming. Moreover, in instances where the examined artwork may be in unreachable areas (e.g. ceiling murals), analysis without the use of scaffolding is impossible. PRISMS (Portable Remote Imaging System for Multispectral Scanning), the spectral imaging system developed in our group [13], overcomes these limitations by enabling the automatic imaging of large areas, even if these are in unreachable locations. As the field of view of this spectral imaging system is relatively large, the imaging of large paintings surfaces can be obtained fast. Another advantage of using spectral imaging is that it provides both imaging and spectral information about the analysed areas, which consequently reveal

important information about both the applied painting methods and the materials. Despite the benefits of large scale data gathering, their effective management remains an issue. In this direction, the aim of this study is the development of methods based on statistical analysis for the automatic processing of large scale data obtained by spectral imaging systems. Regarding the manipulation of large scale spectral information, the aim was to develop a methodology for the classification of this information into a manageable number of clusters. It is known that the spectral similarities in the visible regime of the various paint areas are related to similarities in their pigment composition. Therefore, the classification of the spectral information can assist the identification of the pigments by narrowing down the analysis in a small number of areas, representative for each class. The detailed examination of the pigment composition of these spectrally representative areas could be extended to the whole class afterwards, providing information about the pigment composition of the large scale analysed area. In addition, the observation of the spectral images of the different bands is known to provide interesting information about the painting methods applied. Therefore, another aspect was to investigate which methodology should be followed in order to automatically reveal hidden information.

In the context of this study, three types of East Asian artworks were analysed. The variation concerning painting materials, as well as the differences in their environmental conditions, provided a very heterogeneous statistical sample that enabled the in-depth investigation of the complementarity of the various non-invasive analytical techniques in different painting systems. From an art historic point of view, the analysis of different East Asian artworks is of significant importance as, in contrast to the study of Western European objects of art, information on materials and techniques applied in East Asian painting tradition is limited. The scientific multi-modal analysis of these artworks provided very important information about their history as well as the cultural exchanges and influences in the area of East Asia in different periods of time. More specifically, the first study is conducted on the analysis of the murals of cave 465 of the Mogao complex, a world heritage UNESCO site near Dunhuang in western China. The analysis of these murals is very important for art historians, as the dating of the cave is still a subject under debate. The second study was related to the analysis of the collections of Chinese export watercolour paintings of the Victoria and Albert Museum (V&A) and the Royal Horticultural Society (RHS). Contrary to the cave 465, the dating of these paintings is known and placed in the period between late eighteenth to

nineteenth century. Therefore, the historical interest of this study is the investigation of the trade and cultural exchanges between China and Europe in this specific period of time. The last study is related to the investigation of the origins of the Selden map, an early seventeenth century map of great historical importance as it illustrates the maritime trade routes in East Asia. The historic aspect of the last study was to provide scientific evidence on its origins.

In order to provide a description of the structure of this dissertation, chapter 2 contains a brief presentation of the analytical methods and techniques that have been used in this study. In chapter 3, the application of statistical analysis methods for the efficient management of large scale spectral imaging data is illustrated. More specifically, the application of statistical methods for the automatic revealing of information that is not obvious under visual observation and the development of a method for the automatic classification of large scale spectral information is presented. In chapter 4, a thorough investigation of the limitations that the individual non-invasive analytical techniques face is illustrated, but, most importantly, how their combined use overcomes them. In particular, the complementary use of various non-invasive techniques for the holistic examination of a wide range of objects of art is presented. In chapter 5 to 7, the application of the multi-modal, non-invasive approach is followed for the examination of the painting materials and methods applied on three types of East Asian artworks. Chapter 5 illustrates the examination of the murals of cave 465 of the Mogao complex, a world heritage UNESCO site near Dunhuang in Western China. In addition to the scientific evidence provided for art historic purposes, and more specifically the dating of the cave, the analysis of these murals also enabled the detailed investigation of the application of in situ, non-invasive measurements for the analysis of painting layers of different degradation levels and the extraction of important information regarding the applied painting methods. In chapter 6, the importance and the abilities that the complementary use of non-invasive techniques for the holistic analysis of fragile artworks, such as paper-based watercolour paintings, are presented. More specifically, the multi-modal approach was applied on the examination of a large number of Chinese export watercolour paintings of the Victoria and Albert Museum (V&A) and the Royal Horticultural Society (RHS), dated in late eighteenth to nineteenth century, are analysed. The extracted scientific evidence provided very important information for the trading and cultural exchanges between China and West in the period of their creation. In chapter 7, the analysis of Selden map, an early seventeenth century map of great

historical importance as it illustrates the maritime trade routes in East Asia, is illustrated. The analysis of the painting materials used is indicative of the unusual origin of the map. Moreover, information about the painting techniques and alterations that the creator made during the production of the map are revealed.

## **Chapter 2:**

### **Analytical techniques and methods**

In the context of this study, various non-invasive analytical techniques were used for the holistic examination of different types of artworks. The complementarity of these techniques derives both from the differences on the principles of their operation and from the special features of the instrumentation used. In this chapter, the basic principles of these non-invasive techniques are illustrated. Moreover, a brief presentation of the in-house built instrumentation and the analytical methods applied is provided.

#### **2.1 Spectral Imaging**

Spectral imaging is a combination of imaging and spectroscopy, where images of an object are collected in a series of spectral windows, providing a complete spectrum at every pixel of an image plane (Figure 2-1b,c). The separation of the wavelengths is achieved using either separate filters sensitive to a particular wavelength range or a diffraction grating.

Most of the spectral imaging systems used for the analysis of paintings require scanning in close distances (less than two meters) from the analysed object in order to obtain high resolution spectral images. Moreover, the scanning is performed using mechanical scanners that are built to move either the imaging device or the painting under examination. Although these requirements do not affect the imaging of paintings of small size, in the case of large scale movable paintings the size of the surface that can be imaged is restricted by the size of the studio and the scanning system. Furthermore, in cases like murals and extremely large paintings, *in situ* analysis is necessary and therefore the use of such spectral imaging systems is not suitable due to their scanning limitations. On the other hand, high spatial resolution imaging of large scale paintings or paintings at great heights (e.g. ceiling paintings) using free standing spectral imaging cameras with normal lens is not possible without scaffolding. In addition to the difficulties of using heavy scaffolding in the field, the major disadvantage of a scanning system where the imaging system moves in position relative to the painting is that it causes parallax effects (i.e. displacement in the apparent position of the imaged object)

in the imaging of a 3D structure, resulting in problems in the mosaicing of the collected images.

PRISMS (Portable Remote Imaging System for Multispectral Scanning) is a simple, low-budget instrument designed by our group in order to overcome all these restrictions by providing portable and versatile remote imaging from a fixed position. It comes in two configurations; one using a telescope for imaging at distances greater than three meters and another that uses a lens and is suitable for close range imaging. The use of a telescope enables the *in situ*, high resolution imaging of wall paintings and other large scale artworks, providing spatial resolution of  $8.2 \mu\text{rad}$  (or  $1.7''$ ) which translates to  $80 \mu\text{m}$  at a distance of 10 m.

The PRISMS version for observation in the VIS/NIR regime (i.e. 400 nm to 900 nm), consists of a lens, or a telescope, a filter wheel of ten filters and a CCD camera [13]. The first nine filters are centred from 400 nm up to 800 nm with spacing of 50 nm and have a bandwidth of 40 nm, while the last filter is at 880 nm with a bandwidth of 70 nm.

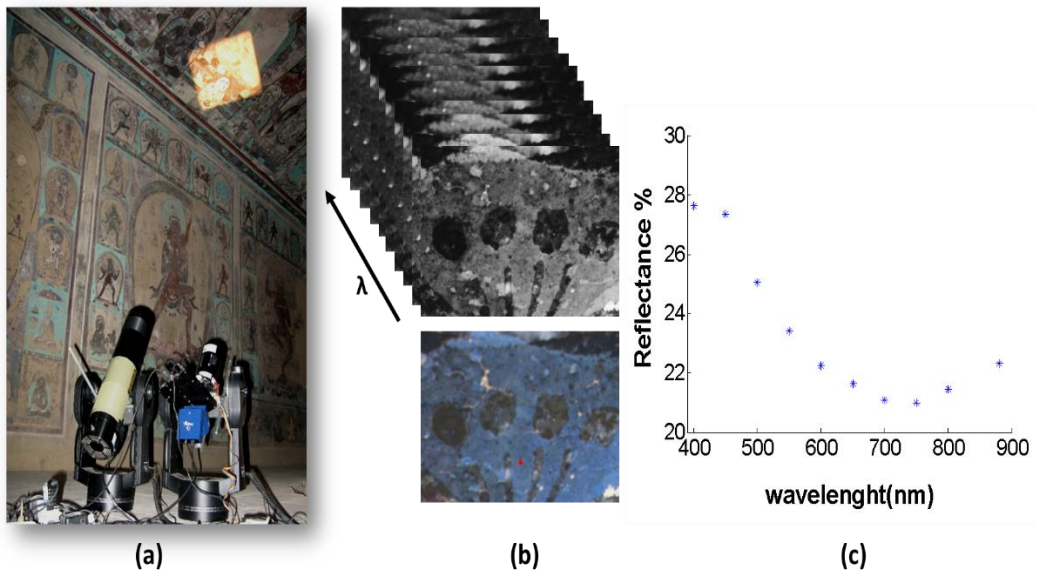


Figure 2-1 (a) PRISMS imaging system in the telescope configuration imaging murals at Mogao caves in China; (b) Spectral cube obtained from spectral imaging and the colour image derived from the spectral cube; (c) Reflectance spectrum for a point on the blue area (red dot in (b)) which can be identified with the pigment azurite.

The observation in the different spectral bands can be very informative in revealing past interventions and damages to the paintings, since the colours that conservators add are selected in such a way so that they match the paint for retouching to the original without necessarily using the same pigment. Moreover, the observation in the near infrared bands (e.g. 800 and 880 nm) allows the observation of sketches and drawings located underneath the paint layer, providing information about the paint sequence followed. Such information is invaluable to art historians in terms of studying painting techniques as well as debating on issues of attribution and authentication.

High resolution coloured images of the examined areas can be obtained through the post-processing of the spectral images collected using the PRISMS system assuming a standard D65 daylight illumination and the CIE 1931 2° standard observer colour matching functions [14][15]. Even though capturing from a fixed position is beneficial for avoiding parallax, it also results in an imaging geometry that is not constant relatively to the target which could create issues in the accuracy of the reflectance measurements. However, since the geometries of the measurements are being recorded this limitation is being overcome, as the reflectance measurements are accurate with respect to the known geometries. In particular, the colours of the imaged painting surface are presented as they would be viewed by a person standing at the position of the camera. The automatic stitching of the individual coloured images (Figure 2-2a) into a mosaic (Figure 2-2b) enables the high resolution imaging of very large surfaces even if they are located at great distances, which can be a very useful tool for their examination. This mosaicing is achieved using an algorithm based on the cross-correlation routine from the VIPS library [16], which returns a maximum when the overlapped regions between the images are matched.

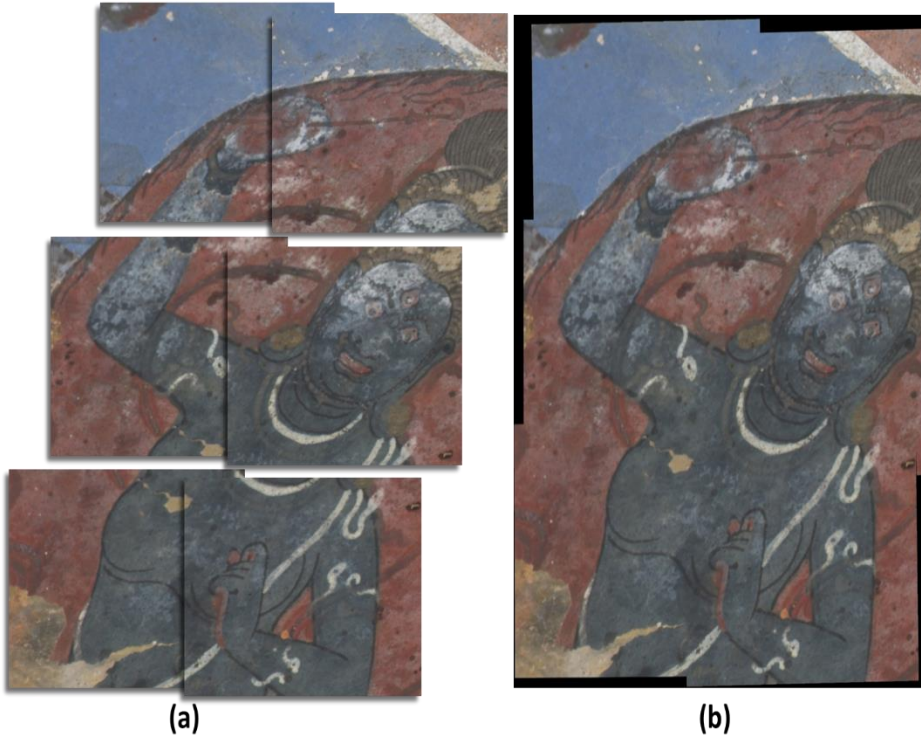


Figure 2-2 (a) Colour images derived from PRISMS data collected for the ceiling of cave 465 of Mogao caves are stitched into a (b) high resolution mosaic of the paint area.

As the various pigments have differences in their chemical composition and therefore in their reflectance spectra, the pixel-level spectral information provided by the PRISMS system can be used for the identification of the palette of the analysed artwork. In general, most of the pigments have broad reflectance spectra and therefore the low spectral resolution of PRISMS system (40 nm) does not cause any problems in their identification (Figure 2-3a). However, there is a handful of pigments, such cobalt blue and red dyes (e.g. lac and cochineal dyes), which have fine spectral features in the visible regime (Figure 2-3b) and for which a spectral resolution of 10 nm is required.

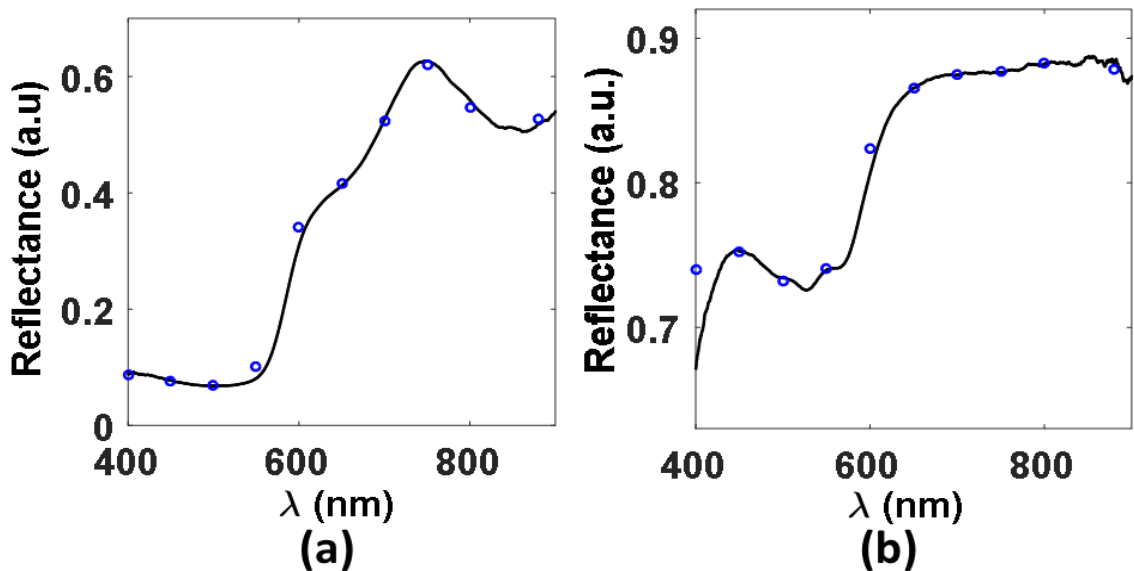


Figure 2-3 Spectral comparison between PRISMS system (blue circles) and high resolution spectrometer (black curve) for the identification of (a) pigments that have broad spectral shape (red ochre) and (b) pigments that have fine spectral features (lac dye) in the VIS regime.

Despite its low spectral resolution, PRISMS system enables the distinction even of pigments that have similar spectra with slight difference in spectral features, due to the position of the central wavelengths of its filters. Figure 2-4 shows a characteristic example, with the distinction between red lead and vermillion, two red pigments that have broad spectral features in the visible regime, but also the same ‘S’ shape and a spectral shift of only 50 nm.

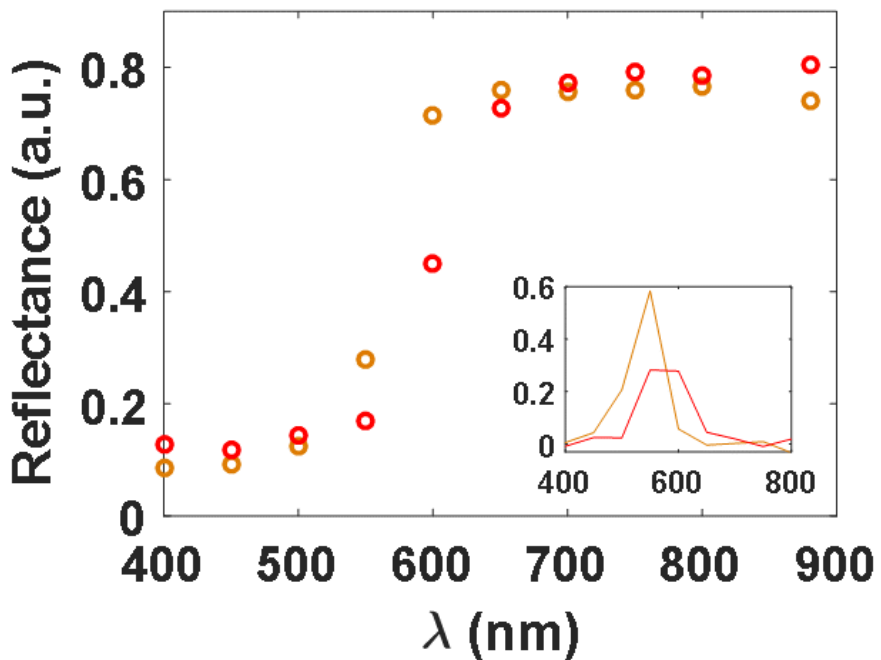


Figure 2-4 PRISMS data of red lead (orange circles) and vermillion (red circles) showing that the distinction between these two pigments is possible. The inset shows the corresponding derivatives of the spectra.

It should be highlighted that, in addition to the importance of the spectral resolution, the selection of a proper sampling step is also crucial. For example, for the identification of the fine lines of the red organic dyes, additional to the minimum spectral resolution of 10 nm, a sampling step of 5 nm is required in order to avoid loss of the fine spectral lines. Figure 2-5 illustrates the importance of both spectral resolution and sampling step through the example of the identification of lac dye, showing that in the case where the spectral resolution is less than 10 nm or the sampling step is greater than 5 nm, the characteristic absorption lines are not obvious.

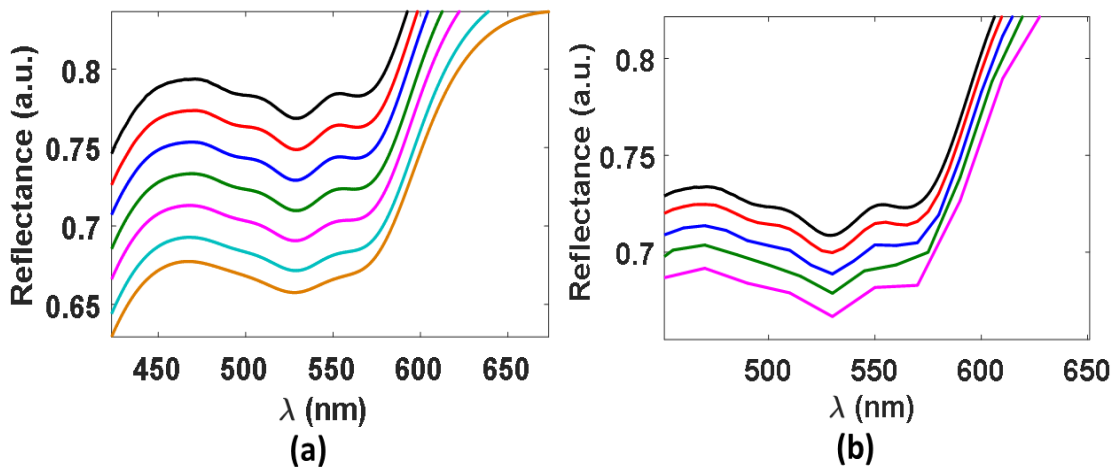


Figure 2-5 Reflectance spectra of lac dye collected using a spectrometer of spectral resolution 3nm with (a) sampling step 1 nm and smoothing window of 1 nm (black curve), 5 nm (red curve), 10 nm (blue curve), 15 nm (green curve), 20 nm (magenta curve), 25 nm (light blue curve) and 30 nm (orange curve) and (b) no smoothed (smoothing window 1 nm) and sampling step: 1 nm (black curve), 5 nm (red line), 10 nm (blue curve), 15 nm (green curve) and 20 nm (magenta curve)

For the examination of areas located in great distances, the identification of pigments with fine spectral features would require the replacement of the VIS/NIR configuration of PRISMS system with a hyperspectral version. However, a cheaper and simpler solution can be provided by changing the set of filters in the VIS/NIR configuration of PRISMS system. For example, a set of ten filters was strategically selected around the spectral position of interest for the identification of red dyes and smalt (470, 488, 500, 520, 530, 550, 560, 570, 580 and 600 nm) with all of them having a spectral resolution of 10 nm. Figure 2-6 shows that the specific set of filters covers the spectral range of interest for the identification of the red anthraquinone dyes but also covers the most informative range regarding the identification of smalt and therefore can complement the analytical strength of the VIS/NIR configuration.

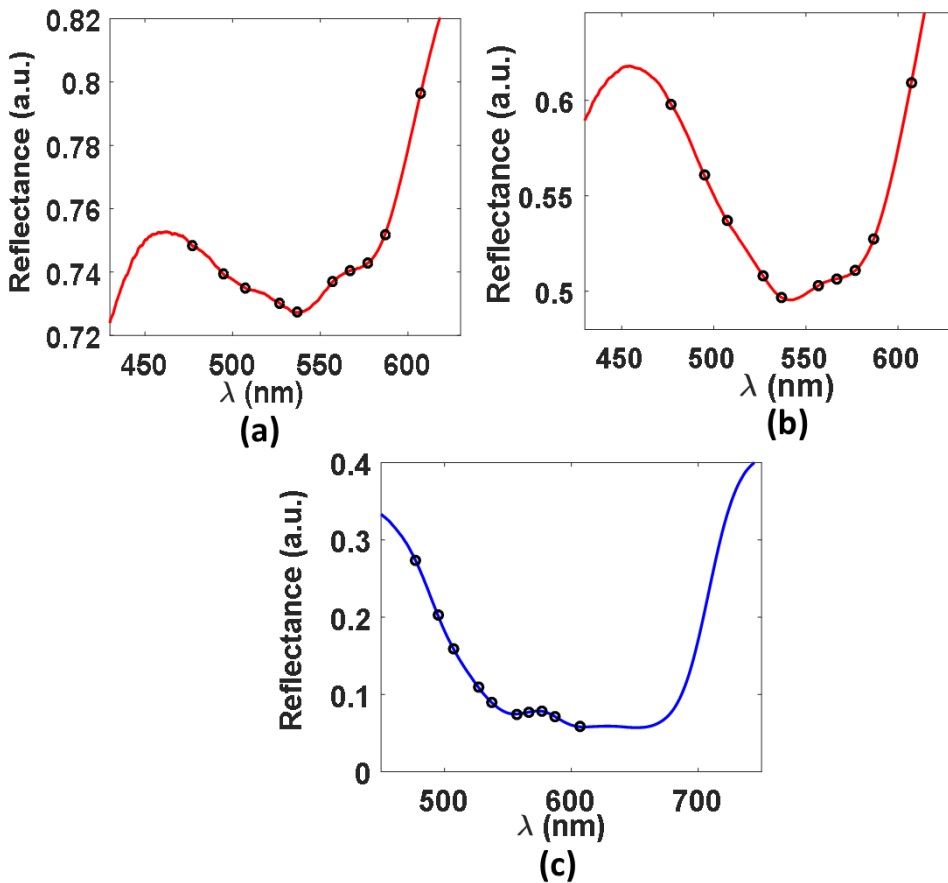


Figure 2-6 Comparison between PRISMS spectra collected using the set of ten filter at 470, 488, 500, 520, 530, 550, 560, 570, 580 and 600 nm (black circles) and high resolution spectra of (a) lac dye, (b) cochineal dyes and (c) cobalt blue.

## 2.2 Kubelka-Munk model for the identification of pigments

The combination of various pigments either in mixtures or in layer by layer application is a very common practise for obtaining different colours and hues. Therefore, for the pigment identification of mixtures, a method based on the Kubelka- Munk (KM) theory for the transport of the light into the matter was used. The simplest form of KM model is given by  $\frac{K}{S} = \frac{(1-R_\infty)^2}{2R_\infty}$ , where  $R_\infty$  is the spectral reflectance of a layer with infinite optical thickness and K and S are the spectral dependent effective absorption and scattering coefficients, respectively. The KM theory works under the assumptions that the analysed paint layers are highly scattering and the scattering particle size is smaller than the thickness of the paint. Therefore, it is possible to be less efficient in the examination of transparent layers or layers with high absorption (K) but low in scattering (S) coefficient. Under the assumption that the absorption and scattering coefficients of a paint mixture are a linear combination of the K/S ratio of the individual

pigment components, the KM theory can be used for the prediction of the reflectance of the paint mixture. Therefore, by importing the reflectance spectra of the reference pigments [17] and setting the concentration of the single pigments as free parameters we can find the best non-negative least squared fit of the predicted reflectance spectrum to the examined spectrum of the mixture. Various indicators that examine the accuracy of the fit can be defined. Cross-correlation coefficient, for example, is an indicator calculated from the predicted and actual spectra of the mixture and shows how closely the peaks and absorption lines match in position. Given that in the identification of pigments it is important to have a match in the spectral feature and not so much the absolute reflectance values, this indicator is well suited. Once the maximum number of components is defined, the algorithm then finds automatically the best combination of pigments from the reference spectral library that fits the examined spectrum.

In order to build the optimum reference database for the identification of the pigment composition of paint layers using the KM method, a detailed examination of the characteristics of the pigments must be performed. The effect of the variations in the concentration of the pigments in the paint layer was investigated through the examination of their spectral behaviour in a range of various concentrations. For the preparation of the samples, solutions of each pigment at mass concentration 25% were first made and then applied in various numbers of layers for the control of the concentration variation (1, 3 and 10 layers for low, medium and high concentration respectively). If K/S scales linearly with concentration, then a change in concentration would result in a shift, up or down, by a constant in the  $-\log(K/S)$  versus wavelength plot, without changing the spectral shape. For most of the reference pigments examined,  $-\log(K/S)$  derived from the application of the KM model on their reflectance measurements seemed to have a more or less linear dependence on concentration (Figure 2-7a). Therefore, the use of reference spectra collected from low pigment concentration paint-outs can produce a good fit to a high concentration paint layer. On the other hand, there are pigments, such as gamboge, that show spectral shifts as large as approximately 50 nm and spectral feature changes from extremely low to extremely high concentrations (Figure 2-7b). In these cases, the use of low concentration reference cannot provide a good fit to areas of intermediate or high concentration and vice versa. For these reasons, both high and low concentration references should be included in the reference spectral list in order to obtain reasonably good fits.

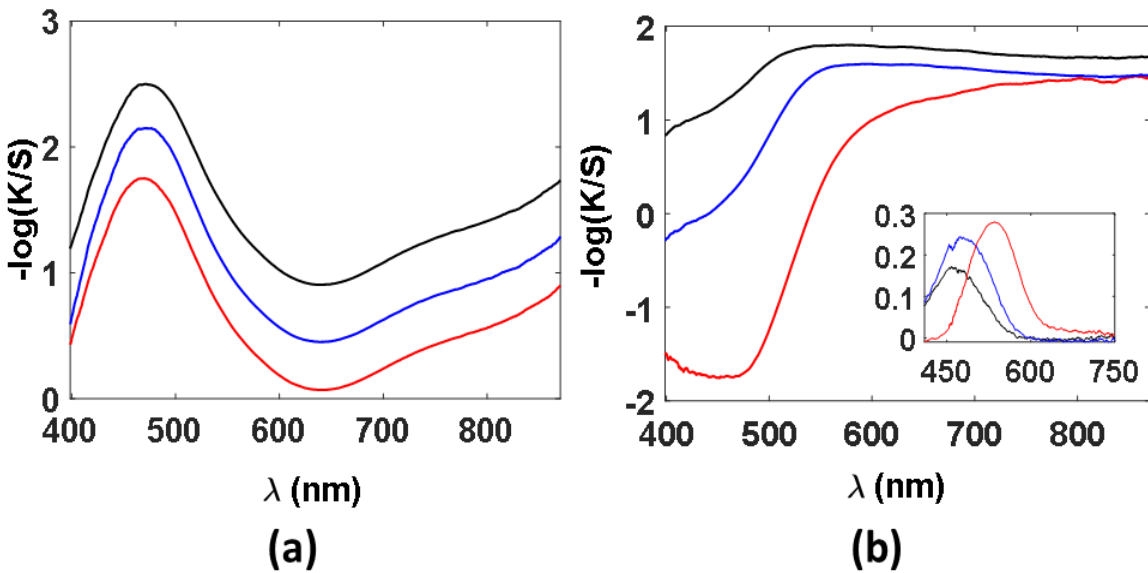


Figure 2-7 The effect of pigment concentration on  $-\log(K/S)$  plot of (a) azurite (grade 5) and (b) gamboge in animal glue at 25% mass concentration applied on watercolour paper with different number of layers (red curve: 10 layers, blue curve: 3 layers and black curve: single layer). The inset shows the corresponding derivatives of the spectra of gamboge in the different concentration in order to show clearer the spectral shift between them.

Variations on the particles size of the pigments can result in differences on the colour appearance. This property has been traditionally used in Chinese paintings in order to achieve different hues of various colours without the addition of white pigments. More specifically, in the case of pigments such as azurite and malachite, coarse grains give more saturated colour than the fine ones. However, these variations in the particle size often result in shifts in the spectral features [17], [18] in addition to the aesthetic effect. These shifts and alterations in spectral features due to differences in concentration and particle size of the pigments have to be taken into account in pigment identification using the KM method and therefore it is important that the reference spectral list covers all of these cases.

A common technique used on artworks, from Chinese paintings to European medieval illuminated manuscripts, is the layer-by-layer application of paint layers of different colour in order to achieve the desired aesthetic result. Despite the fact that the KM method has been designed to identify mixtures of pigments, it was found that it works efficiently in cases where the top paint layer is thin enough, so that the difference between mixed and layered paints is relatively small. For cases like the watercolour paintings in particular, the fact that the colourants are soaked into the fibres of the

substrate, acts as if they had been ‘mixed’ with the highly scattering fibres, enabling a good application of the KM method. A series of experiments were conducted using different types of pigments painted both in mixtures and with layer-by-layer application, with the KM method providing equally good results for both sets (Figure 2-8).

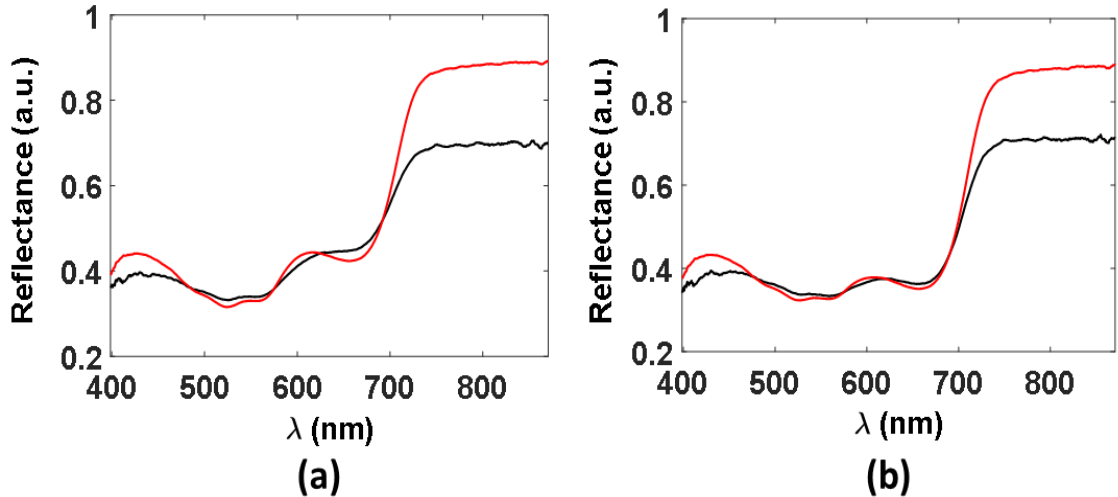


Figure 2-8 Reflectance spectra (black curve) of (a) a mixture and (b) a layer-by-layer application of cochineal lake and indigo fitted with the KM model (red curve) using the reference spectra of the two single pigments.

The examination of the effectiveness of the KM method on samples that combine both mixture and layer-by-layer application was also examined, showing that good fits can also be achieved in these cases. Figure 2-9 shows KM fits of the spectra of green areas, in which a mixture of gamboge and indigo was applied on top of a malachite layer.

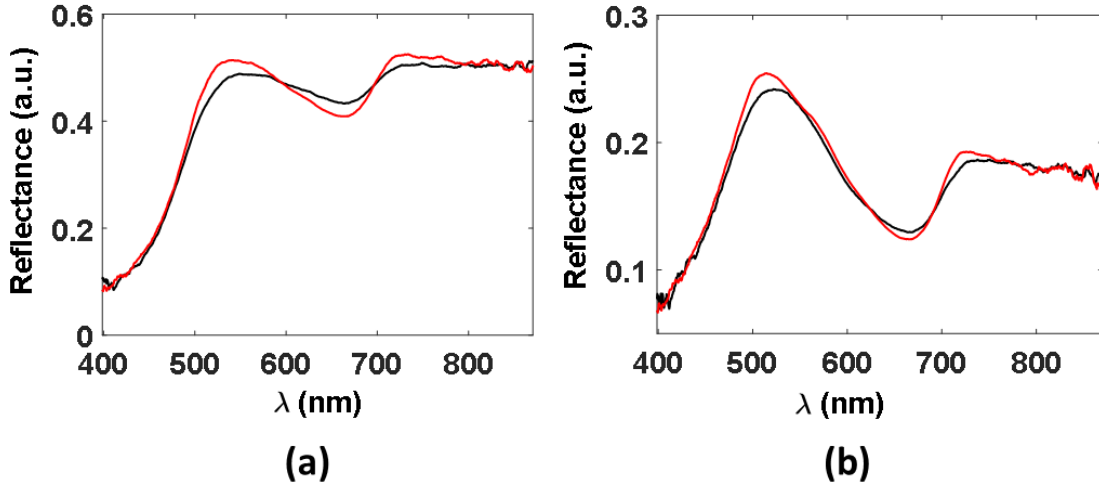


Figure 2-9 Reflectance spectra (black curve) of a (a) dark and (b) a light green area painted by applying a mixture of gamboge and indigo on top of a layer of malachite fitted with the KM model (red curve) using the reference spectra of the 3 single pigments.

Dupuis and Menu [19] have illustrated the combined use of reflectance spectroscopy and a method based on KM theory for the effective evaluation of pigment quantities in semi-transparent paint layers, highlighting the abilities but also the limitations that their method faced. However, their studies were performed on artificial samples, with the application of this method on real artworks requiring taking into account various parameters of the paint layers, such as the particle size of the involved pigments and the aging of the varnishes that have possibly used. In our methodology, KM algorithm provides the ‘weighting’ values of the reference spectra used in the fit, however a systematic work in order to investigate the correlation between the concentration of the reference pigments in the paint combination and these values is required.

## 2.3 Reflectance Spectroscopy

Reflectance spectroscopy is one of the most versatile and widely used analytical techniques, with application in a wide range of scientific disciplines. In the field of the analysis of cultural heritage objects, reflectance spectroscopy extended in various spectral regimes of the electromagnetic range has been used, providing different molecular information about the analysed materials. In the context of this study, the spectral regimes that are examined are defined as the visible/near-infrared (VIS/NIR) that extends at wavelengths from 400 to 900 nm, the near-infrared (near-IR) that covers the range from 800 to 2500 nm and the middle-infrared (mid-IR) regime that goes from 2.5 up to 25  $\mu\text{m}$ .

The reflectance spectroscopy in the UV/VIS regime is indicative of the electronic transitions that the atoms and the molecule of a chemical undergo after its irradiation with light in this regime. The absorption or reflectance in the visible range directly affects the perceived colour of the chemicals involved, with the energy and wavelength of absorption being defined by the difference between the energy levels of an electronic transition.

On the other hand, the energy of infrared (IR) radiation is too low to affect the electrons within an atom. IR radiation, however, corresponds to the energy required for translational, rotational, and vibrational energy transitions. The measurement of the characteristic IR energies that correspond to these transitions results in a spectrum. Based on its atomic structure, each molecule produces a unique and characteristic IR spectrum. The energy of molecular vibration is quantized, which means that a molecule can only stretch and bend at certain frequencies. Therefore, when a molecule is exposed to electromagnetic radiation that matches the frequency of one of its vibrational modes, it usually absorbs energy from the radiation and gets excited to a higher vibrational energy state. This results in an increase to the amplitude of the vibration, with the vibrational frequency remaining the same. It has to be noted that the absorption of IR radiation from a vibrational mode must result in a periodic change of the dipole moment of the molecule.

Developments in the manufacturing of optical fibres have allowed transmittance from 200nm up to 2500nm providing the ability for fibre optics reflectance spectroscopy (FORS) in both UV-VIS/NIR and near-IR spectral regimes. The fibre optic cables provide a flexible solution to interface between the object and the spectrometric devices. This characteristic in the field of cultural heritage has resulted in the development of non-invasive and portable instrumentation for in situ measurements. For the analysis in the mid-IR regime, it is common to use devices whose operation is based on Michelson interferometry. In these cases, the obtained spectrum is resulted from the Fourier Transformation (FT) of the gained interference signal (FTIR spectroscopy).

There are different modes of FTIR operation with the transmittance, which requires the reference beam to pass through the analysed sample, being the oldest one. However, in addition to the transmittance FTIR instrumentation, other types of FTIR spectrometers have been developed, providing different abilities in the mid-IR regime. FTIR-ATR (Attenuated total reflection) systems provide the ability of analysis in small penetration

depth, avoiding the spectral interference of layers beyond the analysed one. The signal measured with the FTIR-ATR spectrometers is related to the changes that occur in a total internal reflected infrared beam after its interaction with a sample. More specifically, an infrared beam is directed into a crystal of high refractive index (usually >2) at a certain angle. The beam is then reflected from the surface of the crystal, creating an evanescent wave that travels only a few microns ( $0.5\text{ }\mu\text{m} - 5\text{ }\mu\text{m}$ ) beyond the crystal surface and into the sample. The IR beam is absorbed by the molecules of the sample and then exits the opposite of the crystal and directed to the detector. Although the FTIR-ATR works in the reflectance mode, its configuration enable its application for the non-invasive analysis only of small objects of art, such as manuscripts. However, given that the operation of FTIR-ATR requires the application of pressure on the sample for the propagation of the evanescence wave, it is not a technique that can be used for the analysis of fragile objects of art. Finally, the development of FTIR spectrometer that operates in the reflection mode, without the need of crystal, provided the ability of non-invasive in situ analysis in the mid-IR spectral regime. However, the interpretation of the spectra collected this kind of instrumentation is not always straightforward as, additionally to the volume reflectance properties of the materials, the spectral information depends strongly on the roughness of the surface, as both specular (occurs on surface) and diffuse (occurs in volume) reflectance contribute to the outcome. This characteristic of reflectance spectroscopy is disadvantageous regarding the material identification, as its sensitivity to the sample morphology can cause spectral distortion.

## 2.4 Raman Spectroscopy

Raman spectroscopy provides highly specific molecular identification, enabling the distinction between different crystalline phases of compounds with the same molecular formula [20]. The Raman scattering technique is a vibrational molecular spectroscopy in which the observed spectra derive from an inelastic light scattering process. More specifically, in Raman spectroscopy monochromatic light (i.e. laser beam) is scattered by the molecules of the materials of the analysed area, resulting in changes to the frequency of its photons. This inelastic scattering is called Raman Effect and provides information about vibrational and rotational transitions in the molecules. When a molecule absorbs an incident photon, it can be excited to a virtual state. Figure 2-10 shows all the three different scenarios that can occur.

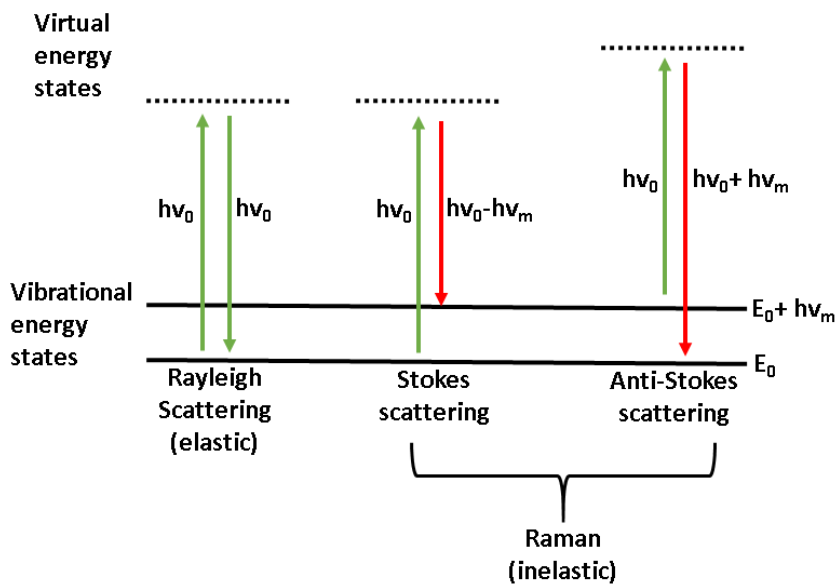


Figure 2-10 Quantum Energy Transitions for Rayleigh and Raman Scattering

The first possibility is that the molecule relaxes back to the ground state and emits a photon with frequency equal to that of the incident one; this elastic process is known as Rayleigh scattering. Another possible transition is from the virtual state to a real energy state with the sequential emission of a photon with frequency lower than that of the incident one; this is one of the two possible inelastic processes and is called Stokes shifted Raman scattering. In the case that the molecule is already in an excited phonon state, it is excited to a higher virtual state and then relaxes back down to the ground state emitting a photon with frequency higher than the incident photon had; this is the second possible inelastic scattering known as Anti-Stokes Raman scattering.

## 2.5 X-ray Fluorescence (XRF) Spectroscopy

XRF is a spectroscopic technique based on the production of characteristic X-ray lines from the different elements of a chemical compound that act as their ‘fingerprints’. More specifically, XRF analysers determine the elemental composition of a sample by measuring the spectrum of the characteristic X-ray fluorescence emitted by the different elements in the sample when it is illuminated by X-rays. The initial X-rays can be emitted either from a miniaturized X-ray tube, or from a small, sealed capsule of radioactive material.

The irradiation of an atom with an X-ray beam of sufficient energy results in the production of a fluorescent X-ray, dislodging an electron from one of the inner orbital shells of the atom (Figure 2-11). The vacancy left in the inner orbital shell is later filled with an electron from one of higher energy orbital shells of the atom. For example, the K line transition is when an electron from the K orbit is ejected from the atom by the incident X-ray and is replaced by an electron from the L orbit.

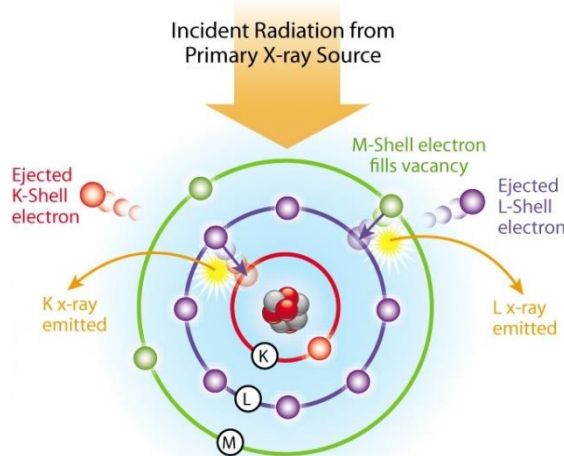


Figure 2-11 Scheme about the production of X-ray fluorescence (<http://www.911metallurgist.com>).

Most of the XRF spectrometers can only detect elements with atomic number greater than 14 ( $Z>14$ ) when they operate in open air. However, some devices enable the attachment of a helium purge, which increases detection sensitivity and extends the detection range up to elements of atomic number 12 ( $Z>12$ ).

## 2.6 Optical Coherent Tomography (OCT)

OCT operation is based on an imaging Michelson interferometer (Figure 2-12), providing the ability of *in situ* and real time non-contact and non-invasive cross-section images of subsurface microstructures. More specifically, the beam of the broadband source of Michelson interferometer is divided in two parts when incident on a beam splitter, with the one part being directed to the target and the other continuing its propagation until it reaches the reference mirror. After both parts reflect back to the beam splitter, they are redirected to the detector and recombined. The recombined beam

is then incident on the detector that detects the interference patterns that are related to the matches and differences of the optical path of the two beams.

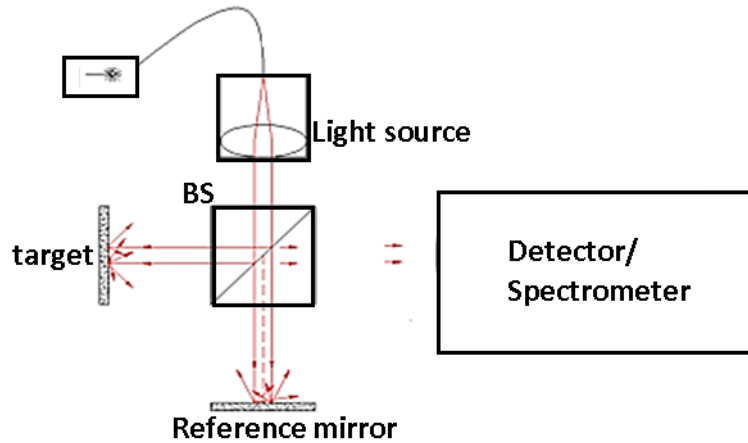


Figure 2-12 Scheme of the operation of Michelson interferometry for OCT scanning.

There are two kinds of OCT systems, the Time-domain OCT (TD-OCT) and the Fourier-domain OCT (FT-OCT), with their differences related to the collection of their axial signal. The operation of the TD-OCT is similar to the operation of the FTIR spectrometry (see section 2.3), with the interference between the two beams being occurred by the mechanical move of the reference mirror.

but in TD-OCT the sample is replacing the stationary mirror (Figure 2-12) and no Fourier transform is necessary since the back-scattered intensity is recorded as a function of depth. However, the depth profile is generated again by the variations in the optical path length due the motion of the reference mirror. In FT-OCT the reference mirror is fixed, with the depth profile being a result of the Fourier transformation of the interference signal that is detected using a grating based spectrometer. It is worth mentioning that given that in FD-OCT there is no mechanical movement involved in the depth scanning, its speed of operation is much faster than the one of TD-OCT.

The combination of the recorded axial signals (A-scans) (Figure 2-13a) results in virtual cross-sectional images (B-scans) (Figure 2-13b). Furthermore, the simultaneous transverse scanning of the incident optical beam through the sample provides high (i.e. micro-scale) resolution information about the stratigraphy of the analysed area. The axial and lateral resolutions of OCT are independent from each other, as the latter

depends on the objective lens, while the axial resolution ( $l_c$ ) is a function of the central wavelength ( $\lambda_0$ ) and the bandwidth ( $\Delta\lambda$ ) of the laser source:  $l_c = \frac{2 \ln(2)}{\pi} \frac{\lambda^2_0}{\Delta\lambda}$ . Three-dimensional, volumetric data (Figure 2-13c) can be generated by scanning the incident optical beam in parallel to the sample, acquiring in this way sequential cross-sectional images.

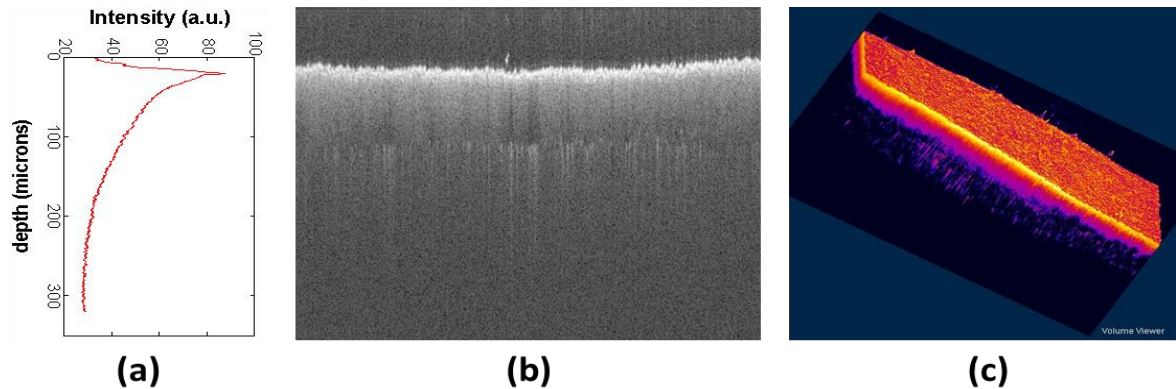


Figure 2-13 (a) Slope of the echo time delay (A-scan), (b) cross-section (B-scan) and (c) 3D representation of analysed area using OCT system.

## 2.7 Scanning Electron Microscopy with Energy Dispersive X-ray (SEM-EDX) Spectroscopy

SEM-EDX is an invasive but non-destructive analytical technique that provides elemental information. In a typical SEM, an electron beam is emitted from an electron gun fitted with heated filament cathode and focused on the analysed sample. The elemental information using this technique derives from the X-ray spectrum that is produced from the sample after its irradiation by this focused beam of electrons. Compared to XRF spectroscopy, EDX offers higher detection sensitivity, enabling the detection of the ‘light’ elements ( $Z < 12$ ), but also the ability for quantitative analysis. Qualitative analysis is based on the same principles as XRF, while quantitative analysis is based on the measurement of the intensity of the elemental lines and their comparison with known lines of standard samples. Another difference between SEM-EDX and XRF spectroscopies is their analytical depth. Given that the energy of the electron beam

typically ranges from 0.2 keV to 40 keV, the penetration depth of the SEM-EDX is lower in comparison to the XRF spectroscopy.

Table 2-1 summarises the operational parameters of both benchtop and portable versions of each of the non-invasive analytical techniques used in this study.

Table 2-1 Spatial and spectral parameters of the non-invasive analytical techniques used in this study

Technique/ Instrumentation	Working distance (mm)	Spatial resolution or spot size (mm)	Field of view or scanned size (mm)	Spectral range
Benchtop Micro-Raman (Horiba XploRA)	~0.5	~0.002	~0.002	532 nm, 638 nm excitation Raman shift range 150-3800 cm <sup>-1</sup>
Portable Raman (Horiba HE785)	~0.5	~0.125	~0.125	785nm excitation Raman shift range 150-3800 cm <sup>-1</sup>
Benchtop XRF (ArTAX)	~1	~0.2	~0.2	2-50 keV
Portable XRF (Niton XL3t Analyser)	~1	~20	~20	2-50 keV
VIS/NIR FORS (Ocean Optics) [adapted with microscope probe head]	~30	~0.5	~0.5	400-950 nm
Near-IR FORS (Polycromix)	~2	~5	~ 5	900-2400 nm
FORS (ASD LabSpec4) & (ASD FieldSpec)	~2	~5	~5	VIS/NIR: 400-900 nm Near-IR: 900-2500 nm
UV-VIS/NIR Spectral Imaging (PRISMS)	2240	~0.085	~115×85	400-900 nm
OCT (Thorlabs)	~10	~0.009 x 0.009 x 0.0045 [on polymer]	~10 (width)	930 nm (100 nm bandwidth)
UHR-OCT (in-house built instrument)	~40	~0.009 x 0.009 x 0.0012	~10 (width)	810 nm (600-1000 nm bandwidth)



## **Chapter 3:**

### **Application of statistical methods for automatic post-processing of large-scale data**

The extraction of accurate results about the holistic analysis of objects of cultural heritage requires the examination of large statistical samples. However, the analysis of the total surface of large number of artworks (e.g. examination of large collections of paintings) or the examination of large scale painting surfaces, such as murals), using analytical techniques of small spot size can be extremely time-consuming or even humanly impossible. The PRISMS system (see section 2.1), given its relatively large field of view and its ability for automatic capturing enables the automatic spectral imaging of large painting surfaces. The issue that arises, therefore, is the development of a method for the efficient management of the large scale spectral imaging dataset.

In this chapter, the application of statistical analysis for the automatic processing of both the spectral imaging and the pixel-level spectral information that the PRISMS system provides is illustrated. More specifically, the application of different statistical methods and the characteristics that the spectral imaging data must have in order to enable the revealing of information, which is not obvious in the visual observation, are examined. Moreover, the development of an automatic way for the management of large scale spectral information is presented. The development of methods for automatic processing of spectral imaging data collected from large scale painted areas makes the analytical procedure more time efficient by highlighting the areas that should be further examined either because they contain interesting information about the drawings and the structure of the paint layers or because they are representative of the various pigment compositions.

### **3.1 Application of Blind Source Separation (BBS) techniques for the revealing of hidden information**

#### **3.1.1 Introduction**

For the examination of objects of art, statistical analysis methods, and more specifically BSS techniques, have been widely applied in order to interpret the data collected using various analytical techniques. Among the various BSS methods, the principal component analysis (PCA) is the most commonly applied and has been proven to be a very useful tool for the interpretation of both spectroscopic and spectral imaging data. The application of multivariate statistical methods on spectroscopic data, also known as chemometrics in chemistry, is widely used for their interpretation in various studies about the analysis of painting materials. The application of PCA on XRF spectral images has been successfully used for the improvement of their interpretation. Rodriguez et al [21] showed that the application of PCA on XRF elemental maps enabled the detection and subtraction of any misleading artefacts, allowing therefore the detection even of trace phases of the present elements. The PCA of FTIR-ATR spectra, collected from mock-up samples, has assisted on the examination of the degradation procedure, enabling the identification of the effect caused it, as well as the determination of the specific time that it started [22]. The PC analysis of data obtained by Laser Induced Spectroscopy (LIBS) improved their interpretation, enabling in-depth elemental profile studies of archaeological objects of irregular surface [23]. However, in the context of this study, our interest is focused on the application of BSS methods on spectral imaging data for the automatic revealing of visually hidden information. Studies conducted on the revealing of hidden texts, drawings and textures, as well as the enhancement of erased texts in palimpsests [24], [25] showed that the observation in single spectral band is not always enough. In these cases, the application of further post-processing methods, such as IGB (i.e. using infrared, Green and Blue channels) False Colour Generation [26], [27], thresholding [28] and Blind Source Separation techniques [27], [29] were required. The application of BSS techniques has been proven to enable the detection of the features of the spectral image dataset without the interference of the operator. The operation principle of the BSS techniques is based on the assumption that the observed images derive from the superposition of individual patterns that are combined linearly to form the final appearance. More specifically, if  $\mathbf{X}(i, j)$  is a N-

vector map corresponding to the spectral image and  $\mathbf{y}(i,j)$  a N-vector map that corresponds to the collection of original patterns then:

$$\mathbf{X}(i,j) = \mathbf{\Lambda} \mathbf{y}(i,j)$$

Equation 3-1

where (i,j) is the pixel index and the  $\mathbf{N} \times \mathbf{M}$  matrix  $\mathbf{\Lambda}$  is called mixing matrix.

The aim of the BSS techniques is to obtain  $\mathbf{y}$  from the spectral data  $\mathbf{X}$  under some statistical assumptions. In addition to PCA, independent component analysis (ICA) is another widely used BSS technique. PCA method is based on the assumption that the vector  $\mathbf{y}(i,j)$  consists of uncorrelated variables and therefore N spectral channels produce N images, representing mutually uncorrelated patterns, by maximizing the variance. Another assumption of this method is that the neighbouring bands of spectral images are highly correlated and often provide almost the same information about the object [30]. The outcome of the application of PCA on the spectral images derives from the performance of a linear projection of the data from the higher variance to the lowest using the eigen vectors and the eigen values of either the covariance or the correlation matrix of the original spectral cube. The covariance matrix consists of the variances of the variables along the main diagonal and the cross-correlation between each pair of the variables in the other matrix positions and it is calculated by:

$$\text{Cov}(\mathbf{X}) = \frac{1}{n-1} \sum_{i=1}^n \left( \mathbf{X}_i - \bar{\mathbf{X}} \right) \left( \mathbf{X}_i - \bar{\mathbf{X}} \right)^T$$

Equation 3-2

where  $\bar{\mathbf{X}}$  : the mean vector.

The correlation matrix is the normalised version of the covariance matrix. ICA method is based on the assumption that  $\mathbf{y}(i,j)$  in Equation 3-1 is a matrix containing non-Gaussian (i.e. independent) components and  $\mathbf{\Lambda}$  is the linear mixing matrix. The purpose of the ICA is the ‘un-mixing’ of the data by estimating an un-mixing matrix  $\mathbf{W}$ , where  $\mathbf{X}(i,j)\mathbf{W}=\mathbf{y}(i,j)$ . According to the Central Limit Theorem, when independent random variables are added, their properly normalised sum tends towards a Gaussian distribution, even if the original variables themselves are not having a Normal distribution. Therefore, it is assumed that the  $\mathbf{X}(i,j)$  variables tend to be ‘more Gaussian’

than the source components in  $\mathbf{y}(i,j)$  and sequentially the extraction of the independent components requires the un-mixing matrix  $\mathbf{W}$  to maximize the non-Gaussianity of the sources. There are various ways to measure the non-Gaussianity, with the negentropy being one of the most common. Entropy is an important concept in information theory, with the Gaussian distributions having the maximum entropy among any random distribution, whereas spiky distributions having the smallest entropy. The negentropy is defined as the difference between the entropy of a random and a Gaussian distribution. Therefore, maximizing negentropy would yield source components that are non-Gaussian [31], [32], which is the requirement for the operation of the ICA. It is worth mentioning that it is the signal rather than the noise distribution that we refer to.

Both of these methods have been promising when applied on the examination of artworks, in studies related to the revealing of hidden information. Bacci et al.[33], illustrated the complementary use of the art historical records with reflectance spectroscopy and PCA elaboration of the spectral data for the analysis of a selection of Parmigianino's drawings. The PCA outcomes enabled the revealing of details of the drawings, not noticeable under simple visual examination. Salerno et al. [27], performed both PCA and ICA on IGB data collected from a mural of an Etruscan tomb in Chiusi (Italy). The application of these statistical based methods provided the visualisation information that was not obvious in the individual bands. Alexopoulou et al. [34] applied PCA on spectral images collected from fragments of ancient Greek papyrus, in the VIS/NIR regime. It was observed that neither the spectral images at the individual bands nor the image subtraction managed to enhance the original writings. On the other hand, the application of PCA and the further processing of the principal component images enabled the distinction between the writing and its background, enhancing the readability of the script. The application of BBS methods on spectral bands has been used for the enhancement of the original writings in palimpsests. Salerno et al. [29], applied both PCA and ICA on bands that were carefully selected, and preliminarily processed, to achieve the desired results. The outcome showed that the statistical processing of spectral images enabled the distinct visualization of both the original and the overwritten writings, as well as the pattern of the mold that was developed on the substrate. However, palimpsests can be very complex systems, as the two scripts can be written in different periods and possibly using different materials. In those cases, the application of PCA on spectral data failed to reveal of the original writings. Bloechl et al.[35] showed that the application of PCA on colour images of fluorescence produced

under ultraviolet illumination can overcome this issue . The combined application of PCA and ICA on the analysis of ancient documents provided complementary information in the enhancement of faded writings and the revealing of hidden patterns belonging to their substrate [36]. Tonazzi et al [37], in their study about the restoration of documents gave a formulation of ICA application for the separation of overlapped texts using a simplified RGB artificial case.

The aim of this work is the investigation of the application of BSS methods on the spectral imaging data, obtained by the PRISMS system, in order to reveal of any hidden information automatically. More specifically, given that BSS analysis contains a wide range of post-processing statistical methods, our investigation was focused on the application of the most widely used methods, PCA and ICA, on a wide range of heterogeneous examples. In most of the studies published so far, the nature of the hidden features was known and therefore specific pre-treatment of the spectral imaging data was performed in order to enhance the revealing of the hidden features. This section illustrates how these BSS methods can be used to reveal hidden information, using spectral imaging data that have not been prior treated. Moreover, most of the studies in the literature are using RGB or IGB data, as the corresponding imaging devices are low cost and commonly found in laboratories of art analysis and conservation. Therefore, the dependence of the BSS results on characteristics of the analysed spectral imaging data is also examined.

### **3.1.2 Spectral Imaging Data & Statistical Analysis methods**

#### *Spectral Imaging data*

The spectral imaging data used in this study were collected using the PRISMS system from the murals of the cave 465 in Mogao complex, as well as from '*The Virgin and Child with an Angel*' (NG 3927) after Francesco Francia, an easel painting from the collection of the National Gallery in London.

### **Statistical Analysis codes**

The codes for the PCA and ICA methods examined in this study were written in R by Dr. Golnaz Shahtahmassebi.

For the PCA, the '*princomp*' function from the built-in R stats package was used. The calculation of the principal components using this function was done using the eigen values and vectors of both the correlation and the covariance matrix of the original spectral matrix.

For the ICA, the '*fastICA*' algorithm from the built-in R stats package was used. In this algorithm, the data are firstly centred by subtracting the mean of each column of data of the original spectral matrix  $X(i,j)$ . Sequentially, the  $X(i,j)$  is going through a linear transformation. Through this transformation, each vector of random variables with a known covariance matrix is transformed into a set of new variables whose covariance is the identity matrix.

### **3.1.3 Results**

#### *3.1.3.1 Comparison between the individual spectral images and BSS methods outcome*

Given that PCA is one of the most commonly used BSS methods, the results obtained from its application on the revealing of the hidden information in the various examples were initially examined. The results were very interesting as, in addition to the automatic detection of the information present in the individual spectral images, it provided new information that could not be observed when examining each band separately. Figure 3-1 illustrates the example of a human feature that in visual observation seems to have only outline sketches (Figure 3.1a). However, the application of PCA on the spectral imaging data collected from this area revealed the presence of more drawings, suggesting that a more detailed examination of the area should be performed. Further examination in the individual spectral images discriminated the observed drawings to the outline sketches, the top drawing (Figure 3-1g,h) and the drawings that are located underneath the paint layer (Figure 3-1i-k). Interestingly, the application of PCA enabled the revealing of drawings that do not appear in any spectral bands (e.g. eyebrow in Figure 3-1m,n).

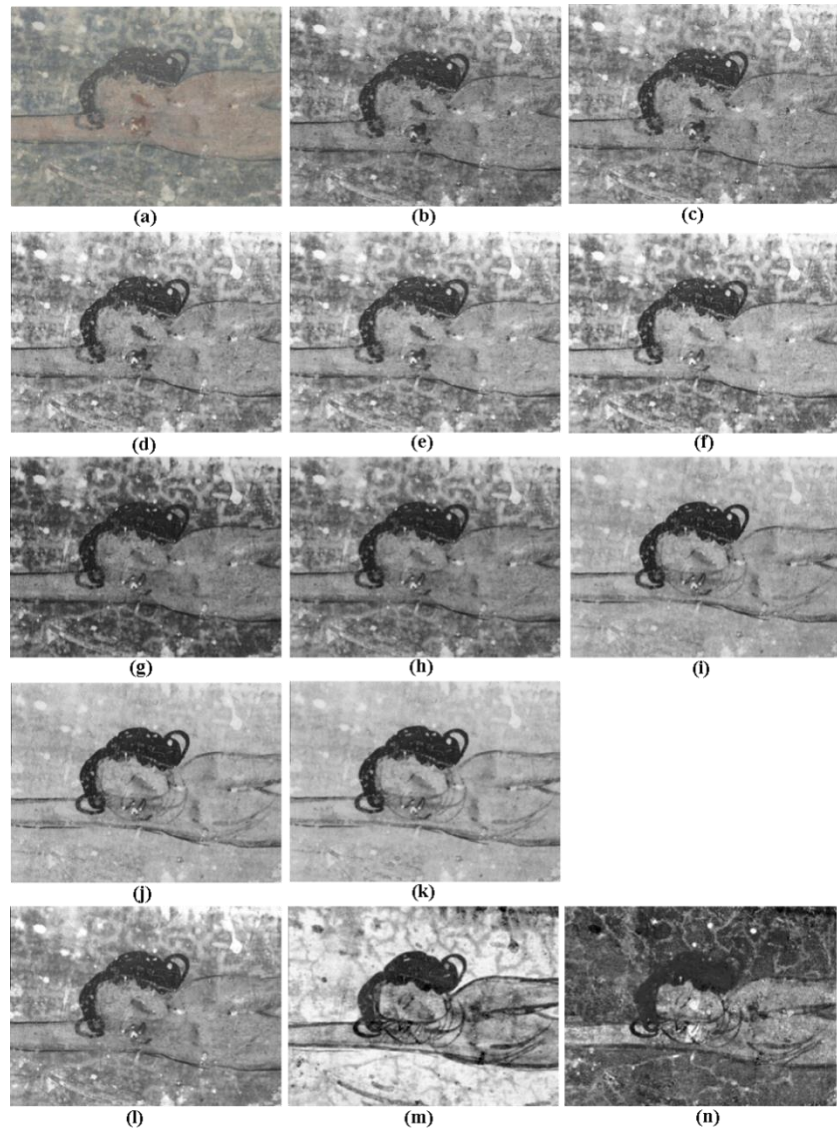


Figure 3-1 (a) Colour image derived from PRISMS data collected from an area with various drawings, (b-k) Spectral images at 400 nm, 450 nm, 500 nm, 550 nm, 600 nm , 650 nm, 700 nm, 750 nm, 800 nm and 880 nm respectively and (l-n) the first three principal components resulted from the application of PCA on the previous ten spectral bands

The revealing of information that the individual spectral images are not showing is becoming clearer in the case of an area containing faded writings. Figure 3-2, shows that neither the coloured image nor any of the spectral images contain any writing. On the contrary, the application of PCA reveals the faded writings in high contrast (Figure 3-2n). It is worth noticing that the first PCA is always the averaged information of the different spectral bands, whereas the last PCAs reveal the imperfections in the data, such as mosaicing issues (Figure 3-2o).

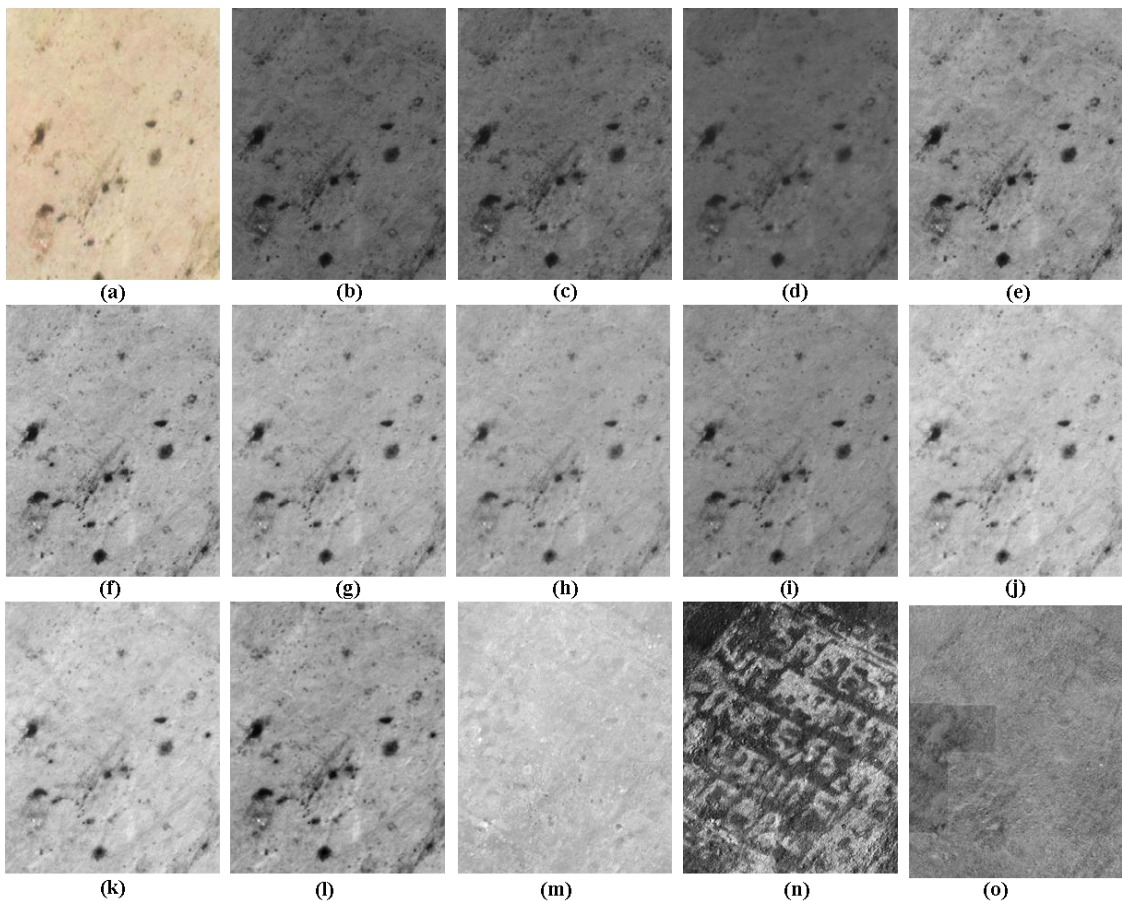


Figure 3-2 (a) Coloured image derived from PRISMS data collected from an area with faded writings, (b-k) Spectral images at 400 nm, 450 nm, 500 nm, 550 nm, 600 nm, 650 nm, 700 nm, 750 nm, 800 nm and 880 nm respectively and (l-o) the four three principal components resulted from the application of PCA on the previous ten spectral bands

The application of statistical analysis on the PRISMS spectral images collected from an easel painting on canvas (Figure 3-3 ) showed that the high contrast in the resulted images enables the revealing of the drawings but also the pattern of the canvas weave (Figure 3-3 m). This information was not observed in the individual spectral bands.

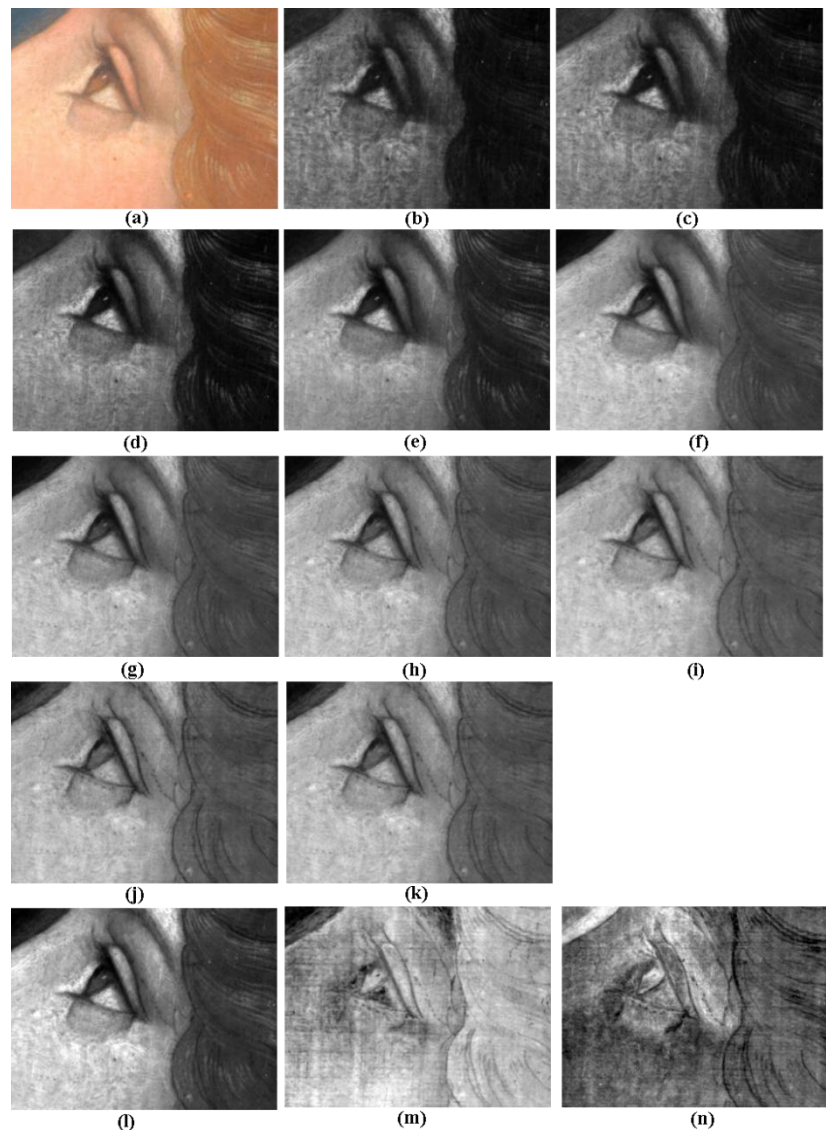


Figure 3-3 (a) Colour image derived from PRISMS data collected from the easel painting The Virgin and Child with an Angel (NG 3927), (b- k) Spectral images at 400 nm, 450 nm, 500 nm, 550 nm, 600 nm, 650 nm, 700 nm, 750 nm, 800 nm and 880 nm respectively and (l- n) the first three principal components resulted from the application of PCA on the previous ten spectral bands

### *3.1.3.2 Comparison between the results obtained by the application of the PCA on the correlation and covariance matrix*

As it has been mentioned, the PCA method can be applied on two types of matrices produced from the input data, either the covariance or the correlation. The examination of the results obtained using both matrices showed that even though both matrices gave similar results for most of the examples, in the case of the faded writings the results based on the covariance matrix were not good. More specifically, the revealed information was divided in two principal components (Figure 3-4b and Figure 3-4c), making the reading of the writings difficult. On the contrary, the third principal

component obtained by the application of PCA on the correlation matrix (Figure 3-4f) contains the whole information, despite the fact that the second one (Figure 3-4e) contains also some information. Therefore, the application of PCA on the correlation matrix of the spectral data is recommended, promising better results in a larger range of cases with hidden information. In the rest of this study, the PCA results that will be presented are obtained by the application of PCA on the correlation matrix unless otherwise specified.

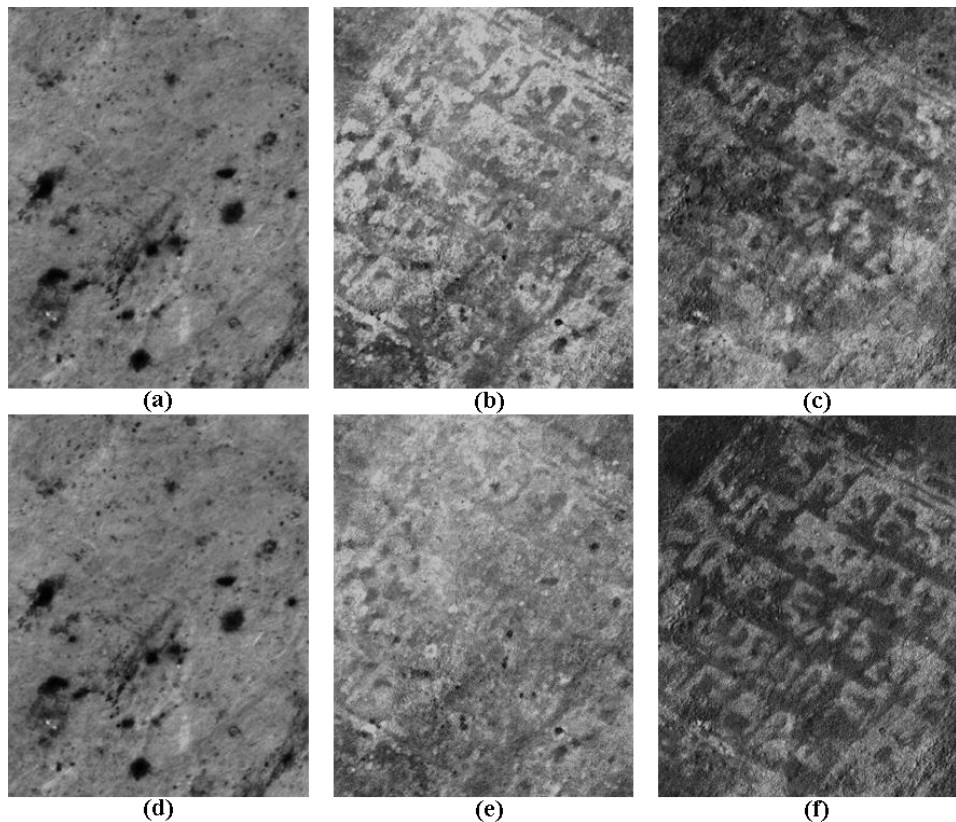


Figure 3-4 First three Principal Components resulted from the application of PCA on (a-c) the covariance and (d-f) the correlation matrices of the data collected in the ten spectral bands from an area with faded writings

### *3.1.3.3 Comparison between the result obtained by the application of PCA or ICA method*

The comparison of the results obtained by the application of PCA and ICA methods showed that both of them seemed to be equally effective on the revealing of the information. The ICA analysis provided also further separation of this information. Figure 3-5 illustrates the results of the application of PCA (Figure 3-5 a-c) and ICA (Figure 3-5 d-f) on spectral imaging data collected from a drawing-containing area of the murals of cave 465. The application of ICA enables the clearer observation of the drawings as, in addition to the revealing of the hidden information, it separates the drawings from the morphological patterns of the background.

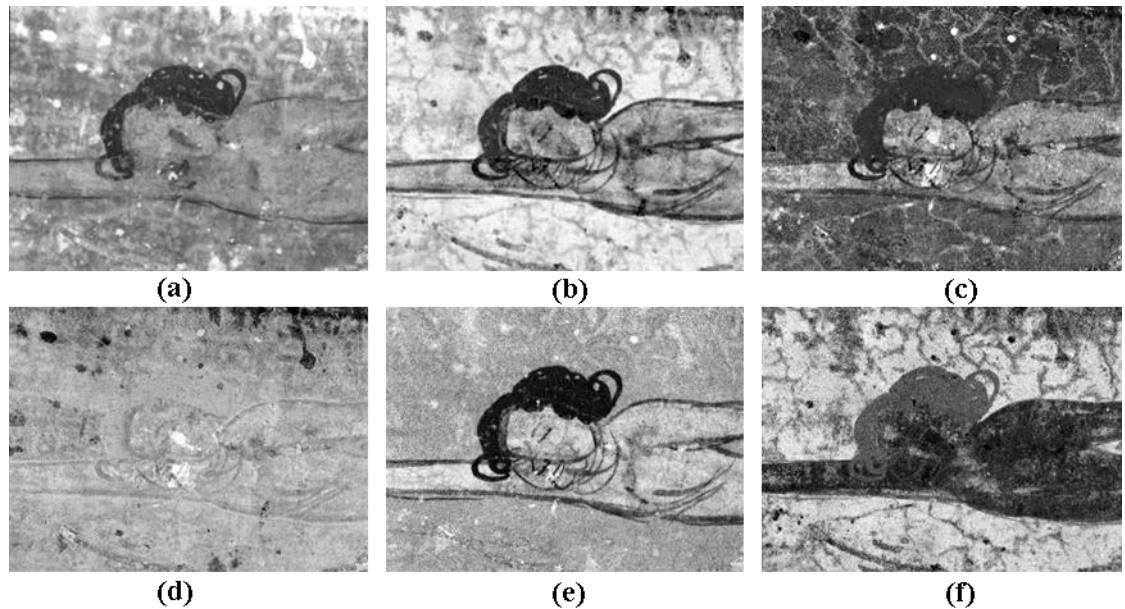


Figure 3-5 (a-c) First three Principal Components and (d-f) three Independent Components of data collected in the ten spectral bands from an area with various drawings

On the other hand, the comparison between the results of the application PCA and ICA on data collected from an area that contains different types of cracks, showed that only PCA enabled the revealing of the total of the cracks. More specifically, the application of PCA (Figure 3-6b) revealed the cracks on both on the painted figure and the surrounding area in higher contrast than any of the individual spectral image. On the contrary, the application of ICA (Figure 3-6d-f) did not offer high contrast observation of the fine cracks and moreover did not reveal the cracks of the surrounding area.

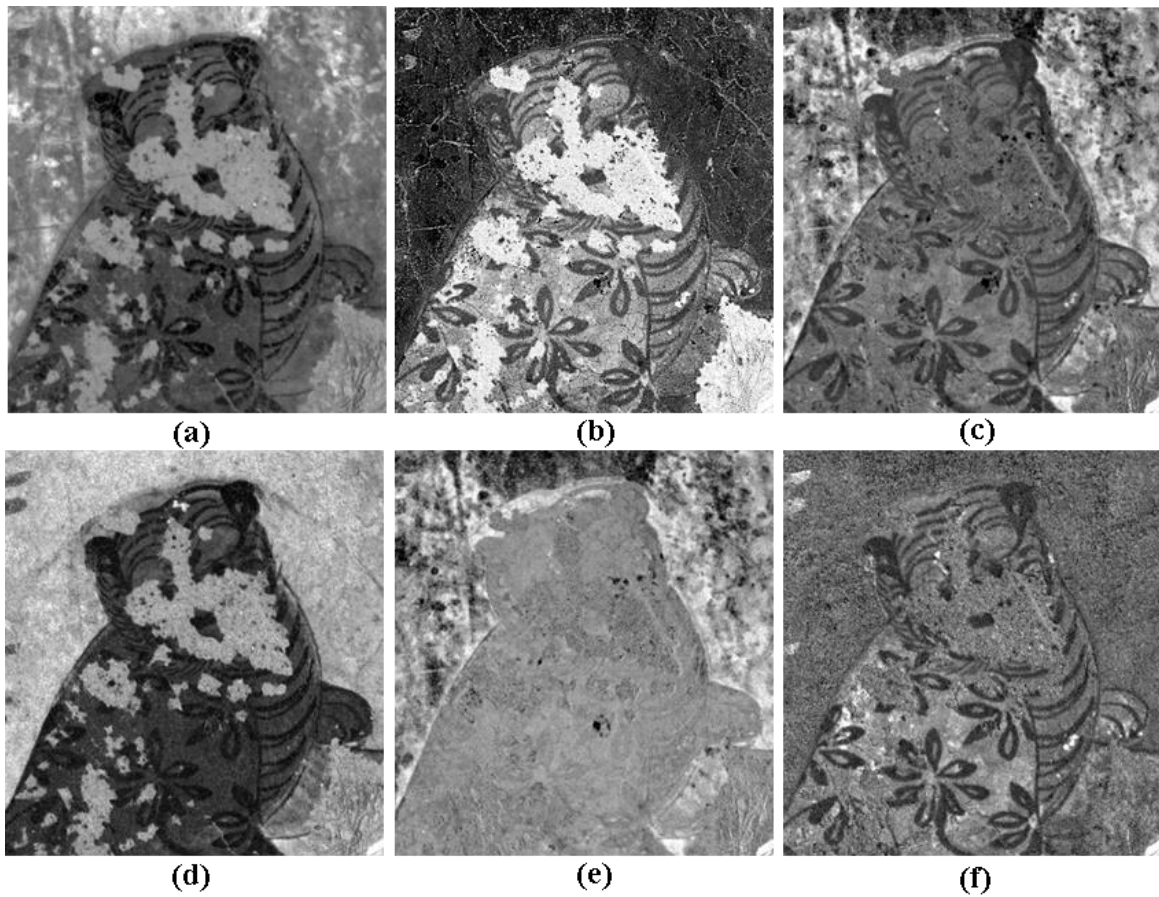


Figure 3-6 (a-c) First three Principal Components and (d-e) three Independent Components resulted from the application of PCA and ICA respectively on data collected in the ten spectral bands from an area with various cracks

The analysis of the various examples showed that PCA and ICA provide most of the times equally good results in the detection of hidden information. However, there were cases where these two methods offered complementary information and therefore their combined use is recommended for a more comprehensive analysis.

### *3.1.3.4 Examination of the dependence of results on the spectral imaging input*

Most of the studies regarding the post processing of spectral images for the revealing of hidden information are based on the application of various processing methods, including statistical analysis, on RGB or IGB data. Therefore, a comparison between the results obtained by the application of PCA and ICA on RGB, IGB and the total ten spectral bands of the PRISMS system in the VIS/NIR regime was performed, investigating the effect of the spectral characteristics of the analysed data on the resulted outcome. Moreover, the optimum combination of the minimum number of spectral images, in the PRISMS range, that is required for efficient revealing of the hidden information was investigated.

In the analysis of the drawing-containing area using RGB data, even though the application of PCA (Figure 3-7c) gave slightly better results than the ICA (Figure 3-8c), the image quality in both cases was low, with the revealing of the eyebrow sketch not being clear. On the other hand, the replacement of the red (R) channel with an IR (880 nm) spectral image improved the results in both; PCA (Figure 3-7g) and ICA (Figure 3-8g). The results of PCA application gave equally good results compared to using the whole ten channel dataset. Finally, the replacement of the blue channel (B) in the previous combination with a spectral image in the near-UV regime (400 nm) was proven to give results similarly good to those obtained using the whole ten bands spectral imaging dataset (Figure 3-7h and Figure 3-8h respectively).

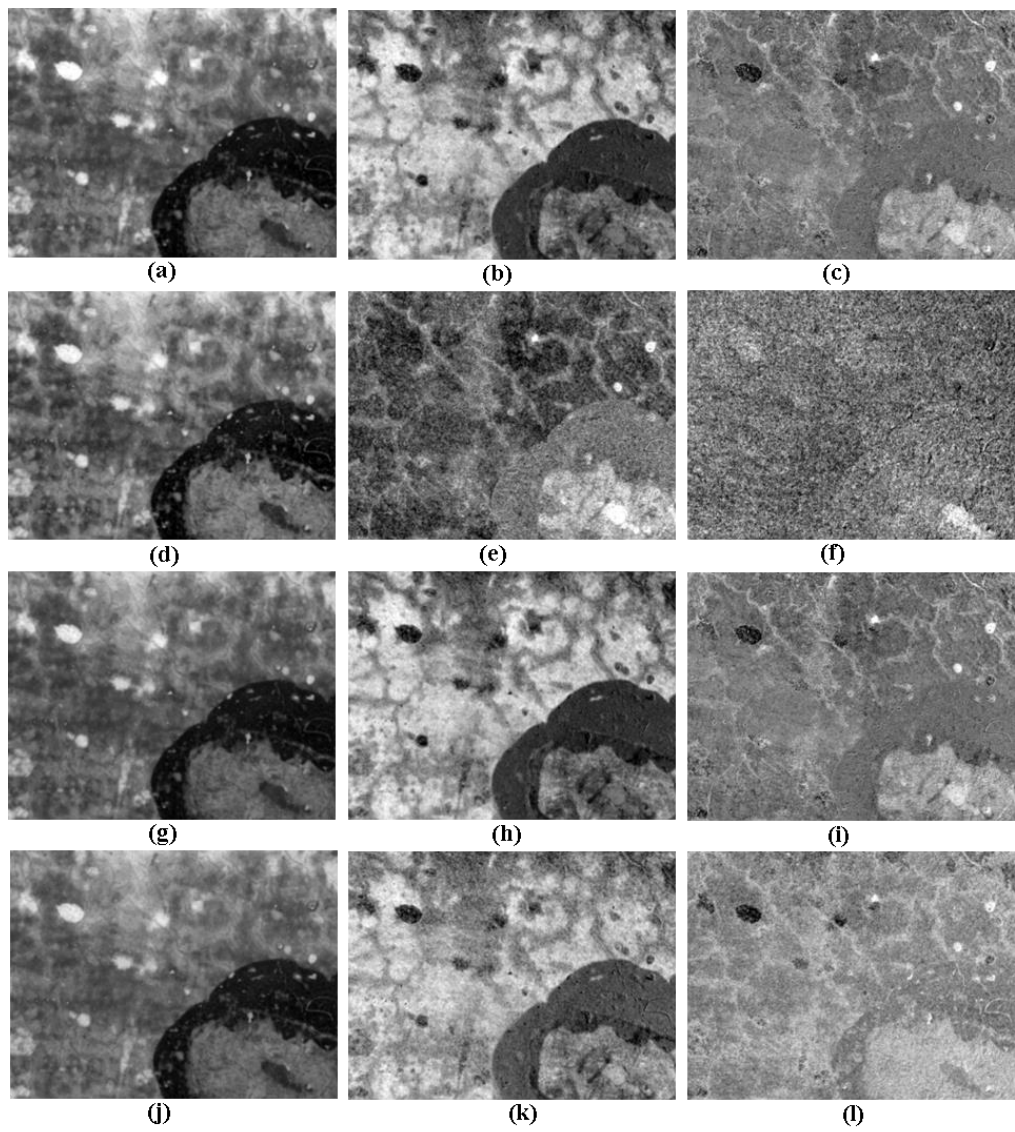


Figure 3-7 First three Principal Components obtained from the application of PCA on the (a-c) ten spectral bands of PRISMS system, (d-f) red (R), green (G) and blue (B) spectral bands derived from PRISMS system, (g-i) blue (B), green (G) and IR (880 nm) spectral bands and (j-l) violet (400 nm), green (G) and IR (880 nm) bands collected from a drawing-containing area

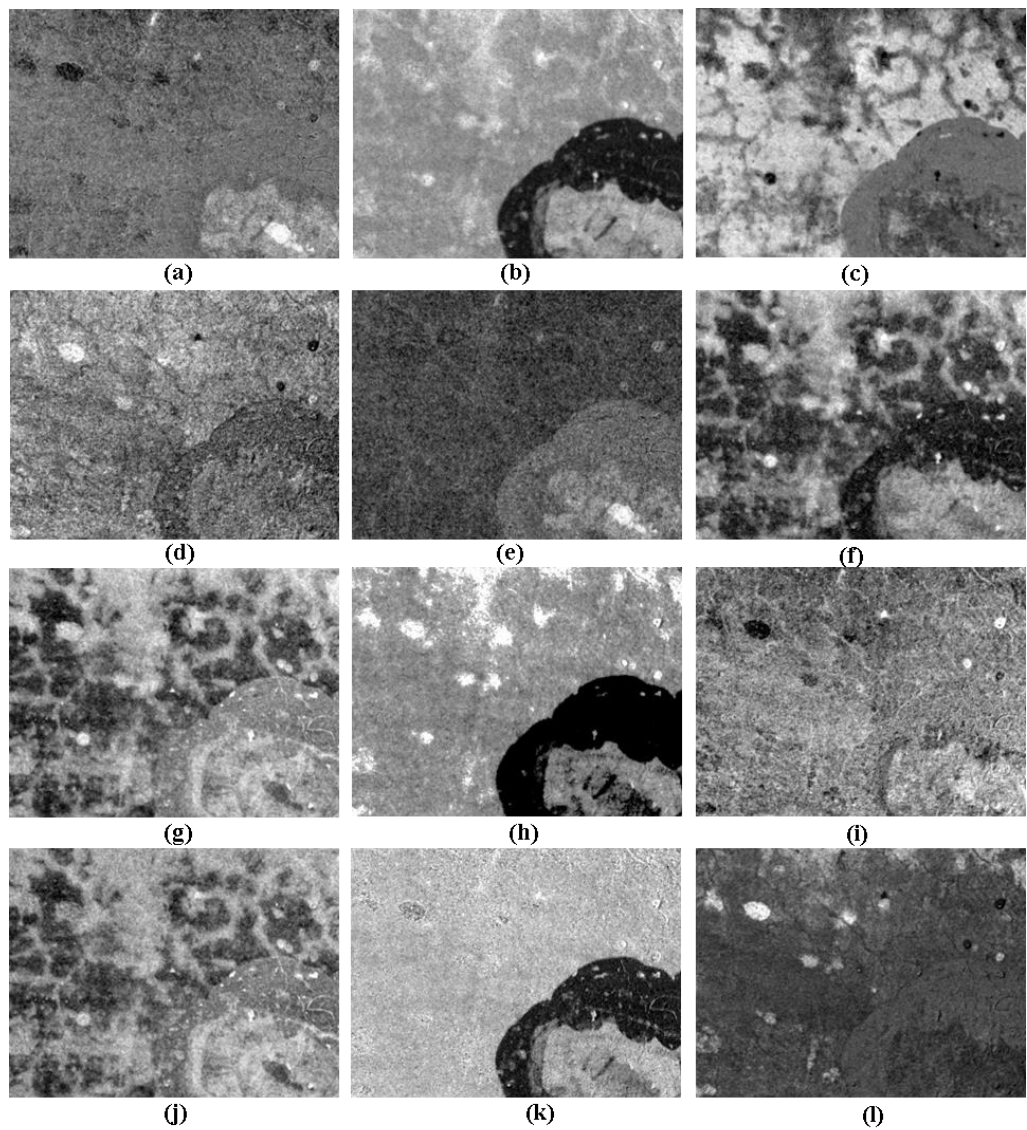


Figure 3-8 Independent Components obtained from the application of ICA on (a-c) ten spectral bands of PRISMS system, (d-f) red (R), green (G) and blue (B) spectral bands derived from PRISMS system, (g-i) blue (B), green (G) and IR (880 nm) spectral bands and (j-l) violet (400 nm), green (G) and IR (880 nm) bands collected from a drawing-containing area

The application of the two BSS methods on RGB data collected from the area with faded writings showed at the same image the writings but also the mosaicing issues (Figure 3-9f and Figure 3-10f). The replacement of the red (R) channel with the IR (880 nm) spectral image was less effective on the revealing of the writings, with information from the background being present in both PCA (Figure 3-9i) and ICA (Figure 3-10i) results. Finally, the combination of the spectral image at 400 nm with the green (G) channel and the IR (800 nm) provided clear images of the writings, with the contribution of the background being insignificant (Figure 3-9l and Figure 3-10l).

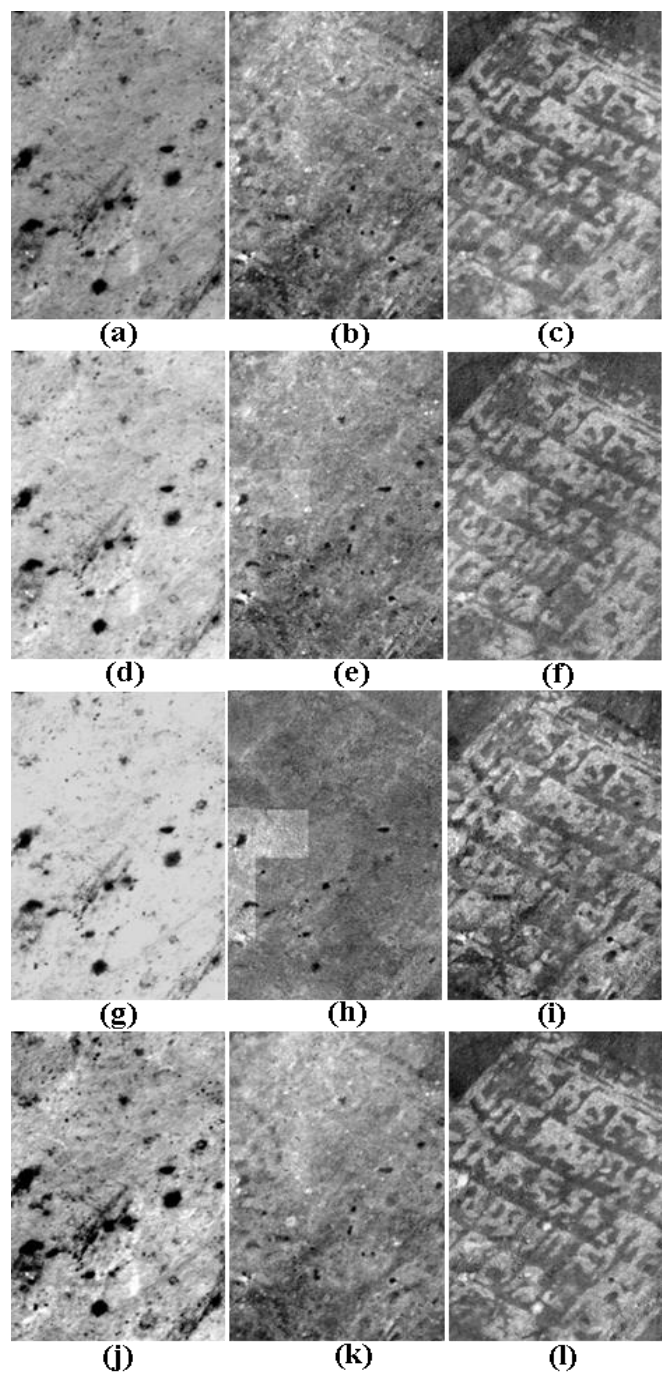


Figure 3-9 First three Principal Components obtained from the application of PCA on the (a-c) ten spectral bands of PRISMS system, (d-f) red (R), green (G) and blue (B) spectral bands derived from PRISMS system, (g-i) blue (B), green (G) and IR (880 nm) spectral bands and (j-l) violet (400 nm), green (G) and IR (880 nm) bands collected from a faded writings-containing area

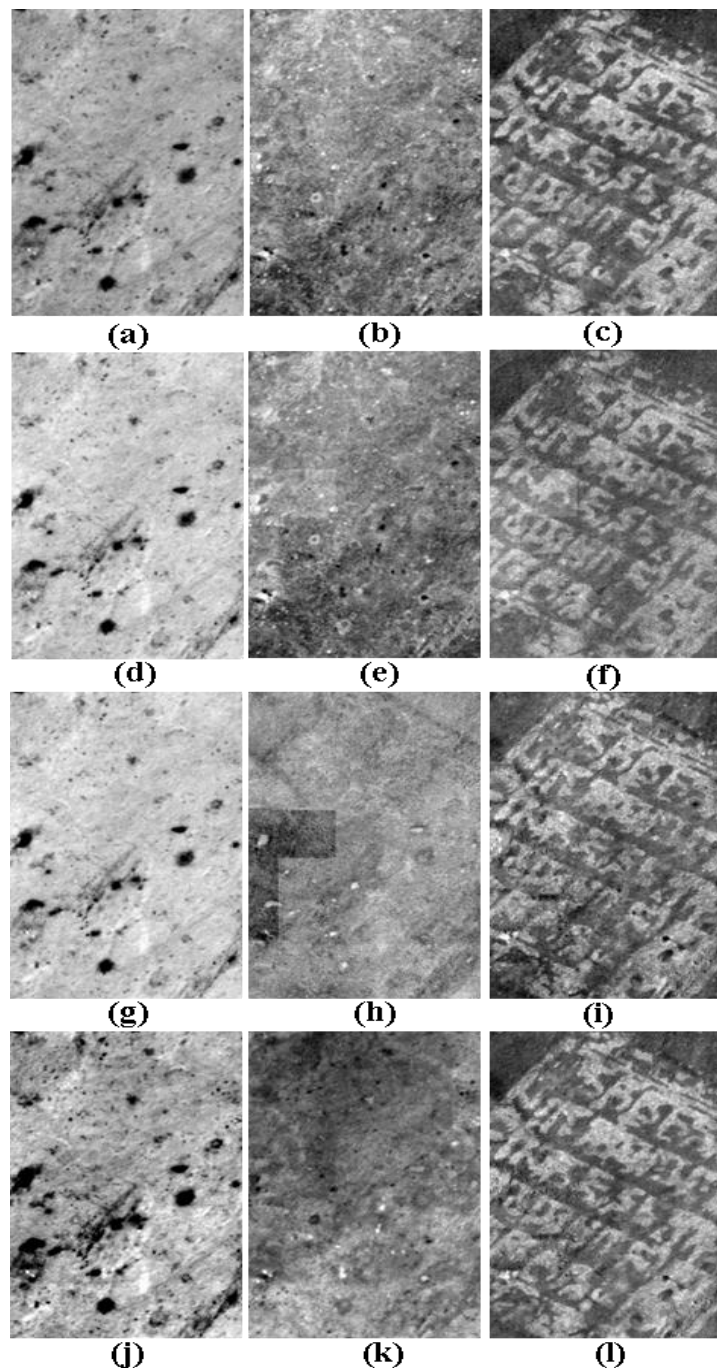


Figure 3-10 Independent Components obtained from the application of ICA on (a-c) ten spectral bands of PRISMS system, (d-f) red (R), green (G) and blue (B) spectral bands derived from PRISMS system, (g-i) blue (B), green (G) and NIR (880 nm) spectral bands and (j-l) violet (400 nm), green (G) and NIR (880 nm) bands collected from an area that contains faded writings.

The application of PCA and ICA on the spectral images of UV (400 nm), green (G) and IR (800 nm) has been examined in cases with different hidden information and of different nature. The fact that the combination of these three spectral bands is so effective can be explained from the fact that the spectral bands used are not in close

spectral positions. Therefore, the information that they contain is highly uncorrelated [30], promoting the efficient operation of the component analytical methods.

### *3.1.3.5 Application of BSS statistical methods on OCT data*

The application of BBS statistical methods, both PCA and ICA, on OCT data was also investigated. The application of both methods on OCT data collected from an area with drawings in different depths gave very interesting results, as it provided a visualization of their difference in depth. Figure 3-11 shows the results of PCA, with the corresponding ICA giving similar results (not shown). Figure 3-11d and Figure 3-11c illustrate the average over a range of OCT depth slides close to the surface and below that respectively. The presence of the shadow of the final drawings cannot be avoided in the examination of areas below the paint surface. The first PCA image revealed the whole set of drawing at once (Figure 3-11d), while the second PCA image showed only the final sketches (Figure 3-11e). Interestingly, the fourth PCA (Figure 3-11f) revealed all the drawings but also distinguished them from each other (final sketches in grey colour) highlighting that their differences which stem from the different level they have been applied.

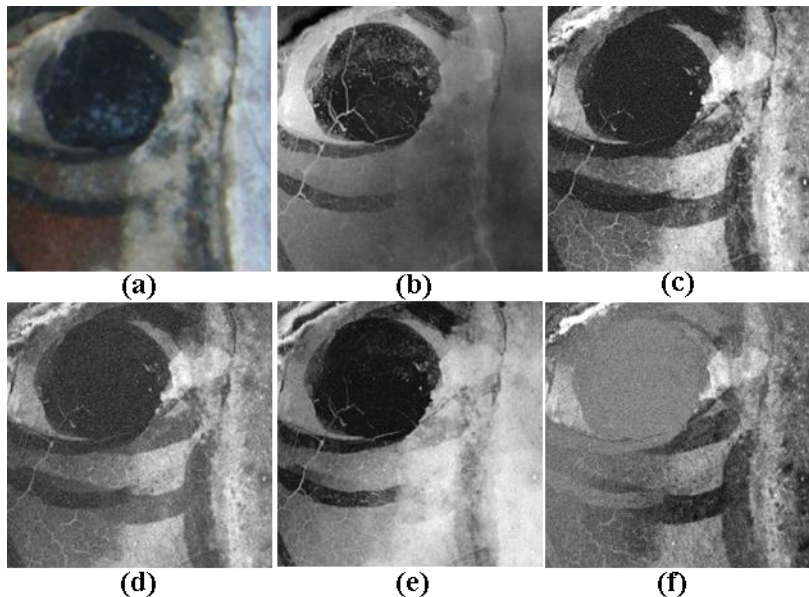


Figure 3-11 (a) Colour image derived from PRISMS data; averages of a 930nm OCT in-depth slices (b) close to and (c) below the paint surface and (d-f) first, second and fourth PCA images resulted from the application of PCA on the ten spectral images of PRISMS system

### **3.1.4 Summary**

The application of BSS methods, PCA and ICA, on the PRISMS spectral imaging data was proven to enable the automatic revealing of information that is not obvious upon visual observation, without the need of any prior treatment of the data. Moreover, the application of these BSS methods enabled the revealing of information that was not shown in any of the individual spectral bands. With regards to the application of PCA, the use of the correlation matrix of the original spectral matrix is proposed, as there are instances in which the use of covariance matrix results to the separation of the information in two PCA images. Moreover, ICA seemed to separate the revealed information (e.g. separation of drawings from morphological information of the substrate), with this characteristic being sometimes a limitation. Consequently, their complementary use is proposed. Moreover, investigation of the application of the BSS methods on different sets of reduced spectral bands, including the combinations that are widely used, showed that RGB and IGB set can indicate the presence of hidden information, with the quality of their results however not being adequately good. Further examination showed that the application of PCA and ICA methods on spectral images collected in the near-UV (400 nm), green (G) and IR (880 nm) bands revealed the hidden information in all the different analysed examples, with the quality of the extracted results being similarly good to the ones obtained using the whole ten spectral imaging dataset. This can be explained by the fact that both the PCA and ICA methods are based on the lack of correlation between the input data. The spread of these three bands in the spectral range covers the desired requirement for the most uncorrelated data among the available spectral images. Finally, the application of BSS methods on OCT data showed promising results on the automatic separation of the information located in different depths.

## **3.2 Development of method for the automatic and unsupervised clustering of spectral information obtained by spectral imaging**

### **3.2.1 Introduction**

The ability of the PRISMS system for automatic spectral imaging of large painting surfaces in high spatial resolution, results in the acquisition of large scale ‘pixel-level’ spectral information. Although the analysis of large statistical sample is necessary for the extraction of representative results about the painting materials of an artwork, the large scale data result in time-consuming analytical procedures. Therefore, the development of methods that would speed up the processing procedure, without affecting the quality of the analysis is necessary. Clustering methods have been widely applied for the minimization of the dimensionality or the more efficient implementation of spectral imaging data in various fields, ranging from remote sensing [38]–[40] to medicine [41]. The automatic application of the clustering methods on large scale data has not been reported. With regards to the identification of pigments of large scale painting surfaces, the minimization of the areas that should be analysed in detail in order to obtain representative results is necessary. The spectral information in the VIS/NIR regime is indicative of the pigment composition. Therefore, the classification of the spectral information collected from a painting in this regime is representative of the distribution of the different pigment combinations on it. In this section, the development of a totally automatic way for the classification of the spectral information of large scale data using clustering statistical methods is presented.

In the field of cultural heritage, the first attempt for the automatic classification of the various painted areas on paintings and its further visualization were performed using PCA [41]. Given that PCA is based on the maximization of the spectral variance, the information that its application provides determines some inherent structure in the spectral data that may be interpreted in chemical terms and therefore can reveal similarities in the pigment composition. However, one important limitation of this method is its strong dependence on noise characteristics of the analysed spectral images. More specifically, when noise variance is larger than signal variance in one band or when the noise is not uniformly distributed between each band, PCA does not guarantee that the image quality decreases for principal components with lower ranking. The application of clustering methods on spectral imaging data collected from paintings has

been illustrated on a limited number of studies conducted on the identification of pigments [27], [42], [43], binding media [44] and substrates [45]. The clustering protocol followed in most of these studies suggests the application of supervised clustering methods, using either the ‘matched tuned filter’ or the ‘spectral angle mapper’ algorithm. In the classification of spectral imaging data, the methods that need a set of reference spectra (also called endmembers) according to which the classification of all other pixels in the image is performed are called supervised. In these cases, the reference spectra are determined from the operator. More specifically, spectral libraries containing the spectra of a wide range of pigments and mixtures of them can be used as the reference database. However, the production of a reference library that can cover all the possible painting mixtures is impossible. Moreover, variations in the concentrations of the various pigments and the binding medium result in spectral differences (see section 2.2), making the construction of a complete database even more difficult. This limitation is becoming more intense in the case of the examination of artworks containing faded or degraded paint layers. The pre-treating methods that are proposed for the reference spectral database directly from the analysed artwork [42] require the interference of the operation in several stages of the procedure, making their application on the automatic processing of the large scale data impossible. The ‘spectral angle mapper’ algorithm treats the spectra as vectors in a space with dimensionality equal to the number of spectral bands, with the classification of the pixels being performed by comparing the angle between the vector of the reference spectrum and the vector of each pixel in the spectral space. More specifically, the classification of the pixels is determined by an angle threshold that is also specified from the user. When the vector of a pixel has an angular distance less than the threshold from the vector of a reference spectrum it gets classified, while pixels further away from the specified maximum angle threshold are not classified. It has to be noticed that the ‘spectral angle mapper’ algorithm is based on the relative reflectance of the pixels. This absence of sensitivity in spectral intensity is beneficial in the field of remote sensing, as the illumination conditions are not controlled and therefore any observed shift of the spectral feature to higher, or lower, intensities is related to the lighting variations, which is unrelated to the material information. However, in spectral imaging of cultural heritage objects, the illumination conditions are controlled and remain stable during the imaging procedure, without affecting the intensity of the resulting spectral features. On the other hand, the spectral contribution of painting materials such as white pigments or black ink in the

mixture is appearing as a shift of the spectral feature to higher or lower position. Therefore, the clustering according to the relative reflectance (that methods such as ‘spectral angle mapper’ provide) can result in misleading conclusions. The clustering using the ‘matched tuned filter’ algorithm is based on the maximization of the response of a known reference spectrum but also the suppression of the response of the composite unknown background, matching therefore the known signature. Although ‘matched tuned filter’ is an algorithm that decreases the computational time, it has been reported to give misclassification of pixels that contain rare spectral information. Salerno et al [27] suggests the application of an unsupervised statistical method, the Kohonen Self-Organising Mapping (SOM), for the classification of the painted areas of an easel painting. However, given that the clustering was performed on a set of data of images collected in four broad spectral bands (i.e. RGB and near-IR), the spectral resolution was not enough to distinguish the various pigments from each other.

In this section, the development of a method that overcomes all these limitations providing automatic and unsupervised clustering of the PRISMS spectral imaging data collected from large scale painting surfaces, is presented.

### **3.2.2 Spectral Imaging Data & Developed Clustering Algorithm**

#### **Spectral Imaging data**

For the developments of the method for the automatic and unsupervised clustering method, spectral imaging data collected from the V&A and RHS watercolour paintings was used. Moreover, in order to test our method on very large spectral imaging dataset, large scale PRISMS spectral imaging data collected from the murals of cave 465 from Mogao complex were used as well.

#### **Clustering Algorithm**

The code was written in R by Dr. Golnaz Shahtahmassebi, using the ‘Self-Organising Map’ (SOM) clustering algorithm.

Self-organising map (SOM) is a clustering method that belongs to the group of artificial neural network methods that is trained using unsupervised learning to produce the clustering maps. The difference between SOMs and other artificial neural networks is

that they apply ‘competitive learning’, in which the output neurons compete among themselves to be activated from the input information space. For the implementation of this competition, the lateral inhibition connections between the neurons are necessary. The principal aim of application of SOM on spectral imaging data is to transform the incoming spectral information into a two dimensional discrete map in a topographically ordered fashion. The principle of the formation of topographic maps is that the spatial location of an output neuron in a topographic map corresponds to a particular feature drawn from the input space. Therefore, the SOM is formed by placing neurons at the nodes of a two dimensional lattice, with their selectively tuning to various input patterns being performed through the competitive learning. The self-organization procedure consists of four main processes: the initialization, the competitive, the cooperative and the adaptive.

In the initialization process all the connection weights are initialized with small random values. Considering that the input space is N-dimensional, the input patterns can be written as  $\vec{x} = \{x_1, x_2, \dots, x_N\}$  and the connection weights between the input units i and the neurons j can respectively be written as  $\vec{w}_j = \{w_{ji}\}$ , where  $j = 1, \dots, D$  and  $i = 1, \dots, N$ . In the competitive process, for each of the input patterns, the neurons of the discrete two dimensional lattice compute their respective values of a discriminant function. This function can be defined as a squared Euclidean distance between the input vector  $\vec{x}$  and the weight vector  $\vec{w}_j$  for each neuron j:

$$d_j(\vec{x}) = \sum_{i=1}^N (x_i - w_{ji})^2$$

Equation 3-3

with the winning vector therefore being the one that comes closest to the input vector. As the winning vector belongs to a network, it is then determining the spatial location of a topological neighbourhood of excited neurons, providing the basis for cooperation among neighbouring neurons. This topological neighbourhood in SOM is defined in such a way that has its maximum at the winning neuron, being symmetric about it, decreasing monotonically to zero as the distance goes to infinity and also being independent from the location of the winning neuron on the lattice. The importance of this topological neighbourhood is that, in addition to the weight of the winning neuron, the weights of its neighbouring neurons are updated as well. The adaptive process

includes the update of the learning weights that results to the move of the weight vector of the winning neuron ( $\vec{w}_j$ ) and its neighbouring neurons towards the input vector ( $\vec{x}$ ), with the procedure of updating being repeated leading to their topological ordering. The competitive, cooperation and adaptation processes are being continuously repeated until the clustering map stops changing.

Figure 3-12 gives a brief description of the method that we developed for the automatic and unsupervised clustering of the spectral information deriving from large scale spectral imaging data. The whole procedure consists of three main steps: the unsupervised clustering of the reference spectral cube, the automated analysis of the large scale spectral images and the summary and the resulting final clustering maps, with a detailed description of each step following.

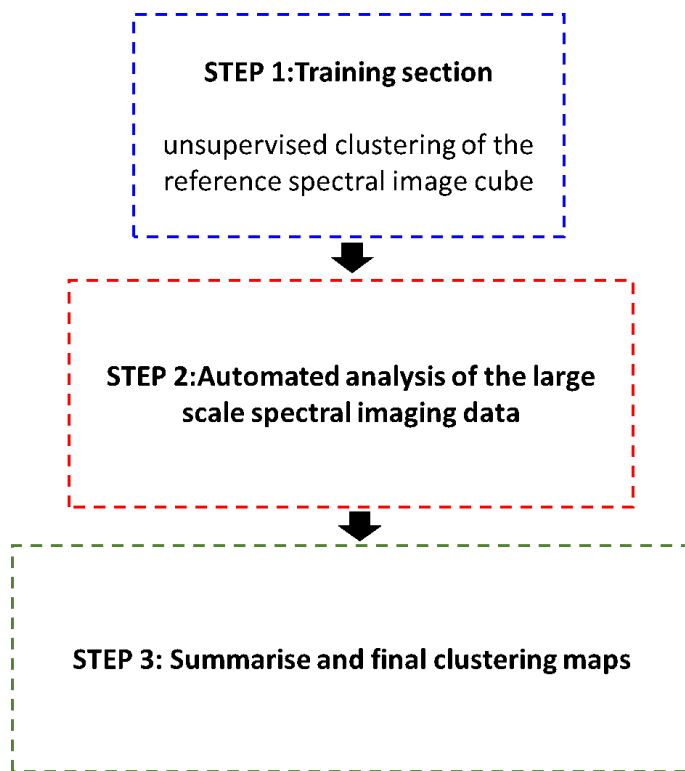


Figure 3-12 Diagram describing the method for the automatic and unsupervised clustering of large scale spectral imaging data

### Step 1: Training Section: Unsupervised clustering of the reference spectral imaging set

Given that the individual spectral imaging data consist of a large number of pixels (average image size approximately 1000x1000 pixels), their pixel-by-pixel clustering could result to computational issues. In order to avoid this issue, their dimensionality is decreased by applying unsupervised SOM on them, resulting to their classification into a smaller number of clusters. This set was decided to consist of ninety nine ‘fine’ classes, as it is a number that is both small compared to the initial number of pixels but also larger than the spectral variation that an image collected from any surface less than 100 cm<sup>2</sup> can have, avoiding any loss of spectral information.

Sequentially, unsupervised SOM is applied on these ninety nine ‘fine’ classes, classifying them further into a smaller number N (‘N-clusters’). Given that the database of the clusters is constantly updated, the number of the initial ‘N-clusters’ is not important. Each of the ninety nine ‘fine’ classes is assigned to one of the ‘N-classes’ according to their spectral information. The information about both the mean value of the spectra of each of the ninety nine ‘fine’ classes and the label of the ‘N-cluster’ that it has been assigned to is stored and consists of the reference spectral database.

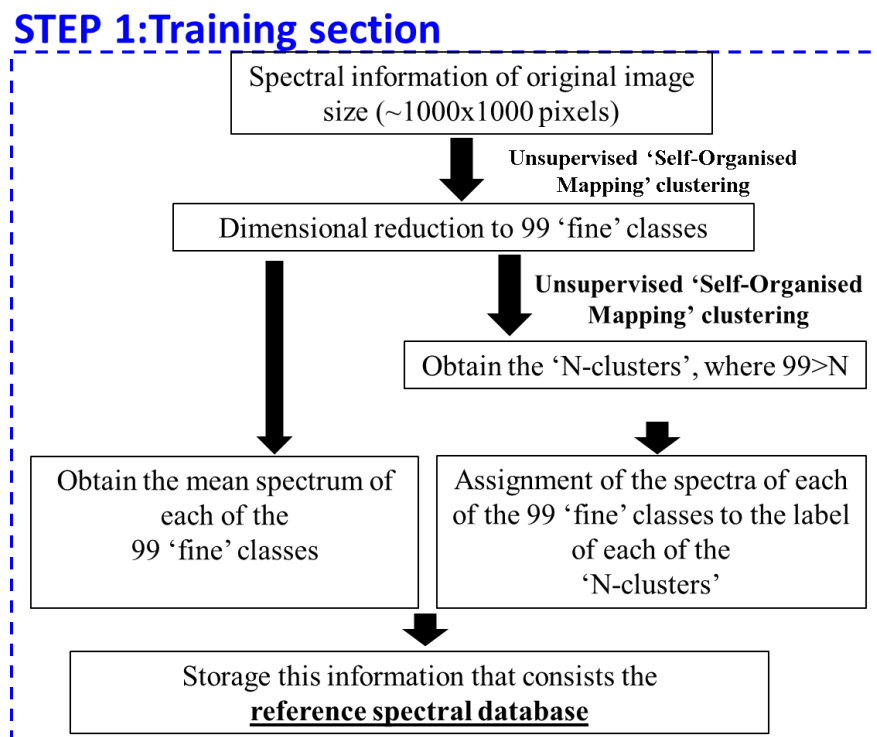


Figure 3-13 Detailed description of the first step of the clustering method which is the training section in which the unsupervised clustering of the reference spectral imaging set that is performed

## Step 2: Automated analysis of the large scale spectral imaging data

This stage consists of a ‘for loop’, that performs the processing described below sequentially for each spectral cube of the large scale spectral imaging set.

For each new spectral cube, the reduction of the large number of pixels in ninety nine ‘fine’ classes using unsupervised SOM is performed, obtaining the average spectral information for each of these classes. This spectral information is used in order to classify these ‘fine’ classes, using this time the SOM in a supervised way, as their clustering is based on the reference ‘N-clusters’, as they arise after the completion of ‘step 1’.

Afterwards, the reference ‘N clusters’ are being mapped on to the original image of the large number of pixels. Based on this mapping, the mean of the spectrum and the standard deviation ( $\sigma$ ) of each ‘N-cluster’ is determined, with the pixels of the original image that are not matching with any of these clusters remaining unclassified.

A final comparison between each pixel of the original image and the mean spectrum of each of these clusters within a range of  $k \cdot \sigma$  (i.e. mean spectrum  $\pm k \cdot \sigma$ ,  $k=1,2,..$ ) is performed, classifying the pixels with similar spectral information. All the pixels that have not been matched with any of the reference ‘N-clusters’ are being saved to a new cluster that is called ‘unclassified’.

Finally, the classification of the pixels that belong to the ‘unclassified’ cluster using unsupervised SOM clustering is performed, obtaining also the mean spectrum of the resulting clusters. Each of the resulting spectra is compared with the spectral information of pixels of the original image that were previously classified in one of the ‘N-clusters’. In case that there is spectral similarity, the pixel is classified to the reference cluster, otherwise a new cluster is created and added to the reference ‘N-clusters’ database. The updated reference database, that after the processing of each image cube becomes ‘(N+w)-clusters’ with  $w=0,1,2,..$  is the one that will be used as the reference clustering dataset for the classification of the next image cube. With the completion of the processing of the whole large scale dataset, a list that contains the ninety nine ‘fine’ classes of all the processed image cubes, as well as the label of the cluster from the resulting ‘(N+w)-clusters’ set that each of them is assigned to is obtained.

## STEP 2: Automated analysis of the large scale spectral imaging data

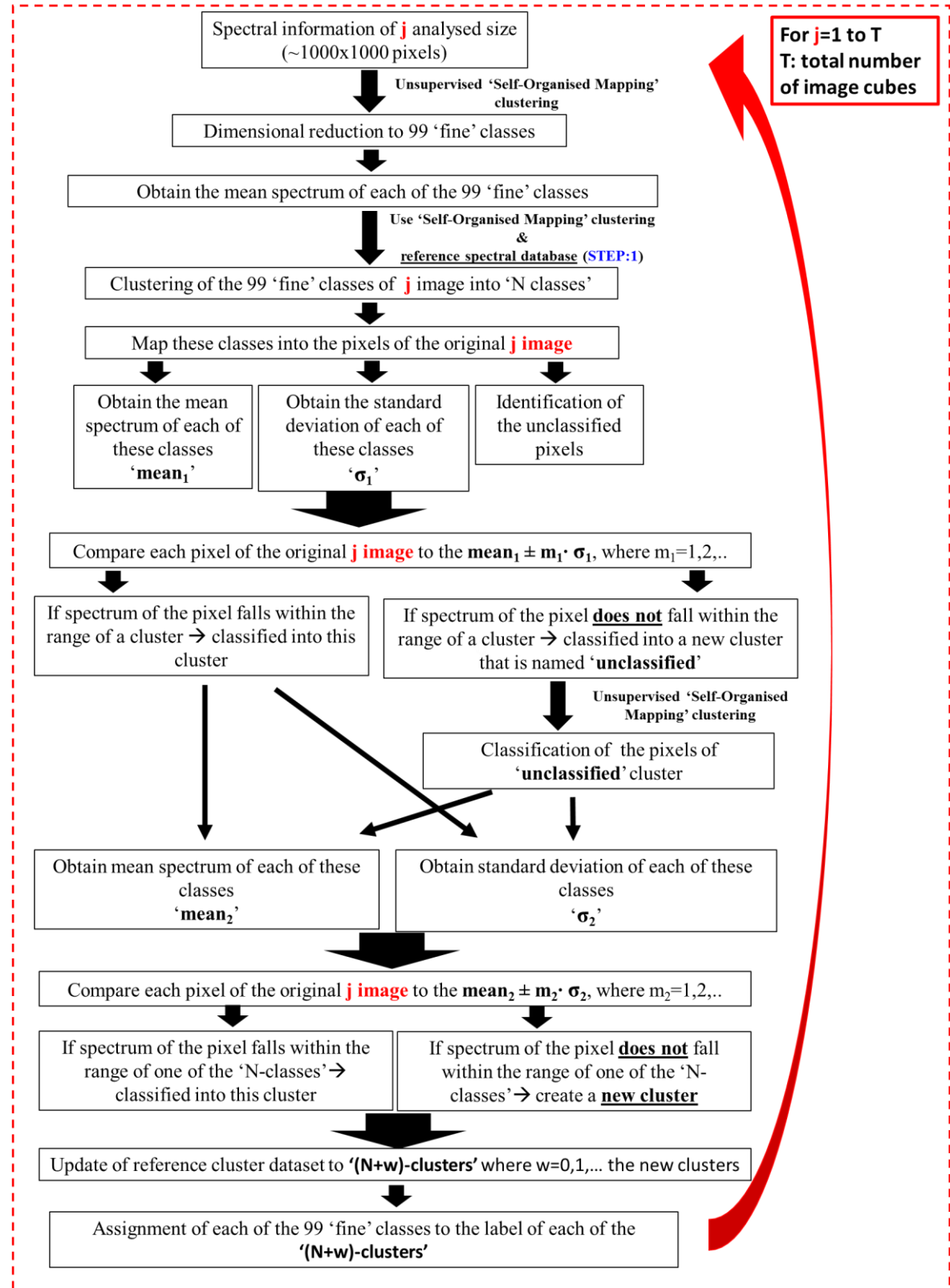


Figure 3-14 Detailed description of the second step of the clustering method which contains the automated analysis of the large scale spectral imaging data

### Step 3: Summarise and final clustering maps

In the final stage, the uniqueness of the spectral information of the updated clusters as they arise after the completion of the process of the large scale spectral imaging dataset is checked by comparing each of these clusters to the others. If two clusters match, then they are merged, otherwise they remain as individual clusters. The final clusters are then mapped on the set of the original images, providing the final ‘clustering maps’.

### **STEP 3: Summary and final clustering maps**

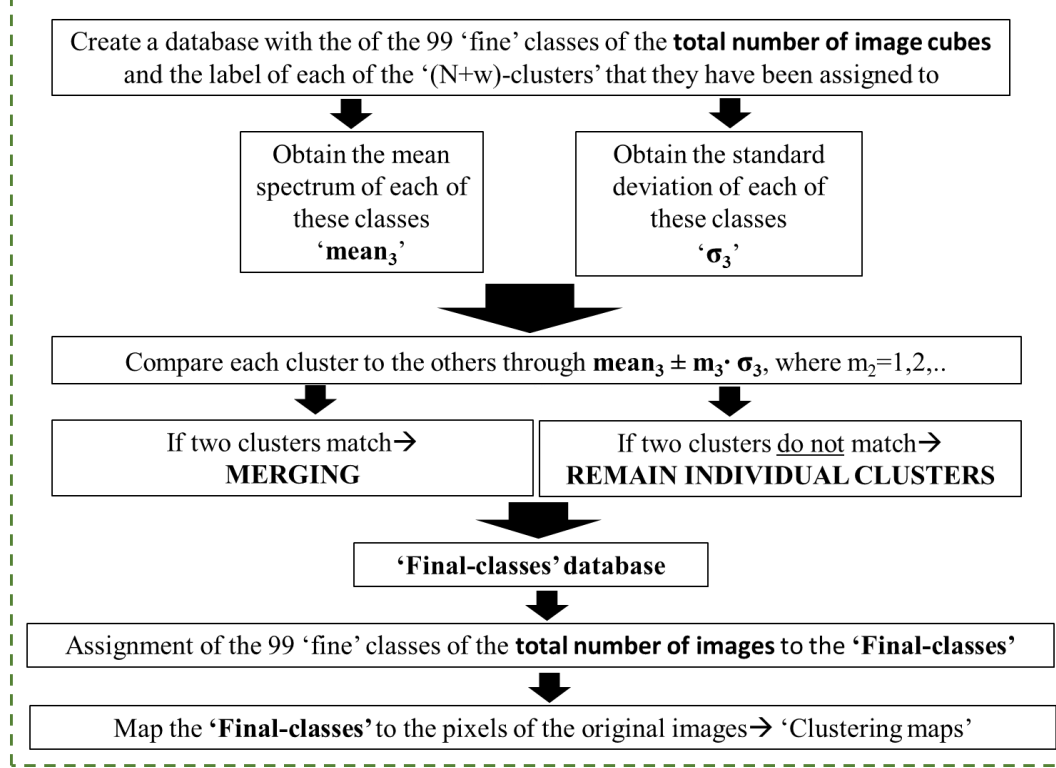


Figure 3-15 Detailed description of the third step of the clustering method which summarises the clustering information and obtain of the final clustering maps

### **3.2.3 Results**

The developed method for the automatic and unsupervised spectral clustering of large scale data was tested using spectral imaging data collected from both the watercolour painting collections of V&A museum and RHS and the murals of cave 465 of Mogao complex. Figure 3-16 illustrates indicative results from the preliminary analysis of the spectral images collected from a watercolour painting of the V&A collection for the spectral classification of the different coloured areas. Given that the spectral imaging data were processed at the same time, the areas with similar spectral features are classified together, with this classification being visualized using the same colour for each cluster. The whole procedure was initialised using a reference spectral cube that did not contain the total spectral information of the analysed dataset. However, this method provides the ability to update the reference database, by adding clusters whenever the spectral information of a pixel does not belong to any of the existing clusters, which results in a final database that describes effectively the spectral variations of the large scale data.

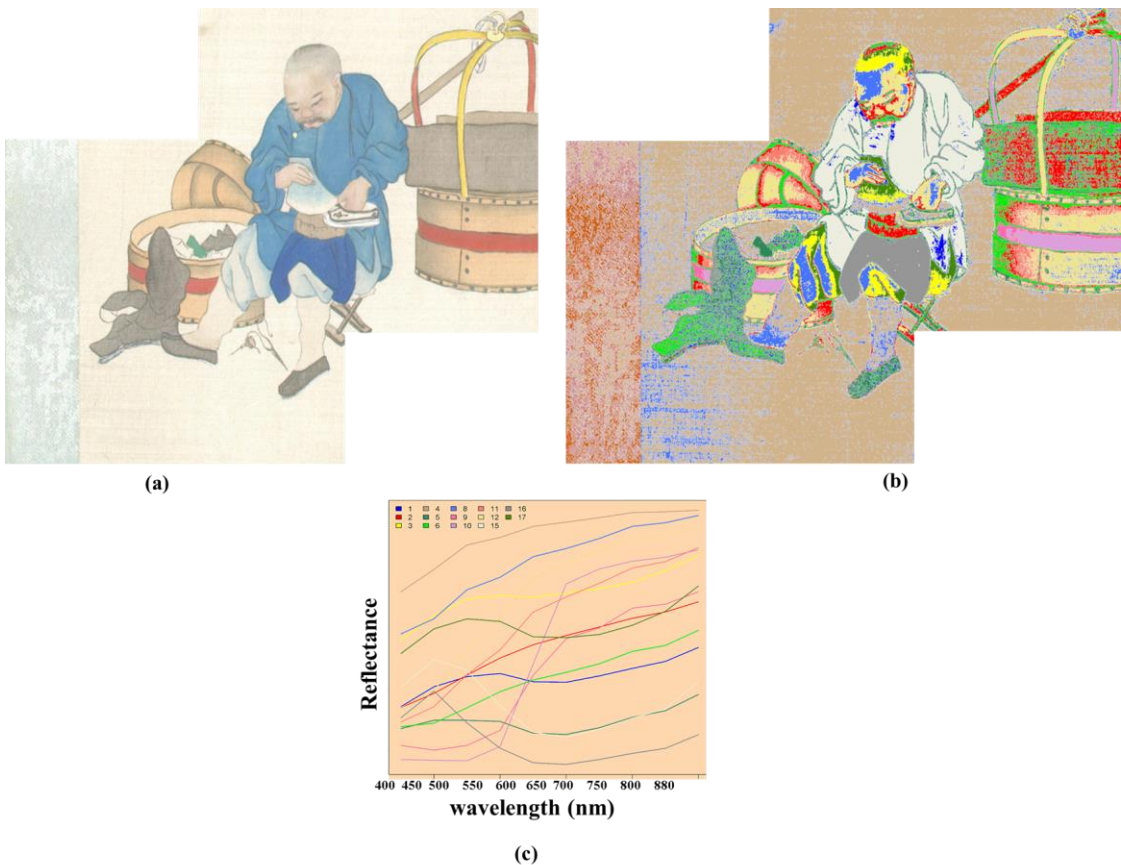


Figure 3-16 (a) 2x2 colour imaging as it derives from PRISMS data collected from the watercolour painting No 7790-18 (V&A collection and (b) the corresponding clustering map; and (c) the final updated reference spectral database that gives the total spectral variations of the analysed spectral data.

It is worth highlighting that the developed clustering method is sensitive enough to enable the distinction between the different hues of the same colour. Figure 3-17 shows the results of the preliminary examination of areas from watercolour painting from V&A and RHS that contain various hues of green and red. The differences in the colour are indicative of differences either in the pigment composition of the paint mixtures or in the concentration of the pigments, therefore, resulting in variations in the spectral features. The sensitivity of the method for classification according to these fine variations provides a precise clustering of the different coloured areas.

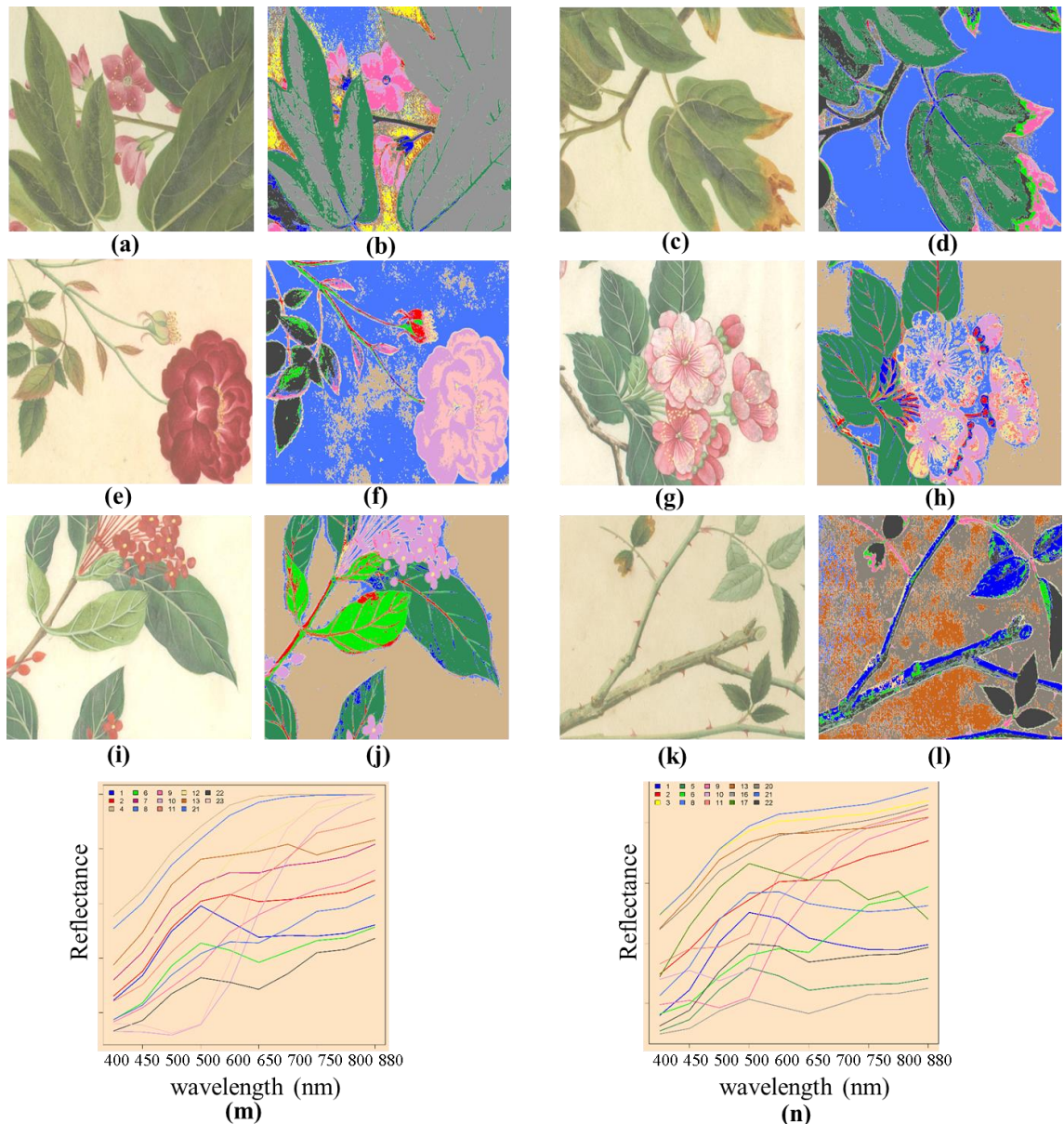


Figure 3-17 (a) Colour image derived from PRISMS data collected from the watercolour painting no.36335 (RHS collection) and (b) the corresponding clustering map; (c) Colour image derived from PRISMS data collected from the watercolour painting no.36335 (RHS collection) and (d) the corresponding clustering map; (e) Colour image derived from PRISMS data collected from the watercolour painting no.60528 (RHS collection) and (f) the corresponding clustering map; (g) Colour image derived from PRISMS data collected from the watercolour painting no. 290-1886 (V&A collection) and (h) the corresponding clustering map; (i) Coloured image derived from PRISMS data collected from the watercolour painting no. 291-1886 (V&A collection) and (j) the corresponding clustering map; (k) Colour image derived from PRISMS data collected from the watercolour painting no.60528 (RHS collection) and (l) the corresponding clustering map; (m-n) the final updated reference spectral database that gives the total spectral variations of the analysed spectral data

The application of the clustering method on the spectral images collected using PRISMS system from the murals of cave 465 of the Mogao complex, provided another example for the examination of the accuracy of our method on processing large scale datasets. Given that the murals of cave 465 are exposed to the environmental conditions, the classification of the spectral information was more complicated due to the spectral contribution of their weathering/degradation. However, the application of clustering on a large painting area of the ceiling gave good results, enabling the spectral classification of large areas. Figure 3-18 illustrated the spectral classification of 2x6 scanned area of the ceiling that enables the visualization of the pigment variations, indicating also their deterioration.

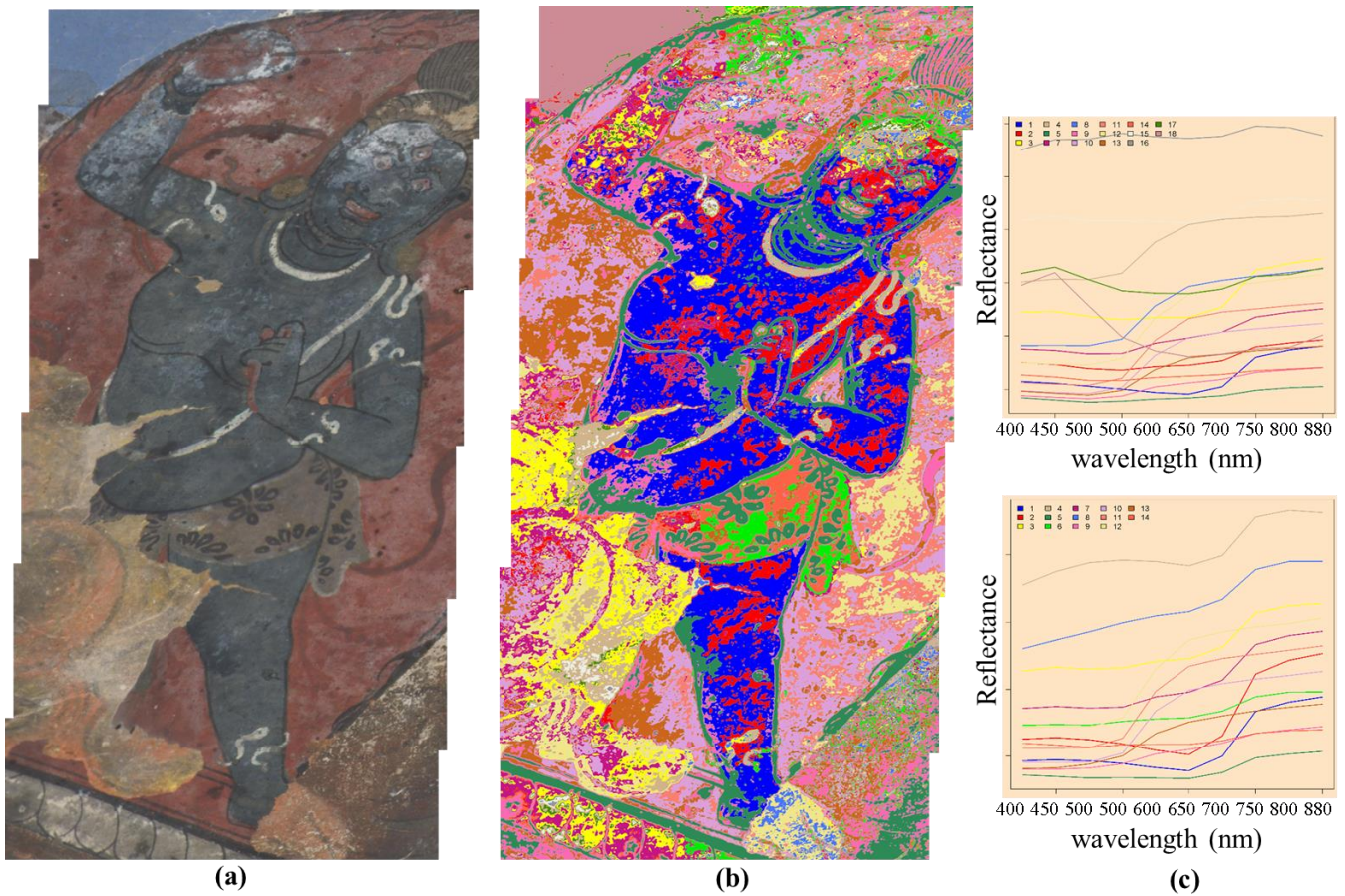


Figure 3-18 2x6 colour imaging as it derives from PRISMS data collected from the murals of the ceiling of cave 465 in Mogao complex and (b) the corresponding clustering map; (c) the final updated reference spectral database that gives the total spectral variations of the analysed spectral data.

The ability to classify the spectral information collected from unreachable areas can be very useful for the identification of their pigment composition. More specifically, the extension of the clustering analysis to areas located on the ground level can enable the

automatic finding of similarities in the pigment composition to areas that can be further analysed in details.

### 3.2.4 Summary

In this section, the development of a method for the automatic clustering of the spectral information obtained from a large scale spectral imaging dataset, without the interference of the operator, was presented. The Self-Organised Mapper (SOM) clustering algorithm was used for both unsupervised clustering of the reference spectral set and sequential clustering of the rest of the large spectral imaging dataset. This method enabled the updating of the cluster database after the processing of each image cube, with the uniqueness of each cluster confirmed before the drawing of the final clustering maps. The application of clustering for the preliminary processing of both large number of watercolour paintings from V&A and RHS collection and the large scale data collected from the murals of cave 465 of Mogao complex gave good results, classifying the areas of the same spectra and narrowing the areas that should be analysed in detail into a manageable number. In the case of the examination of the murals of cave 465, the classification of the painting layers of unreachable areas (e.g. murals on the ceiling) with areas located on the ground level, that have been analysed following a multi-modal and non-invasive approach, would enable the extension of the detailed results about the identification of their pigment composition to the unreachable areas with relative certainty.



## **Chapter 4:**

### **Holistic approach of the non-invasive analysis of painting materials**

The holistic examination of works of art is very important in order to draw conclusions about their history. Given that there is no analytical technique that can individually provide the whole information about the materials and the methods applied on an artwork, the complementary use of a range of techniques is necessary. For a successful analysis, the selection of non-invasive techniques that complement each other in terms of provided information should be made[6]. The information obtained from a technique depends on the principles of its operation, with the special features of the instrumentation used being also an important parameter that can affect the extracted results [6]. Given the above, it is clear that the operational principles and/or the special features of the various instrumentation used define the strengths and the limitations of the individual techniques, therefore, their in depth investigation is necessary. Furthermore, it is important to investigate thoroughly the abilities that the complementary use of the different non-invasive techniques provides on the effective analysis of artworks by overcoming the limitations and combining the strengths that they have individually [6]. In the context of this study, the analysed artworks vary in terms of material composition (e.g. pigments, binding media and substrate) and environmental conditions (e.g. paintings stored in museum storage and murals exposed to the desert environment), offering a sample of heterogeneous painting systems. Moreover, large scale data were collected from the painted areas of the various artworks, providing a large statistical sample, thus enabling the extraction of accurate results about the complementarity of the various non-invasive analytical techniques on the analysis of various painting systems. In this chapter, the complementary use of a series of non-invasive imaging and spectroscopic analytical techniques for the holistic examination of various artworks is illustrated.

## **4.1 Multi-modal approach for the identification of pigments**

### **4.1.1 Introduction**

The identification of the pigments of an artwork provides very important information about its history, as different pigments and combinations of them have been used in different periods of time across the world. The last decades, a lot of non-invasive analytical systems have been developed and complementary used for the examination of objects of cultural heritage. Bouchard et al [46] presented the combined use of micro-FTIR and micro-Raman spectroscopy for the analysis of samples taken from modern paintings. Raman was proven more effective in the identification of both inorganic and organic pigments, while micro-FTIR failed in the identification of almost every inorganic pigment. Rosi et al [47], introduced the complimentary use of XRF with near and mid-FTIR spectroscopy and multivariate statistical analysis (PCA), for the identification of inorganic pigments on modern paintings. In this study, the identification of lead, iron and cobalt-containing pigments was achieved combining the elemental information, provided from the XRF spectroscopy, with the detection of specific functional groups that are correlated with these pigments using FTIR spectroscopy. Furthermore, the application of PCA on the XRF results enabled the chemical analysis of areas consisting of mixtures of pigments. Studies on the examination of leather screen and illuminated title pages, using a combination of non-invasive techniques (namely the Raman and XRF spectroscopy), with the non-destructive one (namely the SEM-EDX), illustrate the limitation that Raman technique faces when degraded varnish layer is present, due to its high fluorescence [5]. Westlake et al. [48] combined Laser Induced Breakdown Spectroscopy (LIBS), which is a micro-destructive technique suitable for *in situ* and depth-resolved elemental identification, with Raman spectroscopy (786 nm excitation) for the pigment identification on Minoan mural fragments. In this study, in addition to the overwhelm of the Raman signal by the fluorescence, it was highlighted that the excitation at 785 nm is not suitable for the identification of copper-containing pigments. Reflectance spectral information, usually obtained by spectral imaging, has been used for the mapping of the spatial distribution of the pigments with their identification, however, being performed using other spectroscopic techniques (e.g. XRF and Raman spectroscopy) [37][38]. In instances where reflectance spectroscopic measurements have been used for the identification of

pigments, their interpretation is performed by comparison of the analysed spectra to reference mock-ups or databases [29]. Although this interpretation can provide accurate results in the case of identification of single pigments, it is possible to fail in the analysis of areas consisting of a combination of pigments. This is the reason why it is commonly believed that, while reflectance spectroscopy can assist the identification of single pigments, it is less effective for the identification of mixtures of pigments [11].

In the previous chapter the development of a method for the effective clustering of large scale spectra data was presented (see section 3.2). After the classification of the large scale spectral information, which were collected from the various painted areas, in a manageable number of spectrally representative clusters, a more detailed analysis of their pigment composition using a combination of non-invasive analytical techniques is necessary. In the context of this study, the combined use of three non-invasive analytical techniques, FORS, XRF and Raman spectroscopy, was decided for the identification of pigments on different painting systems. Additionally to the fact that these techniques are among the most suitable non-invasive techniques for identification of pigments, the availability of portable equipment enables their use for *in situ* analysis. Moreover, given their differences regarding both; the principles that their analysis is based on and their special features (e.g. spot size and spectral resolution), the individual techniques provide different information but also face different detection limitations. This section illustrates, the limitations that each of these analytical techniques faces and how its combined application with the others can overcome them.

## **4.1.2 The use of a multi modal analytical approach in order to overcome limitations that the individual non-invasive analytical techniques face**

### *4.1.2.1 FORS limitations on the identification of a handful of pigments and dyes*

High resolution reflectance spectroscopy, in combination with the KM method (see section 2.2), enables the identification of most of the pigments as well as mixtures of them, however, it faces limitations regarding the identification of a handful of pigments, such as the majority of yellow pigments, and the distinction between the copper (Cu)-containing green pigments.

In the identification of yellow colourants, VIS/NIR reflectance spectroscopy cannot give reliable results (except perhaps yellow ochre) as their reflectance spectra in this regime have an ‘S’ shaped feature with less than 50 nm difference in the position of the points of inflexion. Given that the relative spectral shift is not more than the range of spectral differences in gamboge due to concentration changes (see section 2.2), not reliable identification results can be obtained. On the other hand, as most of the yellow pigments are inorganic compounds with different elemental composition, XRF spectroscopy can provide informative results based on the major, as well as the trace elements detected. However, the identification of organic yellow pigments is particularly challenging as XRF is not generally useful for organics and Raman is often masked by the fluorescence produced due to interaction between the laser and the organic materials. The organic yellow dye gamboge, a colourant traditionally used in East Asia, had been used in the yellow and most of the green areas of the watercolour paintings of the V&A and RHS collections, providing this way a rather large statistical sample for the investigation of the complimentary use of the various non-invasive analytical techniques for its identification. Figure 4-1 illustrates the analysis of a yellow area on a watercolour painting of the V&A collection. XRF spectroscopy detected Pb as the major element (Ca, K and Fe belong to the substrate), while the VIS/NIR reflectance spectrum collected from this area is consistent with a mixture of lead white and gamboge using the KM algorithm. The combined used of gamboge and lead white was finally confirmed by the identification of gamboge and lead white as the yellow and white colourants using Raman spectroscopy.

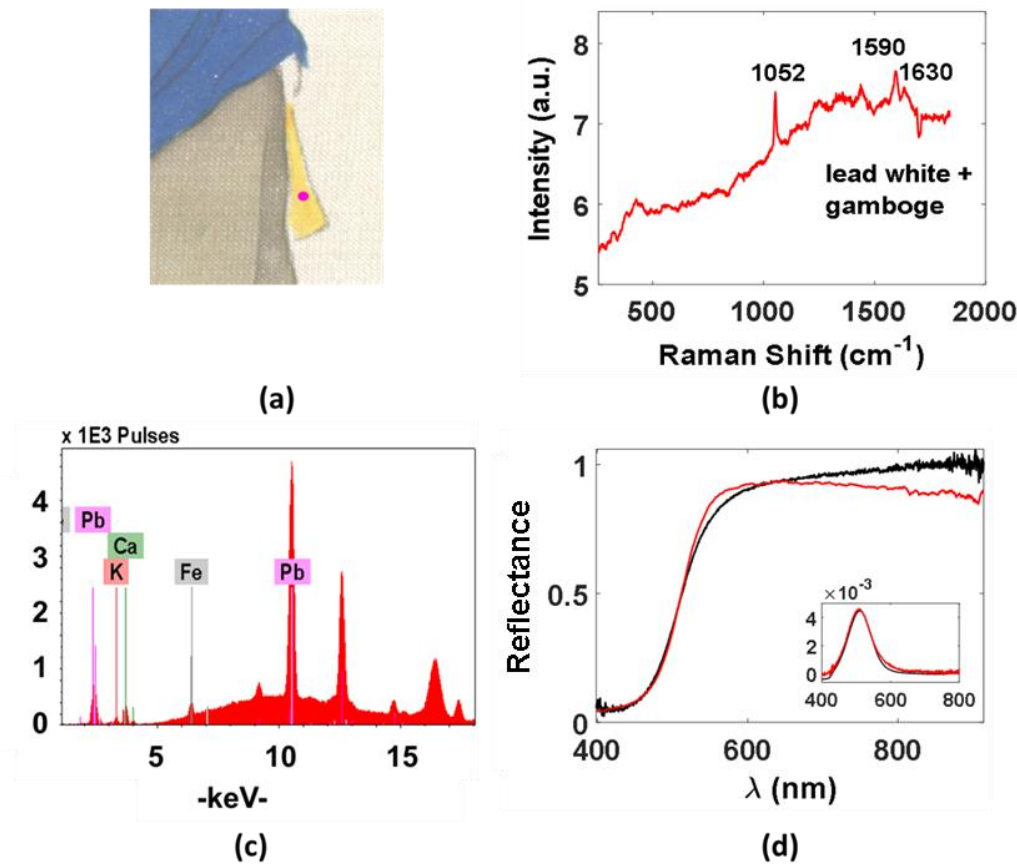


Figure 4-1 (a) Colour image derived from PRISMS data collected from a yellow area of painting no.7790-20 (V&A collection), the magenta dot indicated the analysed area; (b) Raman spectrum of a particle of this area show both lead white and gamboge; (c) XRF spectrum detected Pb as the main element and (d) KM fit (red curve) to VIS/NIR reflectance spectrum (black curve) consistent with a lead white and gamboge mix. The inset shows the corresponding derivatives of the spectra.

It is worth mentioning that Raman spectroscopy not only enables the identification of the pigments but also of their polymorphs as well as the intermediate coexisting phases between them. For the identification of yellow pigments this is becoming particularly interesting in the identification of the As-containing yellow pigments. More specifically, it is known that the formation of pararealgar is related to the photo-degradation of the light exposure of realgar, creating a yellow film usually covering its surface. During the examination of the yellow areas of the watercolour paintings belonging to the V&A collection, a characteristic example of this case was observed. Figure 4-2 shows that XRF detected As and Pb as the major elements, while Raman analysis of yellow particles from this area showed that the yellow colourant is a mixture of two phases, both of which are intermediate between realgar and pararealgar. Realgar and pararealgar along with those intermediate phases coexist in the natural mineral, and therefore, these phases may have been present even in the original painting material. Raman is the only one of the three techniques capable of discriminating between all these phases. It is not

surprising that the FORS spectrum collected from this area was not very well fitted with a standard realgar spectrum with or without the addition of lead white.

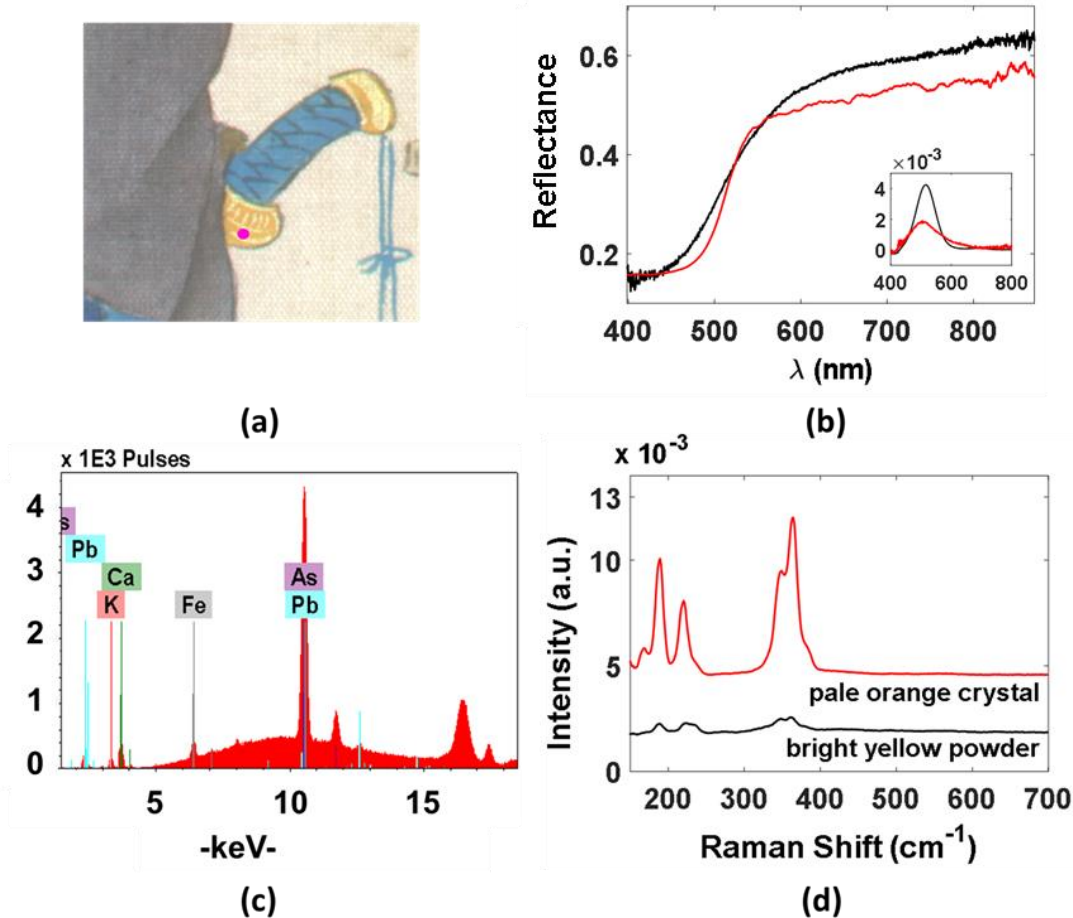


Figure 4-2 (a) Colour image derived from PRISMS data collected from a yellow area on painting no. 7790-8 (V&A collection), the magenta dot indicated the analysed area; (b) KM model fit (red curve) using a combination of realgar and lead white to the measured VIS/NIR reflectance spectrum (black curve); The inset shows the corresponding derivatives of the spectra. (c) XRF spectroscopy detected Pb and As as the main elements; (d) Raman measurement identified a mixture of two phases both of which are intermediate between realgar and pararealgar.

As far as the distinction between the traditional Chinese Cu-containing green pigments, the reflectance spectroscopy cannot provide useful information since they have similar spectral features in both VIS/NIR and near-IR regimes. The elemental information that XRF spectroscopy provides, can only contribute to the distinction between Cu-containing and Cu-chloride pigments. On the other hand, Raman spectroscopy can identify all the different Cu-containing pigments as well as their polymorphs using the appropriate analytical parameters. More specifically, Cu-containing pigments are not a good Raman scatterer upon excitation at 780 nm [11] and therefore its detection is possible only when excitation laser in the VIS regime is used (532 nm).

In the watercolour paintings of both V&A and RHS collections, green leaves are commonly found in the paintings of both collections and therefore provide a significant statistical sample for examining the complementarity of the different analytical techniques on their analysis. FORS spectra collected from the green areas were fitted through the KM algorithm with a combination of malachite, indigo and gamboge (Figure 4-3b). Although reflectance spectroscopy does not provide reliable results about the identification of gamboge, the spectral contribution of both malachite and indigo in the KM fit is clear. Finally, XRF spectroscopy (Figure 4-3c) detected Cu as the major element confirming the presence of a Cu-based pigment (Ca, Ba, K and Fe are elements present on the substrate). Raman spectroscopic measurements (Figure 4-3d), using excitation laser beam at 532 nm, on green and yellow particles identified them as malachite and gamboge respectively.

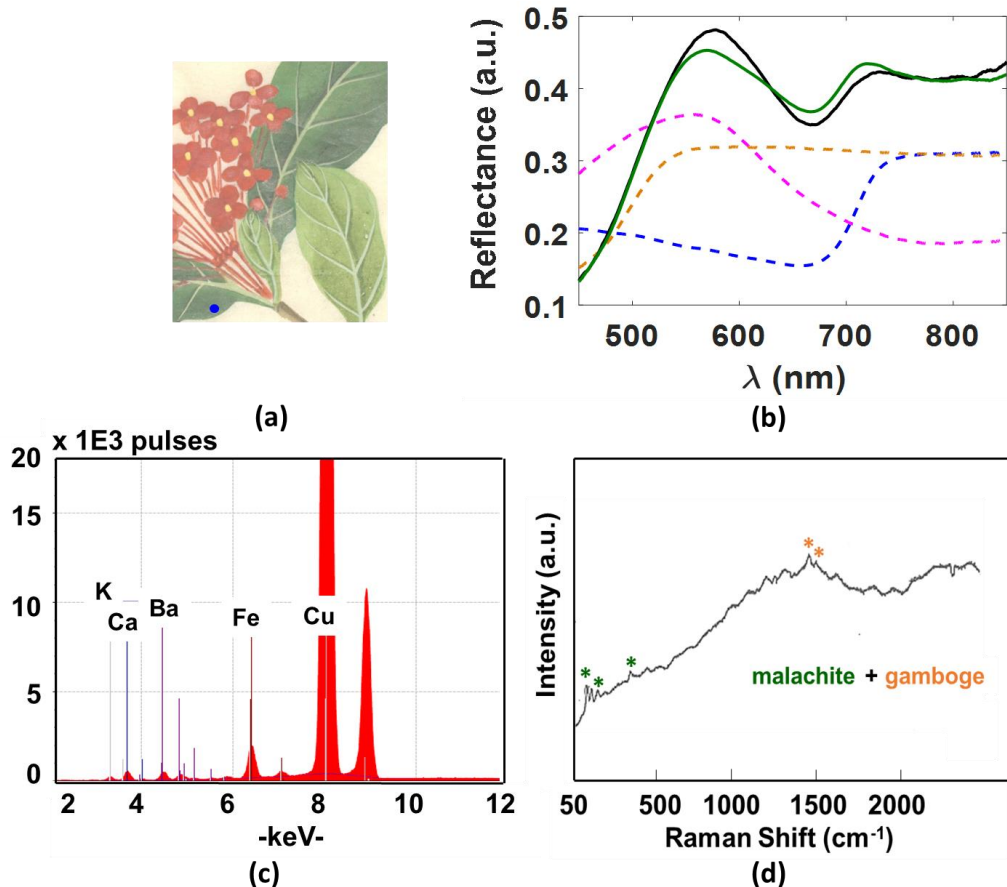


Figure 4-3 (a) Colour image derived from PRISMS data collected from a detail on painting no. 290-1886 (V&A collection), the blue dot indicated the green analysed area; (b) KM model fit (green curve) using a combination of malachite, gamboge, and indigo to the measured VIS/NIR reflectance spectrum (black curve) and the spectra of the KM references: malachite (dotted magenta line), gamboge (dotted orange line) and indigo (dotted blue line); (c) XRF spectrum detected Cu as the major element and (d) Raman measurement for this area detected malachite and gamboge particles

#### *4.1.2.2 Sensitivity of Raman spectroscopy to fluorescence*

The main disadvantage of Raman spectroscopy is its sensitivity to strong fluorescence associated with the interaction between the excitation laser beam and organic materials, such as organic dyes and binders or aged varnishes. This characteristic is problematic as the fluorescing signal emitted from the organic compound(s) can overwhelm the Raman spectrum of the analysed area. The decrease of the spot size of the analytical instrumentation to micro-level (micro-Raman) enables the narrowing of the analysis to the crystal level, avoiding this way the possible spectral contribution of the highly fluorescing environment. However, in the identification of organic dyes, such as red insect dyes, that are highly fluorescent substances by themselves, the drastic contribution of fluorescence cannot be avoided using conventional Raman spectroscopy. Figure 4-4 presents a characteristic example of the analysis of an area containing red organic dye on a watercolour painting of V&A collection. Raman spectroscopic analysis of the area detected vermillion along with a high fluorescence signal suggesting the presence of organic material(s) that was not able to identify though. XRF spectroscopy detected Pb as the main element, with smaller amount of Hg being detected as well (Fe, Ca, K, Ba and S are present to the substrate). On the other hand, high resolution reflectance spectroscopy enabled the clear detection of the characteristic narrow absorption lines of anthraquinone dyes between 500 nm and 600 nm. Moreover, the KM fit to the spectra collected from this area using vermillion, lead white and lac dye references confirmed and supplemented the results of the two other analytical techniques, suggesting that the red area has been painted with a combination of them.

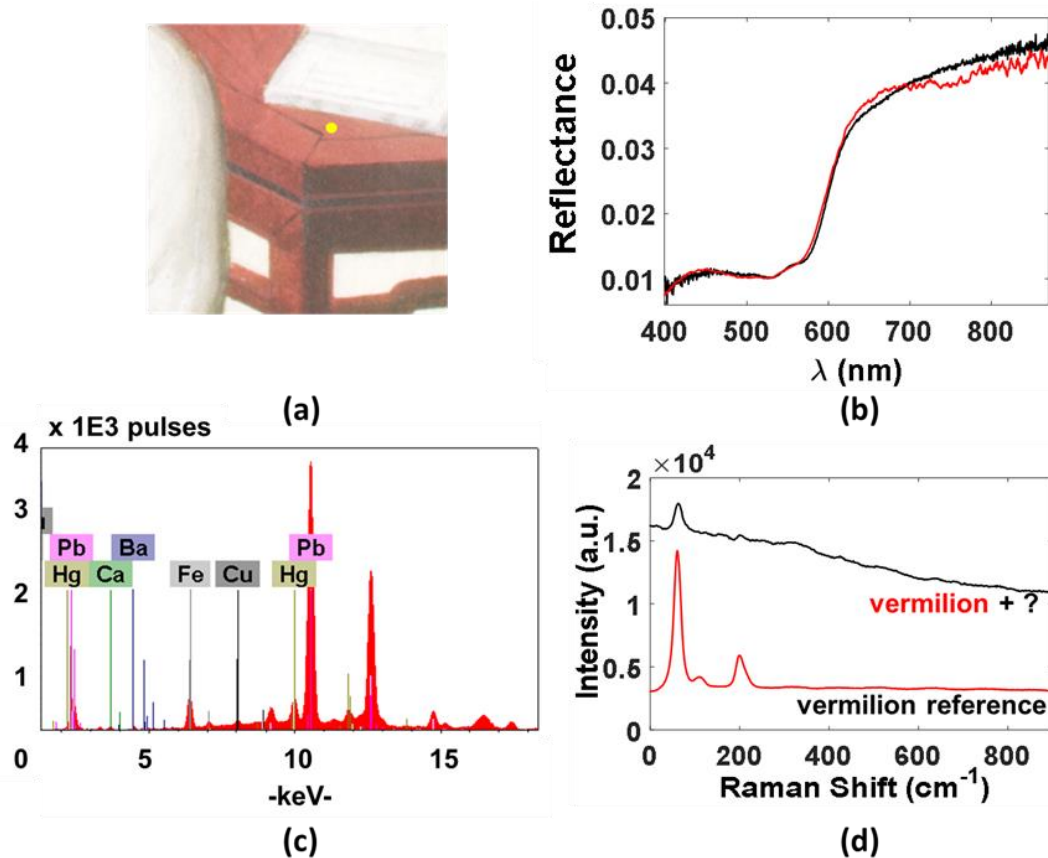
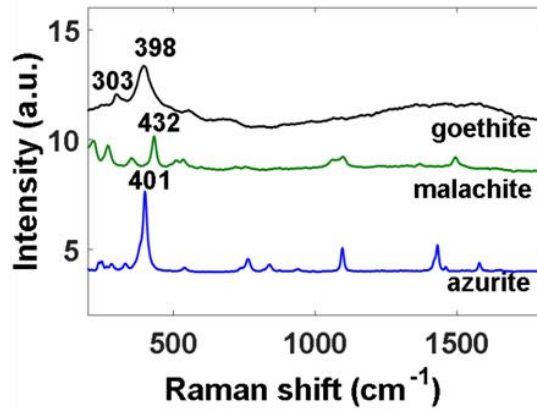
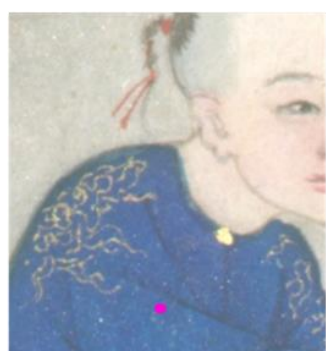


Figure 4-4 (a) Colour image derived from PRISMS data collected from detail on painting no. D82-1886 (V&A collection), the yellow dot indicated the red analysed area; (b) KM fit (red curve) to FORS measurement (black curve) using a mixture of lead white, vermillion and a lac dye; (c) XRF detected mainly Pb and Hg; (d) Raman spectrum (black curve) compared with a standard Raman spectrum of vermillion (red curve) showed that the examined area maybe a mixture of vermillion and a fluorescing material.

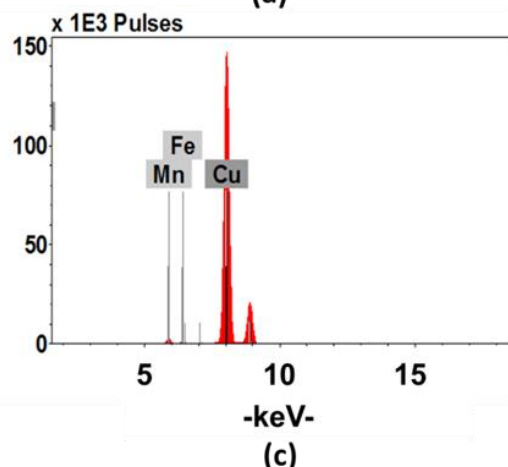
#### 4.1.2.3 Dependence of Raman spectroscopic analysis on spot size

The spot size of the Raman instrumentation used is a factor that can affect significantly the analytical results. The minimization of the spot size has been suggested in order to avoid the possible contribution of the surrounding area. This way helps overcome both issues; the overwhelming of the spectral lines due to presence high fluorescing organic compounds and the possible complication in the interpretation of the collected spectra because of the presence of pigments and/or degradation products that may have overlapping lines. However, the localization of the detection can become also a disadvantage as it can result to no representative, or even false conclusions. This is becoming particularly true when the analysed areas consisting of pigments that have particles of other pigments as impurities. A characteristic example of this limitation can be illustrated through the identification of azurite, a blue Cu-containing pigment that

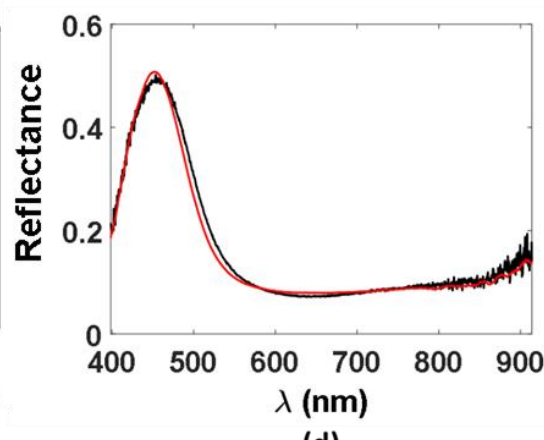
naturally contains malachite and iron oxides (i.e. goethite or hematite) impurities. During the examination of a blue area on one of the V&A watercolour paintings, micro-Raman analysis detected crystals of azurite, malachite and goethite (Figure 4-5b). Although malachite and iron oxides are known as impurities of azurite, they are also minerals widely used as pigments in Asian painting tradition and therefore their presence as compounds of the painting mixture cannot be excluded. Both iron oxides and malachite have a rather distinctive spectrum in the VIS/NIR regime. Therefore the perfect match of the KM fit to the collected from the blue area spectrum using single azurite as reference (Figure 4-5d), confirmed its presence as the blue pigment used, suggesting at the same time that malachite and goethite are present as impurities. The XRF spectroscopic analysis of the same area (Figure 4-5c) showed that the major element is Cu, supporting the identification of azurite, while Fe and Mn were elements detected also on the paper substrate.



(a)



(b)



(c)

(d)

Figure 4-5 a) Colour image derived from PRISMS system from a detail on painting no.7791-12 (V&A collection) with the magenta dot indication the blue analysed area; (b) Raman measurement for this area detected azurite, malachite and goethite p(articles); (c) XRF spectrum detected Cu as the major element and (d) the best fit to the VIS/NIR reflectance measurement (black curve) using the KM model (red curve) was with a reference spectrum of grade 1 azurite.

#### *4.1.2.4 XRF detection limitations and difficulties in the interpretation of the spectra*

In spite the fact that XRF spectroscopy is a powerful tool for *in situ*, non-invasive analysis of artworks, it faces limitations on the detection of elements with atomic number less than fourteen (see section 2.5). This characteristic can become disadvantageous for the analysis of objects of art as it makes the detection of elements, such as Al and S difficult or even impossible. Those elements appear as traces of various pigments and their detection could contribute to the identification of the pigment used. Moreover, careful interpretation of the XRF spectra is necessary as the simultaneous excitation of elements that have their emission lines in close positions can cause the overlap of their lines, resulting to incomplete conclusions. Therefore, the complementary use of other non-invasive analytical techniques that enable the identification of pigments containing elements whose lines are not clear in the XRF spectrum is necessary. The information that derives from the application of these techniques enables a better interpretation of the XRF spectroscopic measurements, based on the detection of the secondary peaks of the specific elements. Figure 4-6 shows a characteristic example where Pb and As-containing pigments are both present on the same orange area on the murals of cave 465 of Mogao complex. Given that Pb has its main detection peak (La) at 10.55 keV, and As has a large Ka peak at 10.54 keV their detection was based on secondary peaks (i.e. Lb at 12.65 keV for and Kb at 11.73 keV respectively). Reflectance spectra collected from the same area were fitted through the KM method and using red lead as reference, suggesting the presence of red lead in the paint mixture. Further analysis using Raman spectroscopy confirmed the presence of red lead and identified the As-containing pigment as orpiment (Figure 4-6d).

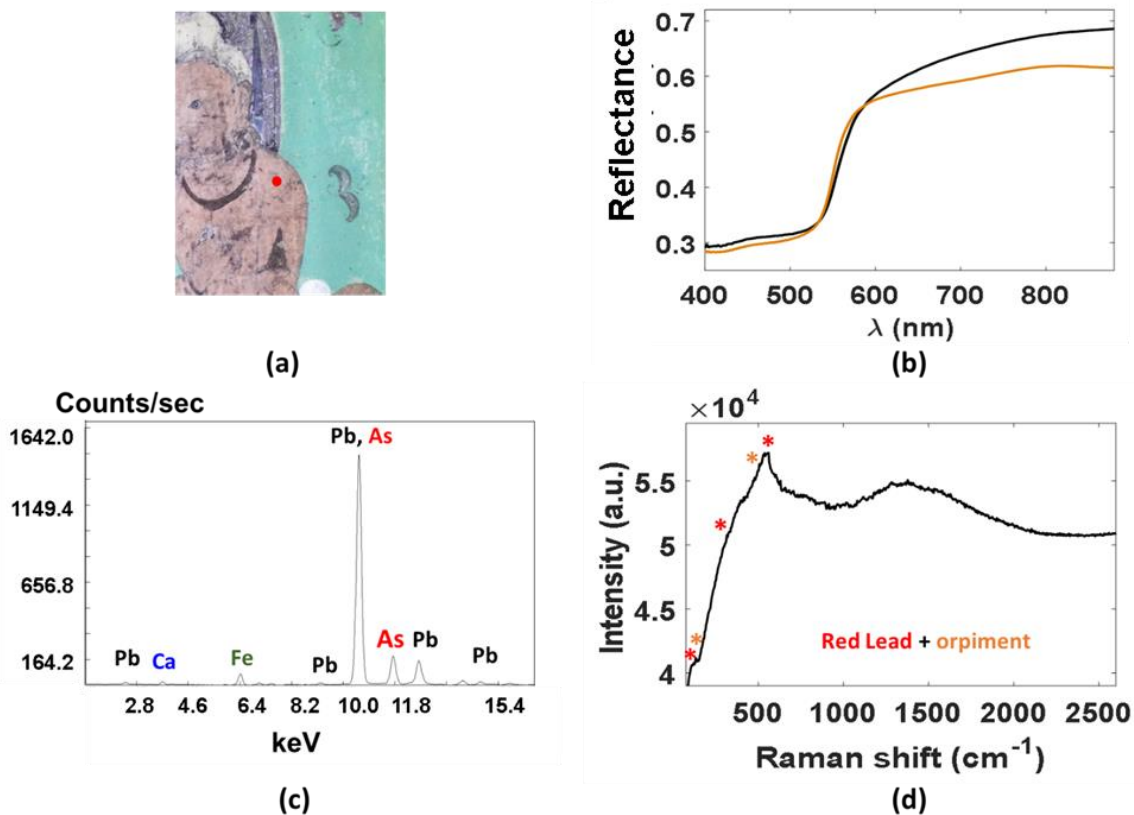


Figure 4-6 (a) Colour image of a detail from the mural on the East wall of cave 465, Mogao complex (red dot indicates the analysed area); (b) KM model fit (orange curve) using red lead as reference to the measured VIS/NIR reflectance spectrum (black curve); (c) XRF spectroscopy detects Pb and As as major elements and (d) Raman measurement for this area detected both red lead and orpiment.

#### 4.1.3 Conclusions

In this section, the necessity of the complementary use of three of the most well-known non-invasive spectroscopic techniques: high resolution spectroscopy with FORS, Raman and XRF spectroscopy for the precise identification of the pigment composition of various paint layers was illustrated. More specifically, the investigation of the limitations of the individual techniques and how their combined use enables overcoming their limitations was presented.

VIS/NIR reflectance spectroscopy in combination with an algorithm based on the KM model enables the identification of most of the pigments of a paint layer in both their single and combined application. However, this method faces limitations in the identification of a handful of pigment such as the majority of the yellow pigments as well as in the distinction between the traditional Chinese Cu-containing green pigments.

This limitation can be overcome with the complementary application of XRF and Raman spectroscopies. XRF detects fingerprint main and trace elements of the various inorganic pigments and Raman spectroscopy provides precise pigment identification, enabling the identification even of the polymorphs of the main pigments as well as their degradation products and their intermediate phases. However, the sensitivity of Raman spectroscopy to the fluorescence emitted from the organic compounds that the analysed area may contain can prevent the identification of the pigments. In order to overcome this limitation, the localization of the analysis in crystal level has been suggested. On the other hand, the localization of the analytic area may cause a drawback regarding the representability of the extracted results about the pigment composition [6]. Moreover, the identification of highly fluorescing organic dyes is impossible using any type of conventional Raman spectroscopic instrumentation, with the application of the micro-invasive surface-enhanced Raman methodology being required [51]–[53]. However, the application of high resolution reflectance spectroscopy showed that it can overcome the limitations that Raman spectroscopy faces in a total non-invasive way.

A factor that also has to be taken into account during the interpretation of the data obtained by various non-invasive analytical techniques, such as reflectance spectroscopy in the near-IR regime and XRF spectroscopy, is the fact that their analytical penetration depth is not always limited on the paint layer, with the contribution of the substrate in their spectroscopic results being possible. The spectral contribution of the substrate is also possible in the analysis of faded painting areas. Therefore, the substrate of the various artworks has to be taken under consideration both; in the preparation of the reference databases but also during the analysis of the real artwork. More specifically, the reference paint layers must be applied on substrates of the same material composition as the original artwork. Furthermore, during the examination of the original object, spectral data from exposed areas of the substrate should be also collected when it is possible and used as reference during the interpretation of the analytical results.

Additionally to the application of the optimum multi-modal analytical approach, the interpretation of the collected data is also very crucial. Some scientific groups suggest different ‘step by step’ analytical protocols for the examination of artworks of various material composition [50], [54]. However, the examination of the large and heterogeneous number of painting areas in the context of this study showed that the strength of the multi-modal analysis does not derive alone from the variety of the

information that the involved techniques provide but also from the complementarity of this information when interpreting their analytical results.

This is particularly obvious in the examination of complex systems like paintings where the nature of the involved materials, their degradation level and their relative concentration in the analysed area may affect the data obtained by the various analytical techniques. In these cases, the interpretation of the analytical results is not a straightforward procedure. The adaptation of a ‘step by step’ analytical approach involves the risk of information loss.

The optimum analytical approach suggested in this study requires the selection of non-invasive analytical techniques that provide complementary information to each other, as well as the in-depth understanding of the analytical limitations and abilities of each them. Moreover, in order to draw safe conclusions about the pigment composition of the analysed objects of art, the collection of as much as possible data using the various non-invasive techniques from the most representative spectral areas should be performed, as they result after the application of clustering on the spectral images collected from them. The collection of the large scale dataset should be then followed by their complementary interpretation as because the analytical results of one technique can provide useful feed-back to another, assisting the optimization of the interpretation of its data. The optimization of the interpretation as well as the complementarity of the spectral information obtained by the various non-invasive techniques increase the accuracy of the extracted conclusion.

## **4.2 Non-invasive identification of binding media**

### **4.2.1 Introduction**

In order to prepare a paint layer, additionally to the pigment that gives the colour, a material that binds the pigment particles to each other and then to the substrate is needed. These materials are called binding media or binders and are either natural (animal or plant derived) or synthetic organic substances. Among the organic products, proteins, lipids and polysaccharides are widespread in objects of art. Animal glues are produced by the dissolving of collagen, a protein derived from the skin, bones and tendons of mammals (e.g. cow, rabbit, horse) and fish [18]. Casein consists of phosphoprotein complexes and is resulted from the precipitation of skimmed milk by the addition of an acid (sulphuric, hydrochloric or lactic). Both egg white and yolk are proteinaceous substances, with yolk having additionally phosphorous-containing lipids. Oil binders belong to the glyceride group of lipids. Gums are amorphous materials, belonging to the group of polysaccharides, with gum Arabic being the most common one, produced by the resin of Acacia trees mixed with calcium and magnesium or potassium salts [55]. Various materials known as waxes have been also used as binding media. This group is quite heterogeneous containing mixtures of hydrocarbons, acids, alcohols, esters, sterols and terpenoids. Additionally to the natural binders, synthetic polymers have been introduced to the fields of art and art conservation since the nineteenth century. Since the twentieth century, synthetic polymers, such as acrylic and polyvinyl acetate (PVA), have been widely used as binding media as well as varnishes. The characterisation of the binders also reveals important information about the history of an artwork and is critical prior to any conservation treatment. For this purpose, a wide range of analytical techniques, both invasive and non-invasive, has been developed, with their applicability being a subject of great interest over the years. Among the invasive analytical techniques, mass spectroscopy (MS), combined with different chromatographic techniques, is the one that has been widely used in the field of cultural heritage enabling the identification of organic materials, like the binders [56]–[60]. However, the nature of the surrounding paint materials can constitute limiting factor to the identification of binders using mass spectroscopy. The simultaneous presence of different organic materials, the dominant use of one material compared to the others and the presence of inorganic materials are some of the cases where the identification of the organic binders can be prevented. The identification of

proteinaceous binders, for example, can be limited when inorganic pigments are present. More specifically, the presence of Cu-containing pigments can potentially block their detection due to the tendency of the metal ions to cluster with amino acids. The same limitation can be faced also when other inorganic pigments, such as mercury (Hg), iron (Fe), calcium (Ca) and magnesium (Mg)-containing ones, are involved [56]. However, recent developments in both pre-treatment protocols and interpolation of the resulted spectra have improved the quality of the extracted information, overcoming several limitations. Extensive work about the optimization of the interpretation of the data obtained by mass spectroscopic techniques for the identification of binders, applying statistical analytical methods (known as chemometrics in chemistry), has been carried out for a long time. A typical example is illustrated through studies on the identification and classification of plant gums [61], [62]. In these cases, the simple analysis of Gas-Chromatography (GC)/MS data does not provide clear information about the type of the gum. However, the application of multivariate analysis (e.g. clustering and PCA) overcame this issue providing clear distinction between the species of gum. The same approach, has been applied successfully for the distinction and therefore precise identification of animal glue and egg binders, even in cases where the proteinaceous binders were used in combination [63]. The application of chemometrics on carefully pre-treated samples was proven to enable also the characterization of all different natural binding material (e.g. oils, proteinaceous materials, polysaccharides and waxes) existing on the same samples combined with MS for the analysis of modern paintings has been presented [63]. More specifically, the initial GC/MS spectroscopic examination of the paintings identified drying oil as the binder. The further distinction between the various types of oil using GC/MS results was based on the ratio of two of the main saturated fatty acids which contain, palmitic to stearic acid ratio (P/S), which is considered relatively unaltered during ageing. However, the environmental contamination as well as the presence of other lipid compounds (e.g. natural waxes, animal fat and egg yolk) can affect this ratio making this differentiation unreliable, particularly in the case of oil mixtures. This limitation was overcome by integrating the results about the fatty acid content to the detection of the entire triglyceride profiles using High Performance Liquid Chromatography (HPLC). Triglyceride derives from the combination of glycerol and three molecules of stearic acids and it is the main constituent of oils. Therefore, the acquisition of the different triglyceride (TAGs) profile of the lipid material extended the analysis to the clarification of the composition of the

oil components. In another study, the application of Matrix-Assisted Laser Desorption/Ionization–Time of Flight (MALDI-ToF) mass spectroscopy on pre-treated samples, was proven to enable the characterization of egg white and yolk proteins of the aged binders of Renaissance paintings [63]. MALDI-ToF analysis on minute samples containing aged lipid binders permitted the discrimination between egg and drying oil-based binding media, even in cases of simultaneous presence [64]. Another invasive analytical technique that has been also extensively used for the identification of binding media is the Fourier Transform Infrared (FTIR) spectroscopy in the transmittance mode. FTIR spectroscopic analysis performed on samples collected from various easel paintings enabled the identification of all the traditional used binders, from egg tempera and oil to animal glue and gums [64]. Moreover, studies about the systematic examination of fresh and naturally aged mixtures of pigments in both egg tempera and oil showed that FTIR spectroscopy in the transmittance mode can determine even the chemical alterations caused by their aging [65]. Despite the analytical advantages of both MS and transmittance-FTIR techniques, their main disadvantage is that they are both micro-destructive techniques and therefore their application on the analysis of Cultural Heritage objects is not always allowed. Therefore, the development of non-invasive techniques for the purpose of the identification of binding media is of a great importance.

Raman spectroscopy is a very well-known, non-invasive analytical technique extensively used for the characterization of both organic and inorganic paint materials. In spite the successful characterization of various natural binders during the examination of samples of pure/fresh media [66], [67], the application of Raman spectroscopy for the identification of the binders of real artworks has rarely provided useful information [68], [69]. The main reason for this limitation is the fluorescence emitted due to their organic nature that is becoming more intense with the aging of the binder. Furthermore, the microenvironment of the binders (e.g. presence of organic dyes) and/or the presence of degradation products of the paint materials can also affect their detection negatively.

Although reflectance spectroscopy in the near-IR regime has been widely used for the identification of various pigments, only a few studies in which this spectral regime has been used for the identification of binders have been published. Riciardi et al [70] in

their work about the examination of illuminated manuscripts using near-IR imaging spectroscopy, showed that the identification of egg yolk is possible (due to its characteristic absorption line at 2309 and 2350 nm) even in the presence of pigment that have intense absorption lines in very close positions (i.e. azurite lines at 2285 and 2350 nm). Vagnini et al [71] in their study about the identification of natural polymers on easel paintings using Fourier Transform- near-IR spectroscopy, applied first derivative mathematical function for the interpretation of the collected spectra. Additionally to the successful distinction between the different binder references, experiments on samples collected from real artworks showed that this method enables the detection of siccative oil, animal glue as well as natural resins. However, the interpretation of the near-IR spectroscopic results is not always a straightforward process, as the signals in this spectral region (see section 2.3) are generally broader and less resolved than the fundamental bands. This results to limitations on the distinction of components existing in a mixture, making often the extension to the mid-IR regime necessary.

Fourier-transform Infrared Spectroscopy (FTIR) is a spectroscopic technique widely used for the analysis of materials in art and archaeology, enabling the accurate identification of both organic and inorganic paint materials. Even though the development of reflectance FTIR seems to be a powerful tool for the non-invasive analysis of artworks, the interpretation of the resulting spectra is not being always a straightforward procedure (see section 2.3). In a comparative study between reflectance and transmittance FTIR spectroscopy, Vetter and Schreiner showed that this limitation can be overcome by the application of Kramers-Kroning transformation on the collected data [72]. It is worth mentioning that the same study highlighted that for the identification of binders both their concentration and pigments of the analysed area should be taken into account. In the direction of the effective interpretation of the reflectance FTIR spectra, the application of multivariate statistical methods has been widely adopted lately. Rosi et al [73], illustrated the complementary use of fibre optics infrared spectroscopy in both mid-IR and near-IR regimes for the non-invasive identification of the binders used in a collection of modern paintings. The application of PCA on Fourier Transform mid- IR spectra enabled the detection of a synthetic, polymeric binder (polyvinyl acetate, PVA) in most of the analysed paintings and furthermore suggested the presence of proteinaceous binder on some others, without being able to specify which one exactly. The Fourier Transform near-IR spectra in

combination with the application of PCA, revealed the presence of lipid components. However, the ageing of the binder caused broadening of its spectral features, inhibiting its precise identification. In another study of the same group [74], PCA was applied for both the pre-treatment and the management of data collected from a series of non-binder, rabbit skin, whole egg and casein-containing replicas, using fibre-optics mid-FTIR in reflectance mode. This application managed to subtract the reflectance effects that are present due to the heterogeneity of the paint layer's surface, revealing the characteristic feature of the various organic binders. Both non-binder and casein containing areas were easily distinguished from the animal glue and egg-containing ones. On the contrary, the low level of lipids of the egg-containing replicas did not enable the distinction between egg and animal glue.

Although the reflectance spectroscopy, in both near and mid-IR regimes, has been introduced as a non-invasive analytical technique that enabled the identification of the binding media of some objects of art, the extend of its detection abilities and limitations has not been investigated in detail. In the context of this study, the ability of the identification of the binding media on various painting systems using near-IR reflectance spectroscopy was investigated through the examination of a series of artificial samples prepared in such a way that they mimic some of the basic categories of artworks. Additionally to the investigation of the strength of IR spectroscopy on identification of various binders, the possible spectral contribution of the surrounding painting materials (i.e. substrate and pigments) is also highlighted and therefore investigated in detail.

#### 4.2.2 Examination of the potential of reflectance spectroscopy in the near-IR regime for the identification of binding media

Preliminary studies were performed comparing the near-IR spectra of a range of common binding media used in European, South and East Asian paintings to a variety of substrates that cover some of the most basic types of works of art (Figure 4-7). For the preparation of the reference samples, thick layers of the various binders were applied on microscope slides that have no spectral contribution in the near-IR regime. During the collection of the reference spectra, the samples were on a long distance from the next possible reflecting surface in order avoid any additional spectral contribution.

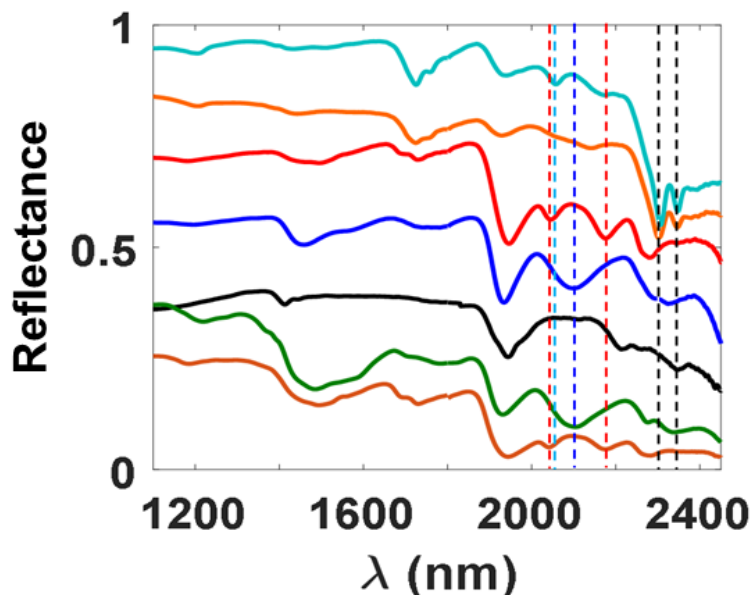


Figure 4-7 Near-IR spectral comparison between binding media applied on microscope slides: animal glue (red curve), egg yolk (light blue curve), linseed oil (orange curve), gum Arabic (blue curve), and substrates of different types of artworks: plaster (black curve), paper (green curve) and parchment (brown curve). The spectra are vertically shifted apart for clarity. The vertical dashed lines are highlighting the position of the characteristic absorption lines of animal glue (red) and gum (blue), as well as the lipid lines of both egg yolk and linseed oil (black lines) and the proteinaceous line of egg yolk (light blue).

The spectral comparison between animal glue and parchment shows their spectral similarity, which is not surprising given that the main component of both of them is the collagen. Similarly results are obtained for the gum Arabic and cellulose (main compound of paper) as they both derive from plants. Further observation of the characteristic lines of animal glue showed that both of its fingerprint lines at 2045 and 2175 nm (C-O bonds of protein's amides) are masked from the broad feature of paper at 2100 nm, making its identification on paper substrate impossible. The only substrate

that does not have any spectral feature at 2045 nm is plaster, which is commonly used in the preparation layer of the murals, suggesting that the identification of animal glue in the paint layers applied on this substrate could be possible. However, the identification of animal glue on murals, even though it is spectrally possible, has been reported to be rather difficult due to the small concentration and/or the degradation of the binder. However, given that animal glue is a binding medium traditionally used in Chinese artworks and more specifically on murals further examination of its potential identification on murals was performed. For this reason, a series of mock-up samples (see section 5.2) which were prepared in such a way that they simulate real mural cases, were examined. The paint layers consisted of pigments traditionally used on Mogao murals mixed with animal glue and applied on both fine and thick paint layers, within the realistic regime. For an accurate examination, the spectra collected from the different painted areas, were additionally compared to the spectrum of the pure animal glue reference and the spectra of the substrate and the raw pigment. Figure 4-8 illustrates the spectral comparison of selected paint layers consisting of pigments that are featureless in the near-IR regime. Interestingly, the spectral contribution of animal glue can be slightly observed only in the paint layer of vermilion. Given that the samples were simulating real paint cases, this observation could be related to the grade of vermilion pigment and the possible need of a more significant amount of binder in order to achieve an applicable paint layer. However, even in this case the lines are not clear, confirming the difficulty of its identification in this spectral regime. For a more detailed investigation, further analysis on samples of a larger variety of pigments and dyes traditionally used on murals that will also cover the whole range of realistic concentrations should be performed.

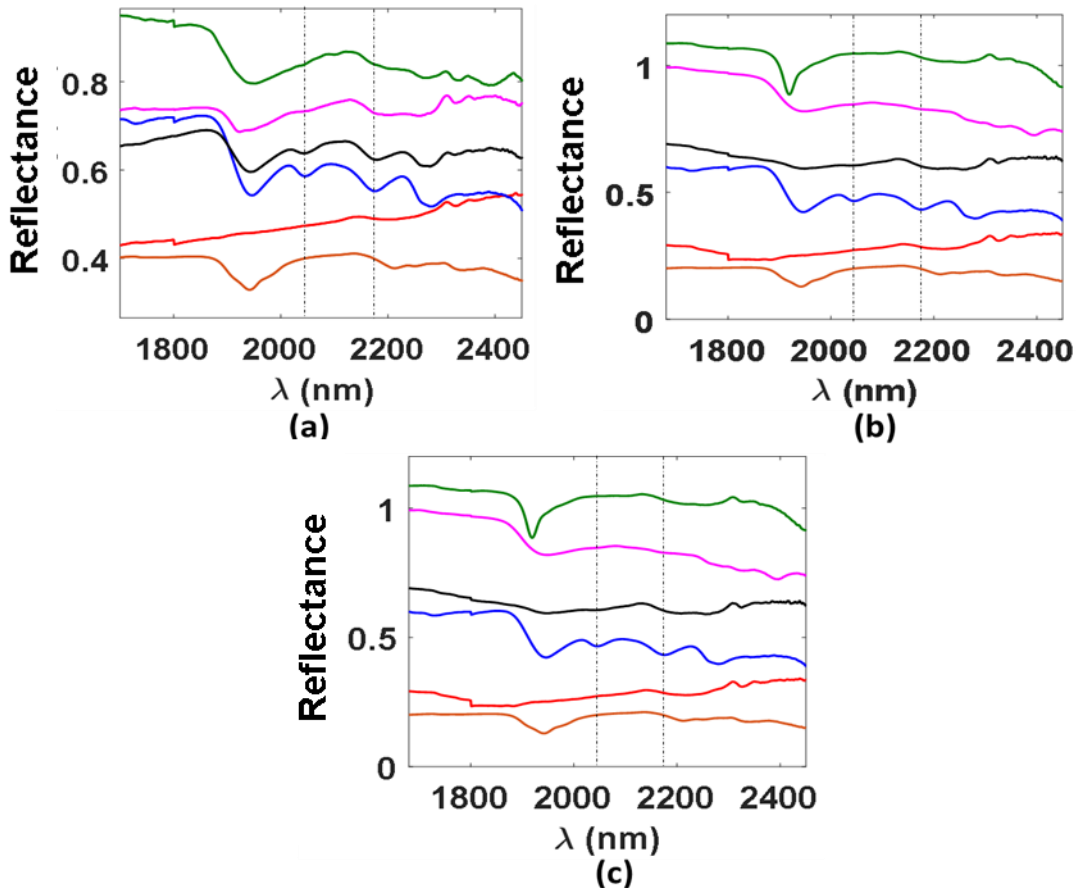


Figure 4-8 Near-IR spectra of fine (magenta curves) and thick (green curves) paint layer of (a) vermillion, (b) red lead and (c) red ochre in animal glue applied on substrate simulation of the Mogao murals (brown curve) compared to the paint layers of the same composition applied on microscope slides (black curves), the reference spectrum of animal glue (blue curve) and the reference spectra of the corresponding raw pigments (red curves). The dashed vertical lines correspond to the position of the characteristic absorption lines of animal glue. The spectra are vertically shifted apart for clarity.

According to the spectral comparison between gum Arabic reference and the different substrates (Figure 4-7) its identification would be expected to be possible on both plaster and parchment substrates its broad line at 2100 nm (OH bonds of polysaccharides). Gum Arabic is one of the binders most widely used on manuscripts and therefore the possibility of its identification in paint layers applied on parchment is very important. Therefore, a series of artificial samples of pigments, commonly used for the illumination of manuscripts, mixed with gum Arabic and applied on parchment were examined. The concentration ratio of the paint-outs was selected in such a way that covers the whole range of realistic paints. Figure 4-9 illustrates the examination of artificial samples that were prepared with ultramarine, one of the pigments that were widely used in the medieval European manuscripts and that is also featureless in this spectral regime. The spectral observation of all different concentration showed that the

characteristic line of gum Arabic is not detected even in the sample of the highest concentration of binding medium. Same results were obtained in the examination of artificial samples made using other pigments, leading to the conclusion that the identification of gum Arabic is not possible using near-IR spectroscopy. Even though the use of gums on murals is not common, further studies on their identification on plaster would be interesting to be performed.

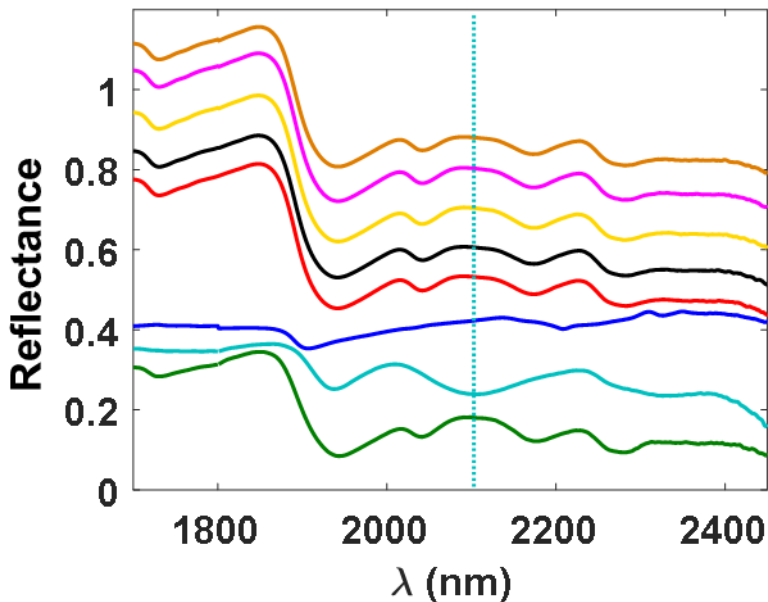


Figure 4-9 Near-IR spectra of ultramarine in gum Arabic paint-outs on parchment in a ratio pigment: binder: (a) 1:1 (red curve), (b) 1:2 (black curve), (c) 1:3 (yellow curve), (d) 1:4 (magenta curve) and (e) 1:5 (orange curve) compared to the reference spectra of gum Arabic (light blue curve), ultramarine pigment (blue curve) and parchment (green curve). The dashed vertical line corresponds to the position of the characteristic absorption line of gum Arabic. The spectra are vertically shifted apart for clarity.

The identification of lipid binders, both egg yolk and oil, seems to be possible in the near- IR regime, as they have characteristic lines (2301 (egg), 2307 (oil) and 2347 (both nm) that are not masked from the spectral futures of any substrate (Figure 4-7). Moreover, the proteineous line of egg yolk at 2057 nm can potentially be the key for further distinction between them. In the case of lipid binding media the spectral contribution of the pigment(s) is becoming very crucial as there are pigments, such as green and blue Cu-containing pigments, that have intensive spectral feature very close to their characteristic lines. One characteristic example is azurite, which has two strong absorption lines at 2285 and 2353 nm, positions very close to the lipid lines of egg yolk and oil. Previous studies on the identification of binders using reflectance spectroscopy in the near-IR regime have shown that egg lines can be detected also in the presence of azurite [70], without however examining the concentration effect. As azurite is also one

of the most commonly used pigments for the illumination of manuscripts, references of azurite in egg yolk have been applied on parchment, with the concentrations covering the whole range of realistic cases. Figure 4-10 shows the spectral comparison between the paint mixtures in different concentrations, the pure azurite powder and the parchment.

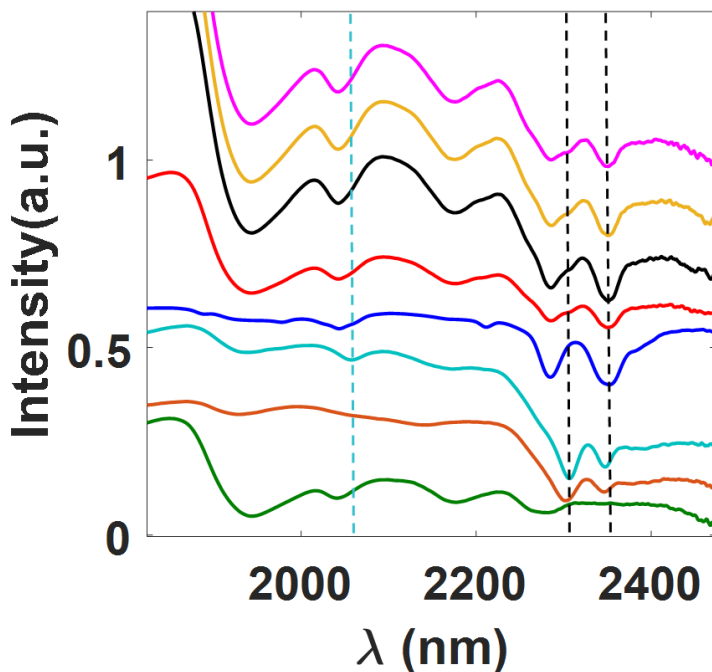


Figure 4-10 Near-IR spectra of azurite in egg tempera paint-outs on parchment in a ration pigment: binder: a) 1:1 (red curve), b) 1:2 (black curve), c) 1:3 (yellow curve) and d) 1:4 (magenta curve) compared to egg tempera (light blue curve) and oil (brown curve) references as well as to the parchment (green line). The vertical lines correspond to the lipid absorption lines of (black dashed lines) and the proteinaceous absorption line of egg (light blue dashed line). The spectra are vertically shifted apart for clarity.

From the lipid lines that are related to the C-H bonds of the lipid fats, only the one at 2307 nm is detectable in all different concentrations, while the lipid line at 2347 nm as well as the proteinaceous line of egg yolk at 2057 nm (C-O bond of amides), are masked from the spectral features of azurite and/or parchment. Given that the proteinaceous line of egg yolk is masked, the characterization of the binding medium as lipid is only possible, without enabling further distinction.

As part of this study, additionally to the examination of the potentials and the limitations on the identification of various binding media using near-IR reflectance spectroscopy through the examination of mock-up samples, the identification of the binder of ‘Selden’ map was also performed. Through this case study, the analytical approach, involving the examination of all the parameters that could affect the detection of the binders, as well as the examination of the extent in which the reflectance

spectroscopy in the infrared regime can be informative are illustrated. As both the pigment(s) and substrate can contribute in the IR spectrum of the analysed area, their identification is required to be performed first. The analysis of the identification of the binding medium was performed on fragments collected from areas where pigment identification showed that indigo is the main colourant. As indigo does not have any characteristic spectral feature in the near-IR regime, only the paper substrate could contribute to the spectra collected from these areas additionally to the binder. Figure 4-11 illustrates the spectral comparison between the map, cellulose (predominant substance of the substrate) and a range of binder references. As it can be observed, the examination in this regime can exclude the presence of oil, egg tempera and beeswax as neither of their characteristic features is present in the spectrum of the fragment. On contrary, no conclusions can be drawn for the presence of animal glue, gum Arabic or peach gum as cellulose has broad absorption lines at similar spectral positions that could possibly mask their characteristic lines.

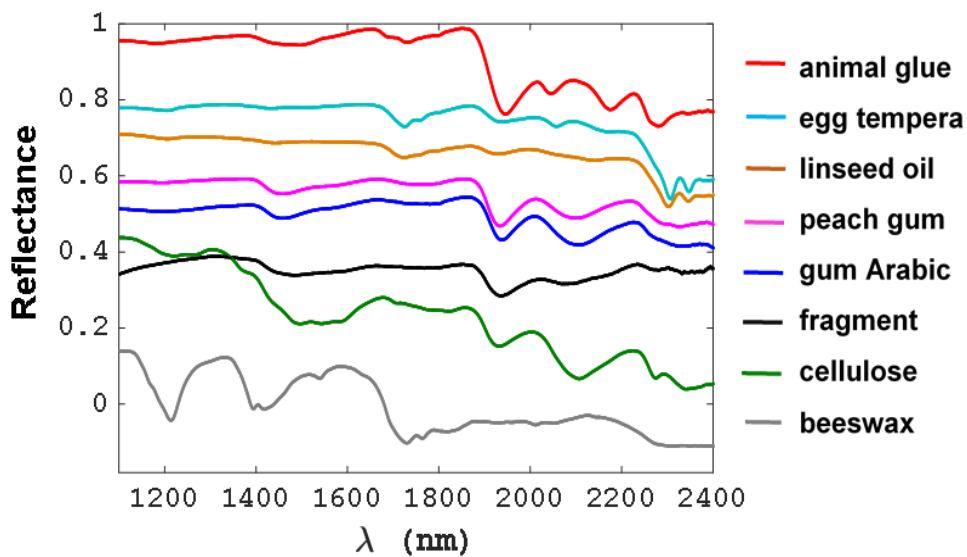


Figure 4-11 Near-IR spectra of binding media applied on microscope slides: animal glue (red curve), egg tempera (light blue curve), linseed oil (orange curve), peach glue (magenta curve), gum Arabic (blue curve), beeswax (brown curve) compared with the corresponding spectrum of a green fragment from the Selden map (black curve) and the spectrum of cellulose (Whatman CC41, green curve). The spectra are vertically shifted apart for clarity.

Consequently the spectral investigation in longer wavelength range, using mid-FITR spectroscopy proved to be necessary. Figure 4-12, illustrates the comparison of spectra collected from the fragment and the various binder references using FTIR-ATR spectroscopy. As it is shown, the spectrum of the fragment matches closely to the gum

Arabic, as the characteristic lines of the gum at 1608 [ (O-H) bending], 1412 [(C-H) bending] and 1032 cm<sup>-1</sup> (C-O stretching)] are also present in the spectrum of the fragment, indicating its presence in it. The spectrum of peach glue is quite similar as it would be expected, given that they are both resins derived from plants. Nevertheless, the ratio of their common lines is not the same and furthermore its lines at 1732 and 1241 cm<sup>-1</sup> are either not present or extremely weak in the spectra of both the fragment and the gum Arabic. Therefore, according to the spectral similarity between the fragment and the gum Arabic reference, the observation in the mid-IR regime suggested gum to be the binding medium of the map.

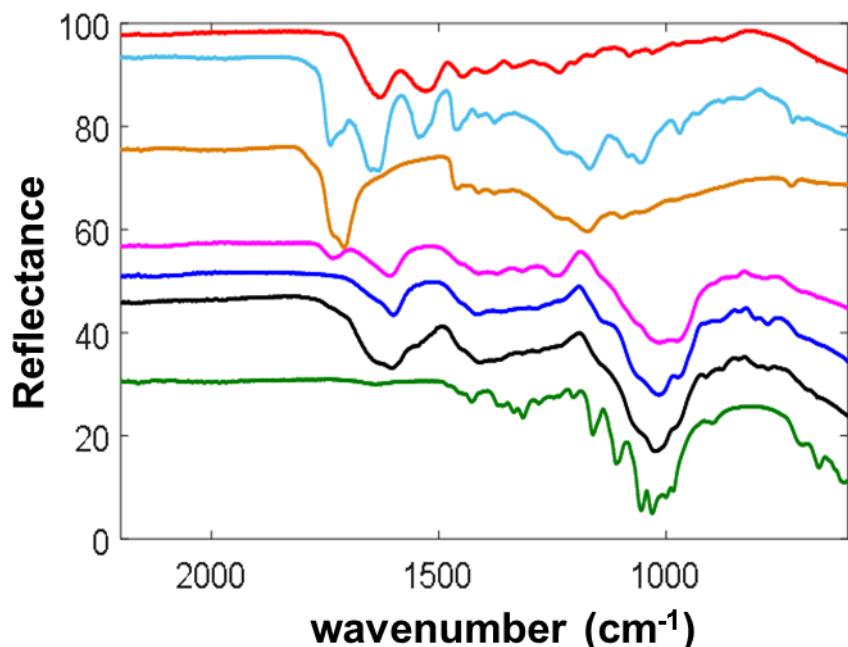


Figure 4-12 FTIR-ATR spectra of binding media: animal glue (red curve), egg tempera (light blue curve), linseed oil (orange curve), peach glue (magenta curve), gum Arabic (blue curve) compared with the corresponding spectrum of a green fragment from the Selden map (black curve) and the spectrum of cellulose (Whatman CC41, green curve). The spectra are vertically shifted apart for clarity.

#### 4.2.3 Summary

This study was conducted on the investigation of the potentials for the identification of binding media using reflectance spectroscopy in the near-IR regime with experiments being performed on samples that simulate different realistic cases. Generally, during the observation in the infrared regime, the possible spectral contribution of both the pigments and the substrate of the analysed areas should always be taken into account, as

can affect the extracted conclusions drastically. More specifically, before any analysis for the identification of the binding medium a thorough identification of the pigments should be performed, while in the sequential spectral comparison additionally to the involved pigments the substrate should be also compared. Preliminary experiments of this study about the identification of animal glue showed that its detection on paper and parchment-based artworks is not possible. The examination of samples prepared in such a way to mimic murals showed that the detection of the characteristic lines of animal glue could be possible only on painting layers of certain pigment composition (i.e. vermillion), with further investigation being necessary. The identification of gum Arabic seems to be impossible on any paper or parchment-based artwork, with further studies on the identification of gums on plaster substrate being needed. The identification of the egg yolk and oil seems possible when they are applied on all different substrates, however, in the presence of azurite the distinction between these two lipid binders was not possible. The examination of their identification in paint layers of different pigment composition that have intense spectral features in the same spectral regime as their characteristic lines is also needed for the investigation of the limitations of the near-IR spectroscopy in their identification. Finally, the identification of the binding medium used on Selden map illustrated the limitations that the analysis in the near-IR regime faces in the identification of some binders in a real case and how the extension in the mid-IR regime in these cases is necessary, providing accurate identification of the binding medium as well as distinction between binders belonging to the same group.

### **4.3 Multimodal approach for the identification of the drawings materials**

The analysis of the drawings of a painting is of significant importance as, additionally to the examination of the painting sequence, the identification of the drawing materials also provides very useful art historic information. During the examination of the Chinese export watercolour paintings of V&A and RHS collections, a multi-modal approach for the identification of the drawing materials was followed. Preliminary examination of the watercolour paintings, using the NIR spectral bands of the PRISMS system, was performed clarifying which of them had preparatory drawings. Further examination, of these areas was then performed using the OCT system that provides the

ability of much higher contrast and spatial resolution observation, therefore showing whether a liquid or solid substance had been used. Given that among the examined paintings there were many with drawings that were uncontaminated by the paint, Raman analysis of the drawings was enabled providing identification of the material used for the drawings. Figure 4-13 illustrates the analysis of a painting that was identified to have pencil drawings. Following the mapping of the drawings, using spectral imaging, high resolution OCT imaging was performed on a selected number of them, with its high resolution imaging showing that the drawing material was a solid substance. Finally, Raman spectroscopic measurements detected graphite which confirmed that it was drawn with a graphite pencil.

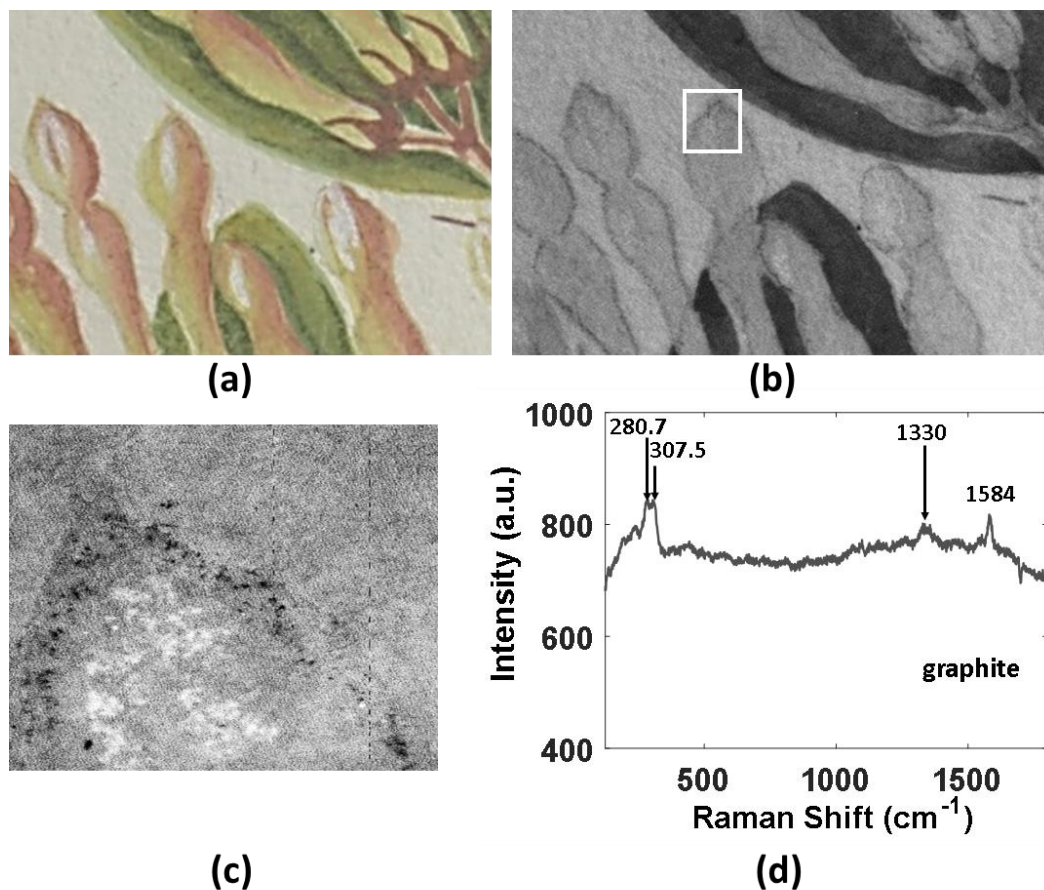


Figure 4-13 (a) Colour image derived from PRISMS data collected from a part of painting no. 35730 of RHS collection, (b) 880nm PRISMS image of the drawings, (c) OCT enface image of the boxed area in b) showing the drawings to be of a solid substance and (d) the corresponding Raman measurement that identified graphite.

Among the watercolour paintings of these collections, cases where both PRISMS imaging and OCT scanning showed that the drawings were made using a liquid substance were found as well (Figure 4-14). Raman analysis of these drawings

identified the material used as carbon black, evidence that is consistent with the composition of Chinese ink. It is worth mentioning that Raman spectroscopy provides the ability for distinction between carbon black (i.e. ink) and graphite, even though both of them consist of pure carbon, due to their differences in their crystal structures. More specifically, carbon black is an amorphous form of carbon, whilst graphite is formed when carbon atoms link with each other into sheets. Therefore, more Raman modes are interfering in the molecule of carbon black resulting to a more complex and noisier spectrum than the spectrum obtained from a well-structured molecule as the molecules of graphite.

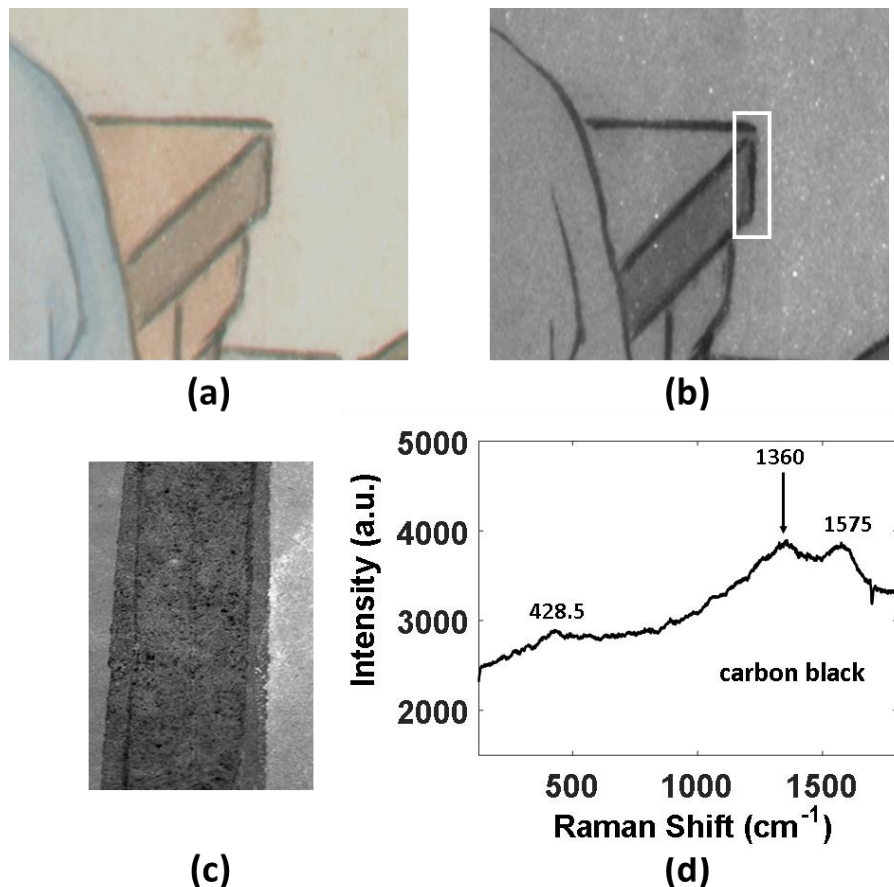


Figure 4-14 (a) Colour image derived from PRISMS data collected from part of painting no. 7791-12 of V&A collection; (b) 880nm PRISMS image of the drawing, (c) OCT enface image of the boxed area in (b) showing drawing to be of a liquid substance and d) the corresponding Raman spectrum that identifies carbon black.

## **4.4 Multimodal approach for the identification of the substrate and the preparation materials**

### **4.4.1 Introduction**

For the holistic examination of an artwork, additionally to the identification of the materials of the paint layer and the drawings, the analysis of the substrate can provide very important information about its history. For the structural examination of the substrate of objects of cultural heritage, optical microscopy as well as various types of photography, from transmitted light to macro photography, have been widely used [18]. More specifically, in the case of paper-based objects, the development of different fibre staining methods in combination to optical microscopic observation has been proven to enable even the identification of the plant origin of the fibres [75]. The fibre length and the thickness of the paper sheet are also very informative characteristics for the identification of the paper substrates, with most of the analyses however being traditionally performed on samples collected from the real artwork. For the identification of sizing materials and fillers, various techniques, both invasive (e.g. SEM/EDX) and non-invasive (e.g. IR spectroscopy and colorimetric methods) have been applied. In this section, a multimodal approach for the non-invasive analysis of paper substrate is presented through the example of the substrate analysis of the watercolour paintings of V&A and RHS collections. In the field of the analysis of artworks, the OCT system, providing both high spatial resolution and the ability of virtual cross-sectional observation has been widely used for the examination of the paint stratigraphy of various artworks. In this study, its application for the structural examination of the different types of papers and their distinction according to the length of their fibres as well as their scattering properties is illustrated. Although OCT has been used to characterise industrial paper, examining the micro-structure and the filler content of paper using the slope of the depth profile of the backscattered light intensity [76], there are no studies contacting on the OCT scanning for the characterisation of the substrate of paper-based artworks. In this direction, the ability of rapid, contactless evaluation of the light scattering properties, the thickness and fibre length of the paper without the need of demount of the painting is the advantage of the OCT scanning, as additionally to the speed of the examination it protects the fragile objects from any possible damage. Moreover, the structural information obtained from the OCT scanning

is combined with the elemental information provided through the XRF spectroscopic analysis of the substrates, revealing information for the sizing and filling treatments that have been followed.

#### **4.4.2 Complimentary use of OCT scanning and XRF spectroscopy for the classification of paper substrates**

The advantages of the combined use of OCT scanning and XRF spectroscopy to the non-invasive analysis of paper substrates were investigated through the examination of real cases in the context of the holistic analysis of the export Chinese watercolour painting collections of V&A museum and RHS. The high spatial resolution and contrast imaging as well as the information about the scattering and absorption properties of the analysed object that OCT provides (see section 2.6) were used for the analysis of the paper substrates. The OCT measurements were performed on unpainted areas, obtaining for each of them a series of virtual cross-sections in an image cube which was sliced in the direction parallel to the painting surface. A number of selected image slices at the region near the surface were then averaged, with the resulted high spatial resolution image enabling the examination of the length of the fibres. Moreover, the profiles of the average backscattered light intensity as a function of depth, obtained by averaging the depth profiles in one cross-sectional scan, were examined in order to investigate the scattering properties of the paper sheet that are related to the density of the fibres.

Among the analysed paintings, there were a few of them painted on papers with western watermarks, confirming their identity and enabling their use as references. Their examination under the OCT system enabled the separation of the total of the analysed substrates into two groups. The first group was including papers that had short and densely packed fibres (Figure 4-15b), matching with the fibres characteristics of the reference western papers. Given that the density of the fibres was high, the thickness of the paper sheet was not able to be measured by the observation of the virtual cross-section (Figure 4-15a). Finally, the match of the average backscattered light intensity profile as a function of depth between the papers of this group and the reference western papers confirmed further the theory that this group consists of Western papers.

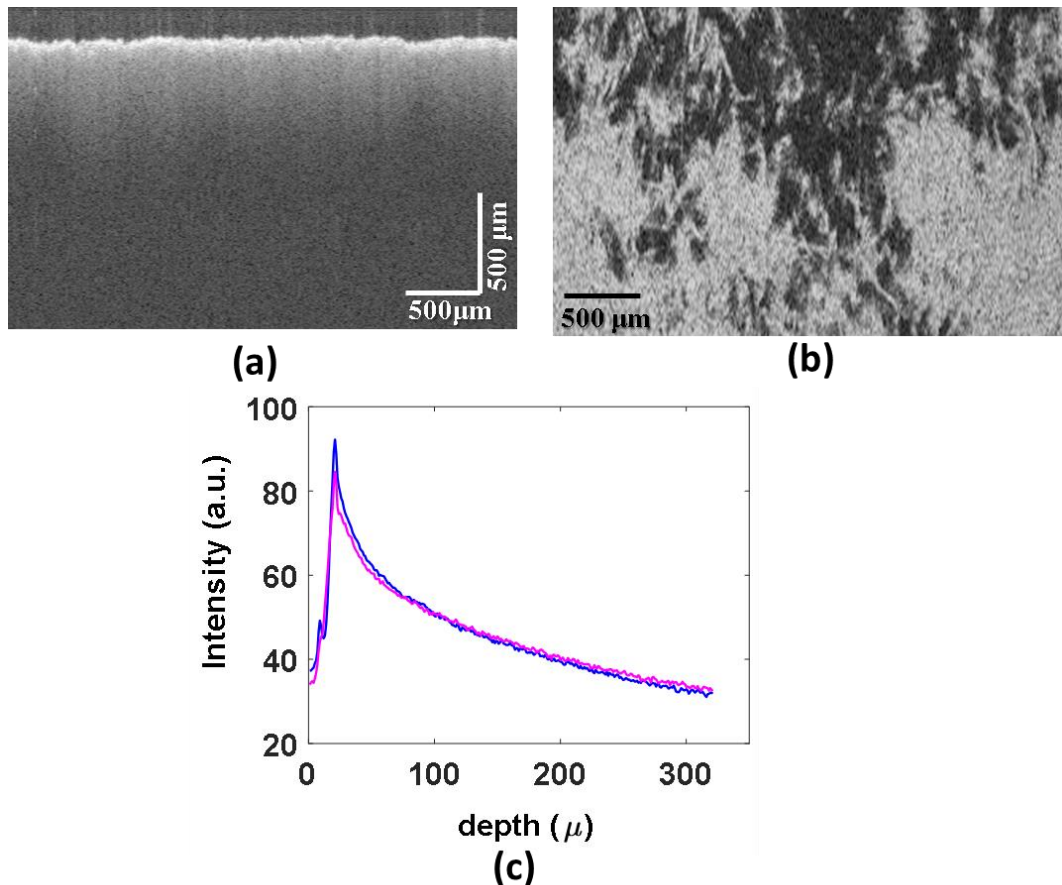


Figure 4-15 (a) OCT cross- section and (b) enface image of the English paper (M. J. Lay) substrate of painting no. 36643 (RHS collection) using the OCT system; (c) comparison between the depth profile of the backscattered light intensity of the M. J. Lay paper (magenta line) with that of the Whatman paper (blue line).

On the other hand, the second group consisted of papers with long fibres (typically at least five times longer than those of the first group) observation that is consistent with Chinese paper. Often this kind of paper was semi-transparent under the OCT allowing the observation of both the paper support and the backing paper (Figure 4-16a) and therefore enabling the measurement of their thickness. It has to be noted that OCT measures the optical thickness, which is equal to the physical thickness multiplied by the refractive index. Based on this and assuming that an average refractive index of the paper is given by that of cellulose which is 1.55, their thickness was calculated between 100 and 300 μm. Figure 4-16b shows the long fibre of a semi-transparent thin paper in an OCT image slice near the surface parallel to the surface of the painting. The low fibre density of this type of paper is resulting to low light scattering properties that is confirmed through the comparison of the slope of the average depth profile of the

backscattered light with that of the reference western paper (Figure 4-16c), as the increased multiple scattering makes the slope shallower. It is important to emphasize that through the examination of paper substrates of both groups it was confirmed that characteristics such as the length of the fibres of the paper as well as its thickness and the intensity of its scattering properties are highly correlated and provide the necessary information for their distinction.

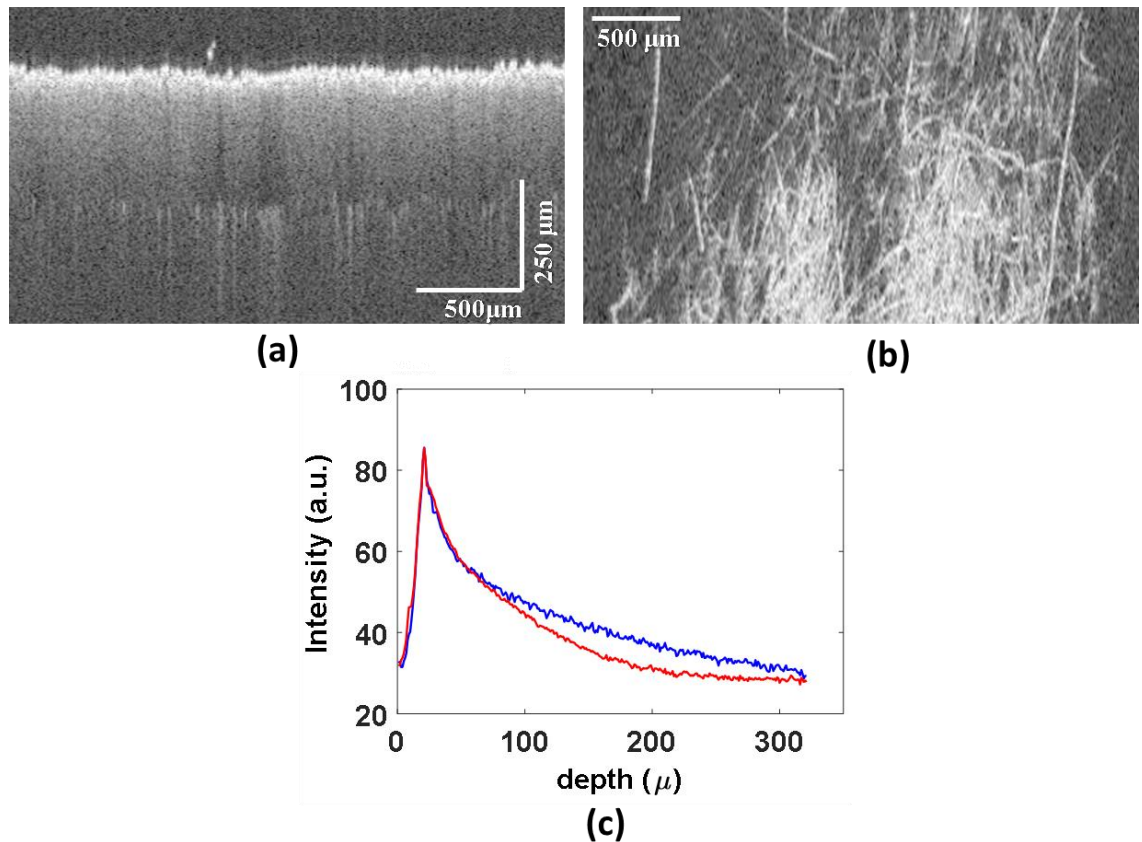


Figure 4-16 (a) OCT cross-section and (b) enface image of the long fibre paper substrate of the painting no. 67107 (RHS collection); (c) Comparison between the depth profile of the backscattered light intensity of the long fibre paper (red curve) with that of Whatman paper (blue curve).

In regards to the identification of the sizing technique and the filler content, XRF spectroscopic measurements were also performed on blank areas of the substrates. The detection of sulfur (S) in all the textile substrates was very informative about the sizing methods that had been applied, as for traditional Chinese paintings, it is common to prepare the substrate with a wash of a solution consisting of alum and animal glue [18]. Since the XRF spectrometer was used with an open beam in air without helium purging, it was only sensitive to elements with atomic number  $Z > 14$  and therefore the detection of Al was not possible. More detailed presentation of the classification of the substrates of the watercolor paintings of both collections is presented in chapter 6.

#### **4.3.1 Summary**

The combined use of OCT interferometry and XRF spectroscopy seems to give promising results about the examination of paper substrates based on the analysis of their structure and chemical composition. More specifically, OCT provides the ability of imaging in high spatial resolution and contrast, enabling the detailed observation of the structure of the substrate. Moreover, the in depth information obtained from this technique reveals information about the optical properties (i.e. scattering and absorption) of the substrate, that can be proven very important for its classification. However, given that it is a technique based on the scattering properties of the analysed material, it can face limitation when highly scattering or absorbing surfaces are attempted to be analysed. Moreover, XRF spectroscopy can provide very useful information about the chemical composition or treatment of the various substrates. However, the detection sensitivity of most of the XRF instruments is limited for elements atomic number greater than 12 making their complete elemental analysis not always possible.

## **Chapter 5:**

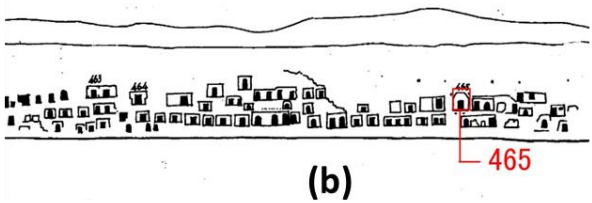
# **Multi-modal approach for the non-invasive and in situ analysis of Murals of Mogao complex in Dunhuang, China**

### **5.1 Introduction**

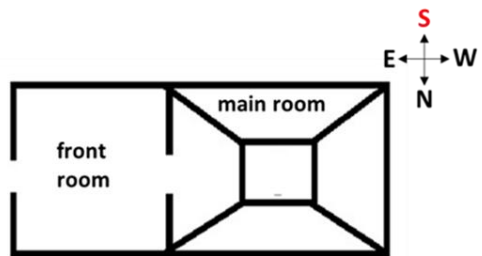
Mogao Caves (Figure 5-1), a world heritage UNESCO site near Dunhuang in Gobi desert in China, is a complex of about 750 caves, located along Silk Road, the ancient caravan routes that used to link China with the West. They were founded by Buddhist monks in the late forth century and gradually grew over the following centuries as monks, local rulers and travellers carved the cave temples with 492 of them being decorated with vibrant murals illustrating the worship of the Buddha, the succession of rulers of the area at the eastern end of the Silk Road but also containing scenes of everyday life [75] [77]. Mogao caves have a significant artistic importance as through the years of their construction, from the period of the Northern Wei Dynasty (386-534) to the Mongol-led Yuan Dynasty (1276-1386), they played a decisive role in artistic exchanges between China, Central Asia and India with the influences being reflected on the murals, the sculptures and the architecture of the monument. Moreover, the exposure of the monument to the environmental conditions of the desert makes its preservation challenging and therefore the detailed analysis of the applied painting materials and methods is necessary for the decision of the optimum conservation protocol. This work was mainly focused on the analysis of the murals of cave 465, a cave of particular interest for the art historians since its dating is a subject under debate with no clear evidences of date of construction found. The various suggestions of dates are based only on the analysis of the iconography of the murals from an art historical point of view.



(a)



(b)



(b)



(c)

Figure 5-1 (a) Mogao complex in Dunhuang, China (image: Flickr user: eviltomthai), (b) diagram showing the location of cave 465 and (c) the main room of the cave 465 (image from: <https://gesaschwantes.com/2012/09/23/mogao-cave-465-conservation-project-dunhuang-gansu-china/>)

The examination of the murals of cave 465 increased the challenges in the multi-modal, non-invasive analytical approach both because the large surface of the analysed painting area (spectral imaging of approximately 100 m<sup>2</sup> painting surface of the murals) and the complexity of the analysed painting materials (i.e. differences on the degradation level of the various paint layers). These challenges highlighted the necessity for the development of an automatic method for the post-processing of large scale spectral imaging data, but also provided a great opportunity for the investigation of the abilities of the multi-modal approach using the portable versions of the non-invasive analytical techniques illustrated in chapter 2, for the in situ analysis of complicated painting systems.

## 5.2 Materials and Methods

Figure 5-2 gives an overview of the analytical techniques. Portable configurations of all the non-invasive techniques have been used, enabling the *in situ* analysis of the murals. As the principles of operation of the various non-invasive techniques have been described in chapter 2, in this section only the special features of portable instrumentation used will be presented.

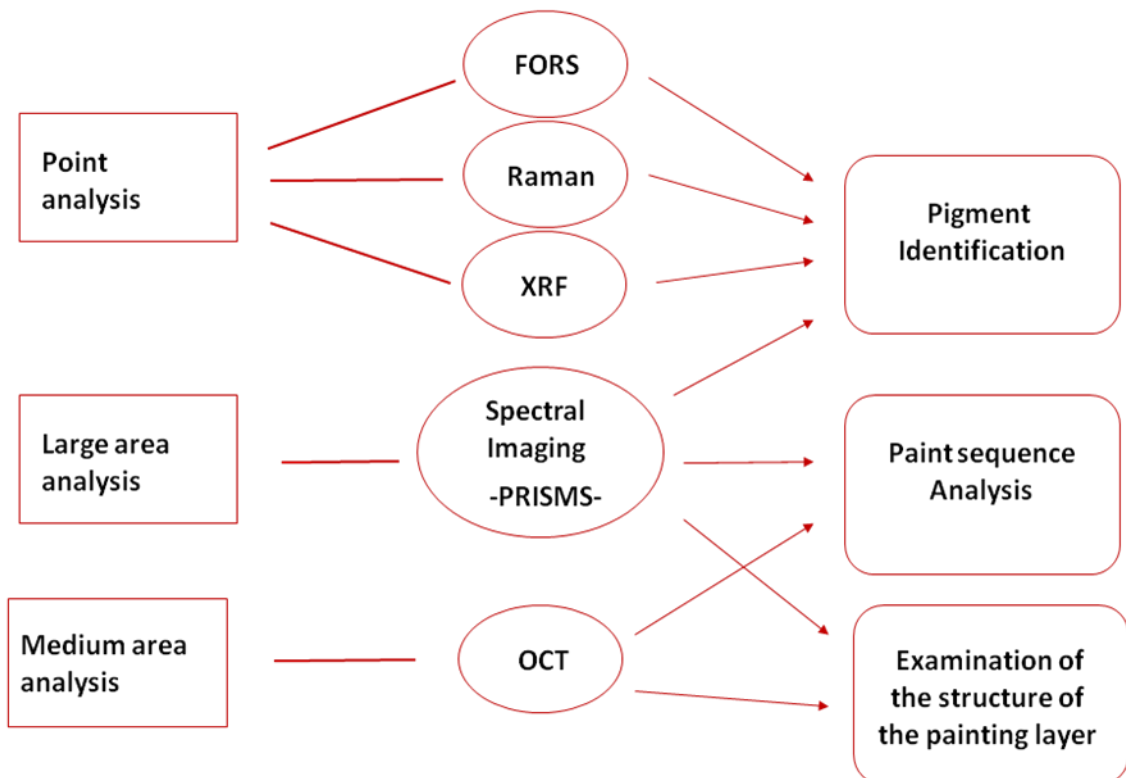


Figure 5-2 Overview of the multimodal analysis strategy

### *Spectral imaging*

PRISMS system in its version for spectral imaging in the VIS/NIR regime and the telescope configuration (Figure 2-1) was used for the preliminary examination of the murals.

### *Fibre Optics reflectance Spectroscopy (FORS)*

High-resolution reflectance spectroscopy was performed using an ASD FieldSpec spectrometer, composed by three spectrometers that cover the whole spectral range from 350 nm to 2500 nm. The spectral resolution is 3 nm in the UV/VIS regime and 10 nm in the NIR.

### ***Raman spectrometer***

Raman analysis was performed using a portable Horiba HE785 Raman spectrometer coupled with a 50x LWD (Long Working Distance) objective with the excitation laser wavelength at 785 nm and laser power of 20 mW. The laser beam was focussed to a spot approximately 30  $\mu\text{m}$  in diameter, allowing a more representative analysis of the painting layers.

### ***XRF spectrometer***

XRF results were obtained using a portable Niton XL3t XRF Analyzer spectrometer. It consists of an Au anode, with maximum voltage at 50 kV and maximum current at 200  $\mu\text{A}$ , enabling the detection of elements with atomic number  $Z > 14$ .

### ***Optical Coherence Tomography***

The OCT used is an adapted Thorlabs spectral domain OCT at 930 nm with axial resolution of  $\sim 7 \mu\text{m}$  in air and transverse resolution of 9  $\mu\text{m}$ .

### ***Reference samples***

Two different reference datasets were used in this study. ‘Reference tile #1’, which was prepared by the Dunhuang Academy, was made in such a way as to simulate the structure of most of the Mogao murals. Therefore, the mock-up consists of a mud substrate with a preparation layer of calcium carbonate ( $\text{CaCO}_3$ ) and five of the most representative pigments that have been traditionally used in China since antiquity (Table 5 -5-1) mixed with animal glue painted on top. ‘Reference tile #2’ was prepared by ShaanXi History Museum, covering a larger range of pigments, also traditionally used in China, as well as a range of different particle sizes for those mineral pigments that are traditionally graded into coarse, medium and fine particle sizes. Standard spectral reference libraries[78], [79], [79] were used for Raman analysis.

Table 5-1 Reference pigments and composition

Pigment name	Composition (major components)
<b>Reference Tile # 1</b>	
<b><u>Red</u></b>	
Iron oxide	Natural red earth
Red lead	$\text{Pb}_3\text{O}_4$
Vermilion	$\text{HgS}$
<b><u>Blue</u></b>	
Azurite (Grade 1)	
<b><u>Green</u></b>	
Atacamite	
<b>Reference Tile # 2</b>	
<b><u>Red</u></b>	
Red ochre	Natural red earth rich in iron oxide
Iron oxide	Synthetic red ochre
Red Lead	$\text{Pb}_3\text{O}_4$
Vermilion light	$\text{HgS}$
Vermilion	$\text{HgS}$
Lac dye	Sticklac soaked in warm water and filtered using cotton patches.
Cochineal dye	Cochineal insects (Kremer Pigmente) soaked in warm water and filtered using cotton patches.
Rouge	Organic red
Madder	Madder dyestuff
<b><u>Yellow</u></b>	
Realgar (Grade 1,2,3)	$\text{As}_4\text{S}_4$
Orpiment	$\text{As}_2\text{S}_3$
Orpiment (Grade 1,2)	$\text{As}_2\text{S}_3$
Yellow ochre	Natural yellow earth
Litharge	Massicot (orthorhombic $\text{PbO}$ )
Gamboge	ready-prepared paints in animal glue
<b><u>Blue</u></b>	
Azurite (Grade 1,3,5)	$2\text{CuCO}_3\text{Cu}(\text{OH})_2$
Indigo	$\text{C}_{16}\text{H}_{10}\text{N}_2\text{O}_2$ ready-prepared paints in animal glue
Indigo	Indigo and siliceous extender
<b><u>Green</u></b>	
Malachite (Grade 1,2,3,5)	$\text{CuCO}_3\text{Cu}(\text{OH})_2$
Atacamite	Synthetic, $\text{Cu}_2\text{Cl}(\text{OH})_3$
<b><u>White</u></b>	
Lead white (Cremnitz white)	$\text{PbCO}_3\text{Pb}(\text{OH})_2$
Shell white:	$\text{CaCO}_3$

## 5.3 Results

### 5.3.1 Multimodal approach for the identification of pigments

PRISMS system was used for the preliminary scanning of large painting areas of the murals extended from the ceiling and the high parts of the wall to areas on the ground level, providing spectral imaging data of high spatial resolution. The subsequent application of clustering on the pixel-level spectral information (see section 3.2), enabled the classification of the paint areas in a narrower number of groups, based on their spectral similarities. As the spectral similarity is linked with similarities in the chemical composition of the different paint areas, the results obtained by the detailed analysis of areas located on the ground level could also be extended rather safely to the pigment composition of the unreachable areas with matching spectra. For the detailed analysis of the pigments, FORS, XRF and Raman spectroscopies were used in their portable and transportable versions.

#### *Single Pigments*

During the analysis of the paint layers of cave 465 only a few areas were identified with single pigment composition. Among them, the grey/blueish background of some scenes on the South wall was identified as indigo. The KM fit on FORS spectra collected from this area gave a perfect match using a combination of indigo reference and a spectrum collected from the support layer (Figure 5-3b), while Raman spectroscopy confirmed the presence of indigo with the clear identification of its characteristic lines (Figure 5-3d). As XRF spectroscopy provides elemental information, it is not expected to assist the identification of organic colourants, such as indigo. However, the match at the elemental ratio between the XRF spectra collected from the grey/blueish areas and the preparation layer (Figure 5-3c) supported the detection of only organic colourant in the area. This is because the presence of any inorganic pigment in the area would contribute to the XRF spectrum either with additional lines or with change to the ratio of the lines in case that the pigment had similar elemental composition to the preparation layer.

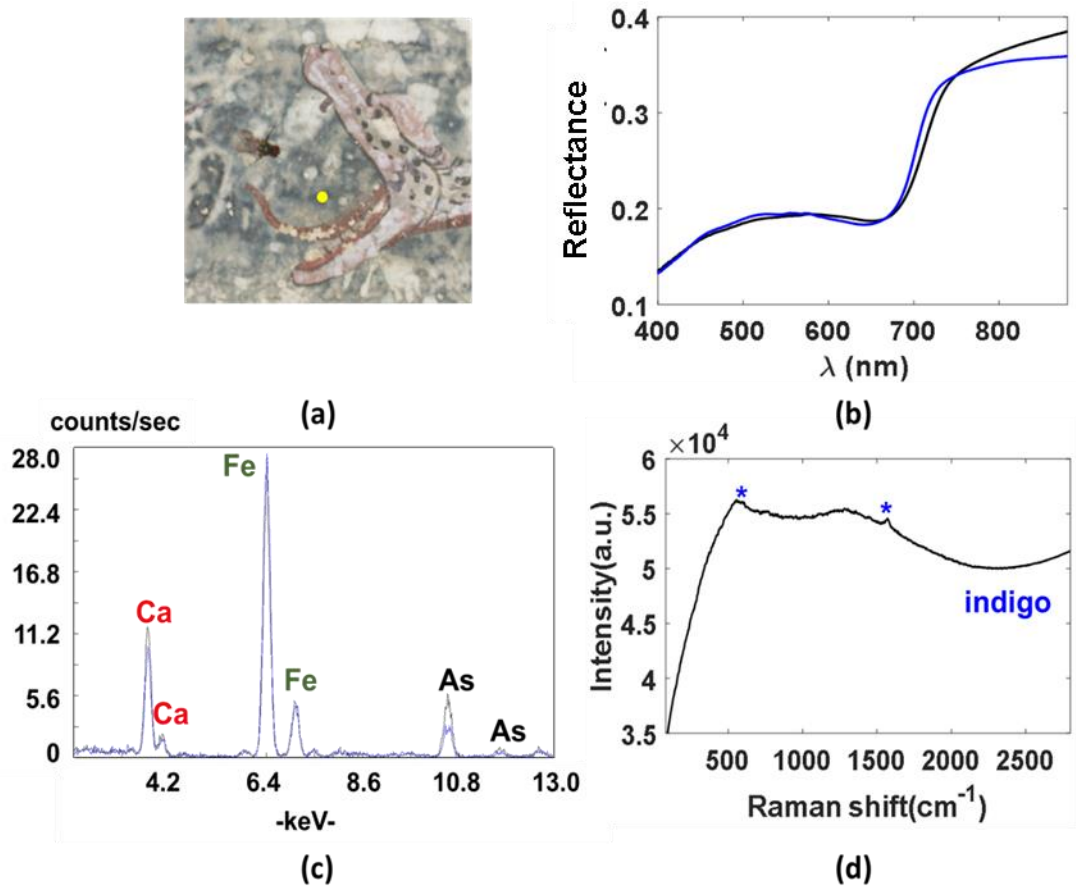


Figure 5-3 (a) Colour image derived from PRISMS data collected from the murals of the Southern wall in cave 465 of Mogao complex (yellow dot indicates the grey/blueish analysed area); (b) KM fit (blue curve) to VIS/NIR reflectance spectrum (black curve) consistent with a combination of indigo reference with the spectrum collected from the support layer; (c) XRF spectral comparison between the greyish/blue (blue curve) area and the plaster support (black curve) and (d) Raman spectrum of the same area containing the characteristic lines of indigo.

Vermilion has been identified as one of the colourants of the red areas either in single application or as part of a painting mixtures. FORS data collected from faded red areas have been fitted using vermillion reference in the KM algorithm (Figure 5-4b). Given that the analysed paint layer was faded, the imperfection of the KM fit using vermillion as reference on the spectra collected from these areas was not surprising. However, the match on the spectral position and the overall good fit are enough for the identification of the red colourants, as vermillion. XRF measurements on these areas (Figure 5-4c) detected Hg, the main element of vermillion, confirming its identification (Ca and Fe belong to the substrate). Finally, Raman (Figure 5-4d) identified clearly vermillion. It has to be noticed that in the analysis of the murals of cave 465 the spot size of the Raman instrumentation used is large (Table 2-1) and therefore the spectral contribution of the various pigments involved or even the substrate and/or any contaminants should

be expected. Therefore, the presence of the characteristic line of gypsum in the spectrum collected from these red areas was not surprising, as the paint loss of the analysed area is leaving parts of the gypsum preparation layer exposed. Moreover, additional lines at the spectral regime where the organic compounds have their lines were observed. However, it did not correspond to any of the reference organic colourants. In order to investigate further the origin of these lines, the hypothesis that they correspond to the organic binding medium of the paint layer was investigated. However, the spectral comparison between the Raman lines of the unidentified organic compound(s) and the reference Raman spectra of all the different binders did not give any match, eliminating therefore the possibility that they are present due to the binder. Given that the murals of the Mogao caves are exposed to various environmental conditions, the possibility that the unidentified Raman lines correspond to the presence of organic contaminants was also examined. Ghosal et al [80], in their study conducted to the characterisation and identification of individual spores from several species of micro-fungi, present micro-Raman spectra related to different compounds of the spores of the fungi. The position of the unknown organic lines of the Raman spectra collected from the murals of cave 465 matches with the lines corresponding the amino acid and lipid bands of the various spores of fungi, suggesting therefore that they are indicative of the fungal contamination of the murals. However, further investigation of the origin of these lines would be interesting with the collection of more Raman spectra from different areas, both painted and unpainted being required.

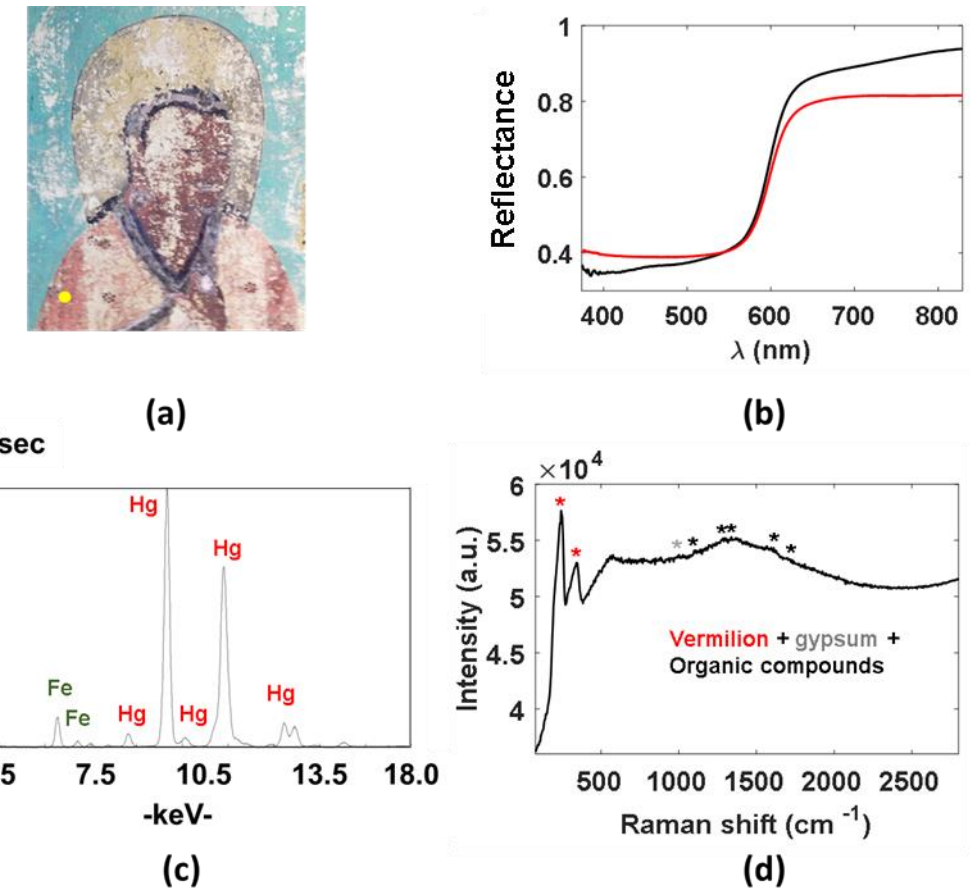


Figure 5-4 (a) Colour image derived from PRISMS data collected from the murals of the Southern wall in cave 465 of Mogao complex (yellow dot indicates the faded red analysed area); (b) KM model fit (red curve) using a vermilion reference to the measured VIS–NIR reflectance spectrum (black curve); (c) XRF spectroscopy found mainly Hg and (d) Raman measurement for this area detects vermilion, gypsum and lines of organic compounds (probably fungi)

Even though no large yellow areas are observed on the murals in cave 465, some small yellow decoration dots enabled the identification of the yellow colourant. The fact that the analytical area of the reflectance spectrometer was significantly larger than the size of the yellow dots resulted to not clear spectra, that were dominated from the contribution of the surrounding area (the spectra are not illustrated). XRF spectroscopy (Figure 5-5c) detected As as the major element, with Hg most probably be detected from the neighbouring Hg-containing area due to the large spot size of the instrument, whereas Ca and Fe belong to the support. Finally, the application of Raman spectroscopy on the dots provided a clear identification of orpiment (Figure 5-5b).

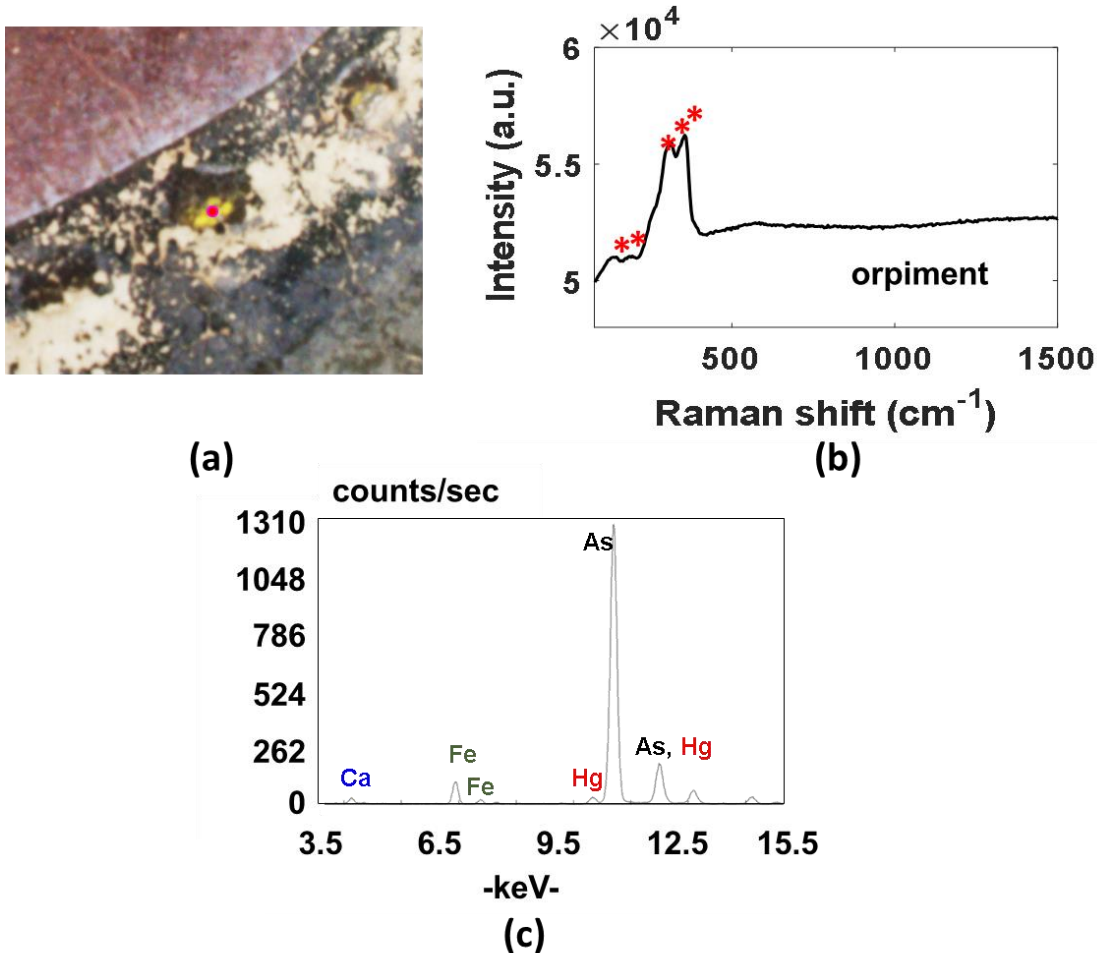


Figure 5-5 (a) Detail from colour image derived from PRISMS data collected from the murals of the Southern wall in cave 465 of Mogao complex (magenta dot indicates the yellow analysed area); (b) Raman measurement detected orpiment and (c) XRF spectroscopy found As as the predominant element and traces of Hg, Ca and Fe

Two hues of green colour were observed on the murals of cave 465, light/vivid and a dark green (see '*Multiple pigments*'). XRF measurements performed on the light/vivid green areas (Figure 5-6b) identified Cu as the major element, but also detected traces of Ca, Fe, Cl and Pb, with Ca and Fe being elements of the support. The detection of Cl exclusively in the Cu-containing green areas, suggests the presence of a Cu-chloride pigment. FORS measurements on the same areas indicated the present of Cu-containing pigment. However, the spectral similarities of the various Cu green pigments in the VIS/NIR and near-IR spectral regimes (Figure 5-6d) are not enabling their precise distinction. In principle, Raman spectroscopy can provide precise distinction between the different Cu-based green pigments, enabling the precise identification of the Cu-containing pigments and their polymorphs. However, the excitation laser beam of the

spectrometer used in this study is at 780 nm where Cu-based greens are not good scatters and therefore no Raman signal was obtained.

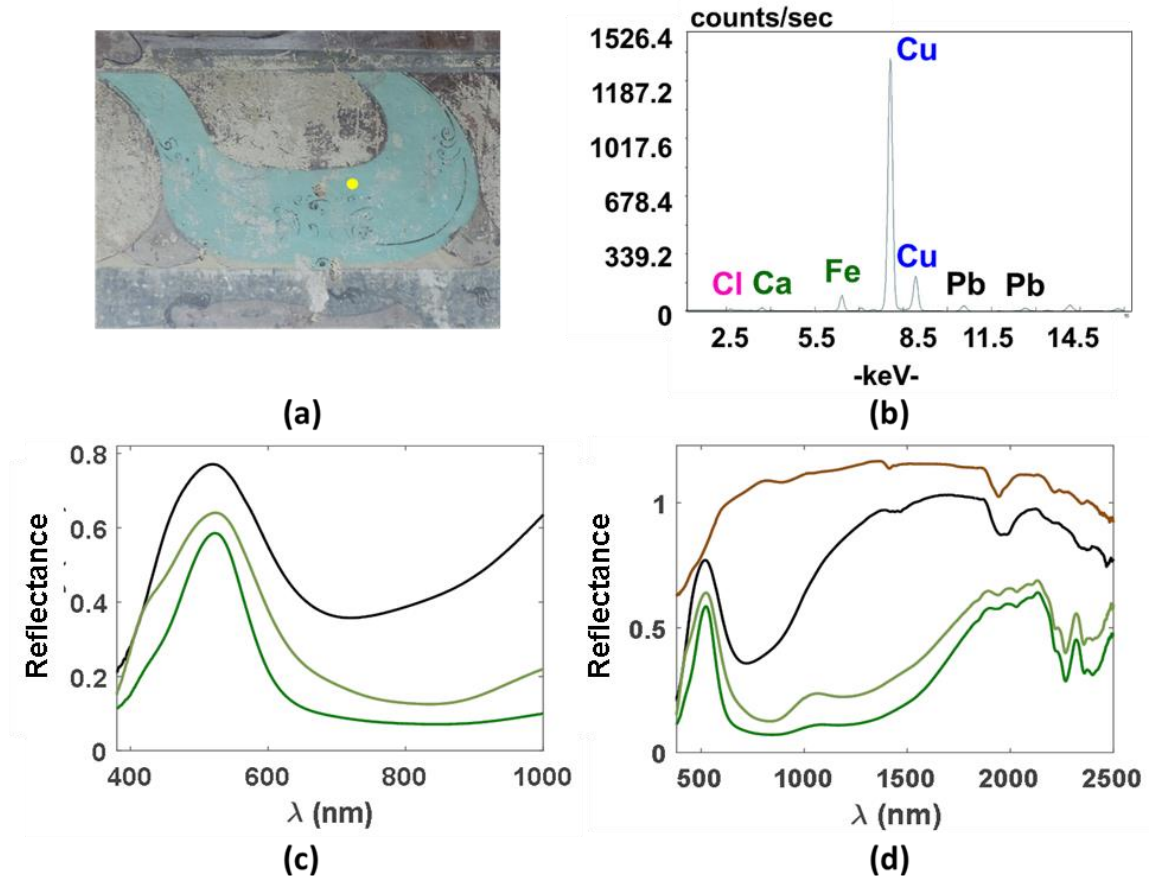


Figure 5-6 (a) Colour image derived from PRISMS data collected from the murals of the Southern wall in cave 465 of Mogao complex (yellow dot indicates the green analysed area); (b) XRF measurement detected Cu as the predominant element with traces of Ca, Fe, Pb and Cl being present as well; comparison between reflectance spectra collected from the analysed area (black curve) and the atacamite (light green curve) and malachite grade 1 (dark green curve) references in the (c) VIS/NIR and (d) VIS/NIR and near-IR regimes, with the plaster support (brown curve) being illustrated as well. The spectra are shifted for clarity.

### *Multiple pigments*

During the analysis of the murals in cave 465, the majority of the paint areas were identified to consist of multiple pigments, with some of the combinations being particularly interesting as they do not belong to the traditional Chinese painting recipes.

Vivid blue areas were observed on the murals of cave 465. XRF spectroscopic analysis identified them as Cu-containing, with the detected traces of Ca, Fe and Pb belonging to the substrate (Figure 5-7c). KM fit on reflectance spectra collected from these areas, in

the VIS/NIR range, gave perfect match using a combination of azurite and indigo as references (Figure 5-7b). The extension of the reflectance spectral observation in the near-IR regime showed that the characteristic lines of azurite at 2284 and 2354 nm are also present in the collected spectra (Figure 5-7c inset), confirming its identification. Raman spectra collected from the same blue areas (Figure 5-7d) confirmed clearly the detection of indigo, with the characteristic Raman lines of azurite being also present. The presence of the line of gypsum in the Raman spectrum indicated the spectral contribution of the support.

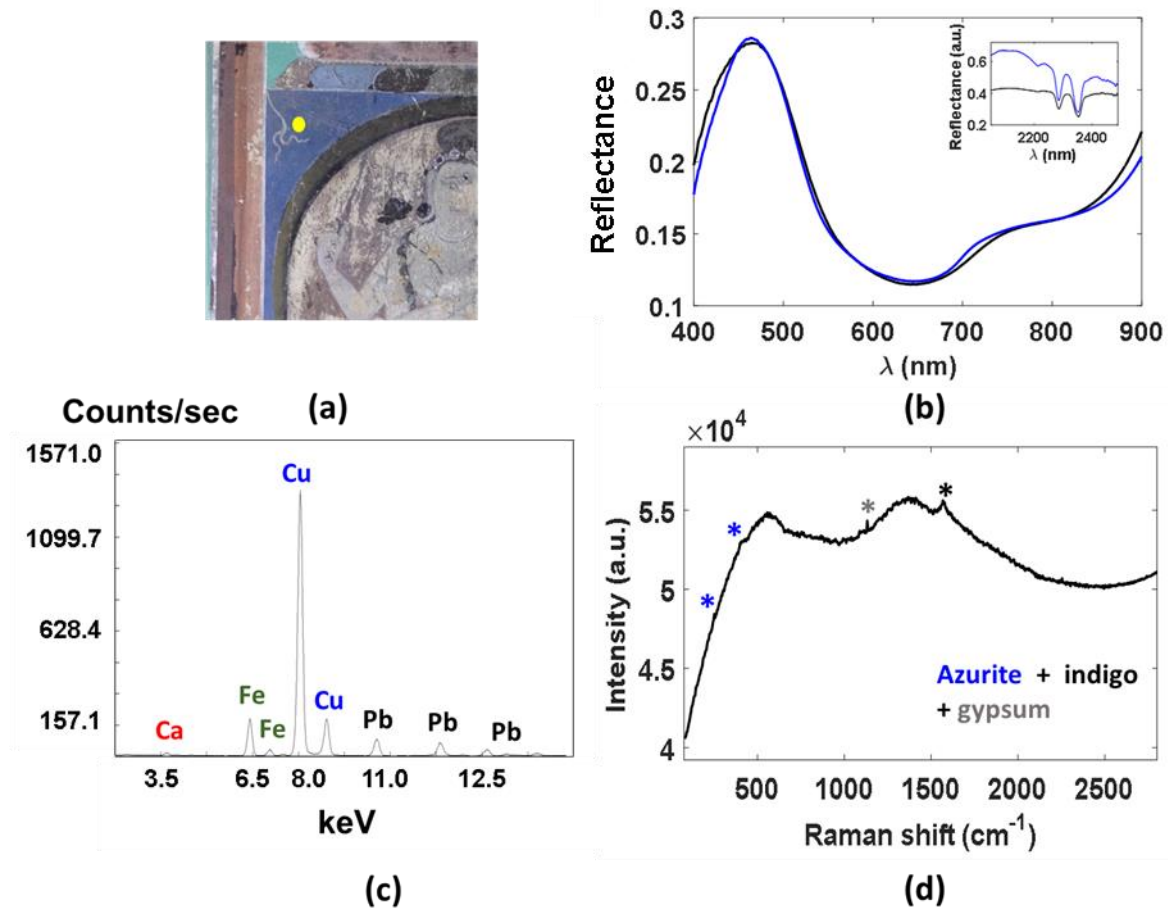


Figure 5-7 (a) Colour image derived from PRISMS data collected from the murals of the Southern wall in cave 465 of Mogao complex (yellow dot indicates the blue analysed area); (b) the best fit to the VIS-NIR reflectance measurement (black curve) using the KM model (blue curve) was with a mixture of grade 1 azurite with indigo; (c) XRF spectrum detected Cu as the predominant element and (d) Raman measurement for this area detected azurite, indigo and gypsum [inset: spectral comparison between the blue area of the murals in cave 465(black curve) and the azurite reference (blue curve)].

Although the use of single orpiment was localised on the tiny decoration dots, the analysis of the paint layer of the murals identified it as part of various paint combinations. More specifically, orpiment was combined with red lead in the

orange/skin colour areas (see section 4.1.2.4) but also in combination with indigo in the dark green areas. KM algorithm gave a very good fit to reflectance spectra collected from dark green areas using reference spectra of indigo and the support layer (Figure 5-8b). XRF spectroscopic results showed that As is the major element on these areas (Figure 5-8c), XRF spectroscopic results showed that As is the major element on these areas (Figure 5-8c), with Ca and Fe belonging to the support layer. Raman spectroscopy identified indigo and orpiment in the green mixture (Figure 5-8d).

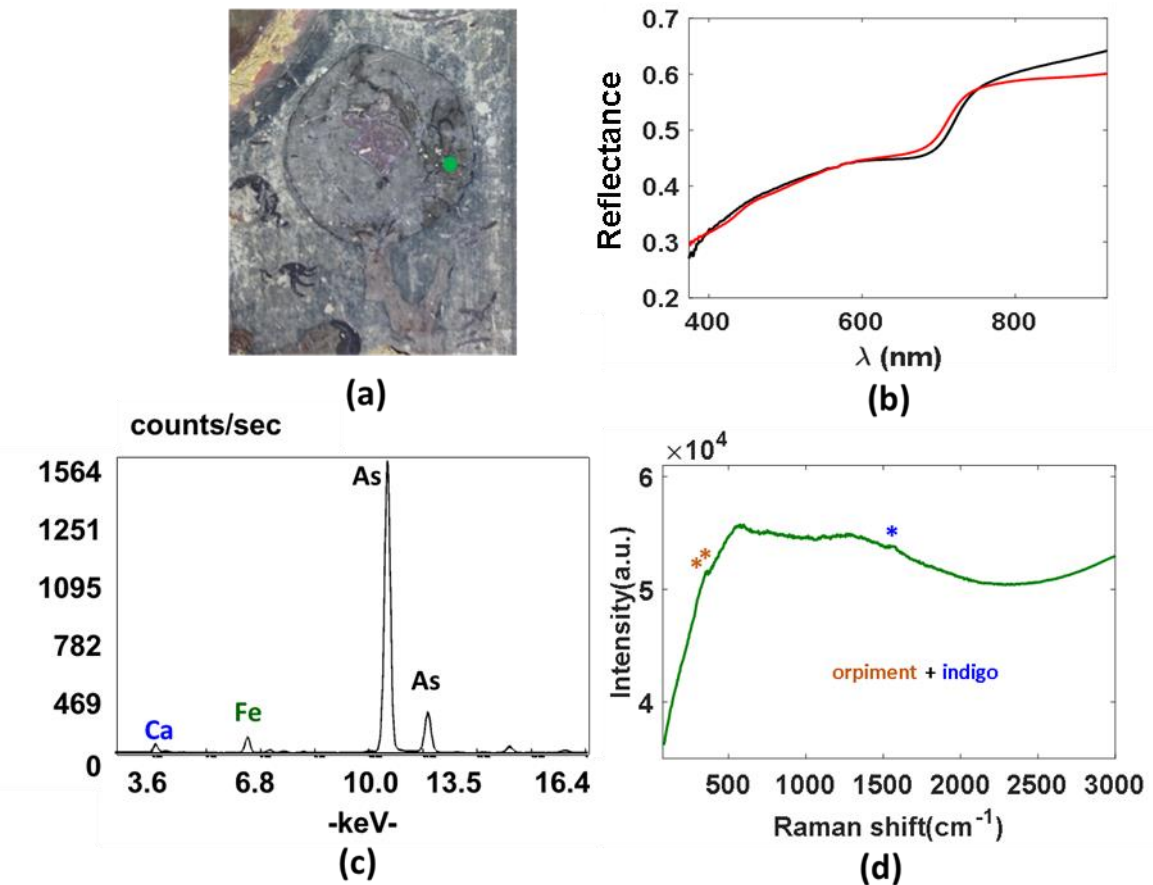


Figure 5-8 (a) Colour image of a detail of the murals of the Southern wall in cave 465 of Mogao complex (green dot indicates the dark green analysed area); (b) KM fit (red curve) on the reflectance spectrum collected from the dark green area (black curve) using a mixture of indigo and orpiment, (c) XRF measurement from this area detected As as the major element, with Ca and Fe belong to the substrate; (d) Raman spectroscopy identified both orpiment and indigo.

Furthermore, orpiment was detected in mixtures with vermillion as well as in paint mixtures with vermillion and red lead. However, the weathering of the murals and their exposure to the environmental conditions (e.g. fungal contamination) as well the

chemical interaction between certain pigments have led to degradation/deterioration of these areas and these are discussed in the next session.

### *Degraded pigments*

During the examination of the murals in cave 465, a lot of areas were found to consist of degraded pigment(s). Although both their degradation products and mechanisms have been extensively examined in the past, the studies have been performed mainly using invasive analytical techniques [81]–[83]. Even in cases where non-invasive analytical techniques, such as RAMAN and FTIR spectroscopies were used, their application was performed on samples detached from the original artwork and more specifically on cross-sections of them [84]–[86]. The challenge in this study was therefore the detailed examination of the degraded paint areas by non-invasive, *in situ* measurements. The degradation of the painting materials results to chemical changes of the original painting layers and therefore alterations on their spectral features. In these cases, the interpretation of the analytical results acquired by the individual techniques is usually difficult making the multi-modal approach necessary.

Extended studies on the degradation of the pigments have shown that it can be caused due to various reasons extending from their interaction with other pigments to their exposure to different environmental factors, such as daylight or humidity. The scenario of degradation due to the presence of humidity is more likely in the case of Mogao caves as they are constructed on the side of a cliff, so humidity coming from the ground could have transferred through the wall to the paint layer, enabling the development of micro-organisms which caused the degradation of the paint layer. Studies have been conducted in the past examining the presence of micro-organisms, showing that their development can cause deterioration throughout the mural, from the substrate to the paint layer. According to the literature, the existing micro-organisms due to the presence of humidity in the caves can be divided into two groups: the lithotrophic and the heterotrophic [87]. For the development of the first group, no organic material presence is required and therefore they are usually related to the deterioration of the substrate of the murals. Heterotrophic micro-organisms, on the other hand, need organic material for their growth and they are therefore related to the degradation of the pictorial layer. The presence of certain groups of micro-organisms has been proven to cause chemical

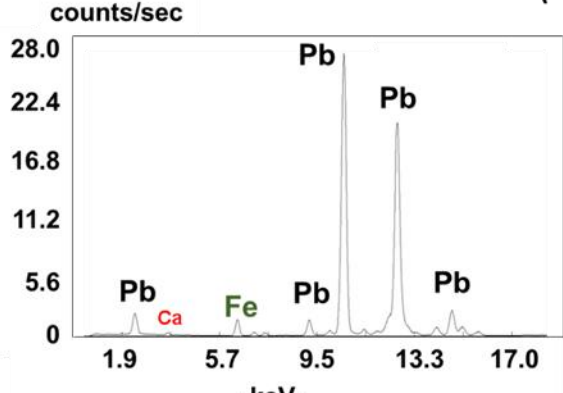
alterations of minerals, including some pigments like orpiment and lead-containing ones, through oxidization [88]. Therefore, the presence of bacteria and fungi on a mural can cause its degradation which can be translated to either altering the stability of both the substrate and the paint layer or the discolouration of the pigments.

### ***Degraded Lead areas***

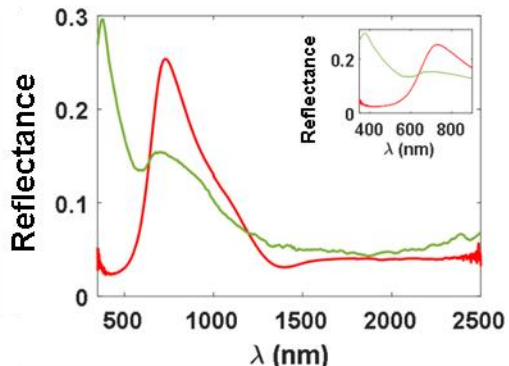
During the examination of the murals of cave 465 a lot of areas of different colours, from purple to bluish and brown (Figure -5-9a), had similar reflectance spectra (Figure 5-9d) despite their colour differences. However, these spectra were not corresponding to any known historic artist pigment. Given that XRF spectra collected from these areas showed that Pb is the major element (Figure 5-9a), the possibility of these unknown spectral features being related to the presence of degraded Pb-pigment(s) was examined. The degradation products of Pb-containing pigments, such as red lead and lead white, have been identified as plattnerite ( $PbO_2$ ) or galena ( $PbS$ ) and their production is related to different environmental conditions. More particularly, plattnerite is the degradation product of the interaction of lead-containing pigments with the air as well as with micro-organisms, such as bacteria or fungi, while galena is produced due to the reaction of the lead-containing pigments with sulphur-containing pollution or pigments such as orpiment or realgar [88]. The comparison between the reflectance spectra of plattnerite, artificially produced in NTU laboratories, and galena, with the spectrum obtained from USGS Digital Spectral Library [89] showed that they have distinct spectral features in the VIS/NIR regime (Figure 5-9c), enabling therefore their distinction and identification using reflectance spectroscopic measurements in this regime. Consequently, the spectral similarity of the reflectance data collected from the various Pb-containing areas to the plattnerite reference (Figure 5-9d) led to the conclusion that the degradation product is plattnerite.



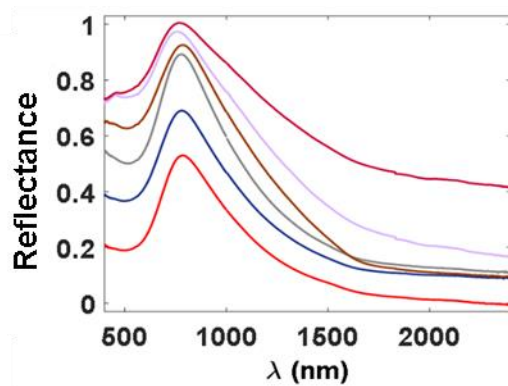
(a)



(b)



(c)



(d)

Figure -5-9 (a) Purple, Bluish/ Black, burgundy, brown and grey areas from the murals in cave 465 with similar reflectance spectral features. (a) XRF spectra collected from these areas showed that Pb is the major element, while Ca and Fe are elements belonging to the substrate. (b) Spectral comparison between artificial made  $\text{PbO}_2$  (red curve) and reference spectrum of galena (green curve) in the whole VIS/NIR and near-IR range [caption: zoom- in of the spectral comparison in the VIS regime] (c) spectral comparison between burgundy (burgundy curve), lilac (lilac curve), brown (brown curve), grey (grey curve), bluish black (blue curve) Pb-containing areas (correspond to the areas in (a)) of the murals of cave 465 of Mogao complex.

The predominant presence of plattnerite in almost all reflectance data collected from these areas, made the identification of the other pigments involved challenging. However, the multi-modal analysis of these areas as well as the combined interpretation of the obtained results, enabled the revealing of very interesting information regarding the original combination of pigments, giving sometimes an indication for the painting

sequence. In this section, the analysis of some of the most interesting cases of degraded Pb-containing areas is illustrated.

#### ***Burgundy area on the east panel of the Southern wall***

The reflectance spectra collected from a burgundy area showed a dominating presence of plattnerite (Figure 5-10b) that resulted in the masking of the features of any other pigments. However, XRF spectroscopy (Figure 5-10c) additionally to the detection of Pb as the major element of the area, also found traces of Hg, indicating the presence of vermilion. Raman spectroscopic analysis of the same area (Figure 5-10d) confirmed the presence of both vermilion and plattnerite and moreover detected lines of red lead and gypsum. The detection of pure red lead using Raman spectroscopy was not surprising as optical microscopic observation, under high magnification, in studies conducted on the examination of the degradation of red lead layers on manuscripts, has shown that their degraded surface is textured and heterogeneous, leaving exposed particles of the originally used pigment [88]. Therefore, the original paint combination is assumed to consist of red lead and vermilion. It has to be mentioned that the Raman spectroscopy detected again the presence of the lines related to organic compound, most probably fungi. Given that the main reason for the degradation of the Pb-containing pigments into plattnerite is the presence of fungi, the presence of intense lines indicating their presence is not surprising.

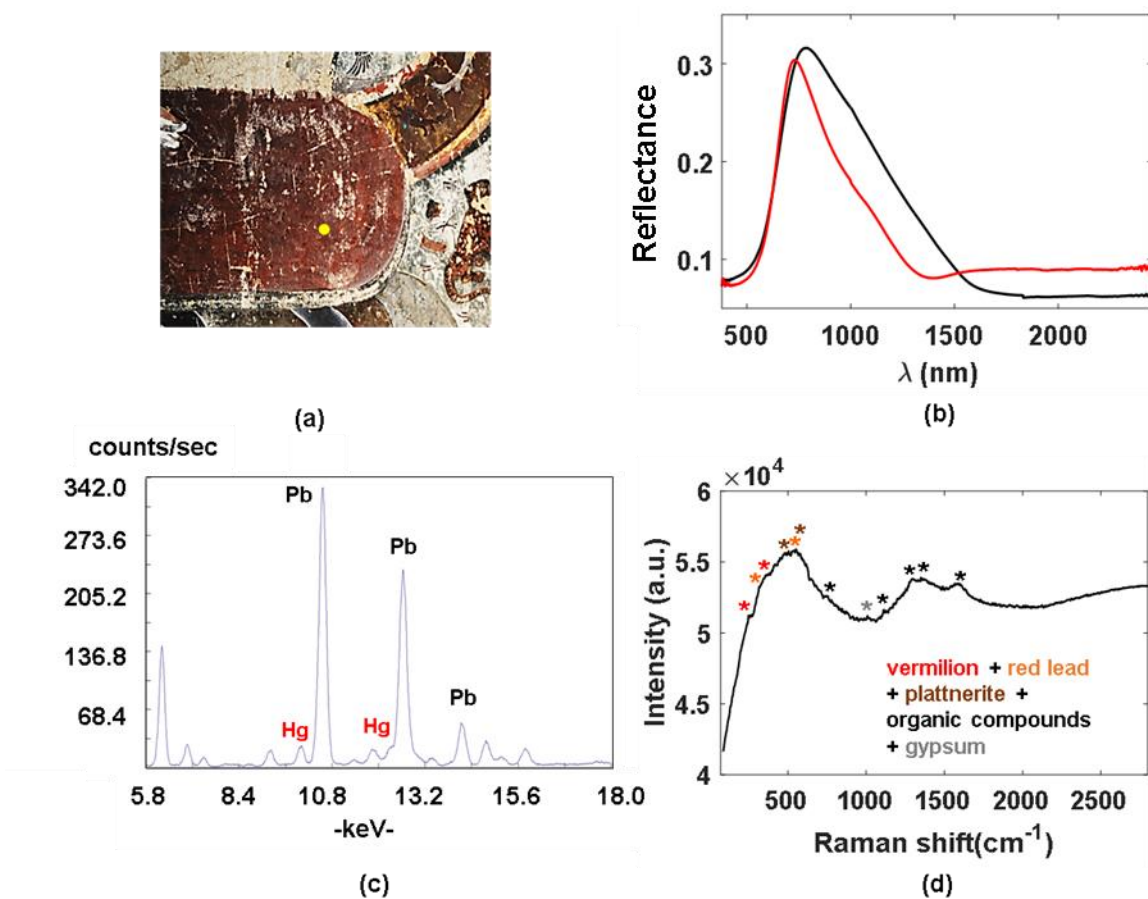


Figure 5-10 (a) Colour image of a detail of the murals of the Southern wall in cave 465 of Mogao complex (yellow dot indicates the reddish/ burgundy analysed area); (b) Reflectance spectrum collected from the burgundy red area (black curve) compared with the spectrum of the artificial produced  $\text{PbO}_2$  (red curve). c) XRF measurement from the same area shows that the main elements are Pb and Hg. d) Raman spectroscopy detects lines of vermillion, red lead, plattnerite, organic compounds (probably fungi) and gypsum.

#### *Reddish/ Brown area on the middle panel of the Southern wall*

The KM fit on reflectance spectra collected from a reddish/brown area showed that vermillion is the main component in the paint mixture. However, the KM fit was not perfect indicating the presence of a highly absorbing or transparent compound. Further spectral observation in the near-IR regime showed a mismatch between the spectrum collected from this area and the reference spectra of both vermillion and the substrate, as it drops at around 1400 nm (Figure -5-11), with only the spectrum of plattnerite, among the reference list, having similar spectral drop in this regime. The presence of plattnerite in the analysed area explains also the mismatch of the KM fit, as it is a highly absorbing compound. XRF and Raman spectroscopic measurements confirmed the presence of vermillion and plattnerite, while Raman also detected red lead, leading to the conclusion

that the original mixture used in these areas was a combination of vermillion and red lead. The intense organic lines, related to the presence of fungi, were also detected in this area.

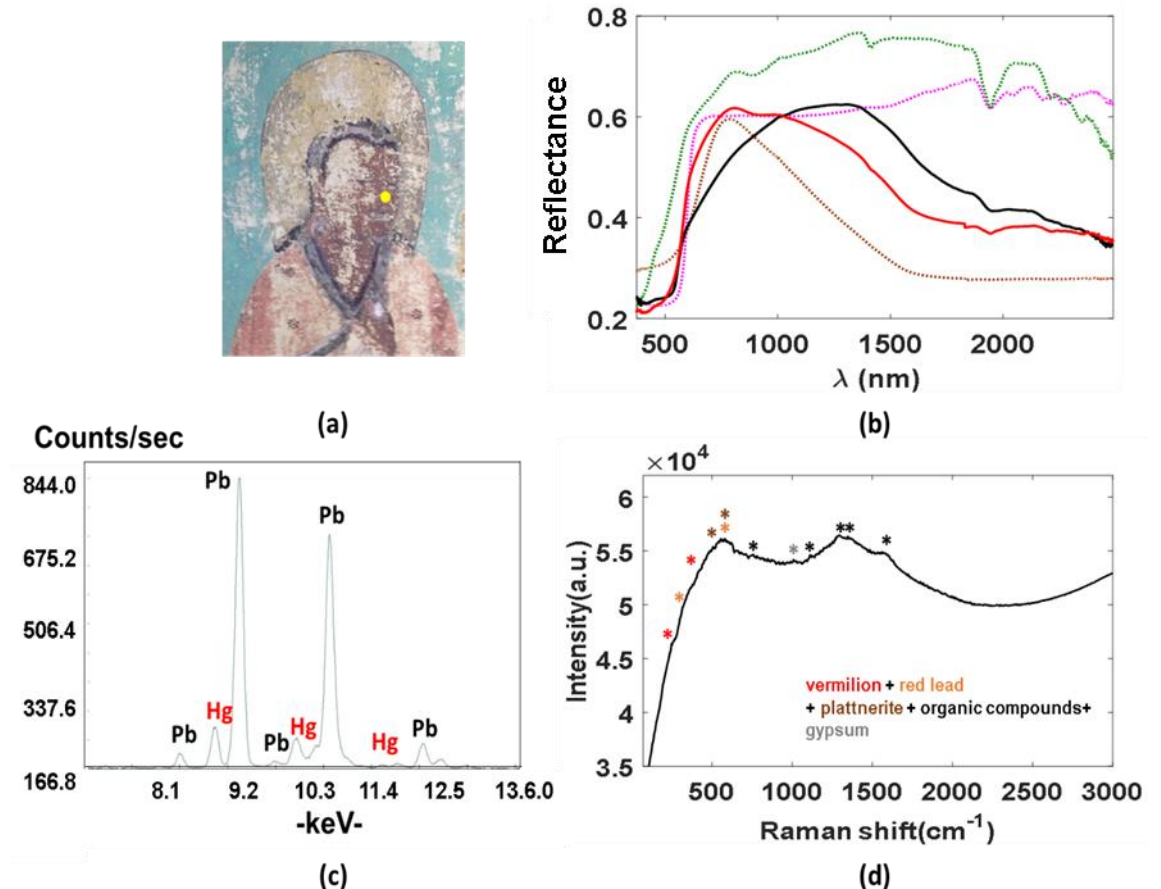


Figure 5-11 (a) Colour image of a detail of the murals of the Southern wall in cave 465 of Mogao complex (yellow dot indicates the reddish/ brown analysed area); (b) KM fit (red curve) on the reflectance spectrum collected from the reddish/brown area (black curve) using vermillion and plattnerite, compared with reference spectra of vermillion (magenta dotted curve), artificial  $PbO_2$ . (brown dotted curve), and the substrate (green dotted curve) references. (c) XRF measurement from the same area shows that the main elements are Pb and Hg. d) Raman spectroscopy detects lines of vermillion, red lead, plattnerite, organic compounds (probably fungi) and gypsum.

The differences between the reflectance spectra collected from the burgundy and the reddish brown areas, despite the similarities on their composition, probably suggest the use of different concentrations of the pigments in the original paint mixtures or differences in application method with the vermillion being applied on top of the red lead and therefore its presence being more intense in the spectrum (Figure -5-11b).

### Purple area on east panel of the Southern wall

The reflectance spectra of the analysed purple areas were dominated by the presence of plattnerite in the whole spectral range, not enabling the identification of any other pigment (Figure 5-12b). A thorough examination of XRF spectra collected from the same areas showed the coexistence of Pb and As but also the presence of traces of Hg (Figure 5-12c). Moreover, Raman analysis detected vermillion, orpiment, red lead, plattnerite, gypsum, as well as the organic lines that most probably correspond to fungi.

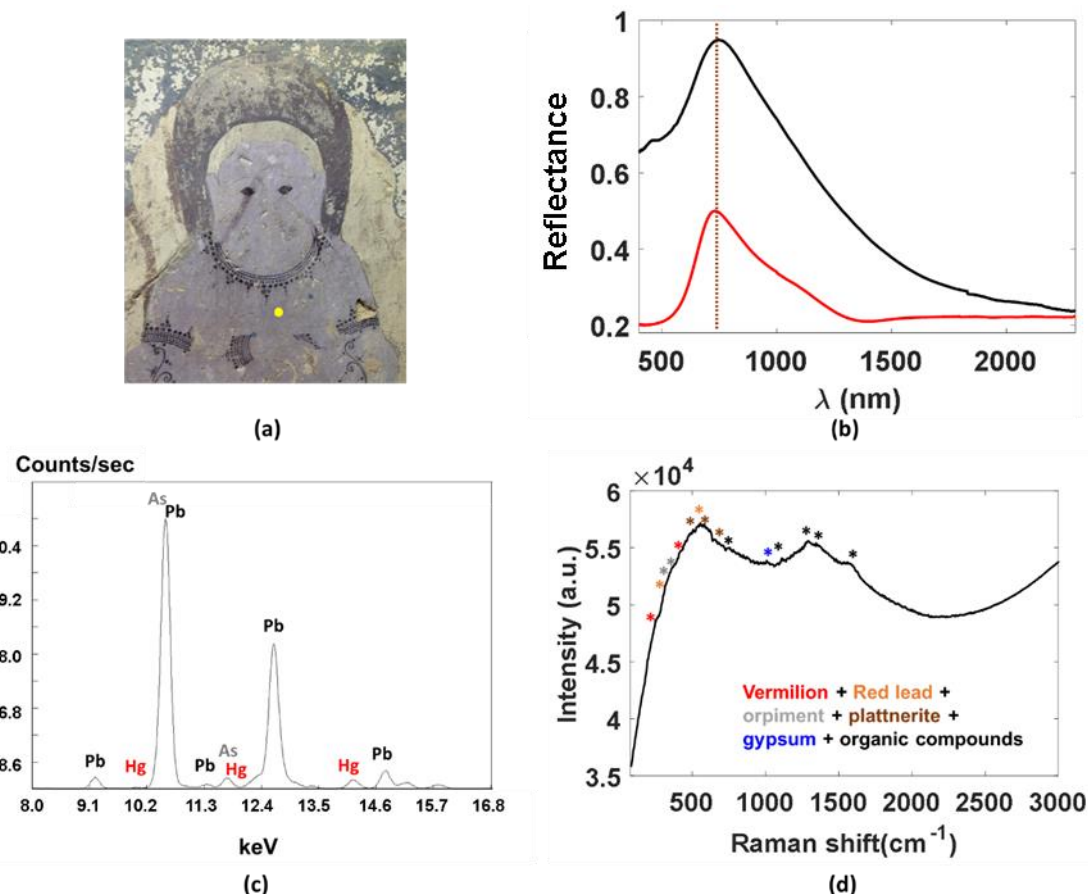


Figure 5-12 (a) Colour image of a detail of the murals of the Southern wall in cave 465 of Mogao complex (yellow dot indicates the purple analysed area); (b) Spectral comparison between FORS spectrum collected from this area and plattnerite reference; (c) XRF measurement from the same area shows that the main elements are Pb and As, with traces of Hg being detected as well. (d) Raman spectroscopy detects lines of vermillion, red lead, orpiment, plattnerite, gypsum and organic compounds (probably fungi).

Studies on the degradation of vermillion have shown that its main degradation products are metacinnabar and mercury chloride, with black and white colour respectively, resulting to a black or grey appearance of the degraded paint layer [88]. However, a lilac colour has been observed as well in cases that the degraded top black layer is thin and

therefore the pure vermilion of the bottom contributes to the colour at the surface. Therefore, regarding the purple areas of the murals in cave 465, it can be assumed that plattnerite is forming a thin, almost black, top layer offering the same visual effect as the metacinabar does in the case of the studies conducted on paint layers containing degraded vermilion. The fact that red lead was also detected, led to the conclusion that red lead was the original Pb-based pigment used. The conclusion that is drawn for the original paint sequence is that a layer of vermilion was applied first, with a red lead-containing layer being applied on top, with orpiment not being sure whether is present on the top or the bottom paint layer.

#### ***Blueish/ Black area on east panel of the Southern wall***

The XRF spectra collected from blueish/ black areas (Figure -5-13b) were dominated by Pb, but also containing Cu and traces of Hg. Analysis on the red paint layer next to and underneath the blueish/black petal, showed that it consists of vermilion. Therefore, it was assumed that the trace Hg in XRF belongs to the bottom paint layer and the petal consists of azurite and plattnerite. Raman spectroscopic measurements on this area detected only lines of red lead and plattnerite, without however detecting any lines of vermilion. Raman spectroscopy does not penetrate as deep as XRF and therefore is less likely to be affected by the composition of the paint layer below. Therefore, the fact that Raman did not detect vermilion supported the scenario that vermilion belongs to the bottom layer and that the bluish/black paint layer consisted originally of a combination of red lead and azurite. The KM algorithm fitted the reflectance spectra collected from these areas with a combination of plattnerite and azurite references (Figure -5-13c), without however giving a perfect match. The fact that the individual reference spectra match the two peaks of the spectrum collected from the bluish/black area, while their combination in the KM algorithm is not giving as good of a fit, revealing again the limitations that the KM method has when highly absorbing components, such as plattnerite, are involved (see 2.2). The spectral observation in the near-IR regime showed that the spectra collected from the bluish/black area contain the characteristic lines of azurite at 2285 and 2351 nm (Figure -5-13d) confirming further its presence.

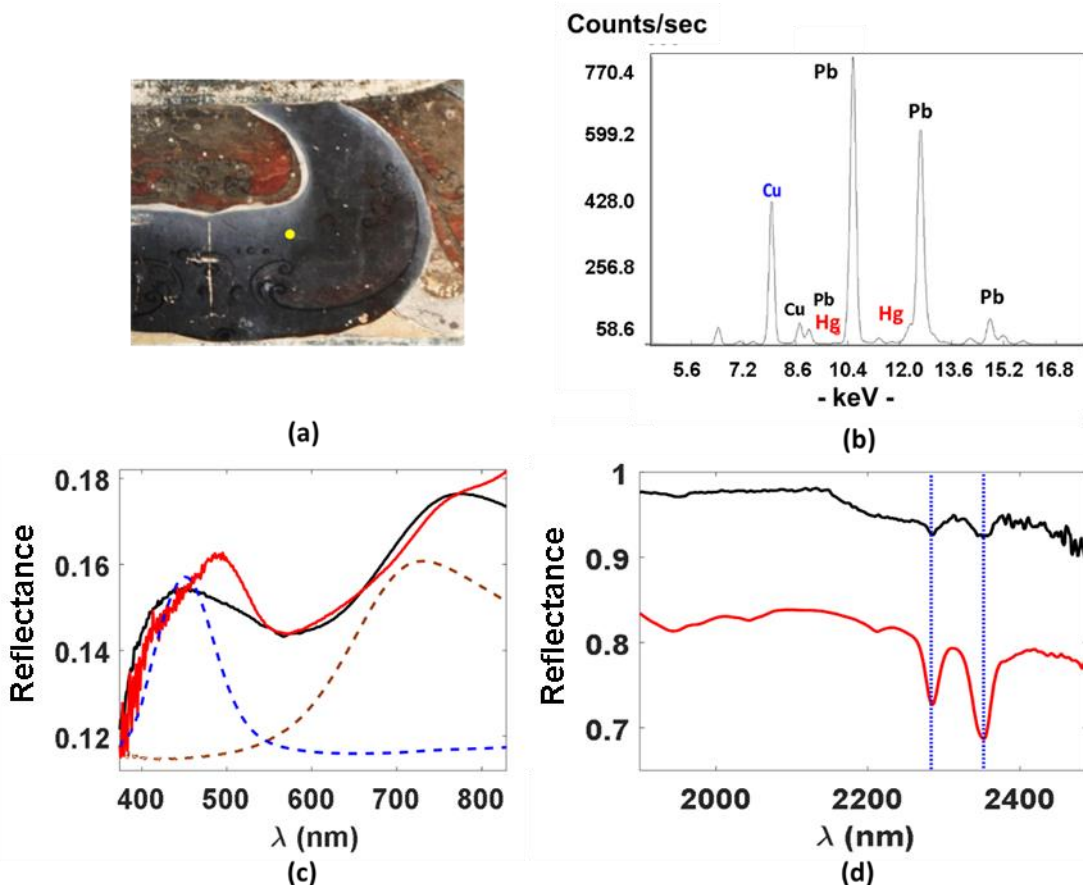


Figure 5-13 (a) Colour image of a detail of the murals of the Southern wall in cave 465 of Mogao complex (yellow dot indicates the black/bleuish analysed area); (b) XRF measurement from the same area shows that the main elements are Pb and Cu, traces of Hg are detected as well; (c) KM fit (red curve) on the reflectance spectrum collected from the Blueish/ black area (black curve) using azurite and plattnerite, compared with reference spectra of azurite (light blue dotted curve), and artificial PbO<sub>2</sub>. (brown dashed curve) references; d) Reflectance spectroscopic observation in the NIR regime detects the characteristic lines of azurite (positions highlighted with the vertical blue dashed lines).

The combination of red lead and azurite has been reported also in previous studies conducted on the analysis of murals from Tangut and Yuan periods. More specifically, X-ray Diffraction (XRD) measurements applied on black samples collected from the murals detected the mixture of plattnerite with azurite, with the original colour supposed to be a combination of red lead and azurite in order to achieve a purple colour. The presence of gypsum was also noticed in the Raman spectra of the bluish/ black areas (not presented), with more intense lines in the whitish parts. Such strong lines can probably be an indication of the degradation cause, as it seems that gypsum, main component of the substrate, has been carried by the water coming from the sandstone and possibly crystallized on the surface.

### **Degraded Arsenic areas**

During the analysis of the murals in cave 465 a number of areas with cracked or detached paint layer were observed, with their XRF spectra being dominated by the presences of As. This was not surprising, as extensive studies regarding the degradation of the As-containing pigments, have shown that they are quite unstable in paintings. More specifically, As-containing pigments are sensitive to photo-degradation, but humidity can propagate their degradation as well. Studies conducted on the analysis of samples collected from degraded As-containing oil paintings [84] have shown that the degradation products of the As-pigments are migrating throughout the multi-layered paint system, due to their solubility in water, with the resulted chemical alterations of the paint layer often leading to physical alterations, resulting in a transparent, whitish, friable and sometimes crumbling paint layer. Both the fragility and the transparency of the As-containing paint layers were observed on the murals of cave 465, leading to the conclusion that they may consist of degraded arsenic pigments. Photo-degradation of the analysed painting areas is unlikely, given that they belong to the murals of the main room of the cave that is not exposed to light (Figure 5-1b).

As mentioned before, the degradation of As-containing pigments results in both structural and chemical alterations of the original paint layer, with the main degradation product being the arsenic trioxide ( $\text{As}_2\text{O}_3$ ).  $\text{As}_2\text{O}_3$  is a whitish compound with its identification on artificial sample being possible using Raman spectroscopy. The fact that no  $\text{As}_2\text{O}_3$  was detected during the Raman examination of the degraded As-containing areas of the murals of cave 465 was not surprising, as its identification in real artworks is difficult even using bench top instrumentation. Studies conducted on the analysis of degraded paint layer of illuminated manuscripts showed that the detection of  $\text{As}_2\text{O}_3$  was not possible on the analysis of their degraded As-containing areas [88]. In studies about the analysis of samples collected from degraded As-containing paint layers of easel paintings [86], the use of synchrotron radiation techniques was proposed in order to overcome the difficulties on the detection of  $\text{As}_2\text{O}_3$ .

## Detached paint layers

The presence of detached As-containing paint layers was observed in different parts of the murals of cave 465. One characteristic example was the detachment of red As-containing paint layers leaving the underneath off-pink areas exposed (Figure-5-14a). OCT scanning on these areas confirmed the fact that the red layers are superposed on top of the off-pink ones, supporting the theory of the detachment of the red paint layer.

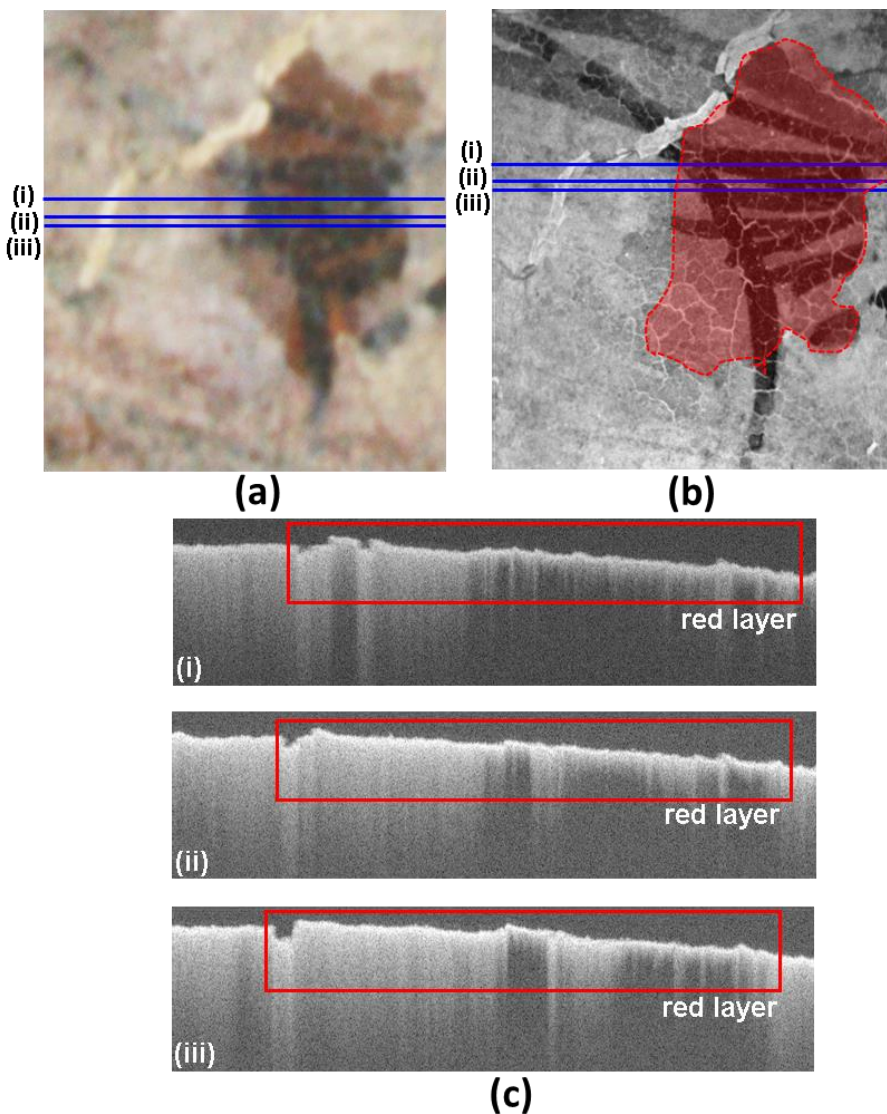


Figure 5-14 (a) Colour image of a detail of the murals of the Southern wall in cave 465 of Mogao containing off-pink and red paint areas and (b) the corresponding ‘en-face’ OCT image, with the blue lines indicating the areas where various ‘virtual’ cross-sections were taken; (c) the corresponding ‘virtual’ cross-sections that show that the red paint layer is applied on top of the off-pink area.

Interestingly, the spectral analysis of these areas, additionally to the identification of their pigment composition, illustrated influence of the paint detachment in the results of all different spectroscopic techniques. KM fit on FORS measurements collected from both off-pink and red areas were consistent with a combination of vermillion and indigo (Figure 5-15d), with the presence of indigo more intense in the off-pink parts (Figure 5-15c). It has to be mentioned that the background of these painting areas was identified as indigo-containing (Figure 5-3) and the fact that the spectral contribution of indigo is greater in the areas where the original paint layer has been detached led to the conclusion that indigo was not one of the pigments of the original red paint layer. Similarly, Raman spectroscopy identified vermillion, orpiment and indigo, with the lines of vermillion and orpiment being predominant in the red spots, whereas the presence of indigo being more intense in the off-pink areas (Figure 5-15e). XRF examination gave As and Hg as the major elements of both areas, with Ca and Fe belonging to the support. However, the comparison of elemental ratio between As and Hg indicated the presence of more significant amount of Hg in the red spots. It is worth mentioning that S was also detected in these areas, despite the detection limitation that the XRF spectroscopy faces due to its small atomic number, most probably because it is an element that both vermillion and orpiment contain and therefore their simultaneous presence enhances its detection peak.

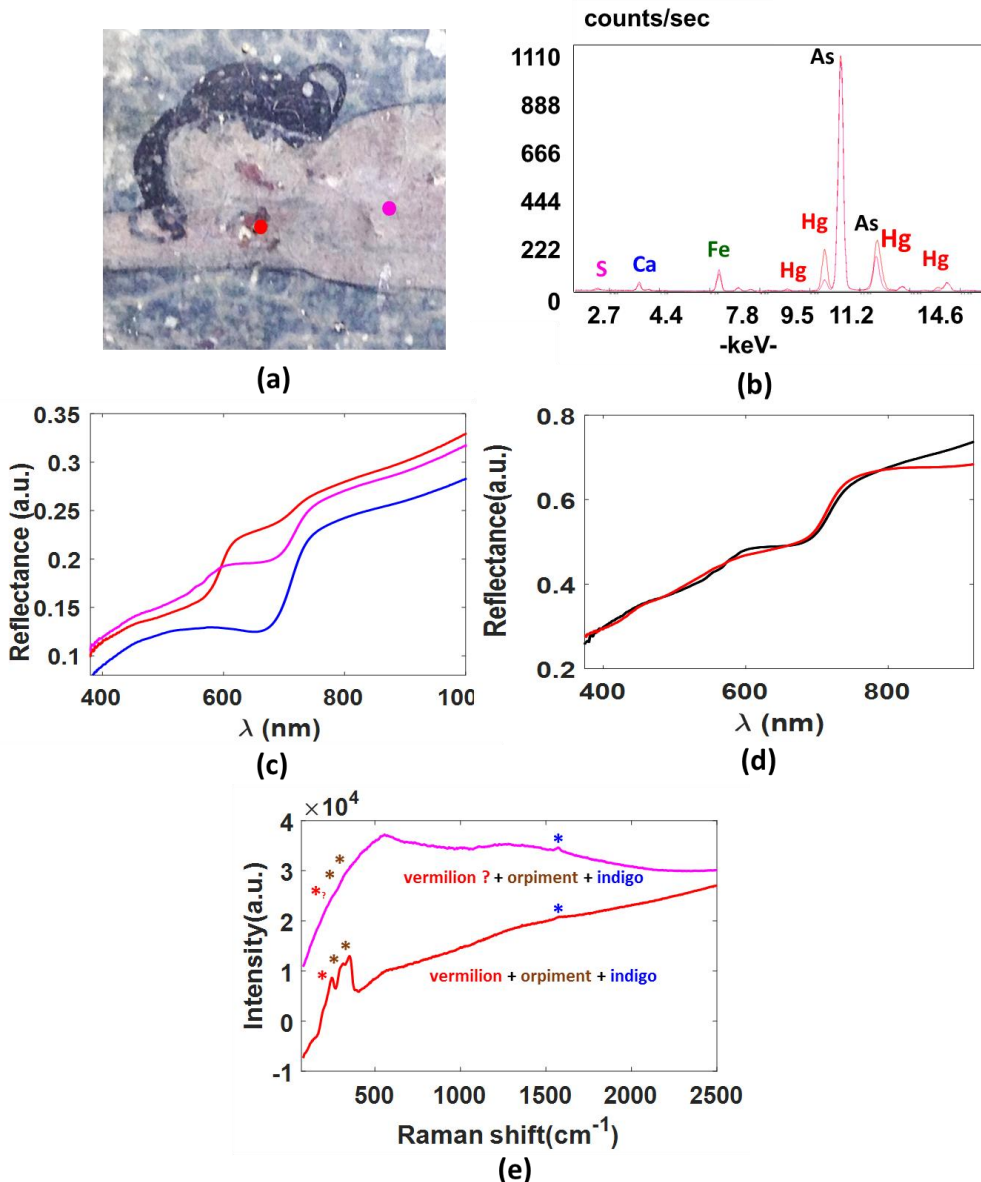


Figure 5-15 (a) Colour image derived from PRISMS data collected from the murals of the Southern wall in cave 465 of Mogao containing off-pink and red paint areas (red and magenta dots indicate the red and off-pink analysed areas respectively); (b) XRF and (c) reflectance spectral comparison between the red (red curve), the off-pink (magenta curve) analysed areas. In the reflectance spectral comparison the spectrum of their grey/blueish background is illustrated (blue curve) as well; (d) KM fit (red curve) on the reflectance spectrum collected from the off-pink area (black curve) using a mixture of vermillion and indigo; (e) Comparison between the Raman spectra collected from the red (red curve) and the off-pink (magenta curve) areas.

### Transparent paint layers with crack formation

XRF measurements performed on various brownish, cracked areas showed that As and Hg are the predominant elements, with traces of Pb being present as well (Figure 5-16c).

KM model gave a reasonable match to the reflectance spectra collected from these areas using a combination of vermillion and a small amount of indigo (Figure 5-16b). Moreover, Raman spectroscopy confirmed the presence of both vermillion and indigo and identifies also orpiment and red lead (Figure 5-16d).

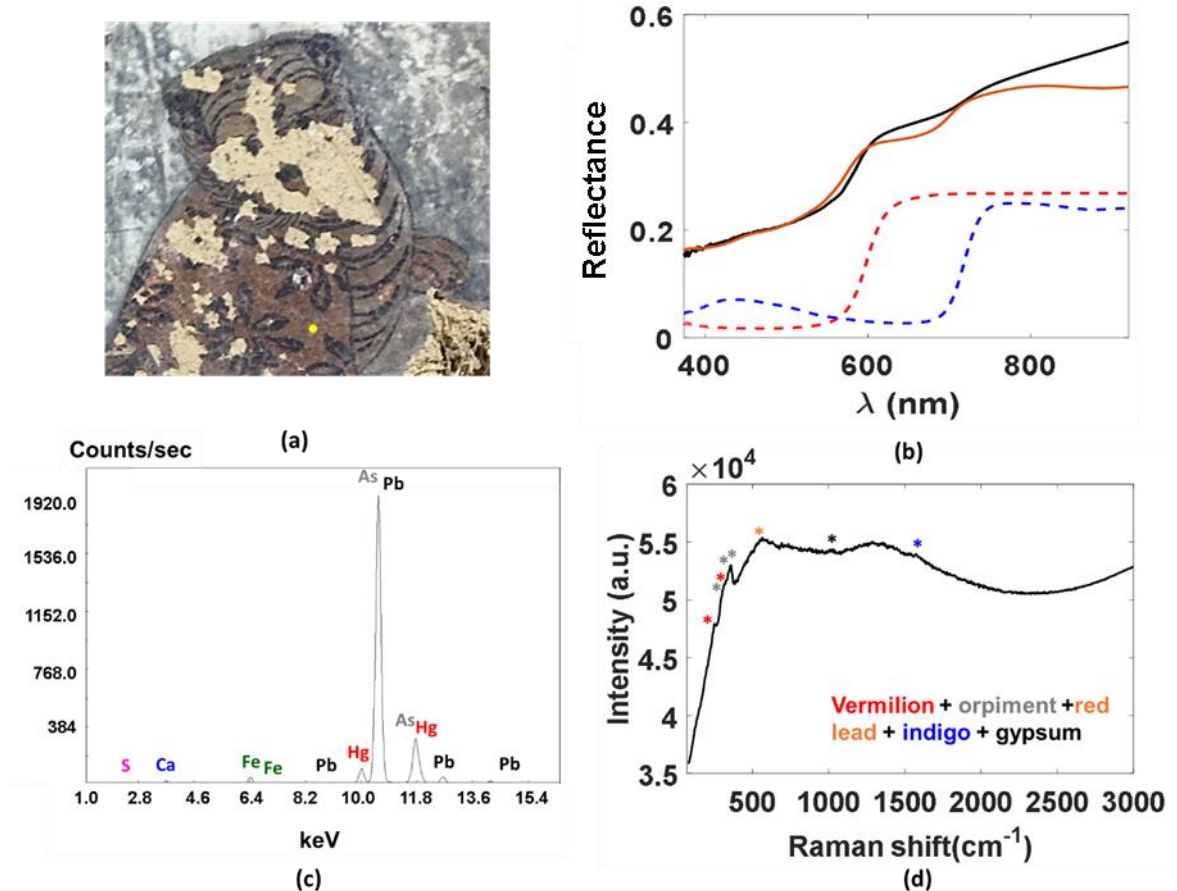


Figure 5-16 (a) Colour image of a detail of the murals of the Southern wall in cave 465 of Mogao (yellow dot indicates the analysed area). (b) KM fit (orange curve) on the reflectance spectrum collected from the brownish area (black curve) using a mixture of vermillion and indigo, the reference spectra of vermillion (red dashed curve) and indigo (blue dashed curve) are presented as well; (c) XRF spectroscopy detected As and Pb as the major elements in this area, but also a small amount of Hg and trace elements of Ca, Fe and S; (d) Raman spectroscopy detected vermillion, orpiment and indigo.

The fact that indigo was detected in small amounts in both FORS and Raman spectroscopy, in combination with the detection of gypsum in Raman, indicates that most probably it does not belong to the paint mixture but to the substrate and that the detection of it is due to the transparency of the brownish paint layer.

## Comparison of the palette of cave 465 with the palette of other caves of Mogao complex and historical records

As one of the aims of this study was to provide scientific evidences for the art history of the cave, and more specifically its dating, a comparison between the pigment composition of the murals of cave 465 and three other caves (i.e. caves 159, 65 and 95) whose dating is better established and also placed in different periods, within the range that the dating of cave 465 is proposed, was performed (Table 5-2). It has to be noticed that the multi-modal examination of the additional three caves was limited to reflectance and XRF spectroscopic analysis.

Table 5-2 Comparison between the palettes of various caves of Mogao complex

Colour of painted area	Pigments/ Degradation products			
	Cave 465 (?)	Cave 159 (Tibetan)	Cave 65 (Tangut?)	Cave 95 (Yuan)
<b>Red</b>	Vermilion Vermilion + orpiment Red Ochre Red lead + orpiment	Vermilion   	Vermilion Red Ochre Red Lead	Vermilion   
<b>Purple</b>	Plattnerite	-	Vermilion (XRF detects Pb)	-
<b>Orange</b>	Red Lead + orpiment Ochre	Realgar		Red Lead
<b>Brown</b>	Vermilion + orpiment Plattnerite	Yellow Ochre	-	plattnerite
<b>Yellow</b>	Orpiment	Yellow Ochre	-	As-containing [no Raman measurements]
<b>Blue</b>	Indigo Azurite + indigo	Lapis lazuli	Lapis lazuli	Azurite
<b>Green</b>	Copper Chloride green (atacamite?) Indigo + orpiment	Copper Chloride green (atacamite?)	Copper Chloride green (atacamite?)	Copper green (malachite?) [XRF no Cl]
<b>Black</b>	-azurite+plattnerite	Ink (?) Plattnerite	Ink (?)	

For the extraction of more accurate conclusions, the scientific results of this study were also compared with the results obtained from other studies conducted on the analysis artworks, produced in Asia through the years, as well as historical records about the

fabrication and use of different pigments in Chinese tradition. The analysis of the paint layers of the murals of cave 465 showed that additionally to the use of single pigment, a lot of combinations of pigments were used for the achievement of the different colours and hues. On the contrary, the analysis of the murals of the other caves showed that the application of single pigment paints was more prevalent. As most of the inorganic pigments identified on the murals of cave 465 have been widely used in the Chinese painting tradition, their presence cannot assist the extraction of conclusive results regarding the history of the cave. The red pigments vermillion, red lead and red ochre as well as the blue pigment azurite are colourants traditionally used in China, and as regards to the murals in Mogao caves, their use is recorded since the early period of their construction. The multi-modal analysis of the pigment composition of cave 159, which is dated to the Tibetan period, were in agreement with the historical records identifying yellow ochre and realgar as the yellow and orange pigments respectively and lapis lazuli as the blue colourant. However, the identification of the pigments used on the murals does not agree with this palette making therefore the dating of its construction in Tibetan period unlike. The paint area analysed in cave 95, which is dated in the Yuan period, was not significantly large and therefore the conclusions are based on a small statistical sample. It was interesting, however, that it was the only one from the three comparison caves in which yellow As-containing pigment has been used, with the precise identification not being possible as Raman measurements were not performed in these caves. On the other hand, it is the only cave where no Cl was detected upon the XRF examination of the Cu-green areas, suggesting that malachite is the green colourant. In the palette of cave 465, the presence of indigo, orpiment and the green copper chloride (most probably atacamite) as well as combinations of pigments was very interesting. The earliest use of indigo on murals is reported in studies conducted on the analysis of fragments detached from Buddhist caves located in the province of Xinjiang Uyghur Autonomous Region in China, that have been constructed between the second and the tenth century [90], while it was also identified as one of the blue colourants of an eleventh century Buddhist Temple in Southwest China [90]. Orpiment is a yellow inorganic pigment mined in Eastern Tibet and therefore widely used in Tibetan paint tradition. However, orpiment mines can be also found in Gansu province, where Mogao complex is located, making its use on the murals of cave 465 possible because of its availability. According to historical records, copper tri-hydroxychlorides seem to have played a more important role than malachite in Chinese

paintings since Northern Song Dynasty (960 to 1127). The start of synthesis of copper chloride pigments is dated back to Five dynasties (907 to 960), with its presence without any traces of malachite placed in Tangut period (1038 to 1227). During Yuan period, the synthesis of copper chlorides is established [91]. Therefore a more detailed analysis of the Cu-green areas using Raman spectroscopy could provide important information related to the dating of the cave 465. The fact that large parts of the murals of cave 465 are covered with paint layers consisting of a complex combination of pigments was a very distinctive characteristic of cave 465. The combination of vermillion and orpiment that was detected on some brownish areas of the murals was also been recorded as the combination used on orange areas on the murals of the Buddhist caves in Uyghur Autonomous Region in China [90]. Interestingly, the combined use of vermillion with orpiment was also reported in the analysis of a wall painting of ninth to twelfth century that was excavated in Central Asia and more specifically Nishapur, a city located along ‘Silk Road’ that played a key role in securing trade and commercial transactions [92]. These evidences suggest that this combination of pigments could be related to cultural exchanges along the Northern Silk Road. The combined use of azurite and indigo has been reported in the analysis of Tibetan manuscripts dated in eighteenth to nineteenth century [93]. The application of non-invasive micro-XRF spectroscopy and cross-sectional SEM analysis on samples collected from Tibetan Thangkas, dating from the thirteenth to the sixteenth century, identified the pigments of the green areas to be a combination of indigo and orpiment [94]. This combination of pigments is not normally found on Chinese paintings. Finally, the combination of red lead and azurite that the multi-modal analysis of the bluish/black degraded Pb-containing areas of the murals of cave 465 suggested, was also proposed after X-ray Diffraction (XRD) measurements on samples collected degraded lead areas in caves 205 and 171 of Mogao complex that are dated in High Tang dynasty (713 to 766). Although the historical records and the results of studies conducted on the analysis of the pigment composition of other Asian artworks are informative about the painting traditions during this time, further examination of the pigment composition of caves of the Mogao complex whose dating is well established should be performed for the extraction of more accurate results about the history of cave 465

### 5.3.2 Examination of crack formation

The application of multivariate statistical methods, and more specifically PCA, on the spectral imaging data collected from various areas of the murals revealed interesting information about the structure of the paint layers. The formation of cracks was observed in the total of the analysed surface with the size of the observed cracks, varying among the different paint layers. Figure 5-17 illustrates a characteristic example, where the analysed area contains paint layers of different pigment compositions. Interestingly, the brownish area that has been identified to consist of a mixture of vermillion, orpiment and red lead (Figure 5-16) seems to have fine and small cracks, while only large cracks can be observed on the surrounding indigo-containing area (Figure 5-17b).

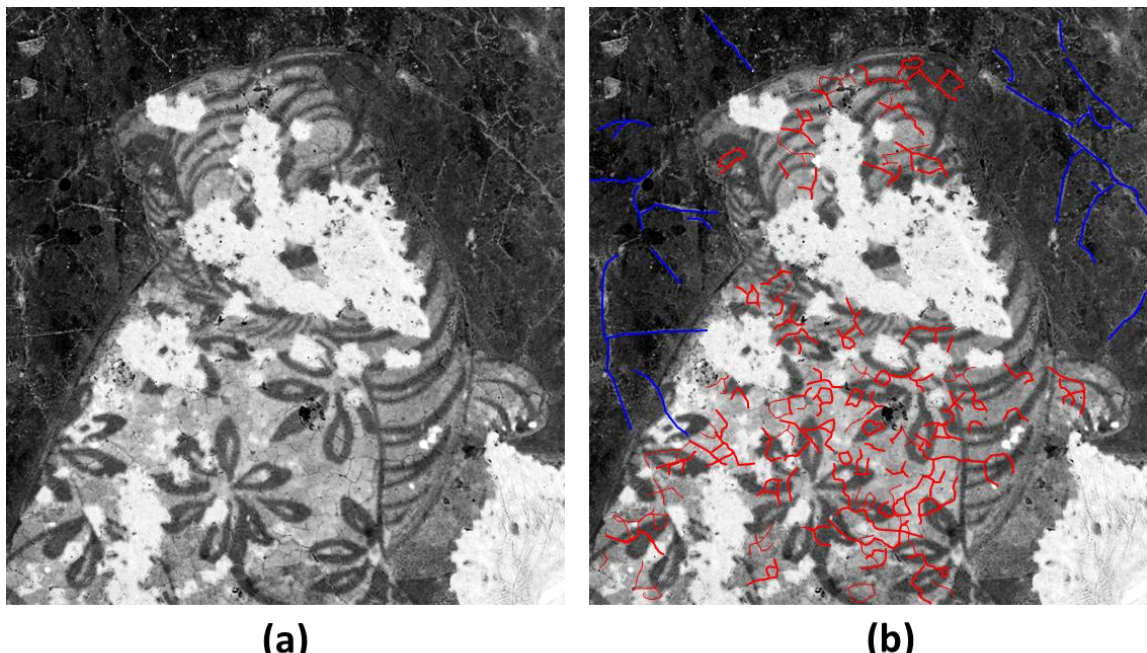


Figure 5-17 (a) PCA applied on the ten spectral images collected using PRISMS system and (b) the same PCA image with markers indicating the presence of the fine and small cracks of the brownish area (red lines) and the large cracks of the surrounding area (blue lines)

The formation of the various cracks could be related to the material composition of the paint layers, the degradation of the substrate or the support layer, while it could also be a combination of these reasons. It has been observed that cracks can be formed on the support layers of the murals during the drying process in their preparation. The main reason for the deterioration of the plaster substrate is the crystallization of gypsum

(sulfation) that is caused due to the weathering of the murals and often results to cracking of the plaster layer, with a possible side-effect the micro-flacking of the paint layer. The deterioration of both, the paint layer and the substrate of the murals is often linked to the presence of salts. More specifically, studies on the deterioration of murals in cave 85 of the Mogao complex [95] have shown that the deterioration is correlated with the amount of hygroscopic salts on both sides of the plaster layer. As the Mogao caves are constructed on the side of a sandstone cliff, the enrichment of salts is considered to be related to the diffusion of water from the porous network of the sandstone body. The migration of salts towards the plaster layer is explained from the humidity difference between the rock bulk and the cave atmosphere that provokes their move to the evaporative front due to the capillary action. After they reach the plaster layer and the water evaporates, salts are getting crystalized and remain there. As the enrichment of salts on the surface of the murals is based on the humidity difference, the presence of moisture is required. Despite the actions for monitoring and stabilization of the humidity levels in the Mogao caves, the deterioration of the murals due to the presence of moisture should be expected given both the construction of the caves (i.e. built in the excavated side of a cliff) and the fact that they have been exposed to the environmental conditions for centuries. On the other hand, the fact that the fine and small cracks were observed only in specific paint layers, supports the scenario that the size of the cracks is possibly related to their material (i.e. pigment or binder) composition.

In order to investigate whether the formation of the small cracks is related to the deterioration of the support layer or the material composition, observations in other parts of the mural were also performed. The analysed areas were selected in such a way that they contain on only paint layers of various pigment composition but also that they are located in different parts of the wall, covering the whole range of different moisture conditions. The examination of an area located at approximately the same height as the brown one, but to the other side of the panel, about two meters away, showed that fine cracks can be observed only on the black, most probably ink-containing, areas (Figure 5-18). The fact that the fine cracks were observed only on the brownish (As-containing) and the black (ink-containing) paint layers of these areas, led to the conclusion that the observation of different types of cracks is probably related to the material composition of the paint layers.

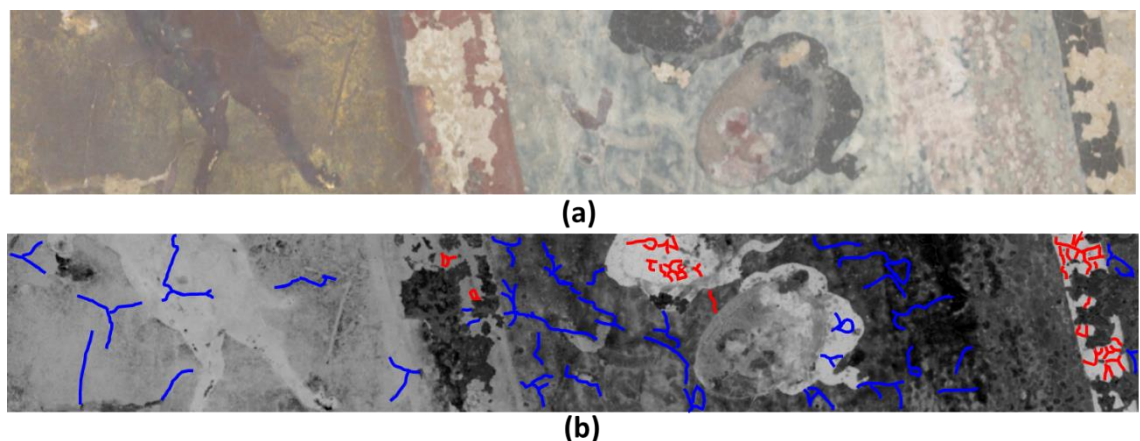


Figure 5-18 (a) Colour image derived from PRISMS system and (b) PCA applied on the ten spectral images of PRISMS system, with the indication of fine (red lines) and large (blue lines) cracks

This conclusion was supported further through the examination of areas of the same panel that were, however, located close to the ceiling. The results were interesting, as fine cracks were observed on the area that was classified with the areas of the ground level that consist of a mixture of orpiment and indigo but also on a whitish area with unidentified pigment composition (Figure-5-19b). On the other hand, areas that have been classified with the plattnerite-containing ones seemed to contain only large cracks.

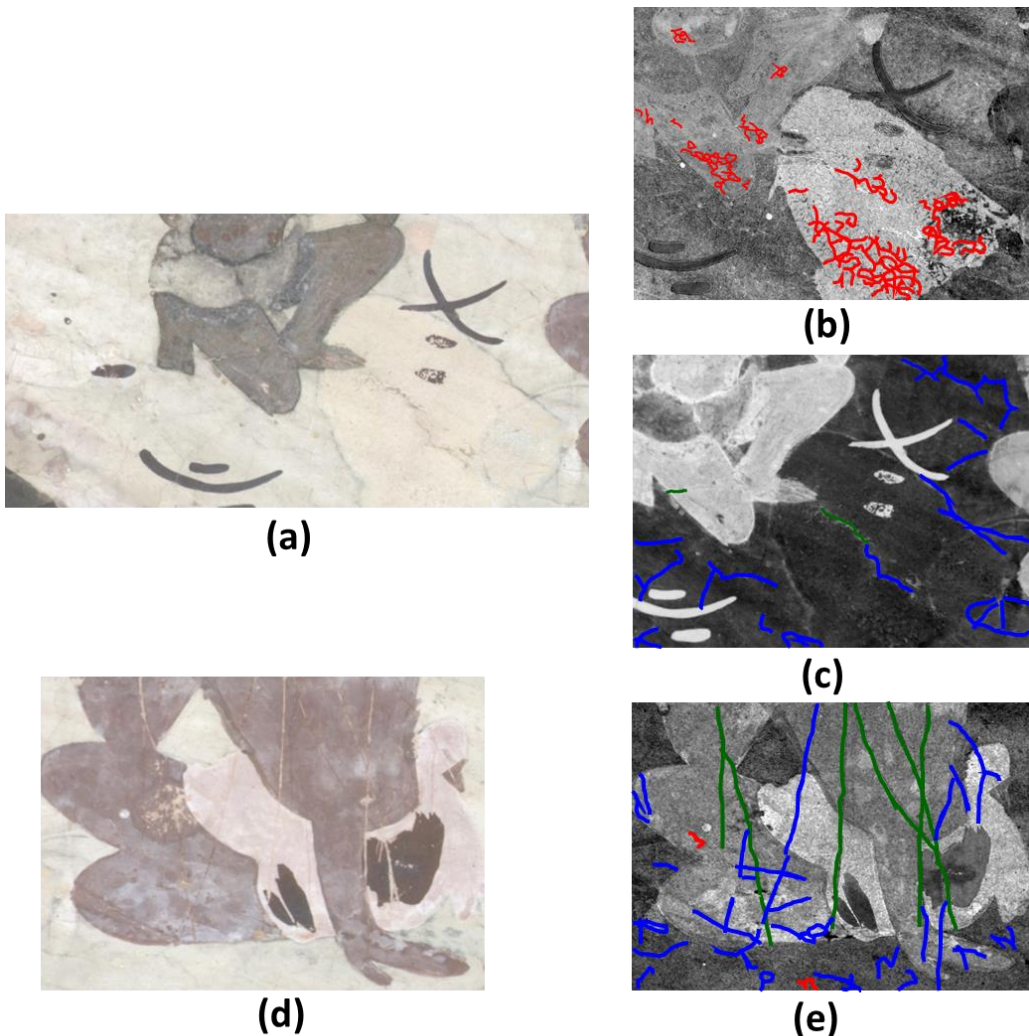


Figure-5-19 (a) Colour image derived from PRISMS data collected from an area close to the ceiling that contain grey/ grenish paint layer that was classified with areas consist of a combination of orpiment and indigo; (b,c) the results of the application of PCA on the spectral imaging data collected from this area that reveal the formation of fine (red lines) and large (blue lines) cracks as well as the presence of deep marks (green lines). (d) Colour image derived from PRISMS data collected from a neighbouring to the previous area that contains burgundy paint layer and was classified with areas consist of a plattnerite; (e) the results of the application of PCA on the spectral imaging data collected from this area that reveal the formation of fine (red lines) and large (blue lines) cracks as well as the presence of deep marks (green lines).

For a more detailed examination of the formation of different cracks on the different painted areas, OCT scanning was also performed on some of them. The examination of red and pink As-containing areas showed that the presence of the fine cracks is localised on the red paint surfaces (Figure 5-20). However, given that the paint layers are very thin and transparent, the specification of the depth of the formation of the cracks was not possible.

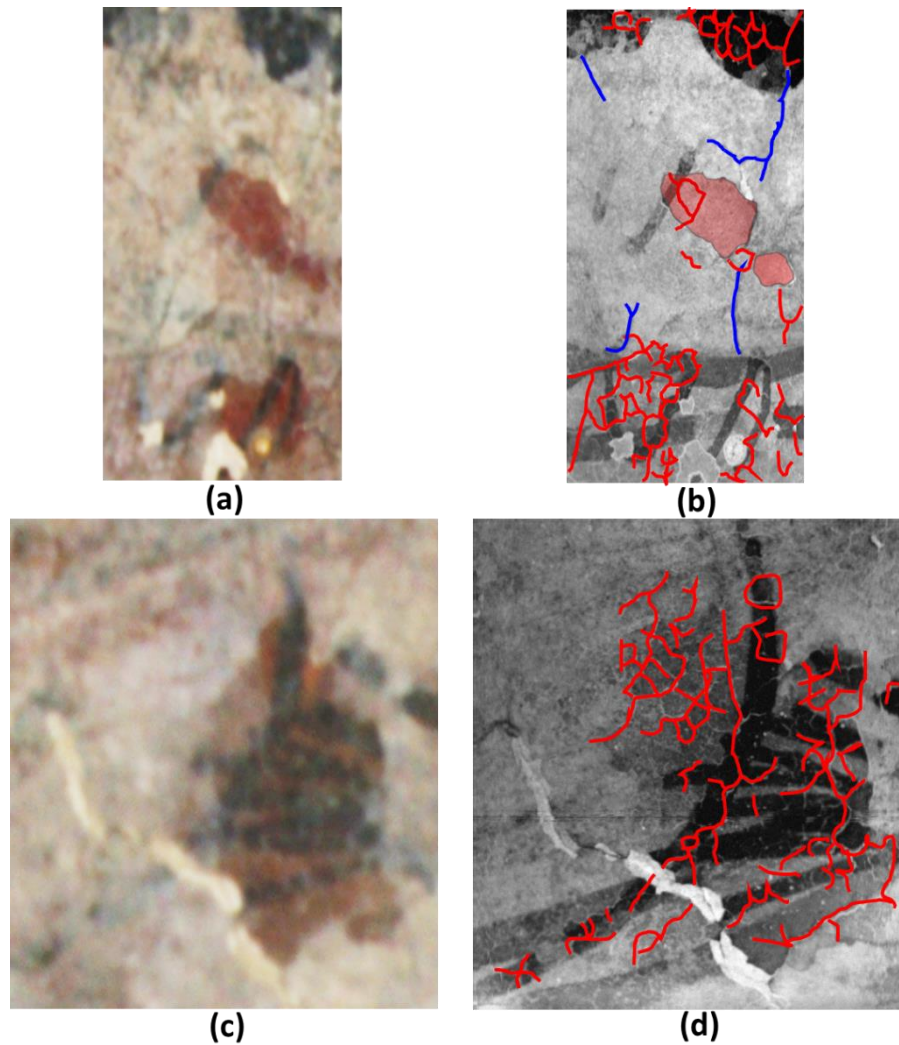


Figure 5-20 (a, c) Colour images derived from PRISMS data collected from pink areas with red spots of the murals of cave 465 and (b, d) the corresponding en-face OCT images indicating the fine cracks (red lines) that are localised on the red paint areas [image dimensions: (b) 100mm x 18.6 mm & (d) 100mm x 11.5 mm]

The examination of the brownish, As-containing area (Figure 5-16 and Figure 5-17) gave a different crack appearance, with the fine cracks being clearly located underneath the paint surface (Figure 5-21d), while large cracks being observed on the paint surface (Figure 5-21c). It has to be noted that the multi-modal spectroscopic analysis of the red As-containing and the brownish areas showed that they have similar pigment composition, except that the brownish area contains also traces of red lead. The combination of this observation with the fact that the fine cracks in the brownish area are located below the pain surface could be indicative of the paint sequence. More specifically, an As-containing layer is likely to have been applied on the bottom with a red lead-containing layer applied on the top.

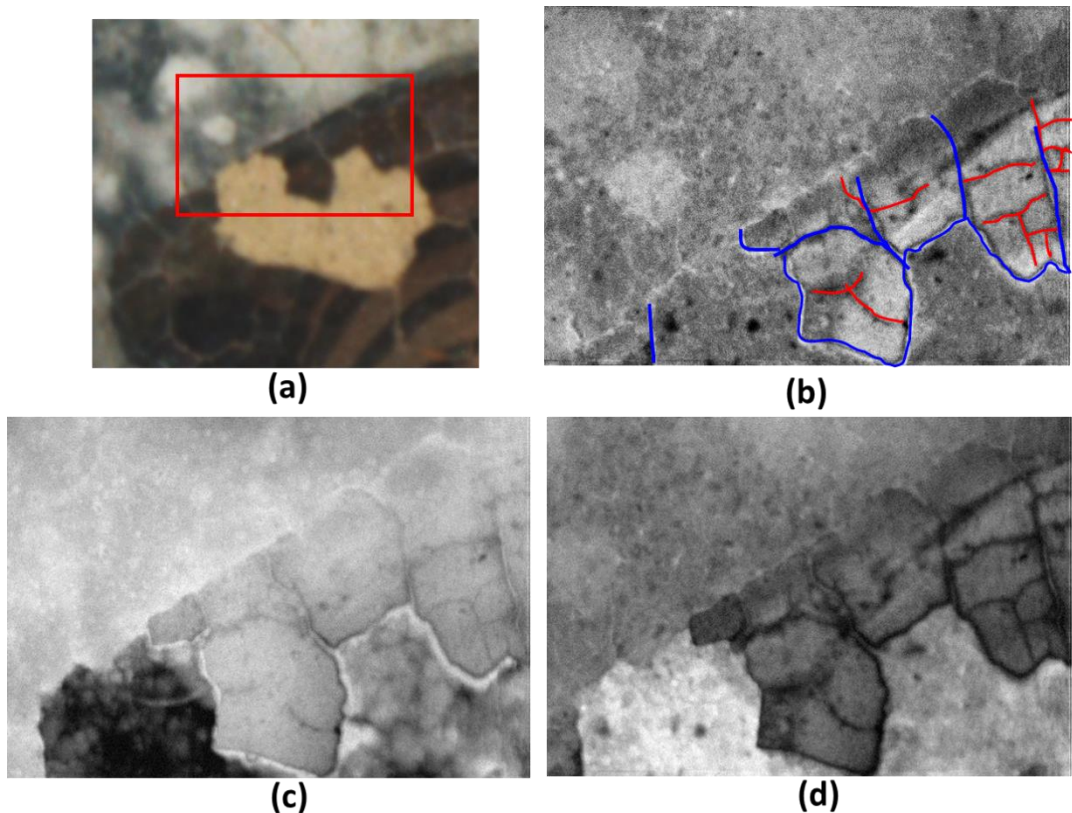


Figure 5-21 (a) Colour images derived from PRISMS data collected from an area on the murals of cave 465 that is on the border of a brownish paint, greyish/blue and exposed substrate areas on the murals of cave 465 and (b) the corresponding en-face OCT images indicating the fine (red lines) and the large cracks (blue crack) that are localised on the red paint areas. Average of en-face images collected from: (c) the top 30  $\mu\text{m}$  of the brownish paint layer and (d) the area underneath the surface, showing clearer the formation of the large and fine cracks respectively. [OCT en-face images dimensions: 100mm x 7 mm]

The examination of paint layers from various parts of the murals using OCT scanning showed that, additionally to the pigment composition of the paint layer, the concentrations of the different painting materials (i.e. pigments and binding medium) as well as the way that they interact with each other could contribute to the observation of various cracks. Interestingly, among the analysed areas the deterioration of the two paint layers of that were identified as plattnerite-containing, seems to result in different structural alteration. More specifically, observation of an area where the plattnerite layer applied on top of a white paint layer (Figure 5-22c, f) showed that it contains cracks similar to the ones formed on an a greyish area that was identified to consist of a combination of orpiment and indigo (Figure 5-22a, d). On the contrary, observation on burgundy areas dominated from the presence of plattnerite revealed the presence only of large cracks, while the deterioration of the paint layer resulted to its micro-flacking.

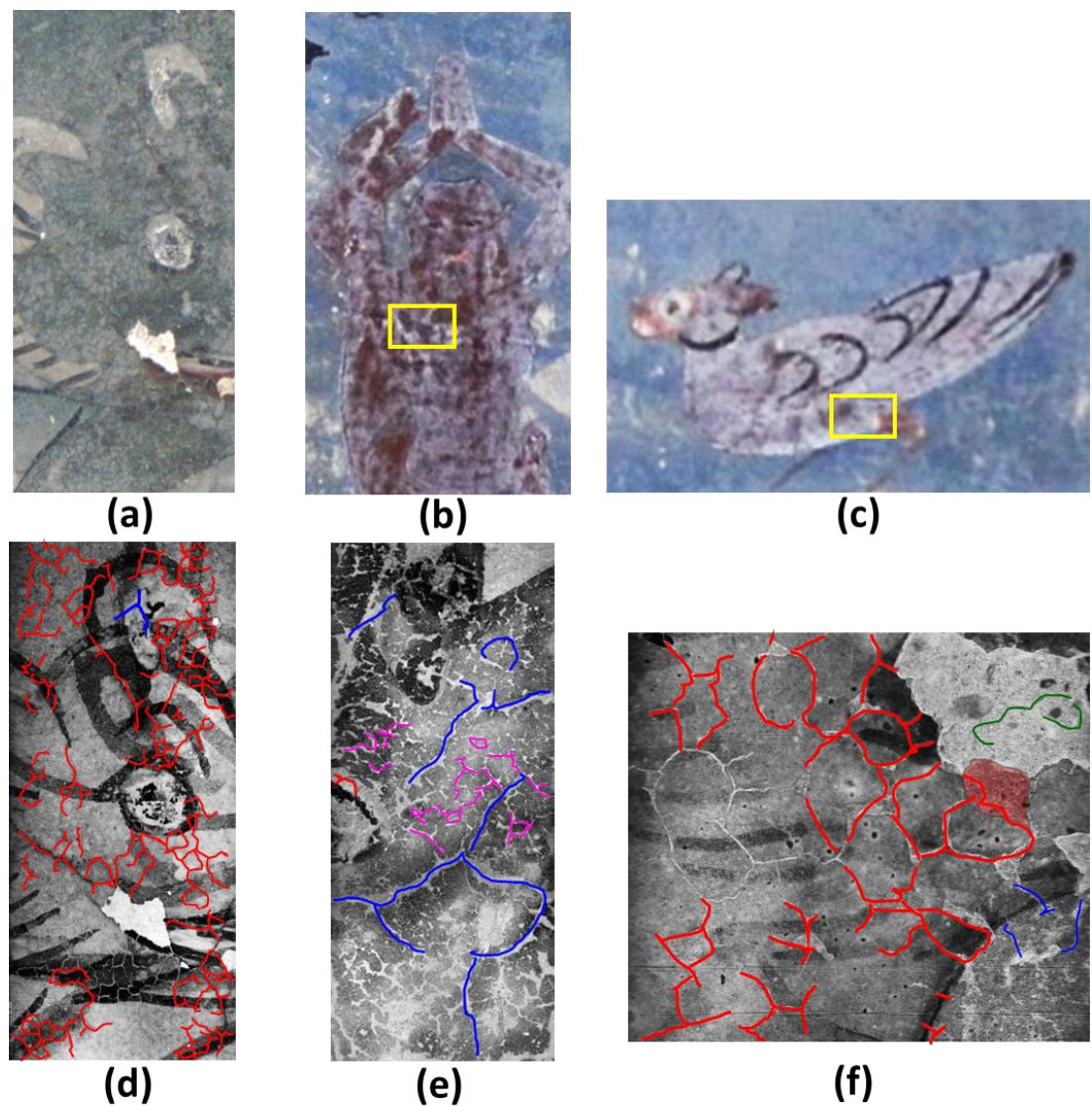


Figure 5-22 Colour images from: (a) a greyish/green area which pigment composition has been identified as a combination of orpiment and indigo (b) a burgundy plattnerite-containing area (yellow box indicates the area that was OCT scanned) and (c) an area where the plattnerite-containing layer is applied on a white paint layer, possibly gypsum (yellow box indicates the area that was OCT scanned). En-face OCT images from (d) the greyish/green area, with the red lines indicating the presence of fine cracks [image dimensions: 100mm x 23.0mm], (e) the burgundy area, with the blue lines indicating the large cracks of the supporting layer, while the magenta lines indicate the flacking formation [image dimensions: 100mm x 20.6 mm] and (f) the area where plattnerite layer has been applied on top of a white paint layer, with the red lines indicating the fine cracks [image dimensions: 100mm x 6 mm]. Some cracks and flacking parts have been left without indication lines enabling the observation of the different crack and flacking formation

In order to investigate whether the particular crack formation is related to the construction of the murals and/or the location of the cave, spectral imaging comparison between cave 465 and caves in different locations of the Mogao complex was performed. The caves analysed are cave 55 that is located on the ground level of the complex and cave 386 that is located on the same level as the cave 465 but in a totally different part of the complex. Both caves have support layers of similar composition as

cave 465 (i.e. gypsum). The application of PCA on the spectral imaging data collected from the murals of these two caves (Figure-5-23b, d, e) did not reveal any crack formation neither on the painted areas nor on the support layers, with some observed marks probably being related to the tools used for the application of the support layer. The only degradation evidence observed on the murals of cave 386 was the formation of some stains that could be possibly related to the presence of micro-organisms (Figure-5-23e).

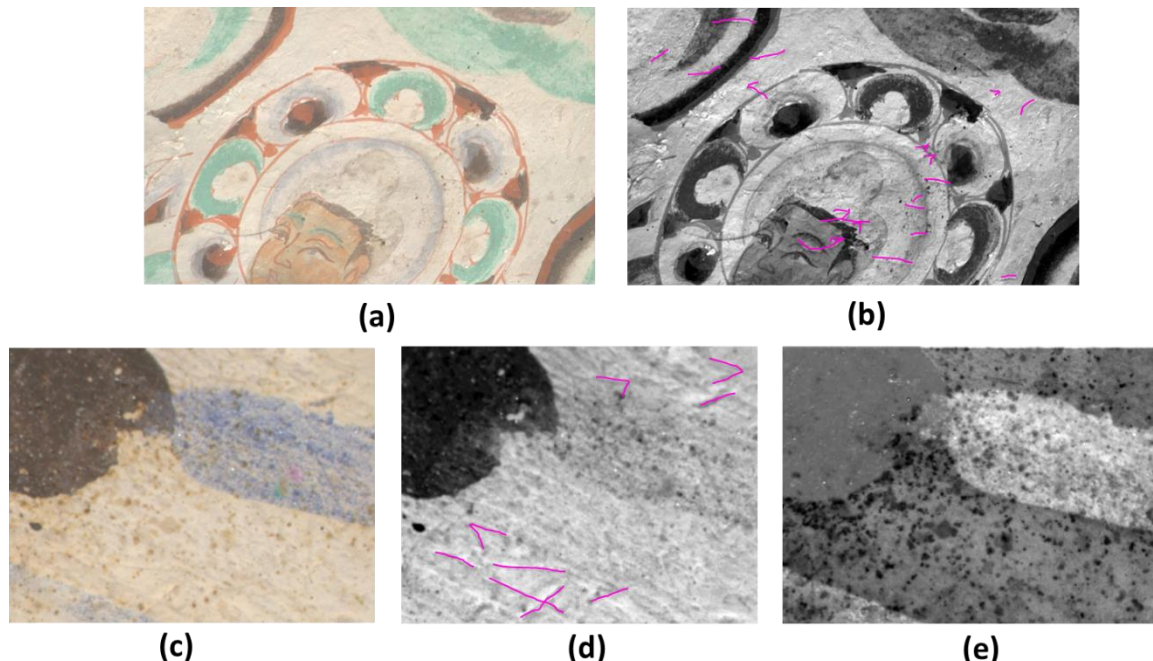


Figure-5-23 (a,c) Colour images derived from PRISMS data collected from the murals of cave 55 and 386 respectively and (b, d) the corresponding PCA on images of the ten spectral bands indicating some marks from the tools used probably for the preparation of the substrate (magenta lines); (e) PCA on images of the ten spectral bands collected from the murals of cave 386m showing clearly the formation of stains that could be related to the cultivation of micro-organisms (black marks)

The combined use of both spectral imaging and OCT scanning enabled the observation of different cracks formed on the various painted areas of the murals of cave 465. The reason of their formation could be the material composition of the paint layers that are observed, the deterioration of the support layer or a combination of them.

The fact that the formation of cracks was not observed on the murals of any of the other caves examined lead to the conclusion that the weathering of the cave and/or differences on the preparation of the support layer are factors that contribute to the observation of cracks. On the other hand, the observation of small cracks on specific painted areas of

the murals of the cave 465 lead to the conclusion that they are most probably related to the composition of their painting materials and/or their relative concentration. Further examination of a larger and heterogeneous statistical sample of paint areas, with variations in the composition of pigments, using an UHR-OCT system (see section 7.2) that provides higher depth resolution, should be performed in order to obtain more informative results about the origin of the different cracks observed.

### **5.3.3 Examination of painting techniques and sequence**

The application of multivariate statistical analysis on the spectral imaging data collected from the murals of the cave 465 enabled the automatic revealing of the ‘hidden’ drawings (see chapter 3), highlighting the areas of particular interest, on which a more detailed examination should be performed. The observation of the PRISMS data in the different spectral bands provided a preliminary examination of their depth location relatively to the paint surface, while further OCT scanning of the drawing-containing areas allowed the high-resolution and in-depth observation of their depth location. More specifically, the application of ICA on the spectral images, indicated the areas where drawings are present, revealing further information that the observation in the individual spectral bands was not able to provide (Figure 5-24a, b). On the other hand, the observation in the individual bands showed how the revealed drawings are spread in the different depths relatively to the paint surface (Figure 5-24c, d, e), illustrating that in a lot of figures thick brushes have been applied for the underdrawings, while fine lines have been used for the final sketches (i.e. outlines and features).

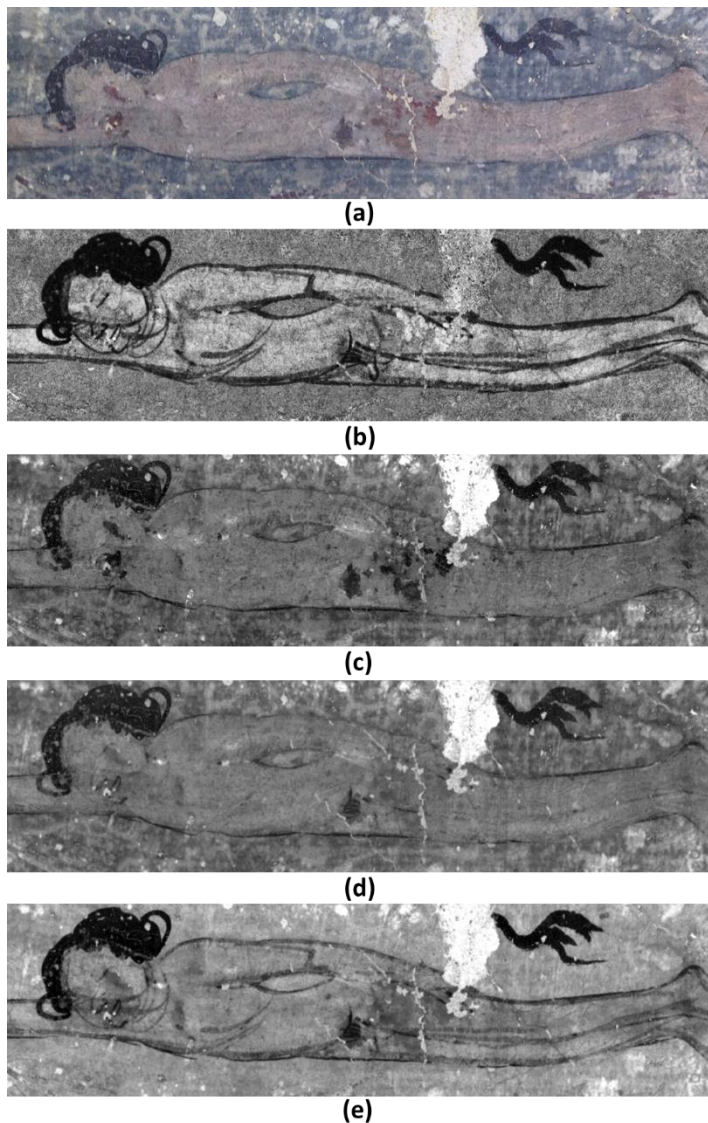


Figure 5-24 (a) Colour image derived from PRISMS data collected from a detail from the murals of cave 465, (b) ICA applied on the ten PRISMS spectral images reveal of the drawings, even the ones that the observation on the individual bands is not enabling, automatically and in high contrast; spectral images at (c)400 nm, (d) 600 nm and (e) 880 nm

Further examination of the drawing sequence was performed with OCT scanning, which allows a finer in-depth observation than the spectral imaging, due to its higher resolution in the depth direction. Furthermore, the ability of the specific selection of the depth of the observation enabled the distinction between the final (Figure 5-25a) and the preliminary (Figure 5-25b) drawings. It has to be noticed that in the observation of the underdrawings the shadows of the final sketches are also present. The virtual cross-sections derived from the OCT scanning (Figure 5-25 c, d) also enabled the observation of the differences in the depth of the various drawings through the observation of their scattering behaviour. The comparison of the scattering depth profiles (also called A-scan) corresponding to the areas that contain final sketches and underdrawings illustrated their

difference, with the signal of the final sketches dropping faster than the one of the preliminary sketches, as the absorbing substance (i.e. ink) is located in higher position.

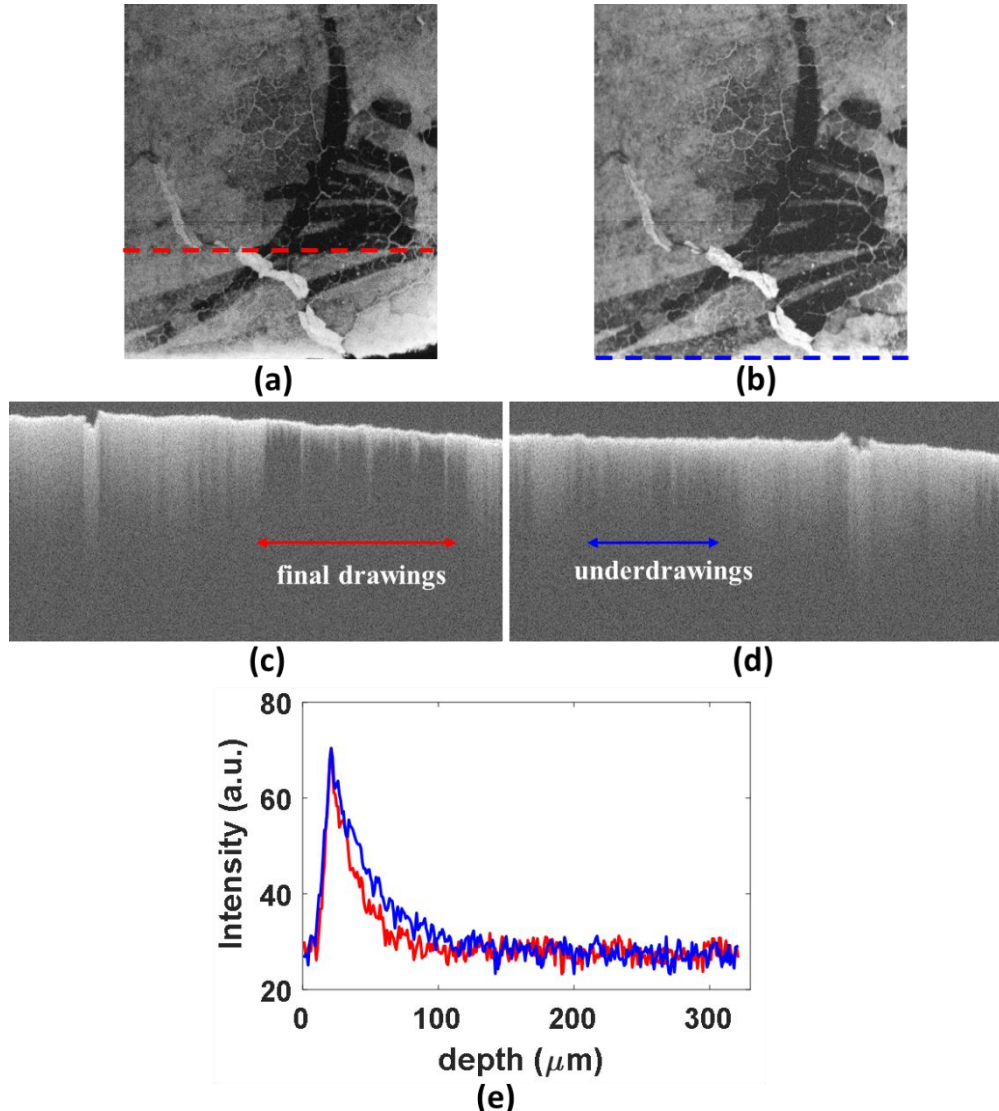


Figure 5-25 En -face average (a) of the upper 0.3 mm of the paint layer that shows the final sketches and (b) area underneath the paint surface; cross-sectional imaging showing (c) the final sketches and (d) the underdrawings; (e) comparison between the depth profile of the backscattered light intensity of the final sketches (red curve) with underdrawings (blue curve) that shows that the final sketches have a significant faster drop given that there are located on the upper part of the analysed area and therefore absorb the incident light, not enable the gain of scattering information from the area below

The examination of the ceiling showed that parts of the mural containing detailed figures, such as faces, were painted on paper stuck on the ceiling surface. One of the assumptions that could be made is that this observation is indicative of the painting methods followed for the painting of the ceiling, with the detailed parts being produced on the paper, possibly at the ground level for convenience and for avoiding of mistakes, and afterwards added on the ceiling painting. However, the observation of other areas of

the ceiling that also contained detailed figures showed that they were painted directly on the support layer. This led to the conclusion that the paper parts were most probably corrections or additions that were made either during the construction of the murals or in later interventions. In this direction, the examination of the paint sequence of these areas, as well as the investigation of whether the paper parts were painted at the same time with the rest of the painting or they were later additions was performed. Given the great distance of these areas from the ground level, the whole analysis was based on the spectral imaging and the spectral data collected using the PRISMS system in its telescope configuration.

For the investigation of the painting sequence and given that some parts of the paper have been detached, the existence of any correlation between the neighbouring area to the paper area and the area that was underneath the paper was initially performed. Initially, the correlation between the patterns of the drawings that both areas contain was examined. The spectral imaging observation in the NIR band (Figure 5-26), showed that the ‘cloud’ pattern of the surrounding area continued also in the area underneath the paper, with the drawings continuing from the one area to the other.

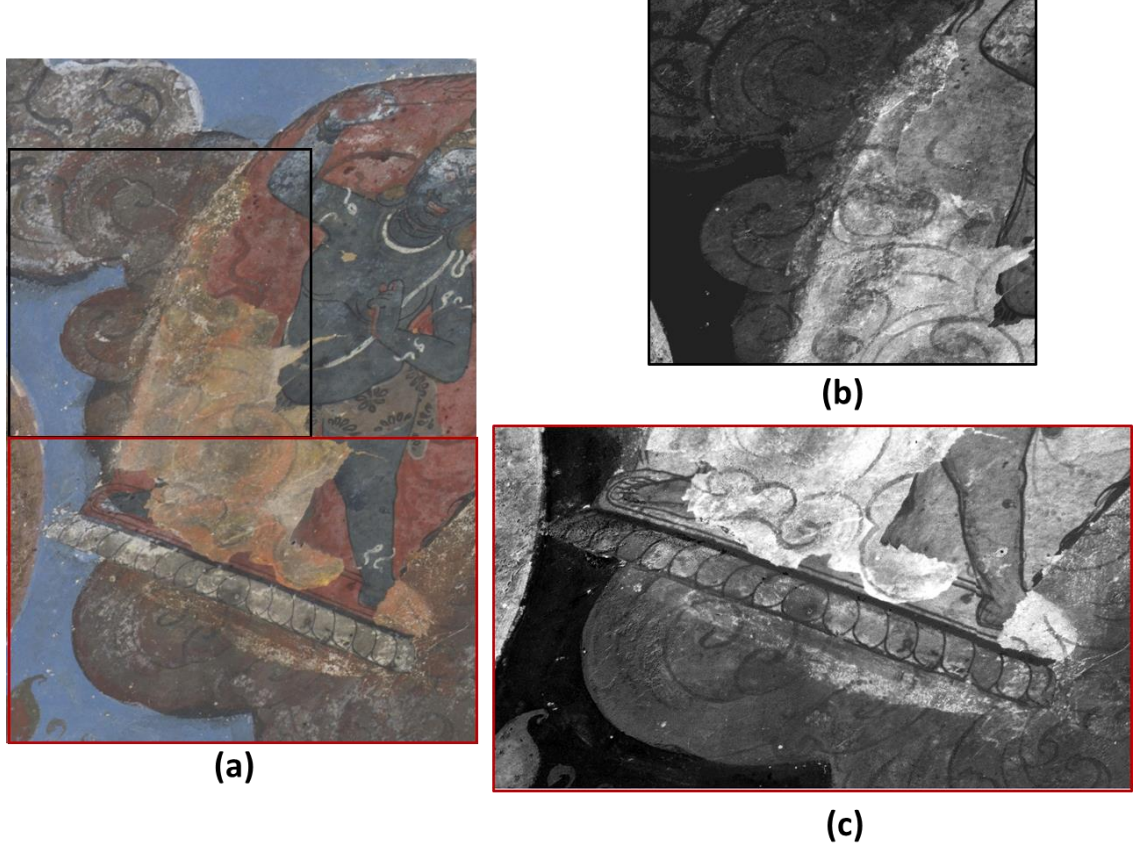


Figure 5-26 (a) Moisaced colour image derived from PRISMS system of an area on the ceiling of cave 465 where stuck paper is present; the black and the red boxes indicate the (b) and the (c) areas that are examined in the NIR regime for the revealing of the continuation of the drawing between the degraded and the exposed orange areas

The correlation between these two areas was further investigated through the comparison of their pigments composition. Figure 5-27 shows that the spectra collected from the areas that used to be underneath the paper were classified with the areas of the ground level that have been identified as red lead-containing in their multi-modal, non-invasive analysis. On the other hand, the spectra collected from the grey/ brownish area, neighbouring to the paper area were clustered with areas that have been identified as plattnerite-containing, with the plattnerite being the degradation product of lead-containing pigments when exposed to moisture.

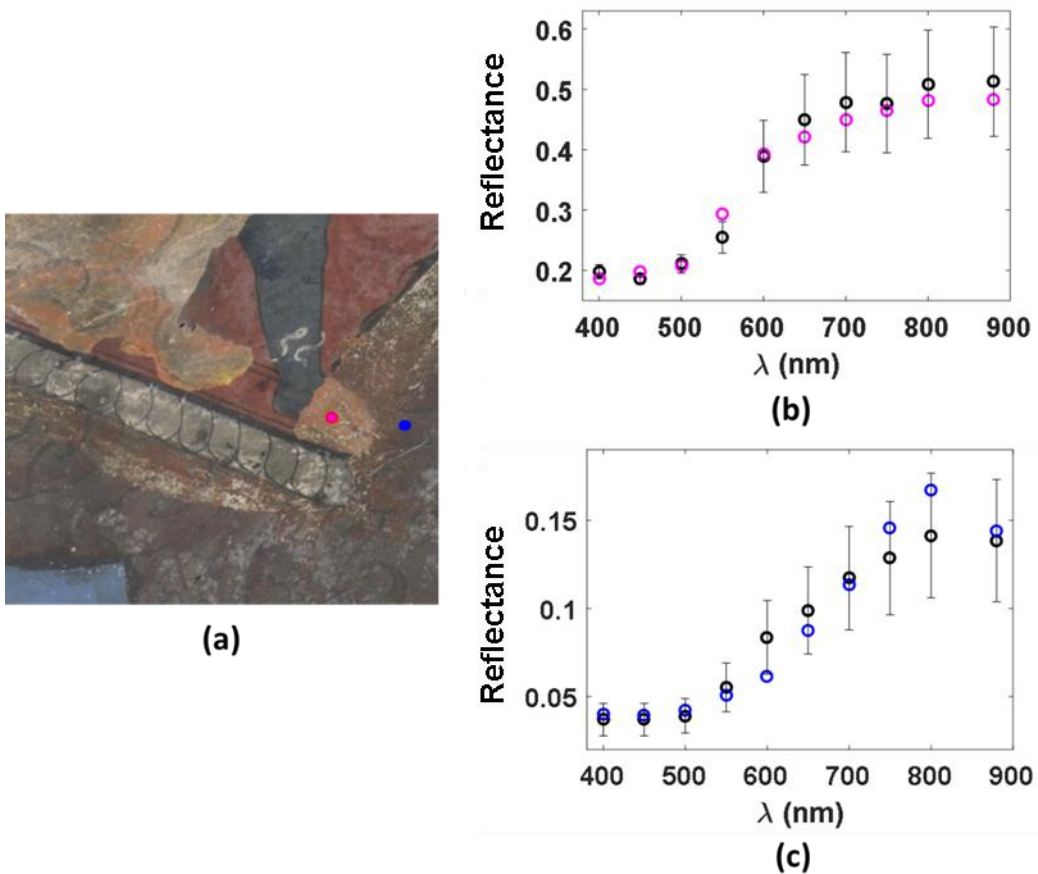


Figure 5-27 (a) Colour image derived from PRISMS data collected from an area located on the ceiling of cave 465 at the edge of the stuck paper and the surrounding area, that also contains exposed underneath the paper areas, with the spectra collected form the surrounding (blue circles in (c)) and the underneath the paper (magenta circles in (b)) being classified with area of the ground level that have been identified as plattnerite (black circles in (c))and red lead-containing (black circles in (b)) respectively.

Combining the continuation of the drawings and the correlation of the pigment composition between the neighbouring to the paper area and the one that used to be underneath it, the conclusion that can be drawn for the painting sequence followed is that the ‘clouds’ pattern was painted initially, using a red lead-containing paint, while the paper part was added afterwards.

In order to investigate whether the paper part was added during the construction of the murals or it was a later addition, the pigments composition of its painting was analysed. More specifically, the application of spectral clustering on the data collected from this area showed that the red and greyish/blue areas of the painting on the paper (Figure 5-28) are consistent with areas that have been identified as vermillion and indigo-containing respectively. Therefore, as both vermillion and indigo belong to the palette of the murals

of the cave, the possibility that the addition was made if not during the construction of the murals in the same period is more likely.

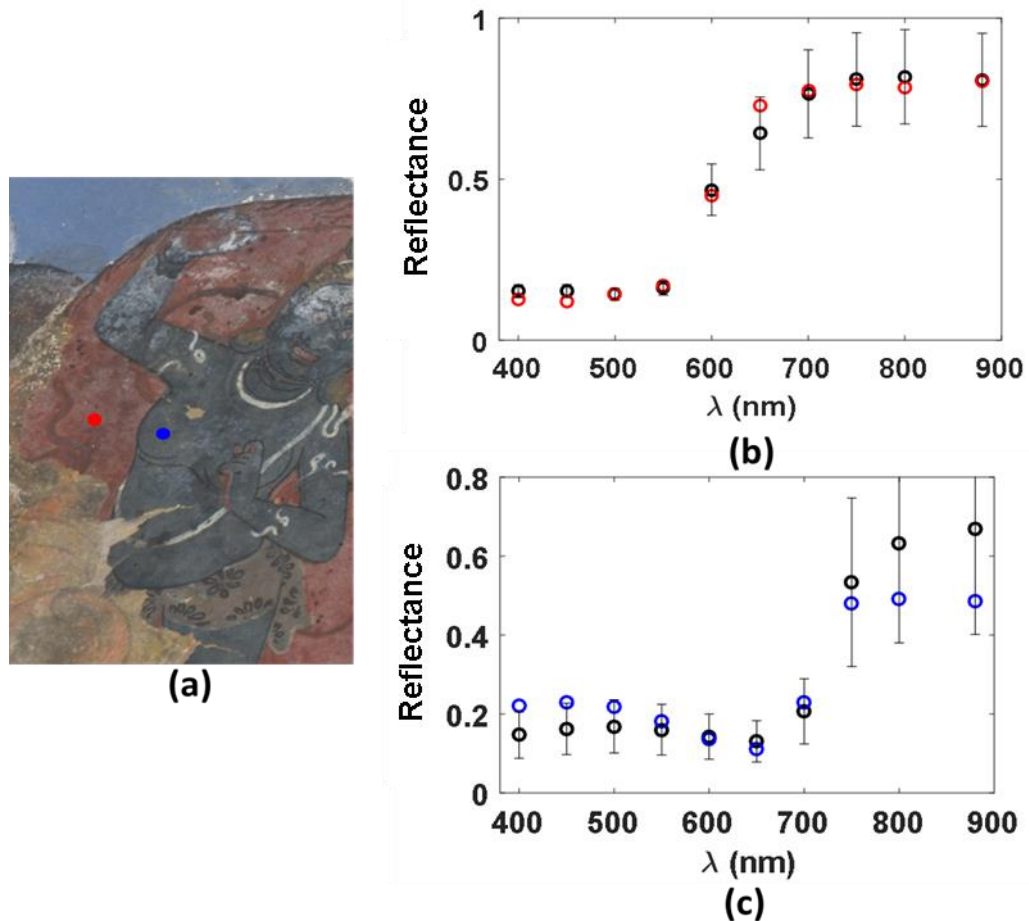


Figure 5-28 (a) Colour image derived from PRISMS data collected from the stuck paper located on the ceiling of cave 465; (b) the spectra collected from the red area (black circles) are fitted with the vermilion (red circles) and (c) the spectra collected from the greyish/blue area (black circles) are fitted with the indigo (blue circles) references respectively

## 5.4 Discussion

A multi-modal approach using a range of non-invasive techniques extended from spectra imaging (PRISMS) and point based spectroscopic techniques (FORS, XRF and RAMAN) to OCT scanning was followed for the in situ analysis of the painting materials and methods applied on the murals of cave 465 of Mogao complex. Moreover, the fact that the analysed murals are of large scale provided a very good example illustrating the necessity of the development of methods for the automatic process of large scale spectral imaging data. Preliminary examination of a large surface of the murals located even in unreachable areas of the cave was performed by applying statistical analysis methods on the spectral imaging data collected using the PRISMS system, highlighting the areas of special interest. For the identification of the pigments, the application of the clustering on the pixel-level spectral information of the different painting areas, minimized them in a manageable number of spectral groups, that were further analysed in detail using portable versions of FORS, XRF and Raman spectrometers. Areas containing degraded pigments were found, among the painting areas of the murals of cave 465, with their non-invasive and in situ analysis being rather challenging. In these cases, the multi-modal approach was proven significantly important, providing indications for the original pigment combinations as well as the painting sequence.

Furthermore, the combination of the results obtained from the application of PCA on PRISMS spectral images with OCT scanning provided very interesting results about the structure of the paint layers and the support layer of the murals of cave 465. More specifically, the comparison of the PCA results on spectral images collected from cave 465 and the ones collected from two other caves(caves 55 and 386) located in different parts of the Mogao complex, showed that formation of cracks was observed only on the murals of cave 465. Further examination of the cracks of murals of cave 465 revealed the existence of cracks of different sizes on the various paint areas. Detailed OCT scanning on selected areas, in combination with the information that the multi-modal, non-invasive analysis provided for their pigment composition, suggested that the formation of small cracks should be related to the material composition of these paint layers. The interaction between the pigments involved and/or the binding medium as well as their relative concentration in the various paint layers are some of the factors proposed to contribute to the formation of the small cracks in certain paint layers.

However, further examination should be performed on areas of various pigments composition and in different locations of cave 465 but also different caves in order to extract safe conclusions of the origin of these cracks. Moreover, the use of an UHR-OCT system that provides higher axial resolution would possibly enable the specification of their depth location.

The application of BSS statistical methods on spectral images collected from the different parts of the cave 465, highlighted the areas that contain drawings, whose visual observation was not possible. Further examination of these areas using OCT scanning that enabled more specific examination of their depth location based on their scattering properties.

The examination of the painting areas of the ceiling showed that some parts were painted on paper. The combination of the spectral observation in the NIR spectral band with the clustering applied on the spectral information derived from the PRISMS system provided very interesting information about the examination of the construction of the paintings and/or additions on the initial painting pattern. More specifically, the revealing of the continuum of the ‘cloud’ pattern of the neighbouring area to the paper area to the area underneath it, in combination to the identification of their pigment composition indicated that the ‘cloud’ pattern was made first, painted using red lead-containing paint, while the paper was stuck on it afterwards. However, the clustering of the colours of the figure that is painted on the paper with areas of the ground level that have been identified as vermillion and indigo-containing through their multi-modal analysis gives an indication that they are consistent with the palette of the murals. Therefore, the conclusion that can be drawn is that even if the addition of the paper part was not made when the rest of the mural was also painted, it should have been added on the same period.

The revealing of the faded writings of the stamps located on the ceiling (Figure 3-1) was another important evidence for the history of the cave 465. The examination of these stamps by historians and linguists showed that they are Sanskrit writings, with their dating placed around the eleventh century. However, this information should not be considered particularly enlightening for the dating of the murals as the writings were produced on paper and therefore they could be later addition.

## **Chapter 6:**

### **Multimodal approach for the non-invasive analysis of Chinese export paintings of Victoria and Albert (V&A) and Royal Horticulture Society (RHS) collections**

#### **6.1 Introduction**

The analysis of paper-based works of art, such as watercolour paintings, is rather challenging as, additionally to the friability of the substrate, the painting layers are usually very thin, making the collection of samples impossible without causing significant damage. Therefore sampling from this type of artworks is often prohibited from most institutions, limiting invasive scientific analysis on fragments that have been detached from the original object. Moreover, the restriction of the analysis on fragment level in most cases implies the extraction of analytical results that are not giving a representative view of the whole object. For these reasons, the application of a non-invasive approach for the analysis is becoming necessary as, additionally to the elimination of the damage, multiple non-invasive measurements can be taken from the different areas of the surface on the object, enabling a global examination of the artwork. In this direction, the aim of this study was to examine the advantages of the multi-modal approach in the holistic analysis of the paper-based watercolour paintings and how much useful information about the paintings can be extracted to address conservation and history questions.

One of the major problems with the study of manuscripts, and by extrapolation, of paper-based works of art, is the lack of a wide range of non-invasive instruments to study systematically a large collection of materials [96]. In this project, a total of twenty six paintings from the RHS and twenty paintings from the V&A were examined, providing a significantly large statistical sample which has been studied in a way rarely done previously. The application of a suite of non-invasive imaging and spectroscopic techniques involving spectral imaging, OCT, XRF, Raman and VIS-NIR fibre optic reflectance spectroscopy (FORS) to study not only the palette but also the drawing material, painting techniques and the silk or paper substrates, allowed us to address art historical and conservation research questions related to this large sample of watercolour paintings.

The examination of these two collections, in addition to the analytical challenge that provides, was selected also due to their significant art historical importance. The V&A museum and the RHS have large collections of Chinese export watercolour paintings dated from the eighteenth and nineteenth centuries [97], [98]. The V&A collection contains a wide range of watercolour paintings on paper and silk with their main themes referring to trade and occupations, processions and punishments, shipping, as well as domestic scenes and depictions of birds and flowers. The paintings of this collection have been acquired from antiquarian booksellers and art dealers in the late nineteenth century. However, specific information about their origin and dating is rarely available. On the contrary, the paintings from the RHS collection are well documented and exclusively paper-based, with both Western and Chinese paper being used. These are paintings produced for botanical reasons, commissioned and collected by an East India tea inspector, John Reeves, between 1817 and 1831. Therefore, from an art historical point of view, the systematic investigation of the painting materials and techniques of these watercolour paintings provided scientific evidence for the examination of the trade and cultural exchanges between China and Europe of this period [99].

## 6.2 Instruments & materials

Figure 6-1 gives an overview of the analytical techniques and the examination strategy that was followed in this study, followed by a brief presentation of the instrumentation used.

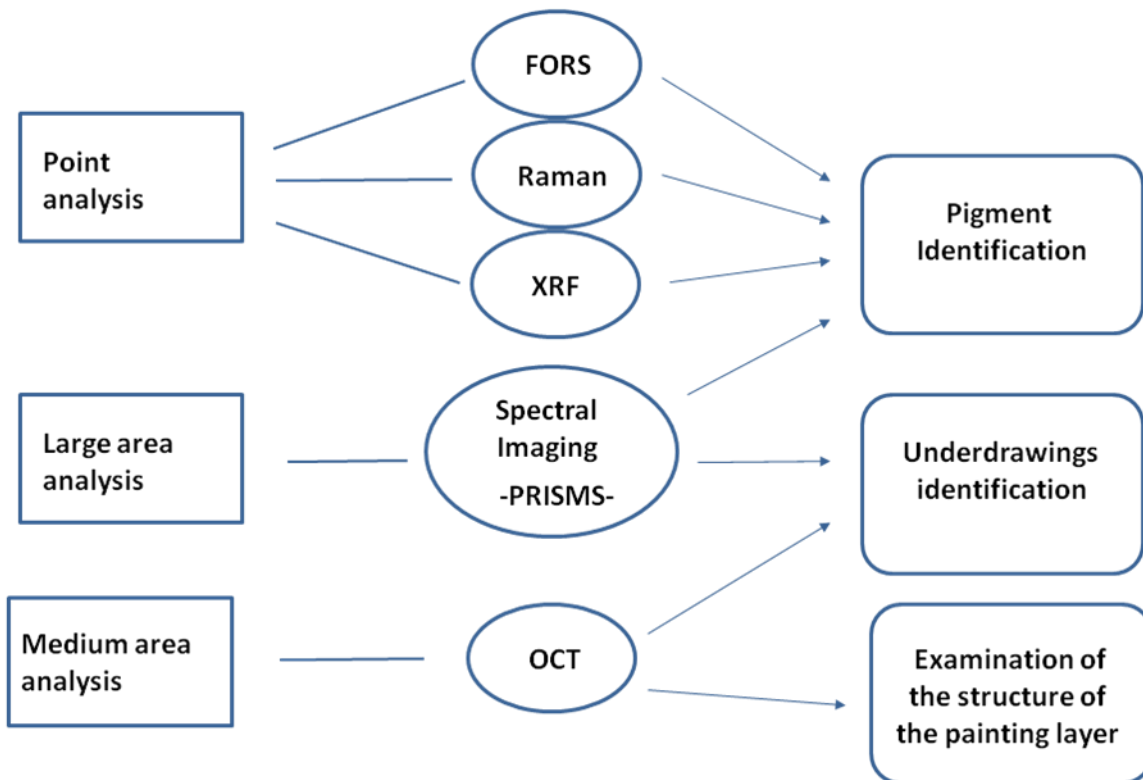


Figure 6-1 Overview of the multimodal analysis strategy

### *Spectral imaging*

PRISMS system, in the lens configuration for close range spectral imaging, was used for a preliminary examination of the paintings.

### *High Resolution Reflectance Spectroscopy*

For detailed pigment identification, FORS spectroscopy (Ocean Optics) with a low intensity tungsten light source (Ocean Optics DH-2000) was used. The spectrometer used covers the VIS/NIR spectral range with spectral resolution 0.9 nm and spectral sampling 0.5 nm.

Two Polychromix fibre optic spectrometers were used for the NIR spectral range: DTS 1700 (900–1700 nm) and DTS 2500 (1700–2500 nm) with spectral resolutions 12 and

22 nm, respectively. Preliminary studies have shown that the spectral examination of paper-based artworks using reflectance spectroscopy in the NIR regime is challenging, as the predominant feature of cellulose is masking the characteristic lines of most of the binders as well as most of the pigments. The low spectral resolution of the specific spectrometers made the detection of the narrow spectral lines even more difficult.

### **XRF**

An ArtTAX XRF spectrometer was used to identify the elemental content of the painting materials and substrates. The operational parameters are 50 kV, 600 µA and 100 s of accumulation live time. Since it was used in open air without helium purge, it was normally sensitive only to elements with atomic number  $Z > 14$ . The collection and interpretation of the data were done by Dr. Lucia Burgio and Sonia Bellesia from V&A museum.

### **Raman spectroscopy**

Micro-Raman analysis was performed with a Horiba XploRA spectrometer coupled to an Olympus microscope using a 638 nm and a 532 nm laser. The laser beam was focussed on a spot of approximately 2 µm diameter, allowing the analysis of individual particles and limiting the interference from surrounding materials. The collection and interpretation of the data were done by Dr. Lucia Burgio and Sonia Bellesia from V&A museum.

### **Optical Coherent Tomography (OCT)**

The OCT used in this study is an adapted Thorlabs spectral domain OCT at 930 nm with axial resolution of approximately 7 µm in air (or 4.5 µm in paint, cellulose and silk) and transverse resolution of 9 µm. In this project, OCT was used to distinguish the different types of papers in terms of both the length of the fibres and the scattering properties of the papers.

### **Reference Samples**

For the preparation of the reference samples, various considerations were taken into account. The selection of the pigments was made so it could cover the whole palette of the various pigments traditionally used in China and some pigments and dyes used in

Europe during the period of interest. The lake pigments were prepared from the dyestuff by J. Kirby at the National Gallery (London) laboratory [100], [101]. Table-6.1 lists the reference pigments and their composition, most of which were analysed and verified in the laboratory in a previous project. The binder was animal glue from the Pigment Factory in Beijing China. The paints were applied on two substrates: Chinese Xuan paper and Canson Aquarelle-300gm watercolour paper. Preliminary studies (see 2.2) showed the necessity of including both high and low concentration paint-outs for each pigment and a range of different particle sizes for those mineral pigments that are traditionally graded into coarse, medium and fine particle sizes. A VIS/NIR spectral library was compiled from the reference samples using FORS instrumentation. Standard spectral reference libraries [78][102] were used for Raman analysis.

Table-6.1 Reference pigments and composition

Pigment name and supplier	Composition (major components)
<b><u>Red</u></b>	
Iron oxide red, natural: Kremer Pigmente	Natural red earth rich in iron oxide
Red lead: Kremer Pigmente	$\text{Pb}_3\text{O}_4$
Vermilion light: Kremer Pigmente	$\text{HgS}$
Lac	<u>Lac dye</u> : sticklac (Kremer Pigmente) soaked in warm water and filtered using cotton patches. <u>Lac Al-based lake (NG laboratory)</u>
Cochineal	<u>Cochineal dye</u> : cochineal insects (Kremer Pigmente) soaked in warm water and filtered using cotton patches. <u>Cochineal Al-based lake (NG laboratory)</u> : 18 <sup>th</sup> century type <u>Cochineal Sn-based lake (NG laboratory)</u> : 19 <sup>th</sup> century type with $\text{SnCl}_4$ Madder dyestuff on Al substrate: 19 <sup>th</sup> century type Madder dyestuff on a sulphate-containing alumina substrate, 19 <sup>th</sup> century type
Madder lake: NG laboratory	Alizarin on a sulphate-containing alumina substrate
Rose madder: L. Cornelissen & Son	Organic dyes, composition unknown
Sappanwood lake: NG laboratory	
Crimson alizarin: Roberson & Co	
Rouge: Pigment Factory Beijing	
<b><u>Yellow</u></b>	
Realgar (Grade 3): Pigment Factory Beijing	$\text{As}_4\text{S}_4$
Orpiment : Kremer Pigmente	$\text{As}_2\text{S}_3$
Yellow ochre: Kremer Pigmente	Natural yellow earth
Litharge: L. Cornelissen & Son	Massicot (orthorhombic $\text{PbO}$ )
Gamboge: Pigment Factory Beijing	ready-prepared paints in animal glue
Buckthorn lake: NG laboratory	Buckthorn dyestuff on alumina substrate
Weld lake: NG laboratory	Weld dyestuff on an alumina substrate
Quercitron lake: NG laboratory	Quercitron dyestuff on a Tingry alumina substrate, 19 <sup>th</sup> century recipe
<b><u>Blue</u></b>	
Azurite (Grade 1,3,5): Pigment Factory Beijing	$2\text{CuCO}_3\text{Cu}(\text{OH})_2$
Indigo: Pigment Factory Beijing	$\text{C}_{16}\text{H}_{10}\text{N}_2\text{O}_2$ ready-prepared paints in animal glue
Indigo: Kremer Pigmente	Indigo and silicaceous extender
Prussian blue (Milori Blue): Kremer Pigmente	Hydrated iron hexacyanoferrate complex, $\text{KFe}[\text{Fe}(\text{CN})_6] \cdot \text{H}_2\text{O}$
Cobalt blue medium: Kremer Pigmente	Cobalt aluminium oxide
Smalt, L.Cornelissen & Son	Cobalt-containing potash glass
Ultramarine synthetic (dark): Kremer Pigmente	Sulphur-containing sodium aluminosilicate, approx. $\text{Na}_{6-10}\text{Al}_6\text{Si}_6\text{O}_{24}\text{S}_{2-4}$
<b><u>Green</u></b>	
Malachite (Grade 1,3,5): Pigment Factory Beijing	$\text{CuCO}_3\text{Cu}(\text{OH})_2$
Atacamite: Kremer Pigmente	$\text{Cu}_2\text{Cl}(\text{OH})_3$
<b><u>White</u></b>	
Lead white (Cremnitz white): Kremer Pigmente	$\text{PbCO}_3\text{Pb}(\text{OH})_2$
Shell white: The Pigment Factory Beijing	$\text{CaCO}_3$
<b><u>Black</u></b>	Carbon
Chinese ink	

## 6.3 Results & Discussion

### 6.3.1 Identification of pigments

#### Blues:

In the examination of the watercolour paintings of the RHS collection, only a limited number of blue areas was observed, with the blue colourant being identified as azurite. On the other hand, a lot of blue areas were observed on the watercolour paintings of the V&A collection, with their multi-modal analysis showing that they are azurite-containing (Figure 4-5). However, the combined use of azurite with prussian blue and cobalt blue was also detected on blue areas of two paintings of the collection. FORS spectra collected from these areas contain the characteristic absorption lines of smalt, while the KM algorithm gave the best fit when reference of smalt, azurite, lead white and Chinese ink were used (Figure 6-2d). The XRF spectroscopic analysis detected Co and Pb as the major elements, supporting the presence of smalt and lead white respectively(Figure 6-2c). Raman measurements confirmed only the presence of azurite, detecting also crystals of its impurities (i.e. goethite and malachite) (Figure 6-2b).

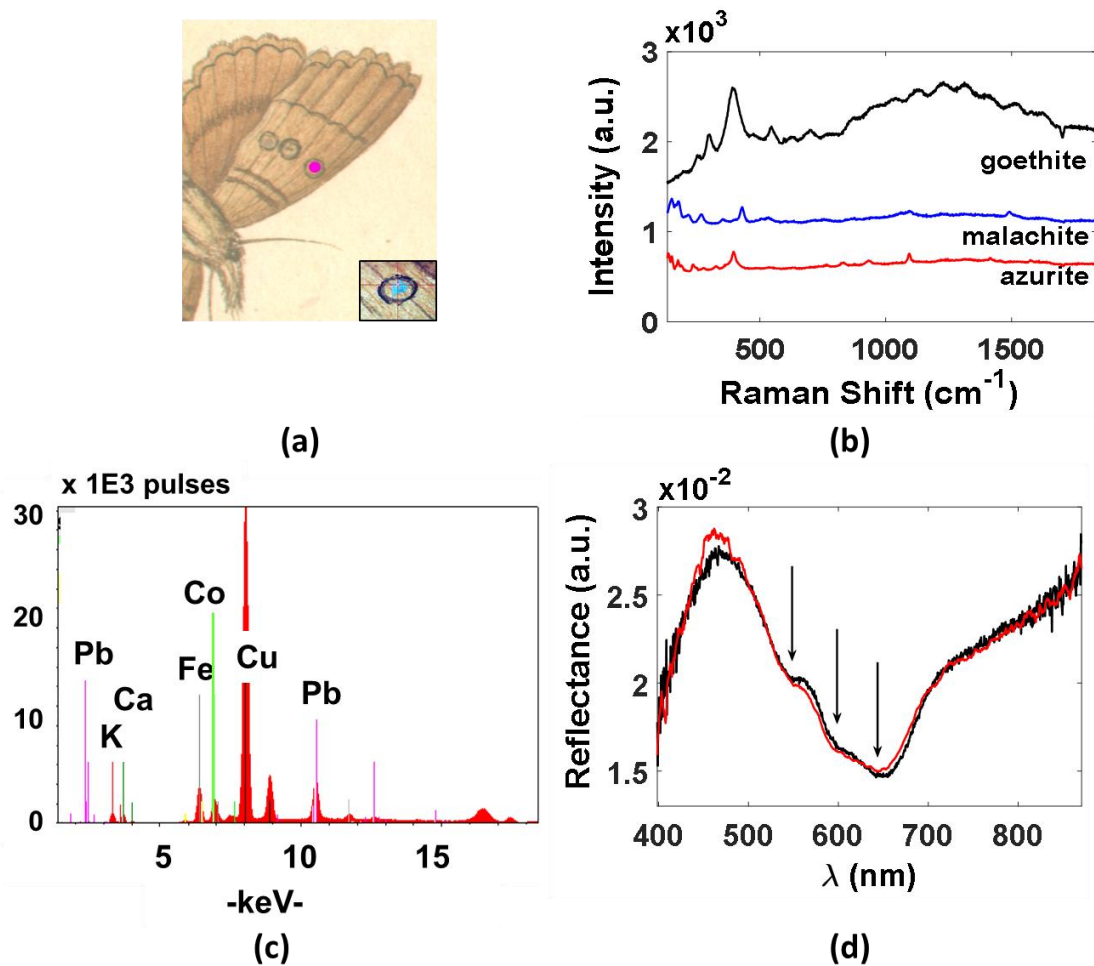


Figure 6-2 (a) Colour image derived from PRISMS data collected from a detail on painting no.1312-1889 (V&A collection) with the magenta dot indicating the blue analysed area[caption: microscopic image of the blue area]; b)Raman spectra for particles in the blue area; c) XRF spectroscopy detected Cu (main element) with small amounts of Co and Pb. d) KM model fit (red curve) to the measured FORS spectrum (black curve) is consistent with a mixture of small, azurite (grade 5), lead white and Chinese ink.

Even though the use of single indigo was not observed in any of the watercolour paintings of the two collections, it was identified as one of the main colourants on green leaves (Figure 4-3) and also used in combination with red dyes in purple areas (Figure 6-7). Moreover, its combined use with other pigments (e.g. hematite, azurite and lead white) in order to achieve the effect of dull colour was observed. Figure 6-3 illustrates the identification of a dull blue area. The application of the KM method on the reflectance spectra collected of the same area gave a perfect match for a combination of azurite, lead white and indigo references, with the spectral feature of indigo being predominant. XRF measurements on this areas detected Cu and Pb as the major elements, with Ca, Ba, Fe and K being detected also on the support. Raman analysis on blue crystals of the area confirmed the presence of indigo.

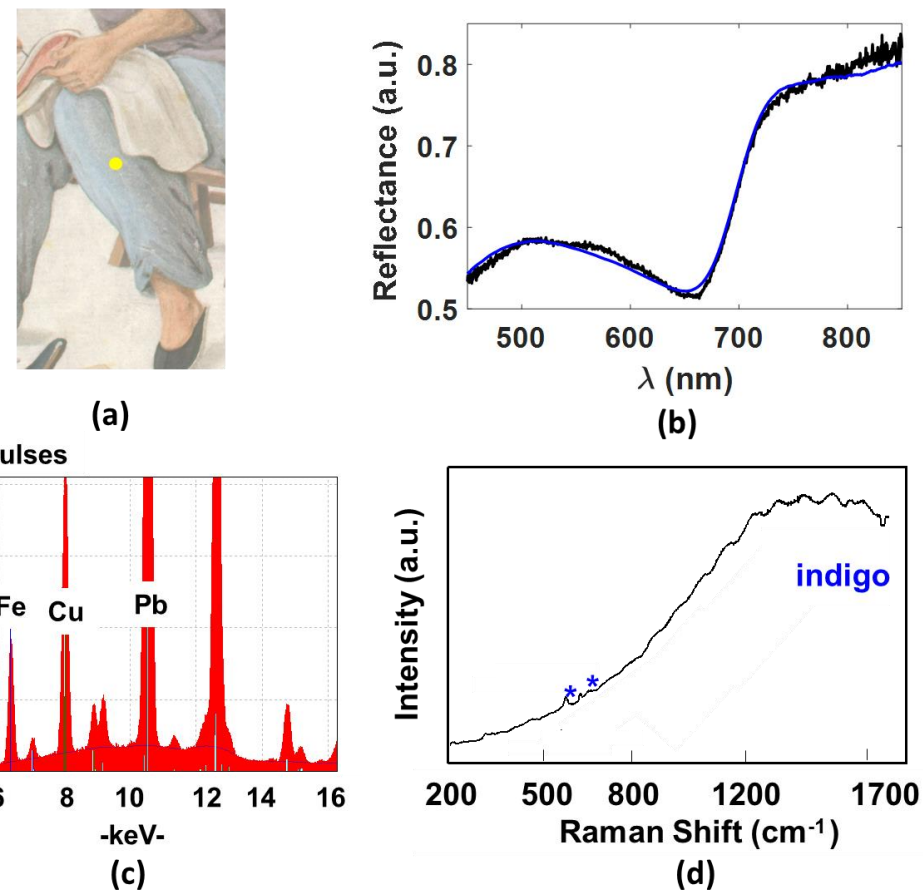


Figure 6-3 (a) Colour image derived from PRISMS data collected from a detail on painting no. 7790-18 (V&A collection)) with the yellow dot indicating the dull blue analysed; b) KM model fit (blue curve) to the measured FORS spectrum (black curve) is consistent with a mixture of azurite, indigo and lead white, c) XRF spectroscopy detected Pb and Cu as predominant elements; d) Raman spectra identified particles of indigo

### Greens:

In both collections, the analysis of the pigment composition of the green leaves showed that a combination of malachite, gamboge, indigo and occasionally lead white was used. This is not surprising, as the traditional way of painting greens when these watercolour paintings were produced was the combined use of Cu-containing greens, mainly malachite, with gamboge and indigo. More specifically, their combined use in a mixture or the application of a first layer of Cu-green layer with a top layer of a mixture of gamboge and indigo were the commonly used methods for achieving green colour. The combined use of non-invasive techniques for the complete identification of the pigments in the green areas was proven necessary. The reflectance spectroscopic analysis of green leaves of different hues showed that, additionally to the identification of the colourants, qualitative information about the relative concentration between indigo and malachite can also be extracted. Figure 6-4b shows that, in the reflectance spectra collected from

light green areas, the contribution of indigo is less compared to the spectra collected from the dark green leaves (Figure 4-3).

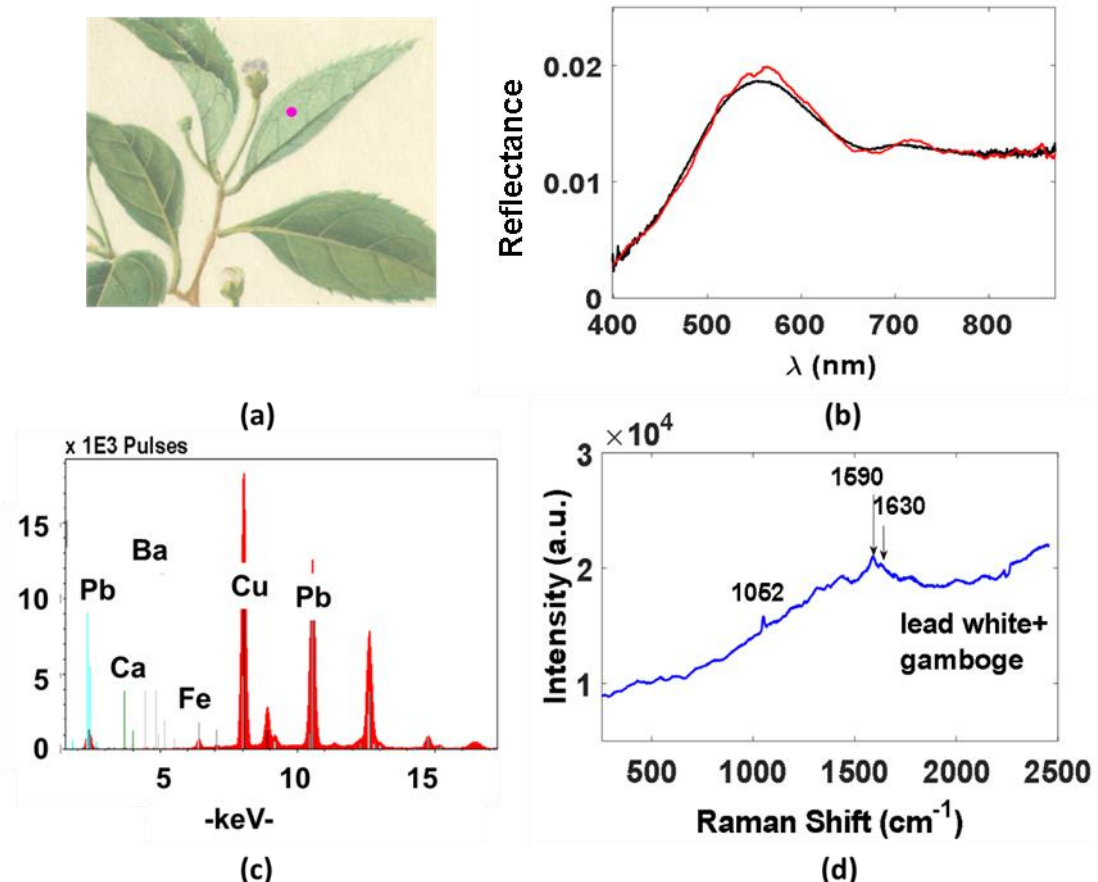


Figure 6-4 (a) Colour image derived from PRISMS data collected from a detail on painting no. 290-1886 (V&A collection) with the magenta dot indicating the green analysed area;(b) KM model fit (red curve) using a combination of malachite, gamboge, indigo and lead white to the measured VIS-NIR reflectance spectrum (black curve); (c) XRF spectrum detected Cu and Pb as the predominant element and d) Raman measurement for this area detected particles of lead white.

### Yellows:

The non-invasive analysis of yellow and green areas of both collections identified gamboge as the yellow colourant (Figure 4-2) that was mainly used. Interestingly, chrome yellow was identified as the yellow colourant of one of the paintings in RHS collection (Figure 6-5). Although the reflectance spectroscopy does not provide precise identification of most of the yellow pigments (2.2), the complementary application of Raman and XRF spectroscopies enabled its accurate identification. More specifically, micro-Raman spectroscopy detected chrome yellow while XRF found Cr confirming that it is not just signal from an isolated particle since the XRF spot size is much larger

and therefore provides more representative results for the composition of pigments of the analysed area.

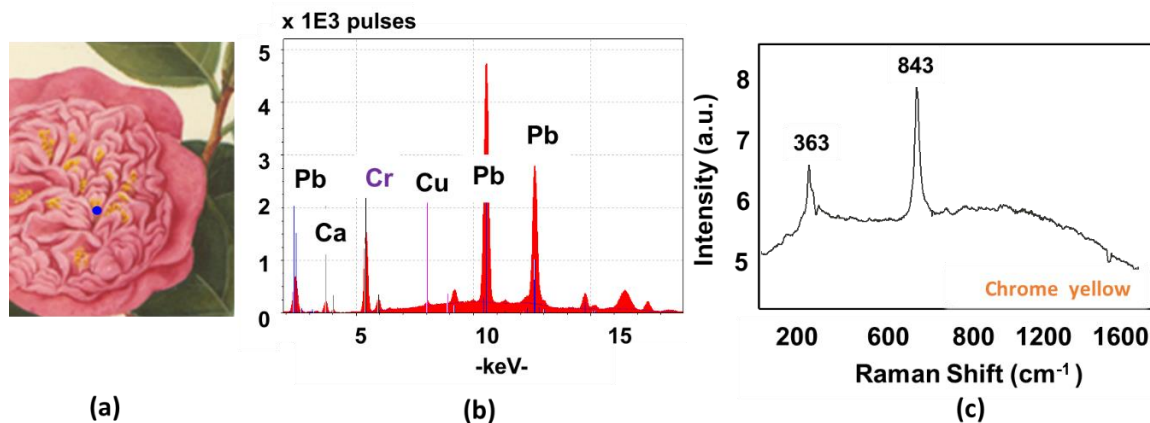


Figure 6-5 (a) Colour image derived from PRISMS data collected from a detail on painting no. 35617 - 1001 (RHS collection) with the blue dot indicating the yellow analysed area; (b) XRF spectrum detected Pb as the predominant element but also a significant amount of Cr and (c) Raman measurement for this area detected chrome yellow.

### Reds:

The vivid red areas, mainly of the watercolour paintings of the V&A collection, were identified as vermilion-containing. More specifically, the analytical spectroscopic results obtained by the various non-invasive analytical techniques agreed on the presence of single vermilion. In their analysis, the results from all the individual non-invasive analytical techniques were in agreement, confirming the detection of vermilion. The KM model using vermilion as reference gave a perfect fit on the reflectance spectra collected from these areas (Figure 6-6b). The detection of Hg as the major element in the XRF (Figure 6-6c) spectra collected from these areas supported the identification of vermilion. Moreover, the identification of red crystals of these areas as vermilion, using Raman spectroscopy, confirmed its presence further (Figure 6-6d).

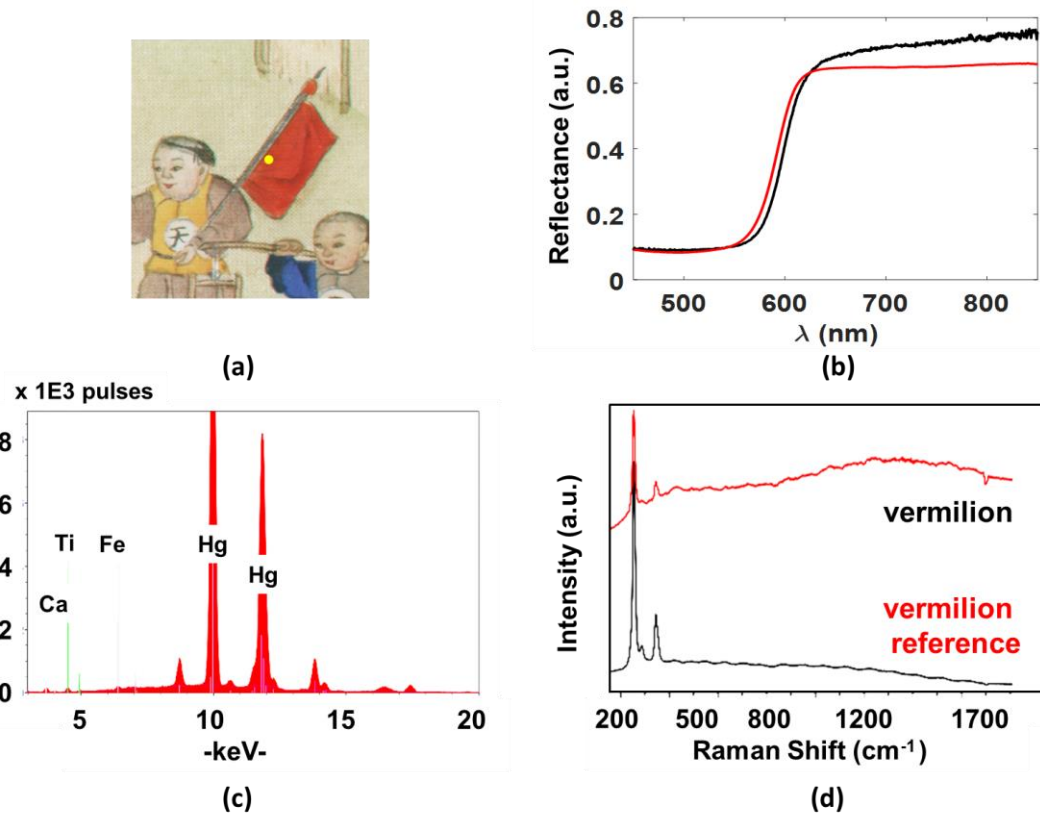


Figure 6-6 (a) Colour image derived from PRISMS data collected from a detail on painting no 7791-8 (V&A collection) with the yellow dot indicating the red analysed area; (b) KM model fit (red curve) using single vermilion as reference to the measured VIS-NIR reflectance spectrum (black curve); (c) XRF spectrum detected Hg as the predominant element, with Fe, Ca and Ti belong to the substrate and (d) Raman measurement for this area (red curve)detected particles of vermilion , while vermilion reference (black curve)is illustrated for comparison

### **Red organic dyes:**

FORS analysis on various painted areas of the watercolour paintings of both collections indicated the presence of red organic dyes and more specifically of anthraquinone dyes (substances with main molecular compound the aromatic organic C<sub>14</sub>H<sub>8</sub>O<sub>2</sub>). The group of anthraquinone dyes includes scale insect dyes, such as lac and cochineal dyes, as well as the plant-derived dye madder. These three organic dyes are of a great importance in the context of this project as it is known that lac and madder had been used in China over the centuries, while cochineal was imported to China during that period [18]. Therefore, the possibility of their identification was extensively investigated in the context of this study. The identification of the anthraquinone dyes is challenging because of the limitations that the various non-invasive techniques face, with FORS being the only analytical technique that is sensitive in their detection (Figure 4-4). For this reason, a detailed examination of the potential of FORS investigation for the precise distinction between them was carried out. Among the anthraquinone dyes madder is very easy to be distinguished from the scale insect dyes, as its characteristic absorption bands are in shorter wavelengths [103], [104]. More specifically, cochineal and lac have their pairs of characteristic absorption bands at 523 nm and 557 nm and 529 nm and 565 nm respectively, while madder has its pair at 513nm and 545 nm. During the examination of the V&A and RHS collections, red dyes were detected in almost every painting, with their use being observed in paint layers of various tones and hues of red colour, paint mixtures of purple colour as well as in fine details and highlights. In all different cases, the characteristic anthraquinone absorption lines were within the range of the scale insect dyes, with the possibility of the use of madder being therefore excluded. Figure 6-7 illustrates the identification of a dull purple area. XRF spectroscopy detected only Pb additionally to the elements of the substrate. Raman spectroscopy identified indigo as the blue colourant of the paint layer, with a high signal of fluorescence being detected as well, suggesting the presence of an additional organic component, without however enabling its identification. Finally, FORS measurements on the area confirmed and supplemented the results of the other two techniques, with KM fit to the spectra of this area using a mixture of indigo, red dye (lac) and lead white.

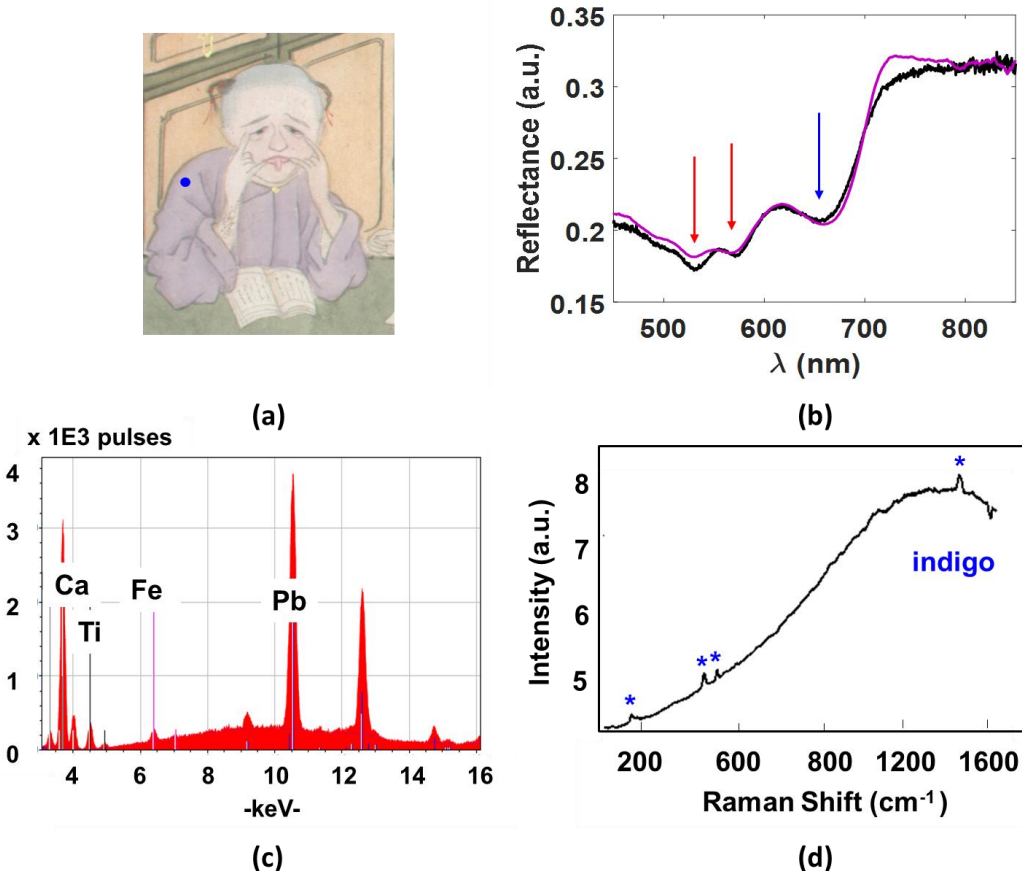


Figure 6-7 (a) Colour image derived from PRISMS data collected from a detail on painting no 7791-12 (V&A collection) with the blue dot indicating the dusty purple analysed area; (b) KM fit (purple curve) to FORS measurement (black curve) using a mixture of indigo, lac and lead white references, the red arrows point the characteristic lines of the scale insect and the blue the line of indigo; (c) XRF measurements showed Pb as the predominant element; (d) Raman spectrum indicated the presence of indigo

Figure 6-8 shows the identification of the red dye as the colourant used for painting the fine veins on the green leaves. KM using malachite, gamboge, indigo and lac as references gave good fit on the reflectance spectral collected from these areas (Figure 6-8b). As it was expected, neither XRF nor Raman spectroscopy assisted the identification of the red dye; they did, however, confirm the identification of the other pigments. More specifically, XRF spectra showed that Cu is the major element, with the elements of the substrate being present as well. Given that the rest of the colourants are organic compounds, XRF did not provide any indication of their presence. Raman spectroscopy confirmed the presence of indigo, with strong signal of fluoresce being present.

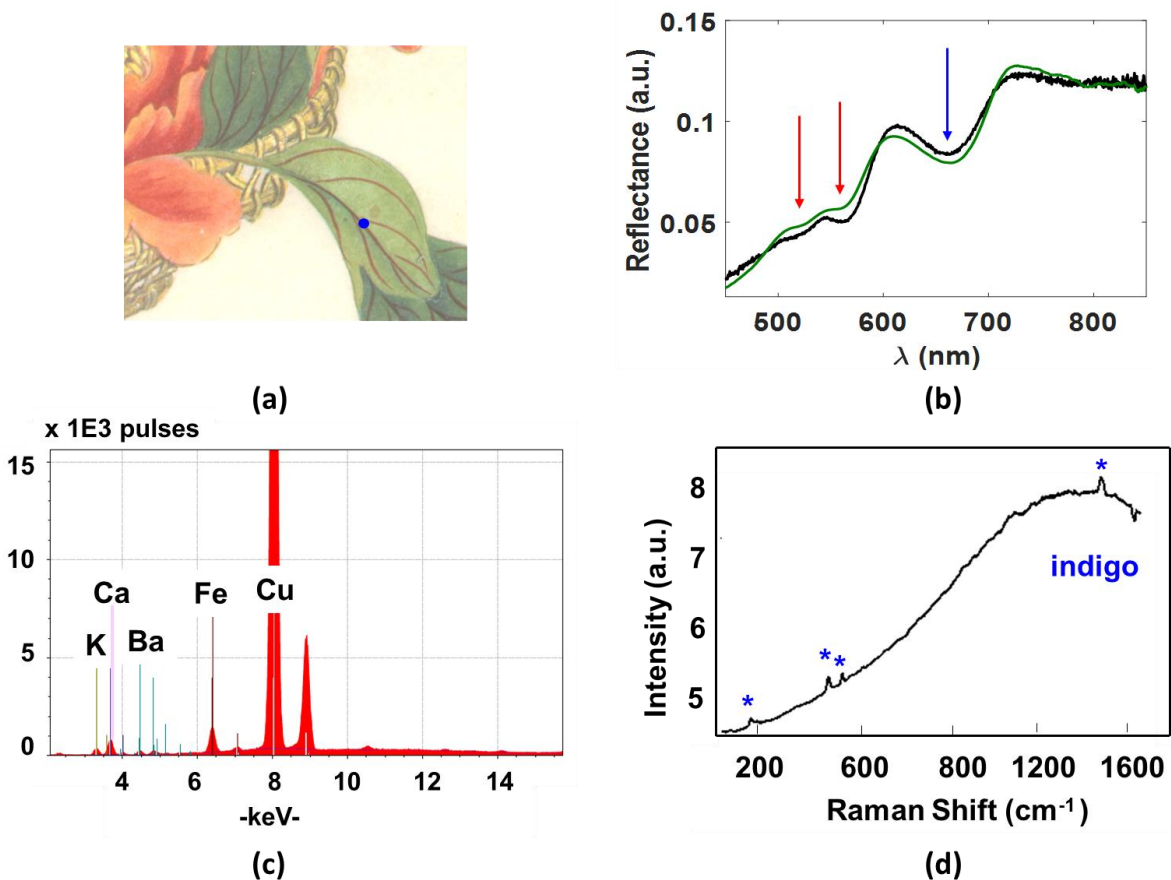


Figure 6-8 (a) Colour image derived from PRISMS data collected from a detail on painting no 554-1907 (V&A collection) with the blue dot indicating the analysed area; (b) KM fit (green curve) to FORS measurement (black curve) using a combination of lac, indigo, malachite and gamboge references, the red arrows point the characteristic lines of the scale insect and the blue the line of indigo; (c) XRF measurement of the a dusty purple area showed Cu as the predominant element; (d) Raman spectrum indicated the presence of indigo

The spectra collected from scale insect dyes-containing areas of the watercolour paintings were classified in two groups according to the position of their characteristic absorption bands (Figure 6-9). The first group consisted of spectra that have their absorptions lines clustered around a mean at 523 nm and at 557 nm respectively, whilst the spectra belonging to the second group had their absorption lines around a mean at 530 nm and at 565 nm. The application of the KM algorithm on the reflectance spectra of these two groups gave good fits when cochineal and lac were used as the red dye reference respectively. Figure 6-9b shows an example where a reflectance spectrum belonging to the first group is fitted better when KM model fit was applied using cochineal reference instead of lac, with the other pigments identified to be present being taken into account. On the contrary, KM model fit on reflectance spectra classified to the second group gave better fit using lac dye as reference (Figure 6-9c). These results

led to the conclusion that the precise identification of the scale insect dyes is possible on these paintings using FORS in combination with the KM algorithm.

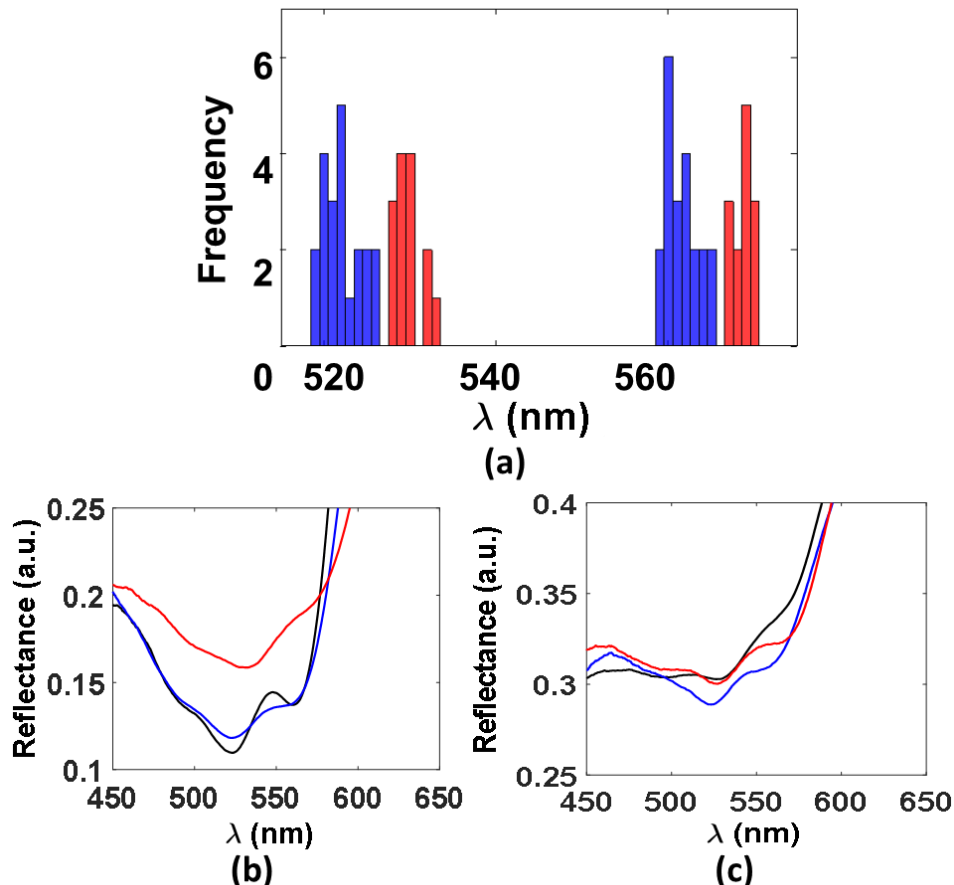


Figure 6-9 (a) Distribution of the central wavelength of the absorption characteristic of scale insect dyes lines detected on the paintings of the V&A and RHS collections. The blue bars correspond to lines of **group A** that are clustered around a mean at 523 nm and at 557 nm, while the red bars correspond to the lines of **group B** and are clustered around a mean at 530 nm and at 565 nm. (b) KM fit to FORS measurement of an area from painting no. 7791-8 (V&A collection) that is clustered in **group A** using a combination of either cochineal (blue line) or lac (red line) dye with vermillion and lead white. (c) KM fit to FORS measurement of an area from painting no. D82-1886 (V&A collection) that is clustered in **group B** using a combination of either cochineal (blue line) or lac (red line) dye with vermillion and lead white

In order to further investigate the possibility of precise identification of the red scale dyes using FORS, further examination of the parameters that can affect their spectral behaviour was performed. The organic red dyes are known to be spectrally sensitive when the pH of their environment changes, with studies having shown that the application of cochineal dye on paper substrates of different pH values resulted in colour changes. Moreover, experiments carried out in buffer solutions of a range of pH values showed that the characteristic absorption lines of cochineal and lac are becoming

less prominent and also shift to shorter wavelengths when added in acidic solutions [105][106][106]. Therefore, further experiments were performed in order to investigate whether the separation of the insect dyes-containing areas into the two groups is observed due to the application of different dyes or due to the spectral shift of the same dye, caused by changes in the acidity of its environment. One of the factors that can affect the acidity of the environment of the red organic dyes is related to the compounds that are added for their laking. Laking is the procedure of manufacturing a pigment by precipitating a dye using a metallic salt. Historical sources about the Chinese painting tradition and methods do not give clear evidence about the use of pure dyes and/or the lake pigments made from them during the period of interest. On the other hand, in Europe, scale insect dyes have been used in both forms, though mainly in the form of lake pigments in easel paintings. Given the extent of the trading relationships between the Europeans and the Chinese in this era, it is difficult to assume that European lake pigments were not exported to China and therefore this possibility should be examined. Another factor that can affect the acidity of the environment of the dyes is the possible treatment of the substrates (e.g. paper or silk) for their sizing. Finally, the use of solutions for the fixing of the paint layers could also affect the acidity of the painting environment. In order to cover all the different scenarios, a series of artificial samples were prepared simulating the various pH environments. Consequently, additionally to the pure dyes, samples of the corresponding lake pigments, both Al and Sn- based, were also examined. The lake pigments were prepared by the National Gallery in London, with the preparation of Al-based cochineal lake being based on an 18th century recipe while the Sn-based cochineal lake on an early nineteenth century recipe [100]. For the investigation of the spectral behaviour of the scale insect dyes according to variations in the acidity of the substrate, a series of samples made of both lac and cochineal dyes applied on paper surfaces with different pH values were examined. More specifically, a series of solutions with pH values extending from 1 to 13 were spread uniformly on paper substrates, with the acidity of the final surface of the paper substrates measured using pH test paper. Even though this method does not provide precise measurements of the pH value, it enabled the confirmation of the spread of the acidities of the paper surfaces along the wide pH range. Finally, reference samples using these dyes were prepared on Chinese Xuan paper in the traditional manner, where the paper substrate was first brushed with a solution of alum and animal glue and then painted with layers of dyes in animal glue followed by solutions of alum and animal glue, with the process

repeated three times to achieve a stronger colour [18][107]. The solution of alum and animal glue was used to fix the paint [107].

The spectral comparison between the various lake pigments of both dyes (Figure 6-10) showed that both the aluminium (Al)-based lac lake and the tin (Sn)-based cochineal lake pigments do not shift from the absorption positions of the pure dyes. However, the Al-based cochineal lake had a spectral shift to longer wavelengths (i.e. 529nm and 567nm), with its characteristic absorption lines being almost at the same position as the lines of lac dye.

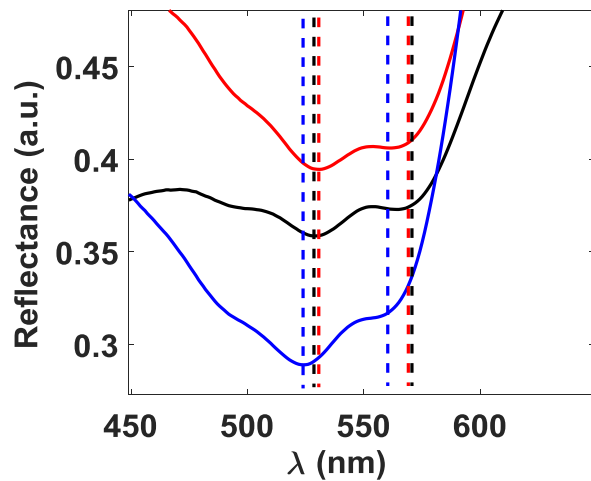


Figure 6-10 Spectral comparison between the reflectance spectra of: Al-based cochineal lake (blue curve), Zn-based cochineal lake (black curve) and lac lake (red curve). The vertical dashed lines indicate the positions of the absorption lines of: Al-based cochineal lake (blue dashed line), Zn-based cochineal lake (black dashed line) and lac lake (red dashed line).

For the investigation of whether the red organic dyes used on the paintings of V&A and RHS collections were in their pure or lake form, the complementary use of XRF spectroscopy proved useful. Preliminary testing on the references samples was performed in order to determine the detection limits of the XRF spectrometer. The examination of the Al-based lake pigments showed the detection of S, as would be expected since alum that contains sulphur was used to make the lake pigments, and Sn was detected in the Sn-based cochineal lake paint out. On the other hand, measurements performed on the samples that were prepared using pure dyes in the traditional Chinese manner did not detect any S even though alum–glue solution was used to fix the paint layers. The most possible explanation is that the amount of alum present in the three thin washes is very low. It has to be noted that the XRF measurements were performed in open air without helium purge, limiting this way its limitation range in elements with

$Z>14$  and therefore the detection of Al ( $Z=13$ ) was not expected. The fact that XRF measurements performed on various red dyes-containing areas of the watercolour paintings of the V&A and RHS collections did not detect S or Sn, led to the conclusion that pure lac and cochineal dyes were used.

The observation of the spectral behaviour of the cochineal and lac dyes depending on the acidity of the paper substrate showed that the characteristic absorption lines remain approximately at the same position (Figure 6-11). More specifically, the line at the shorter wavelength for both dyes being shifted by 1 nm for pH greater than eight, while their lines at longer wavelengths remain at exactly the same position in any acidic case.

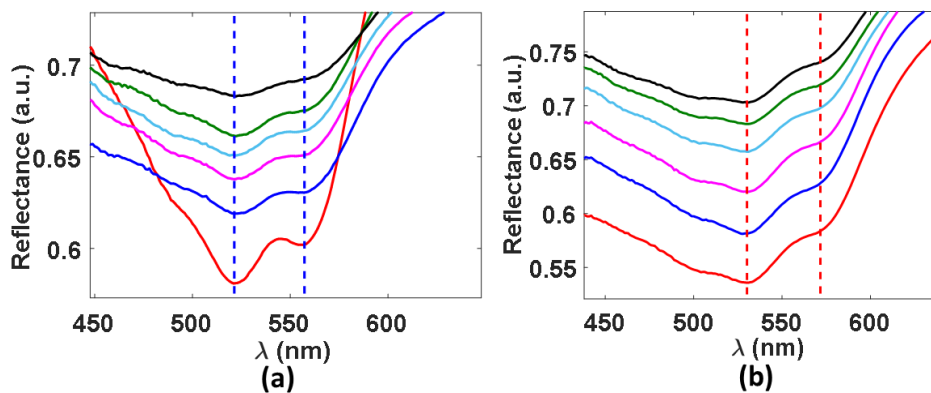


Figure 6-11 Spectral comparison of (a) pure cochineal juice and (b) pure lac juice applied on paper substrates of pH 2 (black line), pH 4 (green line), pH 6 (light blue line), pH 8 (magenta line), pH 10 (blue line) and pH 12 (red line)

Figure 6-12 shows that the only significant difference that is observed when lac and cochineal dyes are applied on papers of different pH value is that as the pH values increases, the absorption features are becoming more intense, with their spectral position remaining fairly the same, enabling their distinction. From these preliminary studies, the conclusion drawn was that the identification of lac and cochineal dyes is likely even when they have been applied on substrates of various pH values. Therefore, in combination with the previous results about lake pigments, we can assume that, in cases where XRF analysis suggests the use of pure dyes, the identification of the insect dyes is likely independent of the acidity of the substrate. However, further systematic experiments in order to confirm the repeatability of these results, as well as experiments that will examine the possible contribution of the other painting materials, such as pigments or binder, should be performed.

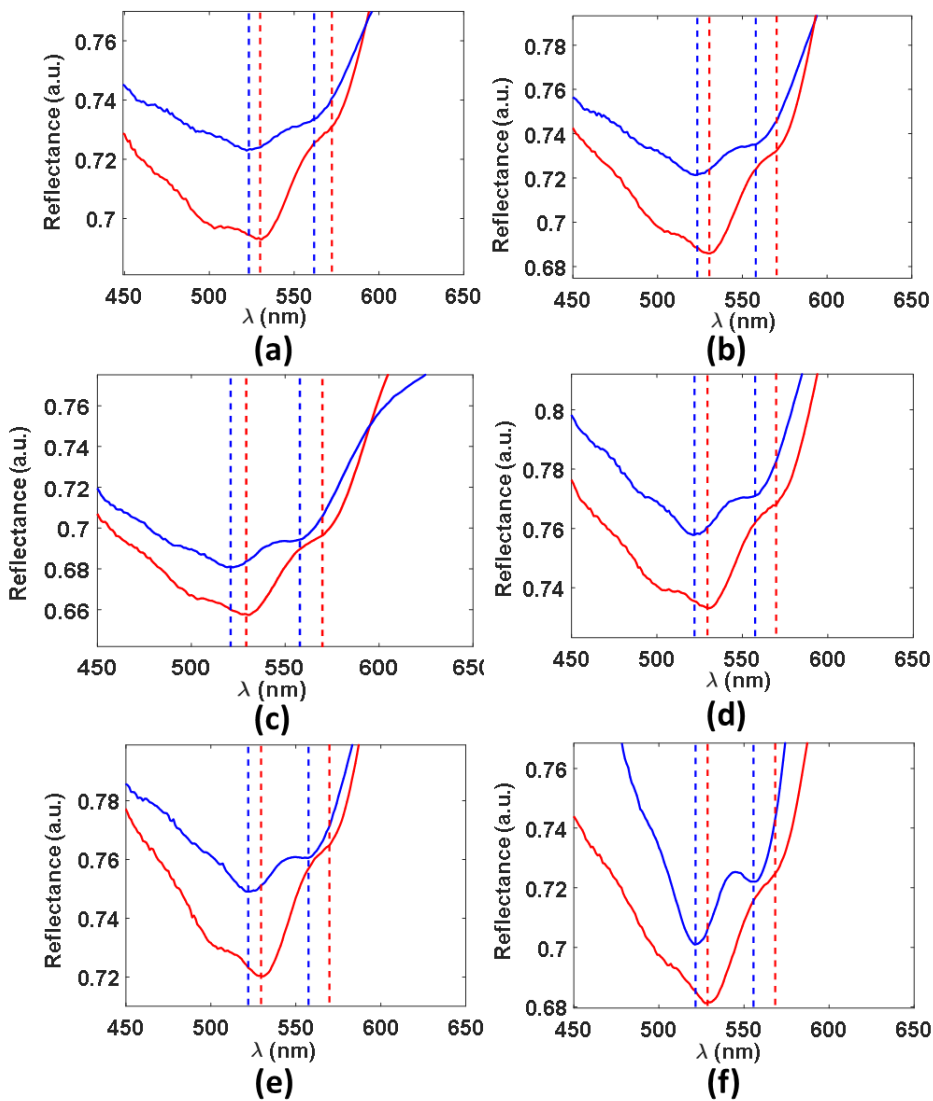


Figure 6-12 Spectral comparison between pure cochineal (blue) and ac (red) juices applied on papers of acidity: (a) pH:2, (b) pH:4, (c) pH:6, (d) pH:8, (e) pH:10, (f) pH:12. The vertical lines indicate the positions of the absorption lines of cochineal (blue dashed lines) and lac (red dashed lines) juices respectively

Figure 6-13 shows the distribution of the two groups of insect dyes, illustrating furthermore the type of the substrate that they have been applied on. As the different types of substrate have gone through different sizing and filling treatments, they provide a realistic sample with possible pH variations. Spectra belonging in both cochineal and lac groups were detected on paintings with Western paper substrate (Figure 6-13b). The examination of the paintings made on Chinese paper showed only one case with spectrum belonging to the lac group (Figure 6-13c), with the rest belonging to the cochineal group. This result is quite surprising as lac is the traditionally used Chinese dye and therefore its presence on the Chinese paper would be expected. Nevertheless, a larger statistical sample should be examined in order to draw more accurate conclusions

regarding the identification of the insect dyes on the export Chinese paintings. Further confirmation of their identification could be obtained by the application of micro-destructive analytical techniques, such as Surface-Enhanced Raman Spectroscopy (SERS) [108], [109]. Developments in these techniques regarding both the instrumentation and the minimization of sampling enable the precise identification of the organic dyes through the analysis of tiny samples.

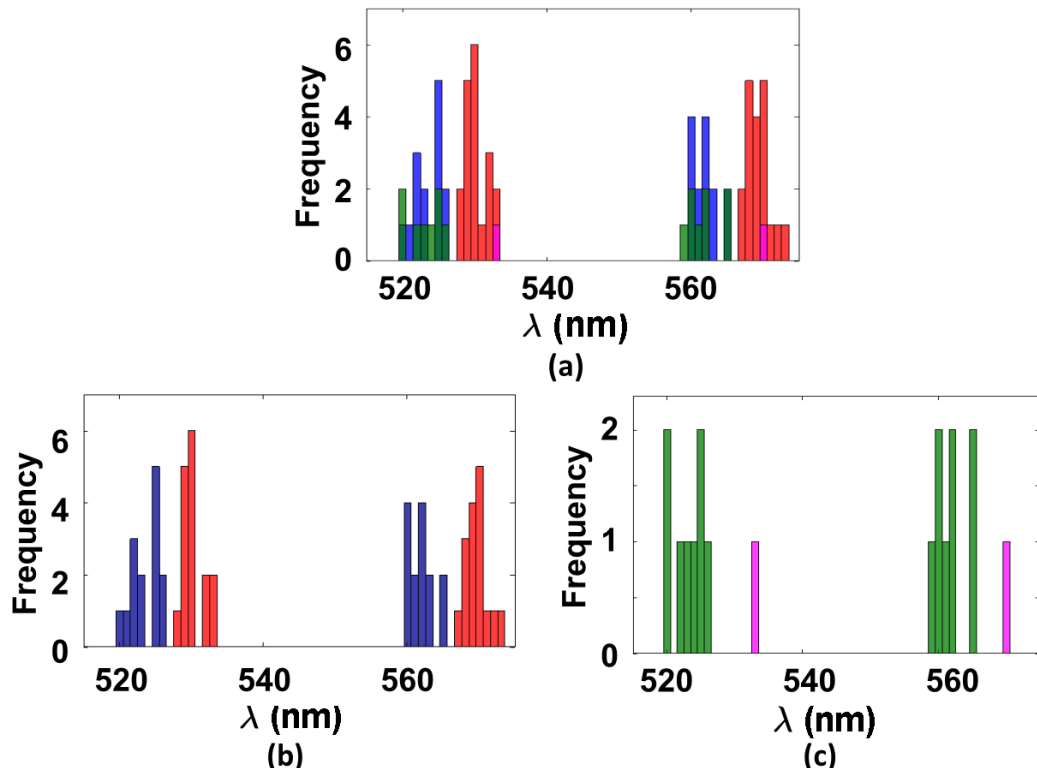


Figure 6-13 Distribution of the central wavelength of the absorption lines detected on the paintings that are characteristic of scale insect dyes a) The blue bars correspond to the lines in group A consistent with cochineal dye painted either on Chinese paper or on silk, green bars correspond to the lines in group A consistent with cochineal dye painted on western paper, the red bars correspond to the lines in group B consistent with lac dye painted either on Chinese paper or on silk and magenta bars correspond to the lines in group B consistent with lac dye painted on western paper; b) examined areas painted on Chinese paper or silk (V&A collection paintings and one RHS painting (Chinese paper sized). The blue bars correspond to the lines in group A consistent with cochineal dye and the red bars correspond to the lines in group B consistent with lac dye; c) examined areas painted on western paper. The green bars correspond to the lines in group A consistent with cochineal dye and the magenta bars correspond to the lines in group B consistent with lac dye.

### Oranges:

Besides the occasional presence of realgar (4.1.2.1), the majority of the analysed orange areas of the watercolour painting were found to consist of a combination of red lead and vermillion. These two red pigments have similar ‘S’-shape spectral features with a

relative spectral distance of 50nm. KM algorithm gave a reasonable good fit on the spectra collected from this area using a combination of vermillion and red lead references (Figure 6-14b), with the contribution of red lead being obvious in the regime below 550 nm and the contribution of vermillion in the regime beyond. Moreover, XRF spectroscopy detected Pb and Hg as the major elements, supporting the presence of these two pigments, with the detection of Cu related to its presence in the surrounding yellow/green details and the large spot size of the instrument. Finally, Raman measurements identified orange and red particles of red lead and vermillion respectively.

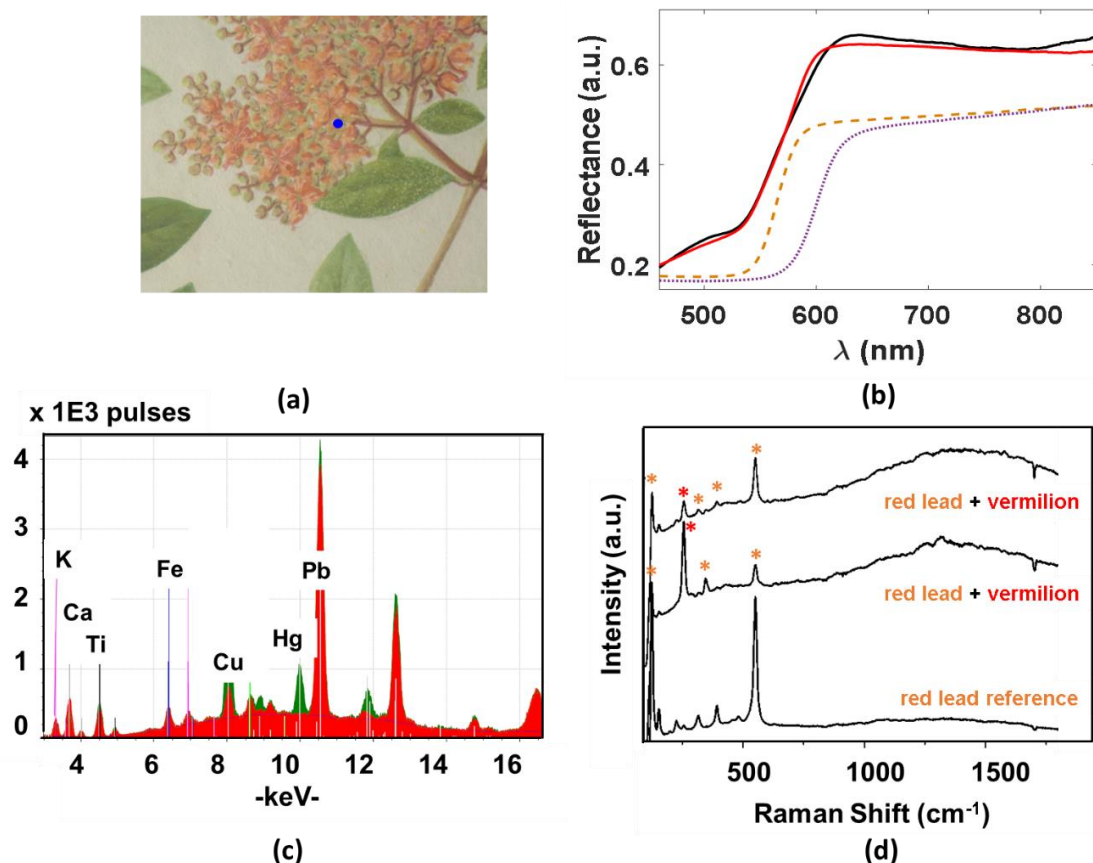


Figure 6-14 (a) Colour image derived from PRISMS data collected from a detail on painting no 67110 (RHS collection) with the blue dot indicating the orange analysed area; (b) KM fit (red curve) to FORS measurement (black curve) using a mixture of red lead and vermillion, the orange dashed and the purple dotted lines are the reference spectra of red lead and vermillion respectively; (c) XRF spectroscopy detects Pb and Hg of the a dusty purple area showed Cu as the predominant element; (d) Raman spectrum indicated the presence of indigo.

## Palette

The significant number of examined areas from paintings of both V&A and RHS collection offered a sample of more than 600 coloured areas, consisting of various pigments and combinations of them. The analysis of the pigments showed that

traditional pigments and organic dyes have been used on all of the paintings. However, pigments that are reported to be imported in China in the period of their production were also detected. More specifically, cochineal dye was detected in the painting of both collections and Russian blue was found on paintings of the V&A collection. Table 6-1 summarises the composition of pigments of the various coloured areas, as it arises from their multimodal, non-invasive analysis.

Table 6-1 Palette

<b>Colour of the analysed area</b>	<b>Pigment/ Combination of pigments</b>
<b><u>Blue</u></b>	Azurite Azurite + ink Indigo + lead white Indigo + azurite + lead white Prussian Blue + lead white Prussian blue + azurite + lead white Smalt* + azurite + Prussian blue Ultramarine* + lead white
<b><u>Green</u></b>	Malachite Malachite + gamboge + indigo Malachite + gamboge + indigo + lead white Indigo + gamboge + lead white + ink
<b><u>Yellow</u></b>	Gamboge + lead white Realgar + lead white Chrome yellow
<b><u>Red</u></b>	Vermilion Vermilion + lead white Vermilion + red dye (lac) + lead white Red dye (cochineal) + indigo
<b><u>Pink</u></b>	Dark: red dye (cochineal) + indigo + lead white Light: red dye (cochineal and lac) + lead white red dye (lac) + indigo + vermilion + lead white
<b><u>Skin colour</u></b>	Red dye (lac) + lead white Red ochre + indigo + lead white Vermilion + indigo + lead white
<b><u>Orange</u></b>	Red dye (cochineal) + gamboge +lead white Red lead + vermilion
<b><u>Purple</u></b>	Dark: Red dye (cochineal and lac) + indigo Red dye (cochineal and lac) + Prussian blue Light: Red dye (cochineal) + indigo + lead white Red dye (cochineal and lac) + Prussian blue +lead white
<b><u>White</u></b>	lead white
<b><u>Gold</u></b>	shell gold
<b><u>Silver</u></b>	Silver

\*Detected only on one painting

### 6.3.2 Examination of the substrate

The complementary use of the OCT scanning and XRF spectroscopy was applied for the non-invasive characterization of the substrates of both collections. As presented previously (see section 4.4), OCT scanning can provide information about the structure of the substrates (e.g. length and intensity of the fibres), while XRF spectroscopy provides information related to the chemical treatment procedure that was followed for their sizing and/or filling. Their complementary use was applied on the substrates of the watercolour paintings of both collections, revealing very important evidence regarding their history. Visual examination of the substrates of the paintings of both collections showed that all the painting of the RHS collection are painted on paper, whereas the V&A collection included also six painting of textile substrate, most probably silk. More detailed examination of two of the paintings with the textile substrate using OCT scanning showed that their weave is plain (Figure 6-15). Moreover, it was observed that the threads were not twisted and the spacing between them was very small, causing strong scattering in the OCT image. Finally, similarity between the spacing of the warp and weft threads was observed, characteristic that comes in contrast to the conventional weave for silk hanging scrolls [18]. However, the statistical sample of textile substrates that was analysed was small, making the drawing of safe conclusions about their characterization impossible. For the extraction of accurate results a larger sample of the textile substrates of V&A collection should be examined.

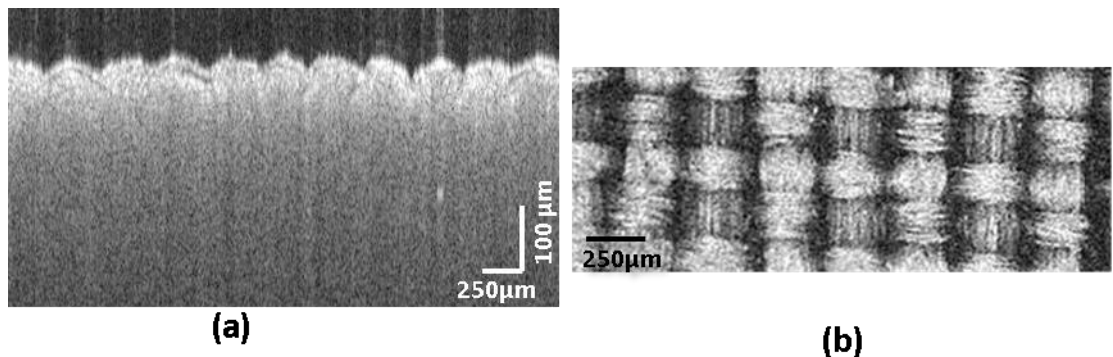


Figure 6-15 (a) OCT cross- section and (b) enface image of silk substrate of painting no. 7790-7 (V&A collection)

Section 4.4.2 describes the procedure followed for the characterisation of the paper substrates of both collections and their separation in two groups. During the examination of the substrates of the paper-based paintings of the RHS collections, some

of them were found carrying ‘M. J. Lay’ and ‘Whatman’ watermarks, indicating both their English origin and their dating in the period before 1830. On the contrary, none of the analysed paper-based painting from V&A collection had any watermark. OCT scanning was used in order to classify the paper substrates of the two collections in two groups, according to the length and the density of their fibres, their scattering properties, two characteristics that are highly correlated to each other. The substrates that had short fibres and were matching with the papers with the English watermarks in all the mentioned characteristics were clustered in the ‘Western’ group, while the semi-transparent substrates with the long fibres (typically five times the longer than those of the ‘Western’ group) were clustered in the ‘Chinese’ group.

For a complete characterisation of the substrates, the structure information obtained by the OCT scanning was combined with the XRF elemental information about their possible chemical treatment. For the examination of the sizing treatment of each painting, the possibility of traditional Chinese treatment was initially investigated. As mentioned before (see section ‘*red dyes*’), the traditional Chinese way for the sizing was the application of a mixture of animal glue and alum and therefore the detection of S is expected. Preliminary XRF measurements on samples mimicking the traditionally Chinese sized paper showed that the identification of S is possible besides its low concentration. The analysis of the substrates of the eleven paintings from RHS collection did not show the presence of S in any of the paper substrates, except from one that was also the only one classified as ‘Chinese’. On the other hand, Cu and occasionally Zn, Pb and Ti were detected on the substrates of RHS collection, both ‘Western’ and ‘Chinese’, that have not been sized following the traditional Chinese way. More specifically, Cu was detected in all ‘Whatman’ papers, while on the ‘M J Lay’ substrate additionally to Cu, Ti was also found. On the other hand, XRF spectroscopic analysis of the ‘Chinese’ substrates of the V&A collection detected S on all of them, suggesting that they may have been treated according to the traditional Chinese way. However, the elemental examination of the ‘Western’ papers of the V&A collection did not give any indication of traditional Chinese treatment. Ca, K and Fe were detected in almost all of the substrates of the V&A collection, both ‘Western’ and Chinese’. The substrate where these elements were not detected was the one that did not have any evidence of traditional Chinese treatment either. Given that all these extra elements detected on the various paper substrates are most probably related either to the filling

materials or to differences in the composition of the sizing solution, their variations between the substrates of the two collections indicate that there is a fundamental difference in the papers used for the RHS botanical collection compared with those in the V&A collection.

Summarizing the results extracted from the examination of the paper substrate of the RHS and V&A collections, a lot of expected but also some unexpected results were observed. The fact that none of the ‘Western’ papers was sized in the traditional Chinese method was not surprising. Similarly, the indication of traditional Chinese treatment on the ‘Chinese’ substrates of the V&A collection was something that could be expected. However, the fact that the paper substrates of the RHS collection that were classified as Chinese appeared not to be sized in the usual Chinese way was unexpected. Moreover, it was interesting that in the RHS papers the extra elements were detected regardless of whether they were classified as ‘Chinese’ or ‘Western’. On the contrary, no additional element was found in any substrate, of any collection, that has been characterised as ‘Chinese and also sized in the traditional Chinese way.

## 6.4 Conclusions

This study was aiming at the in-depth investigation of the advantages that the multi-modal approach provides for the holistic analysis of fragile artworks, such as the paper-based watercolour paintings. Moreover, the analysis of the applied painting materials and methods enabled the extraction of useful information regarding the cultural exchanges between China and West in the eighteenth and nineteenth centuries. The large statistical sample that was analysed, with thirty five paintings and more than six hundred coloured areas examined, enabled the extraction of very important information in both directions. The painting materials of the two collections of Chinese watercolours were analysed non-invasively, using a holistic approach that involved VIS-NIR spectral imaging, high spectral resolution VIS/NIR spectroscopy with FORS, micro-Raman spectroscopy, XRF spectroscopy and OCT imaging.

In regards to the palettes of the RHS and the V&A collections, significant similarities were observed with traditional Chinese pigments (natural or synthetic) and dyes being used in both of them. Moreover, pigments and dyes that were imported in China in the period that the watercolour paintings of both collections were produced, such as Prussian blue and cochineal, were widely detected. It is surprising, however, that while Prussian blue was detected on eight of the analysed paintings of V&A collection, no evidence for its presence was found on any of the RHS paintings. On the contrary, scale insect dyes, both cochineal and lac, appear to have been used on nearly every painting of both collections, with cochineal seemingly having been used more frequently. It is worth highlighting that this study suggests that the identification of the insect dyes on these paintings is possible through the complementary use of high resolution reflectance spectroscopy and XRF spectroscopy. However, further systematic analysis that takes into account also the possible spectral contribution of the other painting materials should be performed. The possibility of non-invasive identification of the insect dyes is very important, as so far only micro-destructive analytical has proved effective. For the evaluation of the results of this study and the confirmation of the identification that the complementary non-invasive approach provides, application of micro-destructive analytical techniques, such as SERS, is required.

The identification of the binding medium using reflectance spectroscopy in the NIR regime was not possible, as the spectra in the region of interest were dominated by the absorption features of the paper substrate (see section 4.2.2). In the future, a portable FTIR could be used to assist in binder identification, although it may still be challenging given the presence of just a small amount of binder.

Regarding the identification of the underdrawings (see section 4.3), a preliminary examination of the paintings by spectral imaging (NIR bands) allowed the rapid visualisation of the preparatory drawings, specifying the areas that should be further examined. Further examination was performed by OCT imaging on selected areas providing detailed, high resolution and high-contrast images of the drawings, assisting therefore their distinction based on whether they were made with a solid or a liquid substance. Finally, micro-Raman spectroscopic analysis of exposed drawings identified the drawing materials to be either graphite (pencil) or carbon black (ink). The analysis of the drawings on paintings belonging to both collections showed that graphite pencil

was used for preparatory sketches on the majority of the RHS paintings, while Chinese ink was used on the V&A paintings.

The complementary use of OCT imaging and XRF spectroscopy was applied for the characterization of the substrate. More specifically, OCT scanning enabled the distinction between papers with long fibres that were thin and semi-transparent (likely to be Chinese) from those with short fibres that were thick and highly scattering (likely to be Western). Furthermore, it provided quantitative measures of the fibre length and the thickness of the Chinese papers in a non-invasive way, without the need of sampling or demounting of the paintings. The majority of the paper substrates in the RHS collection were found to have short fibre, while nearly all of the paper substrates in V&A collection had long fibres. Finally, XRF spectroscopic measurements revealed whether the papers were sized using the traditional Chinese method and whether the size and filler materials for the papers were different. All of the V&A paintings, except one, were sized with alum while only one of the RHS paintings was sized with alum. Surprisingly, elements such as Cu, Zn, Ti and Pb that were detected on nearly all of the RHS papers regardless of whether they were long or short fibre papers, were largely absent from the V&A papers.

The overall analysis of the watercolour paintings of RHS and V&A collections in terms of the drawing material, types of paper and painting techniques, showed that the RHS collection of Chinese botanical watercolours is very different from the paintings in the V&A collection. This conclusion is not unexpected since the RHS paintings were commissioned by the Society to serve as a plant catalogue, while the paintings of V&A collection were acquired piecemeal largely from antiquarian booksellers and art dealers, with details of the original collectors and collection dates being seldom available.



## **Chapter 7:**

# **Scientific Analysis for the investigation of the origin of Selden map**

### **7.1 Introduction**

The Selden map of China is an early seventeenth century map showing the maritime trade routes in East Asia (Figure 7-1). It looks like a combination of a coloured Chinese landscape painting style map and a nautical chart, with detailed annotations in Chinese of cities, ports and countries in Asia. The arrival of the map at the Bodleian Library (Oxford) is dated in 1659 and it was named after John Selden, a prominent London lawyer who donated the map to the library after his death in 1654. After the arrival of the map at the Bodleian Library, it was studied and annotated in Latin in 1687 by the librarian Thomas Hyde with the help of a Chinese Jesuit convert Michael Shen Fuzong who had arrived at the court of James II from China. The map was frequently displayed as an item of curiosity in the eighteenth century but it probably fell into neglect after it was examined and dismissed as cartographically incorrect by the astronomer and mathematician Edmond Halley [110], [111]. However, the Selden map was ‘rediscovered’ by the historian Robert Batchelor with the help of the Bodleian librarian David Helliwell in 2008. After that, a lot of studies have been performed regarding the history and the interpretation of the map [110]–[113] as it is believed to provide new and important information about the global maritime history of the late sixteenth and early seventeenth century. Batchelor noticed the importance of the Selden map through the clear depiction of the shipping routes (Figure 7-1c) and the unique compass rose and ruler as a scale bar at the top of the map which were impressive given that the Chinese maps before the twentieth century did not have compass rose and scale bars [110], [111], [113]. The dating of the map has been narrowed down only after its ‘rediscovery’ based on extensive research by various historians and is set between 1607 and 1624 based essentially on the activities of the Dutch in South East Asia during that period. The first documented conservation of the map is back in 1919, when it was remounted on a thick paper border with cloth lining. This conservation procedure caused severe cracking of the paper support such that fragments would fall out with each unrolling of the map. The final restoration of the map, when it was also stabilized, was done in 2011 and nowadays it is again on display at the Bodleian library.

The aim of this study was the scientific examination of the painting materials and techniques of the map by employing a suite of complementary analytical techniques in order to provide scientific evidence on the origins of the Selden map.

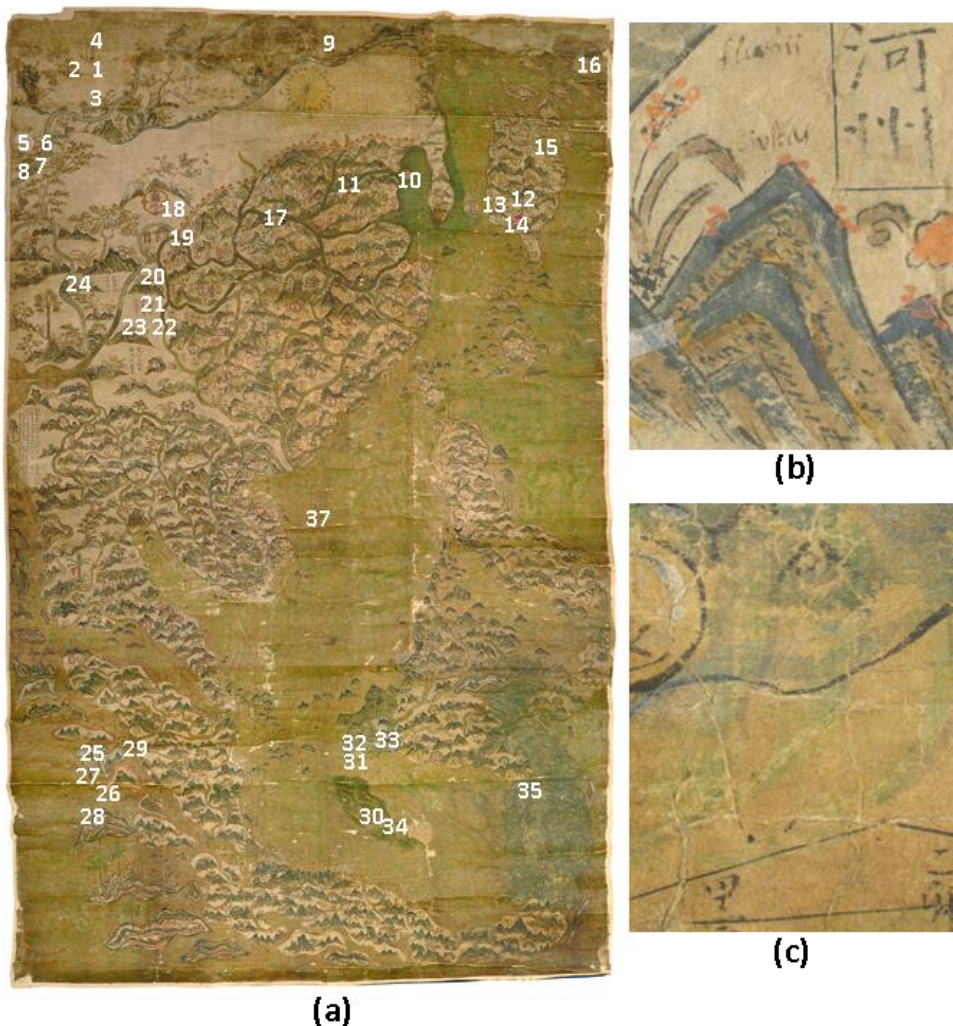


Figure 7-1 a) The Selden map (before the 2011 conservation treatment) with positions marked in white numbers of where spectral imaging data has been collected (the field of view of each image is ~4cm). The map measures ~ 96 cm by 158 cm. The original colour image is © The Bodleian Library, University of Oxford, MS Selden Supra 105; coloured images derived from PRISMS system collected from areas that contain b) details of the landscape and c) trade routes

## 7.2 Materials and Methods

Prior to the recent (2011) conservation of the map, in situ spectral imaging with high spatial resolution of selected regions on the map was performed. Additional analysis (both non-invasive and invasive) on detached fragments fallen out during the unrolling of the map, provided further confirmation and supplementation to the spectral imaging results about the identification of the pigments, enabling also the identification of the binding medium used. Spectral analysis is the only one applied on the map due to the logistics of access, however, the instrumentations of the non-invasive techniques applied on the fragments that were collected from the map have also portable versions, enabling a future in situ analysis of the map. Figure 7-2 gives the overview of the analytical techniques used as well as of the examination strategy that was followed for the analysis of the Selden map. The instrumentation used for the examination of the map is also illustrated briefly.

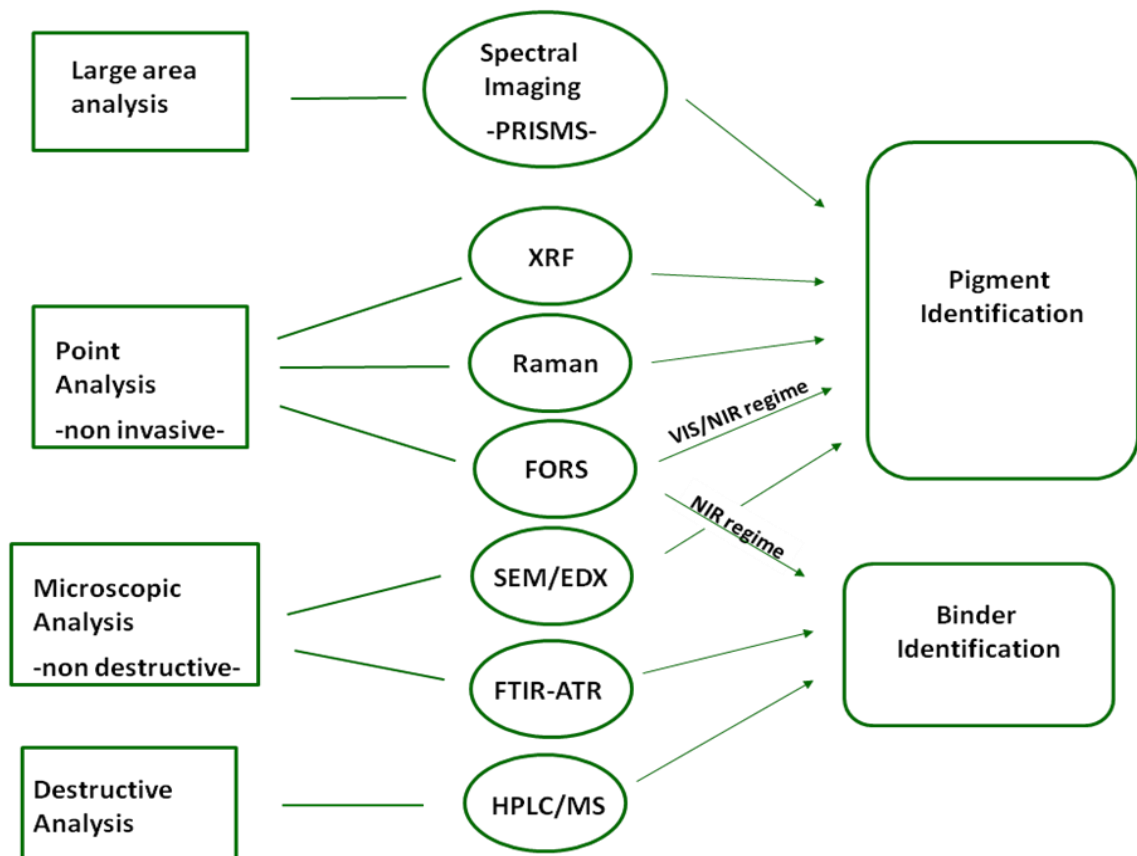


Figure 7-2 Overview of the multimodal analysis strategy

### **Spectral imaging**

Spectral imaging was performed using the PRISMS system, modified for close range imaging specifically for capturing the Selden map (Figure 7-3a).

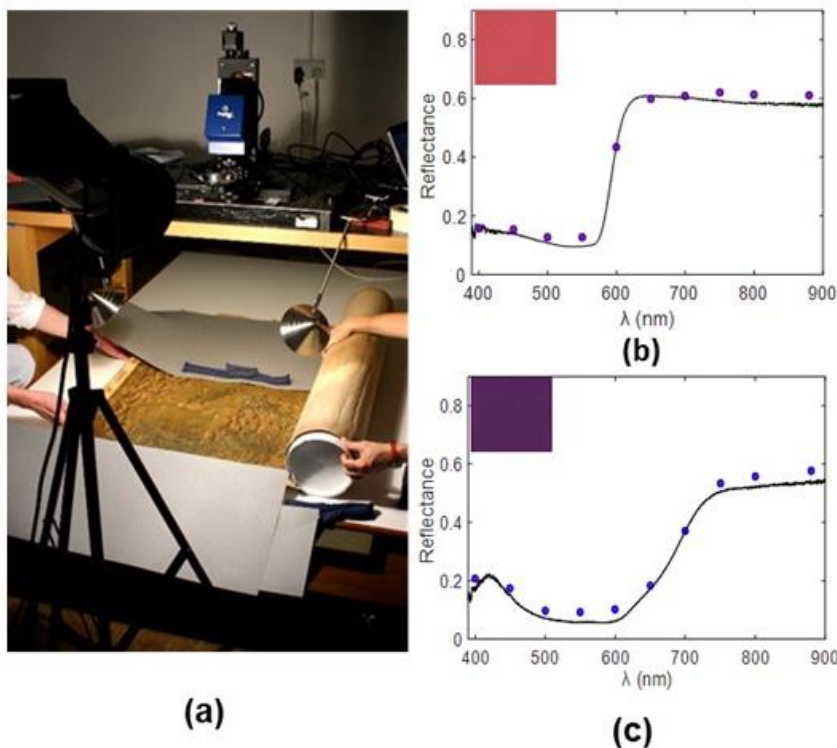


Figure 7-3 (a) Spectral imaging of the Selden map using PRISMS at the Bodleian Library; b, c) Spectral comparison between data collected from patches of a mini Macbeth ColorChecker. The black curves are spectra collected by a fibre optic spectrometer and the blue circles and red crosses are calibrated PRISMS data from the first and second day of imaging.

Calibration was performed with a Spectralon standard (99% diffuse reflectance) at the beginning and end of each imaging session. The imaging of the Selden map was performed on two consecutive days with a change of the bulb of the light source in the middle of the second day. Figure 7-3b,c show representative results of the validation tests of the system that were performed during each imaging session.

### **VIS and NIR reflectance spectroscopy**

A high resolution fibre optic reflectance spectrometer (ASD LabSpec 4 Benchtop Analyser) operating in the 350-2500nm spectral range with spectral resolution of 3-10 nm was used on the fragments to assist the identification of both pigments and binding medium. For the identification of pigments the whole spectral range was used, while the identification of the binding medium was limited to the near-IR regime. It is possible to

use the instrument in situ non-invasively on the map, but given the logistics of access, this has not yet been performed.

#### ***Mid-IR spectroscopy***

A PerkinElmer Spectrum 100 FTIR-ATR was used to examine the fragments for the identification of binding medium and pigment. While the technique is invasive, it cannot be applied directly on the map. However, a Bruker alpha FTIR with a reflection module can be used as an alternative for future application directly on the map.

#### ***Micro-Raman spectroscopy***

For the specific identification of the pigments present on the fragments, a Horiba XploRA Raman spectrometer coupled to an Olympus microscope, using an excitation laser at 638 nm and providing spatial resolution of approximately two microns, was used. The collection and interpretation of the data were done by Dr. Lucia Burgio from V&A museum. While the technique is non-invasive, the size of the map limits the type of Raman instrument that can be used directly on the map. However, in principle it is possible to perform Raman spectroscopy in situ on the map with a portable Raman spectrometer [114].

#### ***Optical Coherence Tomography (OCT)***

OCT enables non-invasive and non-contact imaging of the stratigraphy of paint and coatings layers. The 810 nm ultra-high resolution OCT (UHR-OCT) developed at NTU has an axial resolution of 1.2  $\mu\text{m}$  (in the direction perpendicular to the painting surface) in varnish and paint, and a transverse resolution of 7  $\mu\text{m}$  (in the plane of the painting surface) [115]. OCT was used on the fragments to verify if there were any potential coating layers on the map, as it looked very glossy for an East Asian painting [116]. The ultra-high resolution OCT is transportable and could be used directly on the map in the future to give a more representative view of the map subsurface microstructure.

### ***X-ray Fluorescence (XRF) Spectrometer***

The XRF analysis was performed with the ArtTAX XRF spectrometer (50 kV, 600 µA and 100s of accumulation live time) on the fragments to identify the elemental content. The spatial resolution of the instrument is 200 µm. XRF spectroscopy is a non-invasive technique, with powerful portable instrumentation and therefore it could potentially be applied on the map directly. The collection and interpretation of the data were done by Dr. Lucia Burgio from the V&A museum.

### ***Scanning Electron Microscopy with Energy Dispersive X-ray Spectroscopy (SEM-EDX)***

SEM-EDX is a non-destructive analytical technique that allows the detection of light elements, providing therefore complementary to the XRF elemental information.

### ***High Performance Liquid Chromatography hyphenated to Mass Spectrometer (HPLC-MS)***

Mass spectrometry is a destructive technique that in this study was used to verify whether animal glue was used as a binding medium. The mass spectrometer that was used for the analysis of the sample was a SCIEX Triple TOF 6600 (optimised for proteomic analysis) mass spectrometer hyphenated to an Eksigent nanoLC 425 HPLC system operating in micro flow (5 µL/min). The chromatographic analytical protocol is described in the relative publication. The collection and interpretation of the data were done by Clare Coveney, Amanda Miles and David Boocock from John van Geest Cancer Research Centre, Nottingham Trent University.

## **7.3 Results and Discussion**

### **7.3.1 Identification of the binding medium**

As it has been discussed (see section 4.2.1), the identification of the binding medium of an artwork can provide important information about its history and origin. In the context of the holistic examination of the Selden map, a thorough investigation for the identification of the binding medium was performed. In section 4.2.2, a part of the experiment performed for the identification of the binding medium of Selden map was presented, illustrating the necessity for extension of the infrared spectroscopic observation in the mid-IR regime. The application of FTIR-ATR measurements on detached fragments from the map suggested gum Arabic as the binder used, with the glossy appearance of the overall map surface being consistent with these results. However, the presence of gum Arabic as the binder of the map was a rather surprising finding as historically the most commonly used binding medium for East Asian paintings is animal glue produced from animal skin, tendon and bone, all of which contain collagen. More specifically, for the production of the glue, the collagen was mainly extracted from skins of cow, donkey, horse, pig, fish and deer antler, with cowhides, however, being the most common source used in China and Japan [117]. On the other hand, gum Arabic was the most common binding medium used on paper-based works of art in Europe from the sixteenth century onwards [118] as well as on illuminated manuscripts from the Safavid and Mughal empires [108] [109]. The occasional use of fruit gums has been reported also on Central Asian murals[117]. The Selden map has been conserved at least once in the early twentieth century and possibly once or twice prior to that [100] [105], with gum Arabic being a common consolidation materials for paper-based artworks at that time. Given the consolidation history of the map and the fact that animal glue is the binder used in Chinese painting tradition, the scenario that animal glue is the binding medium of the map with gum Arabic been applied as a consolidation material was investigated. The glossy appearance of the map in combination with the fact that microscopic examination of fragments showed a medium-rich appearance, suggested the possibility of the treatment of the map with a consolidant mixture rich in gum Arabic. In this case, the formation of a layer of the consolidation mixture above the paint layer would be expected. Furthermore, the paper would be expected to have absorbed amount of the gum-containing solution, with spectral evidence obtained on the back side of the map as well. For the examination of

this scenario, both FTIR-ATR measurements and virtual cross-section, obtained using UHR-OCT, were taken from both sides of the fragments. Figure 7-4 shows that only the IR spectrum collected from the front side matches to the gum Arabic reference, with the spectrum of the back side matching to the cellulose reference. Moreover, the UHR-OCT observation (Figure 7-4 insets) did not give any evidence of coating layer presence at a resolution of 1.2  $\mu\text{m}$ , making the scenario of the presence of gum Arabic as consolidant less unlikely.

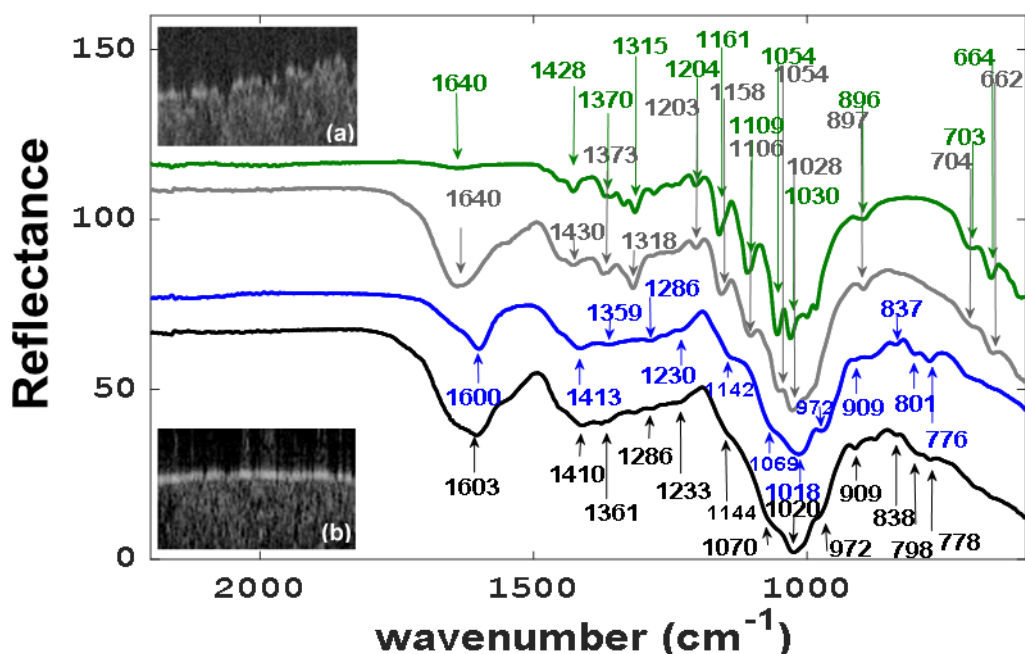


Figure 7-4 FTIR-ATR spectra of a fragment measured from both the paint (black curve) and paper (grey curve) sides compared with the spectra of gum Arabic (blue curve) and cellulose (Whatman CC41, green curve). The spectra are shifted vertically for clarity. Insets: UHR-OCT virtual cross-section images of a) the paper side and b) the paint side of the fragment (the bright line at the top is the interface between air and the painting surface). OCT image dimensions are 0.82 mm (width) by 0.05 mm (depth).

For further investigation of the possibility of animal glue to be the original binder, with gum Arabic being the material used in later consolidation treatment of the map, the performance of HPLC-mass spectrometric analysis on a small fragment was decided. In order to test the sensitivity of this technique using the setup available, preliminary study was performed on a fragment of similar size cut out from an artificial sample. The paint layer of the artificial sample consist of indigo mixed with as little amount of animal glue as possible, painted on Chinese paper and covered in a thick layer (80  $\mu\text{m}$ ) of gum Arabic. The selection of indigo as the dye used on the artificial samples was made

because FORS measurements on the original fragments showed that it was the predominant pigment. Moreover, the artificial sample was prepared in such a way to represent an extreme scenario where the animal glue content is low and the gum Arabic content is high. The digestion protocol followed for the preparation of both artificial sample and the fragment in order to get mass spectrometric analysed has been described in details in the corresponding publication [121]. The examination of the artificial sample showed that the platform was capable of detecting peptides derived from three separate types of bovine collagen (1330 total bovine peptides identified at 1% false discovery rate from the three collagen types). However, the examination of the fragment detached from the map did not show any detection of collagen proteins distinguishable from those identified within the controls. Interestingly, proteins derived from bovine and sheep casein, which are usually associated with a binder sometimes used in European manuscripts but not in East Asian paintings, were identified. This evidence was important as sheep milk has been reported to be used sometimes in combination with gum Arabic binder to improve the texture of the paint layers [122]. However, the possibility that the trace amount of casein is present simply as a contaminant cannot be excluded.

The identification of gum Arabic instead of animal glue as the binding medium on the analysed fragment is an evidence of the unusual origin of the map. According to its paint style the map appears to be Chinese or East Asian style, however, the use of gum Arabic as a binding medium in paintings from Ming China has not been reported or mentioned in the historical sources so far.

### 7.3.2 Identification of the pigments

In this study, the identification of the single or multiple pigments was mainly performed by applying the KM algorithm on PRISMS spectral data collected directly from the map. Occasionally, the observation of the optical behaviour of the paint layers in the NIR imaging bands was used for further confirmation of the identification of the pigment composition. The reference spectral library used was one that is suited to the identification of historic Chinese paints with animal glue used as binding medium and Chinese Xuan paper as substrate [6].

The Selden map was created in the traditional Chinese landscape painting style, with its painting scenes consisting of sea, mountains, plants, rivers and occasionally houses and pavilions. However the largest part of the map is painted on a dark green colour, red, blue, yellow, brown, white and black areas are present as well. More specifically, the seas, some of the mountains, boundaries between provinces in China and between countries outside China were painted in green colour, while the leaves are in a brownish green colour. Red colour was used on some flowers and plants, part of the Sun and some parts of the architectural structure. Moreover, red circles were painted around the constellation signs and some names of places outside China, while red decorations were painted around the names of the provinces and the two capitals of Ming dynasty (1368-1644) in China. Dull red colour was used for the delineation of some islands. Mountains were often highlighted in blue, while the Yellow River was also painted in blue. Bright yellow circles were used for the indication of most of the cities, except of the two Chinese capitals, and ports. The names of the Chinese provinces were circled in brown with red decoration, while names of places in Manchuria and the name of the kingdom of Korea were circled just in brown. Finally, white colour was used on the Sun and the Moon as well the clouds.

KM algorithm fitted perfectly the spectra collected from various dark, almost black, blue areas of the map using indigo as reference (Figure 7-5c). Indigo is known to be transparent in the NIR regime and therefore, the transparency of the dark blue paint layers in the NIR band (Figure 7-5b) provided a further confirmation of their pigment composition.

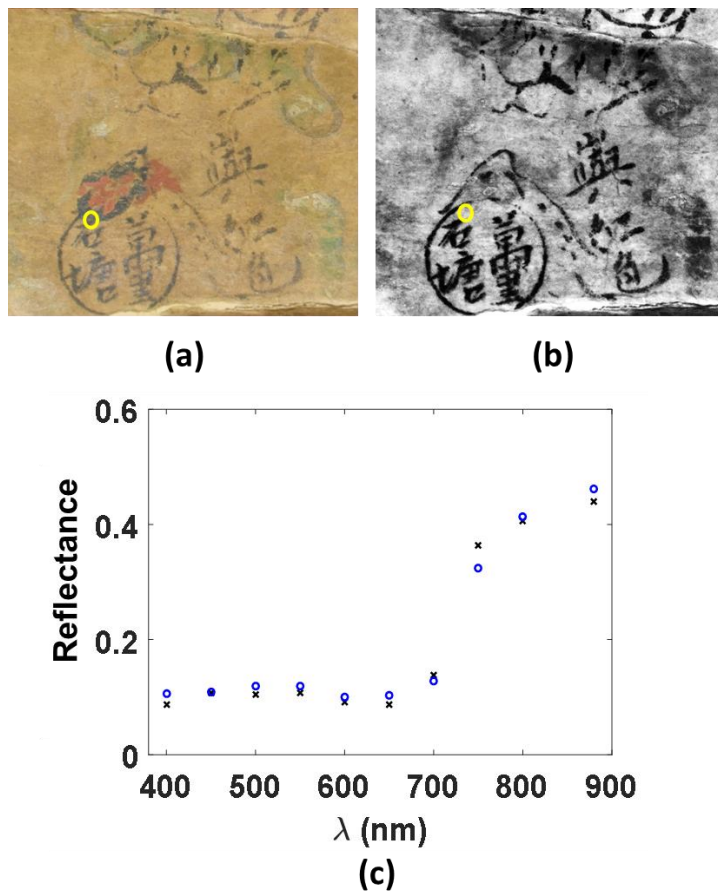


Figure 7-5 (a) Colour image derived from PRISMS data collected from ‘Area 37’ on the Selden map (Figure 7-1) with the yellow circle indicating the blue analysed area; (b) near-IR (880 nm) PRISMS image; (c) The reflectance spectrum extracted from the dark blue area (black crosses in the spectrum) is fitted by the KM model using a reference spectrum of indigo (blue circles).

The precise identification of the majority of the yellow pigments based on reflectance spectroscopy analysis is not possible (see section 2.2). Therefore, the distinction between gamboge, orpiment and massicot, the yellow pigments that were traditionally used on East Asian paintings [18], based on the PRISMS data collected from the map was not expected. However, the application of XRF spectroscopic analysis on the yellow areas could assist drastically in the identification of the pigment, as the predominant elements in both orpiment and massicot (As and Pb respectively) are easily detectable. Moreover, Raman spectroscopy can potentially identify these pigments with certainty, as long as the laser-induced fluorescence, due to the rich presence of binder, does not mask the Raman signal.

The larger part of the Selden map depicts the sea and is painted mainly in a dark/brownish green colour with brighter green highlights also being present. KM algorithm gave a good fit on the PRISMS spectra collected from both dark and bright green areas

using a combination of Cu-containing pigment, indigo and either orpiment or gamboge as references (Figure 7-6b). In order to have additional confirmation and supplementation of these results, further investigation using complementary analytical techniques on the map should be performed.

Even though the application of additional analytical examination directly on the map was not possible, green fragments detached from the map were multi-modally analysed. As the fragments were detached when the map was unrolled, their exact location on the map is not known. However, spectral comparison between the fragments and various green areas of the map showed that they are consistent with those brownish green areas in the ocean (Figure 7-6b).

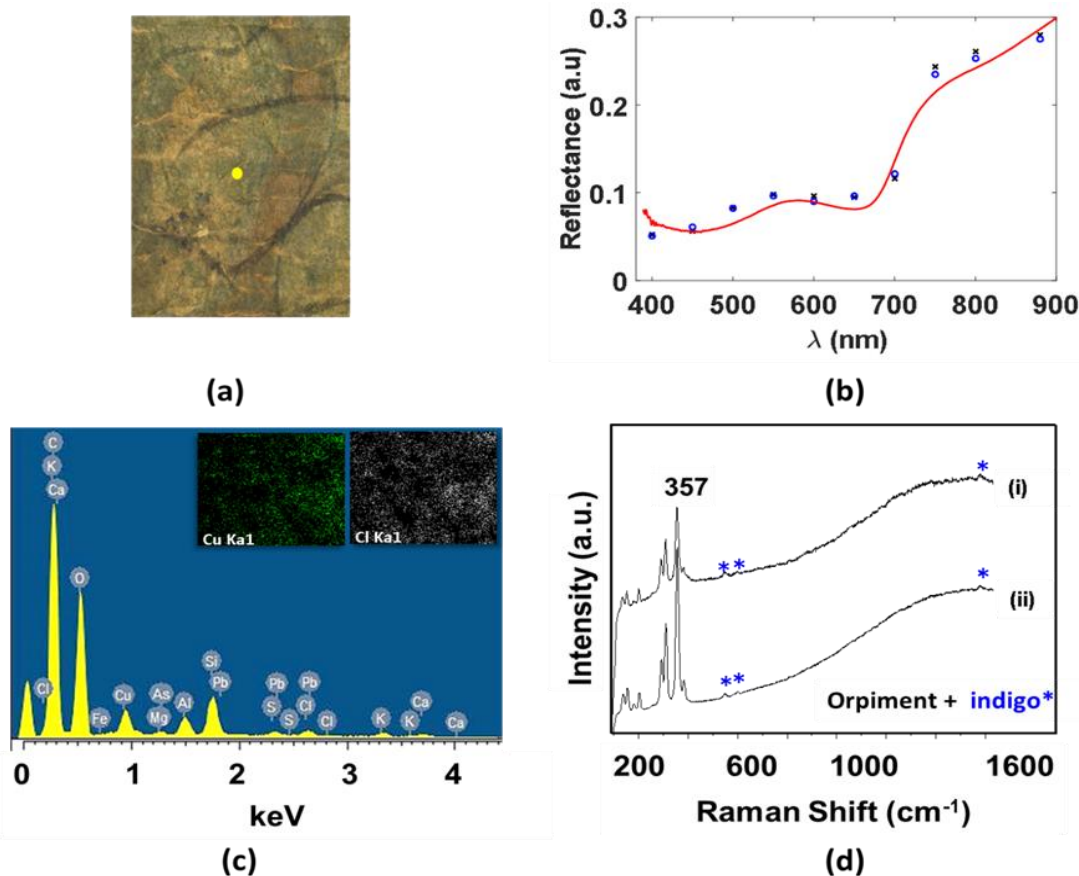


Figure 7-6 (a) Colour image derived from PRISMS data collected from ‘Area 35’ on the Selden map (Figure 7-1) with the yellow dot indicating the green analysed area; (b) KM model fit (blue circles) using a combination of atacamite, indigo and orpiment to the measured PRISMS reflectance spectrum (black crosses) for a green area; the spectrum of a green fragment measured with a spectrometer (red curve) is also plotted to show the spectral similarity between the fragment and the green region on the map; (c) EDX spectra from a green fragment showing the presence of copper, chlorine and arsenic; the left inset shows the SEM copper map and the right inset shows the SEM chlorine map; (d) Micro-Raman spectra from two green fragments showing spectral features corresponding to orpiment and indigo.

The application of KM algorithm on FORS spectra collected from the green fragments in the VIS regime agreed with the results obtained from the analysis of the PRISMS spectra about their pigment composition (Figure 7-6b). For further examination of the pigment composition, the reflectance spectroscopic investigation was extended to the near and mid-IR regimes (spectra not shown). Unfortunately none of the spectral features that could attribute to any of the Cu-containing green pigments (absorption lines in the range 2140-2500 nm and 1700-600 cm<sup>-1</sup>) or the potentially yellow pigment gamboge (absorption line at 1191 nm and 1700-600 cm<sup>-1</sup>) and orpiment (absorption lines in the range 1700-600cm<sup>-1</sup>) was possible to be observed as the spectra was dominated by the presence of the binder. However, the presence of Cu-based pigment on the fragments was confirmed by the application of XRF spectroscopy that detected Cu as the predominant element, with Ca, Fe, traces of K and occasionally As also being detected. Given the availability of fragments the performance of more sensitive and quantitative elemental analysis using SEM/EDX was allowed (Figure 7-6c), enabling the detection of lighter elements, such as sulphur (S) and chlorine (Cl). The detection of both Ca and S, that both XRF and SEM/EDX measurements confirmed, could be indicative of the presence of gypsum that is generally associated with the filling treatment of the supporting paper. Interestingly, Cu and Cl are present in a ratio 2:1 and according to the corresponding SEM/EDX maps (Figure 7-6c insets) and also have a strong similarity on their distribution. Given that only atacamite with its polymorphs, paratacamite and clinoatacamite, have this Cu/Cl molar ratio, the presence of copper chloride as pigment (i.e. atacamite) or as degradation product (i.e. atacamite, paratacamite, clinoatacamite) is suggested. Raman spectroscopy generally enables the distinction between these three polymorphs [18], however, the rich presence of binder and the limitation of the analysis only on the fragments, did not enable the identification of the green copper crystals. The detection of traces of As on the green Cu-containing fragments, under both XRF and SED/EDX investigation, could be an indication of the presence of synthetic Cu green pigment, as arsenic bronze materials have been traditionally used for their synthesis [91]. However, Raman analysis of occasionally present yellow particles identified them as orpiment (Figure 7-6d), attributing the As detection on the presence of this yellow As-containing pigment.

Three hues of red can be observed on the map, orange red used for flowers, deep red used for flowers, as architectural decorations or to circle the constellation signs and dull red used on islands. Figure 7-7 shows that the spectrum of a deep red was consistent

with vermillion, while the reflectance spectra of dull red regions are consistent with the combined use of vermillion and indigo.

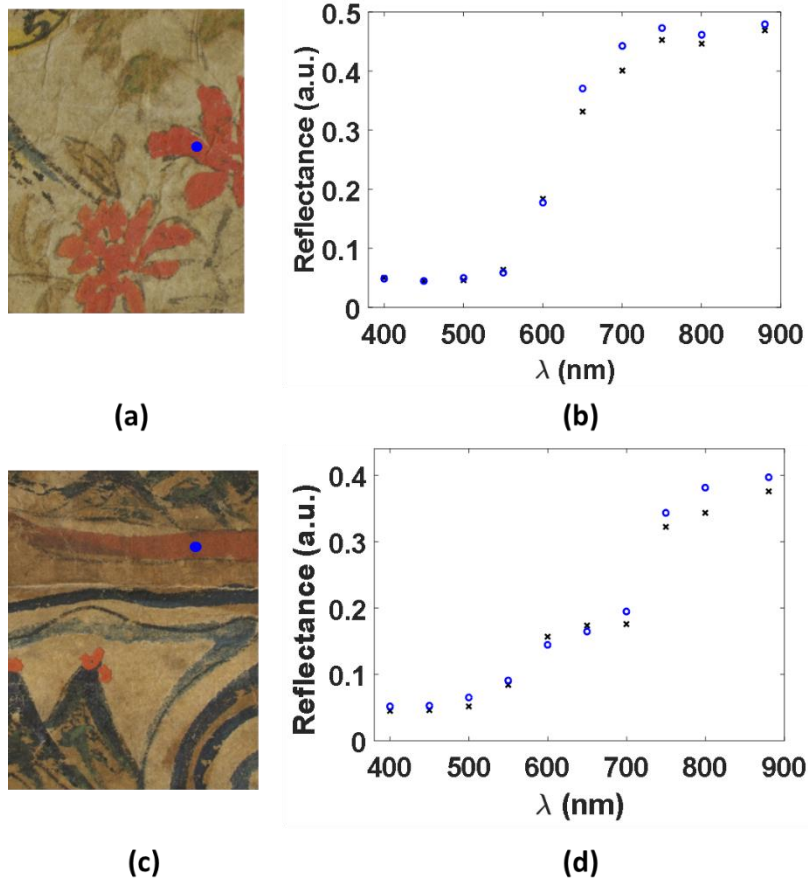


Figure 7-7 (a) A detail from the colour image derived from PRISMS data collected from ‘Area 12’ on the Selden map (Figure 7-1) with the blue dot indicating the red analysed area; (b) the reflectance spectrum extracted for the red area (black crosses) fitted with the KM model using a reference spectrum of vermillion (blue circles); (c) Colour image derived from PRISMS data collected from ‘Area 25’ on the Selden map (Figure 7-1) with the blue dot indicating the blue analysed area; and (d) the reflectance spectrum extracted from a dull red area (black crosses) fitted with the KM model using as reference pigments vermillion and indigo (blue circles).

Unlike the deep and dull red areas, the spectrum of the orange red is not consistent with the spectrum of single vermillion, red lead or a combination of them (spectra not shown) suggesting, therefore, the presence of different or an additional pigment.

In summary, the blue areas were painted with indigo, while the vivid red areas were painted with vermillion and the dull red areas were painted with a combination of vermillion and a small amount of indigo. The dark/brownish green of Selden map is suggested to be produced by the combined use of orpiment, indigo and possible a basic copper chloride (e.g. atacamite) and/or malachite, with the presence of degradation

products of Cu-based pigment not being excluded. The combination of indigo and orpiment in order to create green colour as well as the possible use of copper chlorides on paper-based artworks are two painting practises that are not matching with the Chinese painting tradition of the examined period, providing therefore more evidence for the unusual origin of the map. Generally, even though orpiment has been reported as a pigment in historical Chinese reports, it has been rarely detected in the palette of paper-based works of art from China [91]. On the contrary, the combination of orpiment with indigo is commonly found in European and Islamic manuscripts of this period [111] [114] [115], with the traditional Chinese combination being indigo with gamboge [18]. An alternative explanation of the presence of orpiment on the analysed fragment could be related to protection treatment of the paper substrate for its protection from insect attacks [125][18]. However, examples of such treatment are rare, with the most common material traditionally used for the paper treatment being berberine (or Huangbo), an organic substance that offers also a yellow appearance [126]. The possible presence of Cu chlorides as the green pigment is also an evidence in contrast to the Chinese tradition of paper-based paintings production. Basic Cu chlorides, such as atacamite, are known to be widely used as pigments on murals and temples [90][127] with their use on paper-based paintings, however, never been reported. The use of atacamite and its isomers on paper-based paintings is not common either in the West European tradition [128], while an extensive study, performed by the Freer Gallery, on Japanese Ukiyo-e paintings dated in the period between the sixteenth and the nineteenth centuries showed that basic Cu chlorides were not used in Japan in this period either. On the contrary, atacamite seems to be a common pigment used for the illumination of Persian and Indo-Persian manuscripts of this period [119], [124]. However, more accurate conclusions on the pigment composition of the various coloured areas can be drawn after the application of these non-invasive techniques directly on the map.

### 7.3.3 Examination of painting techniques and signs of alterations

During the examination of the map, various instances of modification were found. Some of them, such as the Latin annotations made in late seventeenth century after the arrival of the map in Bodleian Library, were obvious even with the naked eye. The application of PCA and ICA on the spectral images collected from the various areas of the map using the PRISMS system revealed very interesting information about the paint

sequence but also the alterations and correction that were made during its construction and are not obvious by visual observation.

The application of ICA on the spectral images collected from a section of the western end of the Great Wall revealed the drawings underlying the paint layer of its towers, illustrating the whole of the initial sketches (Figure 7-8b). More specifically, in addition to the obvious rectangles used for the base of the towers, it was shown that squares were drawn at the top part. The identification of the pigment of the red paint on the top part showed that they are painted consist of vermillion, while the composition of the brownish paint layer of the base was difficult to be identified through PRISMS analysis. A mistake made during the construction of the map on one of the tower of the Great Wall is revealed through the comparison between the first two PCA results, which highlight the ink-containing and vermillion-containing areas respectively. More specifically, the second PCA highlights the areas that contain ink (Figure 7-8c), and the third PCA the areas that vermillion-containing areas (Figure 7-8d), making clear that the square sketch of the top part was altered using ink with a vermillion layer being later applied on top. Figure 7-8e shows another modification, where white paint seems to have been applied both for erasing the black and red lines and in the perpendicular direction where there are no lines. The perpendicular lines could probably be made in order to mimic the depiction of the great wall in the map it copied from, where the wall was drawn with dashed lines (see Figure 24 in [110]). In historical Chinese records, orpiment is mentioned to be used as correction ink. Therefore, the possibility that the white layer was initially an orpiment-containing layer that has been degraded resulting to its transformation to arsenic trioxide ( $As_2O_3$ ) [129] could be possible. In contrast to the East Asian painting tradition where the use of white paint for corrections on paper-based artworks was not as common as the use of orpiment, lead white was traditionally used for correction in Persian miniatures [120]. The in situ non-invasive examination of the map could easily identify this white paint by applying XRF and Raman analysis.

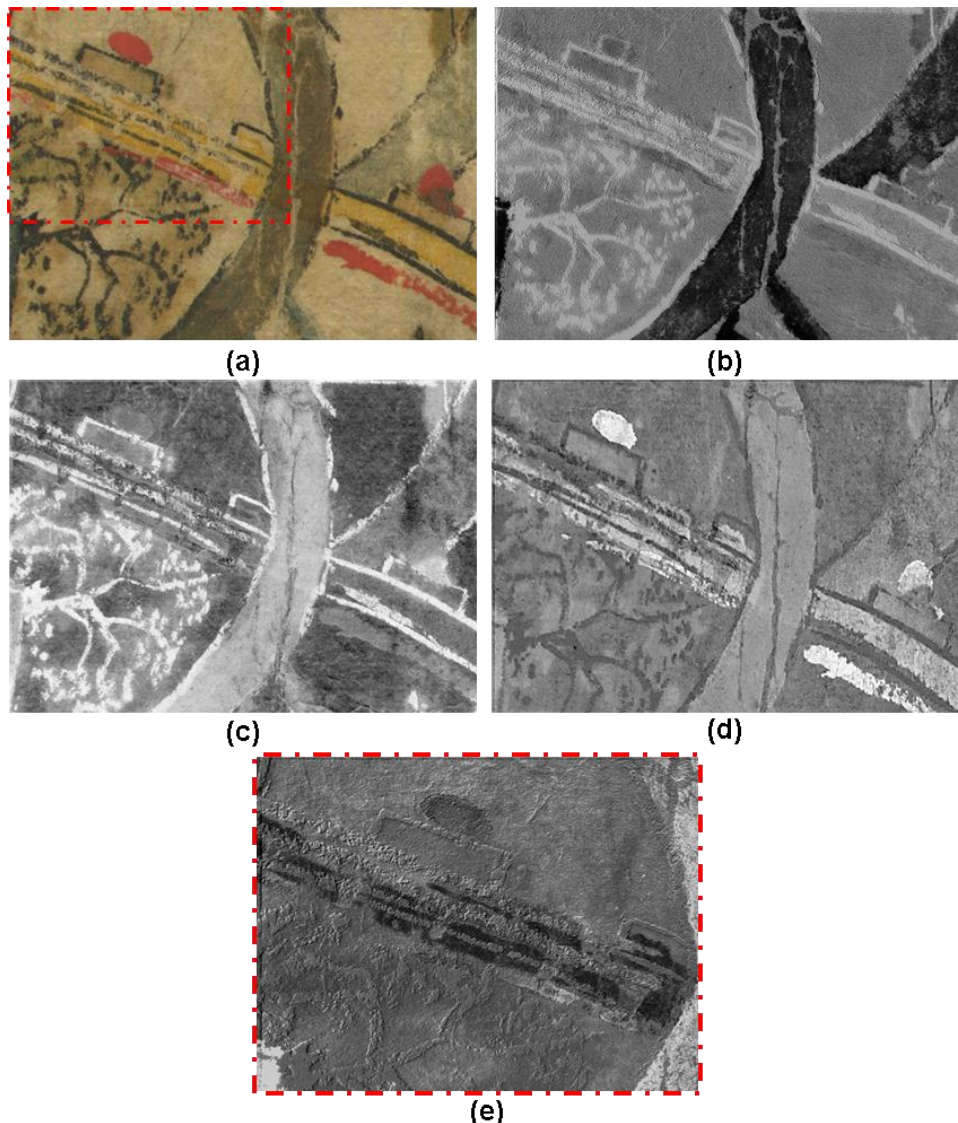


Figure 7-8 (a) Colour image derived from the PRISMS data collected from ‘Area 19’ on the Selden map that contains a part of the Great Wall with red dashed rectangle indicating the area analysed in (e); (b) ICA applied on the PRISMS data reveals the drawings of the map, showing that initial sketch of the Great Wall was made using rectangles and squares that were afterwards overpainted with brownish and red paint respectively; (c) the first PCA highlighted (white) the ink-containing drawings illustrating the mistake that was initially made on the painting of the Great wall; (d) the second PCA highlighted (white) the vermilion-containing paint layers; e) zoomed-in area (red dashed square in (a)) of ICA outcome illustrates clearer the corrections made on the Wall using white paint.

Modifications were also observed in a part of the map than contains boundaries and mountains. Figure 7-9 shows that both green boundaries and blue mountains have the same dark brownish bottom layer. The application of ICA showed that in the area of the mountains the layer of indigo was applied on top of the brownish layer (Figure 7-9c). Moreover, the application of ICA revealed clearly an alteration on the right mountain that was not obvious. More specifically, it can be observed that the drawings of the left

mountain can be observed underneath the indigo-containing layer, while a thick brown/blackish layer seems to have been applied on the drawing of the right mountain, possibly in order to erase some mistake.

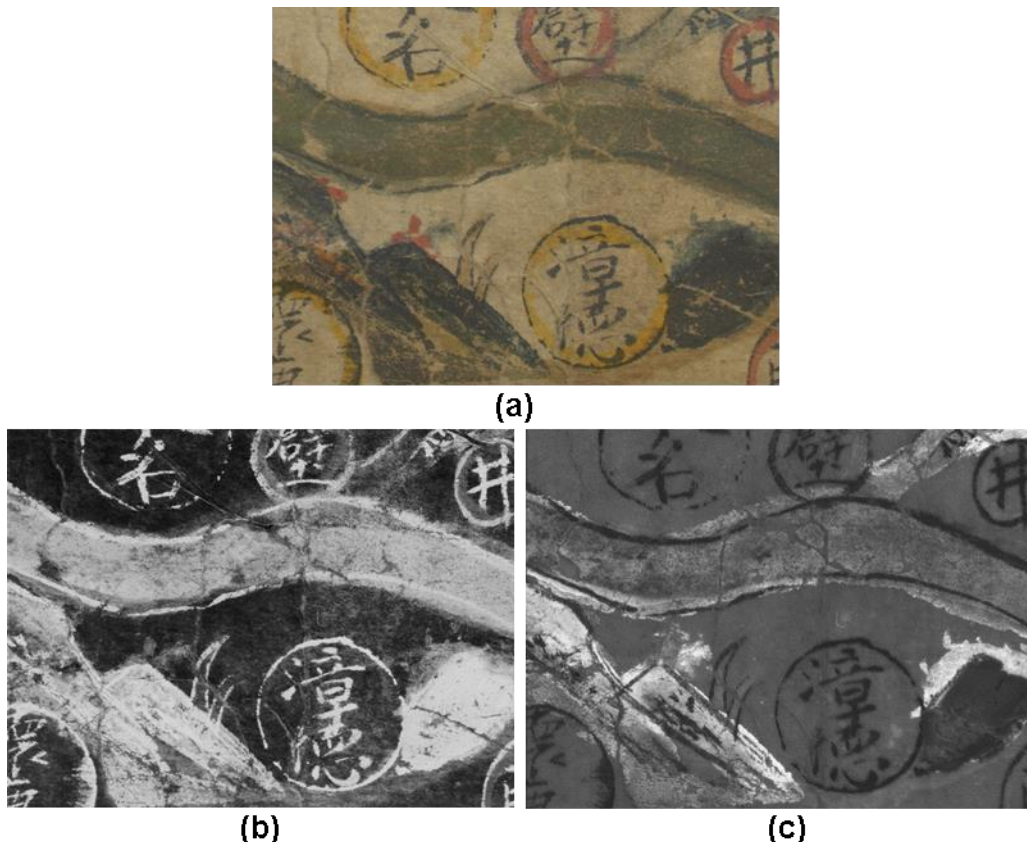


Figure 7-9 (a) Colour image derived from the PRISMS data collected from ‘Area 17’ on the Selden map; (b, c) the results of the application of ICA on the spectral imaging data collected from ‘Area 17’ that highlight the brownish underlying painting layer (white colour); the results of the application of ICA on the spectral imaging data collected from ‘Area 17’ that highlight the blue indigo-containing paint layers (white colour).

## 7.4 Conclusions

The results of scientific examination of the map using mostly non-invasive analytical techniques provided evidences of the unusual origin of Selden map. The palette of the map was found to consist of indigo in blue, dull red and green areas, vermillion in red areas and Cu green (possibly atacamite or one of its isomers) in green areas. Orpiment was detected to be used in combination with indigo and a Cu green pigment in dark green areas. The combined use of orpiment and indigo on Chinese paper-based artworks is quite unusual in the period of our interest, with the combination of indigo with gamboge being the one traditionally used. However, their combined use was commonly chosen to make green in European and Islamic manuscripts. In a similar way, the presence of basic copper chloride pigments, such as atacamite, is not usual on Chinese or western European paper-based works of art but is common for South and West Asian illumination manuscripts. With regards to the identification of the binding medium, the detection of gum Arabic with the additional traces of casein was a surprising result, as animal glue was the binding medium traditionally used in China and therefore its detection would be expected. These unusual findings seem to be more consistent with a Persian or Indo-Persian tradition, suggesting therefore that a fusion between Chinese and South and West Asian painting materials and techniques was applied for the production of the map. For the non-invasive analysis of the map only spectral imaging has been applied directly on the map so far, with the rest of the techniques applied only on fragments. However, all the applied techniques, except for the SEM/EDX and the HPLC mass spectroscopy, have their portable versions, enabling the non-invasive analysis of the map *in situ*. Future application of a non-invasive, multi-modal and *in situ* analysis is necessary for the identification of the complete palette of the map as well as for the confirmation of the results presented in this study. During the examination of the map, it was interesting that the application of PCA and ICA on the spectral data collected from various areas of the map found a number of instances where the creator of the map had made alterations, including stylistic alterations or unintentional mistakes.

Finally, the various hypotheses of the origin of the map that have been suggested by past historical research were examined in view of the new evidences. The scientific evidence that this study provided about the identification of the binding medium and the pigments of the map indicates a South and West Asian influence, suggesting as place of

its origin one of the western ports of the map, with strong Islamic influence. Moreover, the combination of the results of the non-invasive scientific examination with the detailed observation of the relationship between the trade routes and the magnetic declination [120] led to the conclusion of an alternative origin for the map , with Aceh at the north-west end of Sumatra being proposed. Art historical analysis of illuminated manuscripts from Aceh dated in the eighteenth and nineteenth centuries showed that there is a coherent and well-established tradition on the illumination of manuscripts. However, only a few illuminated documents from South East Asia of early seventeenth century have been preserved, restricting the ability for a comprehensive study on the painting materials and techniques applied on the production of paper-based artworks from different regions of South-East Asia.

## **Chapter 8:**

### **Conclusions**

The objective of this work was the development of methods for the automatic processing of large scale spectral imaging data as well as the detailed examination of the complementarity of various non-invasive analytical techniques for the holistic examination of different artworks.

The studies conducted on the automatic processing of large scale spectral imaging data were focused on two directions: the revealing of hidden information and the clustering of large scale spectral information.

Regarding the automatic detection of hidden information, the potentials of principal component analysis (PCA) and independent component analysis (ICA), two of the most well-known Blind Source Separation (BSS) statistical methods, on spectral imaging data obtained by the PRISMS system were investigated through the examination of various examples. It can be concluded that each one of these two statistical analysis methods has its own advantages, but also limitations that notably can be mitigated effectively when both methods are used in combination. In addition, it was shown that the complementary use of PCA and ICA is superior than the use of the observation in the individual spectral bands. Therefore, the addition of their use in the spectral imaging analysis protocols is suggested.

Another conclusion that can be drawn, regarding the revealing of hidden information using PCA and ICA, related to the spectral characteristics that the input images should have. Namely, it was shown that the obtained outcomes showed that the application of PCA and ICA on a minimized dataset consist of three channels in the near-UV (400 nm), G (in the middle of the visible range) and NIR (880 nm) spectral areas gives similarly good results to the ones obtained using the whole ten bands dataset of the PRISMS system. This result is more likely related to the fact that the images collected in these spectral bands contain the most uncorrelated signal information, which is the fundamental principle of the operation of these methods [30]. In practice, this conclusion implies that it is possible to acquire relevant information from an object of cultural heritage even by using a minimised dataset of spectral images, which can be handy in conservation laboratories that do not possess more sophisticated spectral

imaging systems. A future perspective for the automatic revealing of hidden information is the examination of the potentials of other statistical analysis methods.

A method for the automatic clustering of the spectral information derived from large scale spectral imaging data was also developed for this study. As explained before, the disadvantage of the clustering methods presented so far in the field of the cultural heritage is that they require the interference of the operator in many steps of the classification procedure. This can lead into two major limitations:

Firstly, the interference of the human factor in the classification procedure could lead to a biased selection of the clusters diminishing the overall accuracy of the final results.

Secondly, the large number of non-automated steps, which require human intervention, limits the applicability of these methods on large scale spectral imaging data.

The clustering method presented in section 3.2, overcomes these limitations by enabling the automatic unsupervised clustering and at the same time enables the accurate classification of the spectral information collected from large scale painting surfaces. This is achieved by constant updating of the reference database after the processing of each image cube, adding new clusters when it is necessary on the fly. This is becoming particularly important in the analysis of large collection of paintings or artworks of large size.

The clustering of the spectral information of the large painting surfaces specifies the areas that are representative of each pigment composition, thus minimizing the number of areas that should be examined in detail. In the context of this study, the combined use of three of the most well-known spectroscopic techniques (i.e. FORS, XRF and Raman spectroscopy) was investigated through the analysis of a large and heterogeneous statistical sample.

An important conclusion of the aforementioned work is that the information provided by the various techniques, in addition to the principles of operation, depends on the specific features of the instrumentation used. For example, the minimization of the spot size in Raman spectroscopic devices (i.e. micro-Raman) has been introduced for more effective analysis on the individual particles but it could potentially provide non representative results in certain cases (e.g. pigments with impurities, or mixture of pigments).

In addition, it has to be highlighted that a variety of other factors can affect the acquired spectral results of spectroscopic techniques. These factors can be related to the size of the pigment particles (e.g. malachite, azurite), the concentration of the dye (e.g. gamboge), the binding medium and the substrate.

The complementary use of the various techniques was proven to be important not only on the different information obtained from the data but also in their interpretation, as in many cases the results of the one technique confirm or even improve the interpretation of the data collected from the others.

Conflating all the above information enabled us to propose a different approach for the analytical procedure for the identification of pigments. This approach is based on the following concepts:

For the extraction of accurate results about the pigments used, large scale painting surfaces should be examined. Therefore a time efficient preliminary examination of spectral imaging data, applying methods based on statistical analysis, is proposed. This procedure highlights the areas with representative pigment composition that should be examined in detail.

These representative areas should be examined in turn, using a combination of various non-invasive analytical techniques. The selection of these techniques should be made based on their complementarity in terms of both the principles of their operation as well as the specification of the instrumentation used. The in-depth investigation of the limitations and the advantages of the selected techniques should be made beforehand, in a way that the collective information of the sum of the techniques negates their limitations while enhances their strengths.

Following that, a collection of large sample of multi-modal measurements from the representative areas should be performed in order to avoid statistical bias, since the limitations of the individual techniques (see section 4.1) may skew the results when the number of measurements is limited.

The interpretation of the data should be performed by taking into account the possible spectral contribution of the painting materials. In this direction, the reference samples should be produced using materials similar to the ones of the analysed artwork. Moreover, data collected from the substrate of the examined artwork should also be used for comparison.

Finally, the complementarity of the techniques should be extended to the interpretation of the analytical results. This approach differs from the ‘step-by-step’ approach that is commonly proposed in the context that the interpretation of the analytical results is made dynamically and in circularity, in a way that each result is ‘cross-relevant’ to the other and each analysis affects the rest in a reciprocal way. As further work, the examination of other painting systems with different combination of materials and, therefore, different analytical needs would enrich our knowledge about how the complementary use of the various non-invasive analytical techniques increases the accuracy of the results.

For the identification of the binding media, the potentials of reflectance spectroscopy in the near-IR regime were investigated through the systematic examination of a series of artificial samples made in such a way as to mimic a wide range of real artworks. A general observation that should be emphasized is that during spectral examination in this regime, it is important to take into account the possible contribution of the substrate as well as the pigments of the analysed area that could result in misleading or false conclusions. Therefore, before any attempt for the identification of the binding medium, a detailed identification of the pigments of the analysed area should be performed. Both the experiments on artificial samples and the studies on the identification of the binding medium of a real artwork (i.e. Selden map) confirmed the limitations that the examination in the near-IR faces, such as having similar spectral features as the substrate, suggesting the extension of the observation to the mid-IR regime. The extension of the detection in the mid-IR regime using FTIR-ATR spectrometer enables the distinction between the various binders. However, there are only limited types of artworks where this technique can directly applied on, making the use of FTIR instrumentation in the reflectance mode necessary.

For a holistic examination of an object of art the analysis of the drawing materials and the substrate is necessary. In this study, it has been illustrated that the complementary use of spectral imaging (PRISMS), optical coherence tomography (OCT) and Raman spectroscopy enables the classification of different types of drawings (e.g. identification of ink and pencil drawings).

For the identification of the substrate, the complementary use of two non-invasive techniques, OCT and XRF spectroscopy, enabled the effective classification of different types of paper. This is important, as the traditional approaches require fiber sampling,

which is harmful for the artwork. The investigation of the abilities that the non-invasive analysis can provide for the identification of substrates should be further extended in the examination of other types of substrates, such as parchments and support layers of murals, for which the information related to their structure and/or elemental composition can be indicative of the history of the artwork.

In the context of this work, three artworks of significant art historical importance for the East Asian painting tradition were examined.

The analysis of the murals of the cave 465 of the Mogao complex, gave very interesting results about the applied painting materials and techniques. The analysis of the palette of the murals provided interesting information about the pigment combinations that have been used. With regards to the analysis of degraded paint layers, this study illustrated that the complementary use of the various non-invasive techniques enables their efficient and in situ examination, providing useful information about the original painting materials and methods applied. This is a very important result, as the studies conducted on the analysis of degraded paint layers so far are mainly performed following invasive approaches. With regards to the examination of the dating of the cave, the comparison between the pigment composition of the murals of cave 465 and the pigments used in other caves gave interesting results. The elimination of the possibility that the cave 465 was constructed in the Tibetan period, as it resulted from the comparison with the pigments identified in cave 159, is very important evidence as the Tibetan, the Tangut and the Yuan are the three prevailing dating periods in the art historical debate. However, further studies, involving the multi-modal examination of the pigment composition of the murals of other caves of the Mogao complex which dating is placed in the other two periods of interest, would assist the extraction of conclusive results about the dating of the cave 465.

In the case of the cracks of the mural in cave 465, the fact that the size of the cracks appears to be related to the materials composition of the paint layer was interesting. In order to draw safe conclusions about the formation of different types of cracks, the analysis of the material composition (i.e. pigments and binding medium) of areas that contain both large and small cracks in combination with UHR-OCT measurements for the determination of their in-depth location should be further performed.

The analysis of the collections of Chinese export paintings of Victoria and Albert (V&A) museum and Royal Horticultural Society (RHS) collections offered a large statistical

sample that provided the opportunity for the investigation of the complementarity of the various non-invasive analytical techniques. Moreover, the holistic examination of the watercolour paintings of the two collections enabled the extraction of very useful information about the trading and cultural exchanges between China and West in the eighteenth and nineteenth century. Among the interesting results about the palette of two collections, the possibility of the distinction between the scale insect dyes using high resolution spectroscopy is of a great importance, as so far, their identification is possible only using destructive techniques. However, further experiments that would confirm this identification using micro-destructive analytical techniques, such as SERS-Raman, should be performed.

The scientific analysis conducted on the painting materials and methods applied on the Selden map, provided very interesting results for the examination of its origin. The identification of pigments not commonly used in the Chinese painting tradition as well as the identification of gum Arabic as the binding medium of the map provided scientific evidence for the unusual origin of the map. With regards to the non-invasive analysis of the map, only spectral imaging has been applied directly on the map so far, with the rest of the techniques applied only on fragments. Future application of a non-invasive, multi-modal analysis on different part of the map is necessary for the identification of the complete palette of the map as well as for the confirmation of the results presented in this study.



## **Chapter 9:**

### **Bibliography**

- [1] M. Puchalska, M. Orlinska, M. A. Ackacha, K. Polec-Pawlak, and M. Jarosz, “Identification of anthraquinone coloring matters in natural red dyes by electrospray mass spectrometry coupled to capillary electrophoresis,” *J. Mass Spectrom.*, vol. 38, no. 12, pp. 1252–1258, 2003.
- [2] J. J. Perry, L. Brown, E. Jurneczko, E. Ludkin, and B. W. Singer, “Identifying the plant origin of artists’ yellow lake pigments by electrospray mass spectrometry,” *Archaeometry*, vol. 53, no. 1, pp. 164–177, 2011.
- [3] J., Wouters, A., Verhecken, “The scale insect (Homoptera: Coccoidea). Species recognition by HPLC and diode-array analysis of the dyestuffs,” *Annls Soc. ent Fr.*, vol. 25, no. 4, pp. 393–410, 1989.
- [4] S. M. Halpine, “An Improved Dye and Lake Pigment Analysis Method for High-Performance Liquid Chromatography and Diode-Array Detector Studies in Conservation , Vol . 41 , No . 2 ( 1996 ), pp . 76-94.
- [5] T. D. Chaplin, R. J. H. Clark, and M. Martinón-Torres, “A combined Raman microscopy, XRF and SEM-EDX study of three valuable objects - A large painted leather screen and two illuminated title pages in 17th century books of ordinances of the Worshipful Company of Barbers, London,” *J. Mol. Struct.*, vol. 976, no. 1–3, pp. 350–359, 2010.
- [6] S. Kogou, A. Lucian, S. Bellesia, L. Burgio, K. Bailey, C. Brooks and H. Liang, “A holistic multimodal approach to the non-invasive analysis of watercolour paintings,” *Appl. Phys. A Mater. Sci. Process.*, vol. 121, no. 3, pp. 999–1014, 2015.
- [7] Z. E. Papliaka, A. Philippidis, P. Siozos, M. Vakondiou, K. Melessanaki, and D. Anglos, “A multi-technique approach, based on mobile/portable laser instruments, for the in situ pigment characterization of stone sculptures on the island of Crete dating from Venetian and Ottoman period,” *Herit. Sci.*, vol. 4, no. 1, pp. 1–18, 2016.
- [8] P. Vandenabeele and M. K. Donais, “Mobile spectroscopic instrumentation in

- archaeometry research," *Appl. Spectrosc.*, vol. 70, no. 1, pp. 27–41, 2016.
- [9] C. Miliani, F. Rosi, B. G. Brunetti, and A. Sgamellotti, "In Situ Noninvasive Study of Artworks: The MOLAB Multitechnique Approach," *Acc. Chem. Res.*, vol. 43, no. 6, pp. 728–738, 2010.
- [10] P. Moioli and C. Seccaroni, "Analysis of Art Objects Using a Portable X-ray Fluorescence Spectrometer," *X-Ray Spectrom.*, vol. 29, no. May 1999, pp. 48–52, 2000.
- [11] L. Appolonia, D. Vaudan, V. Chatel, M. Aceto, and P. Mirti, "Combined use of FORS, XRF and Raman spectroscopy in the study of mural paintings in the Aosta Valley (Italy)," *Anal. Bioanal. Chem.*, vol. 395, no. 7, pp. 2005–2013, 2009.
- [12] Z. Li, L. Wang, Q. Ma, and J. Mei, "A scientific study of the pigments in the wall paintings at Jokhang Monastery in Lhasa, Tibet, China," *Herit. Sci.*, vol. 2, no. 1, p. 21, 2014.
- [13] H. Liang, A. Lucian, R. Lange, C. S. Cheung, and B. Su, "Remote spectral imaging with simultaneous extraction of 3D topography for historical wall paintings," *ISPRS J. Photogramm. Remote Sens.*, vol. 95, pp. 13–22, Sep. 2014.
- [14] "CIE Colorimetry", Vienna, 2004.
- [15] B. McLaren and K. Rigg, "XII-The SDC Recommended Colour-difference Formula: Change to CIELAB," *Soc. Dye. Colour.*, vol. 92, no. 9, 1979.
- [16] J. Cupitt and K. Martinez, "VIPS: An image processing system for large images," *Proc. SPIE*, vol. 2663, pp. 19–28, 1996.
- [17] H. Liang, "Advances in multispectral and hyperspectral imaging for archaeology and art conservation," *Appl. Phys. A Mater. Sci. Process.*, vol. 106, no. 2, pp. 309–323, 2012.
- [18] J. Winter, *East Asian Paintings—Materials, Structures and Deterioration Mechanisms*, 1st Editio. London: Archetype Publications, 2008.
- [19] G. Dupuis and M. Menu, "Quantitative evaluation of pigment particles in organic layers by fibre-optics diffuse-reflectance spectroscopy," *Appl. Phys. A Mater. Sci. Process.*, vol. 80, no. 4, pp. 667–673, 2005.

- [20] R. J. H. Clark, “Raman microscopy: application to the identification of pigments on medieval manuscripts,” *Chem. Soc. Rev.*, vol. 24, no. 3, p. 187, 1995.
- [21] M. A Rodriguez, P.G. Kotula, J. J. M. Griego, J. E. Heath, S. J. Bauer, D. E. Wesolowski, “Multivariate Statistical Analysis of Micro-XRF Spectral Images,” in *Denver X-ray conference on Applications of X-ray Analysis*, 2009, vol. 16, no. 1, pp. 1–7.
- [22] E. Marengo, M. C. Liparota, E. Robotti and M. Bobba, “Multivariate calibration applied to the field of cultural heritage: Analysis of the pigments on the surface of a painting,” *Anal. Chim. Acta*, vol. 553, no. 1–2, pp. 111–122, 2005.
- [23] F. Borba, J. Cortez, V. Asfora, C. Pasquini, M. Pimentel, A. Pessise and H. J. Khoury “Multivariate treatment of LIBS data of prehistoric paintings,” *J. Braz. Chem. Soc.*, vol. 23, no. 5, pp. 958–965, May 2012.
- [24] R. L. Easton, W. A. Christens-Barry, and K. T. Knox, “Spectral image processing and analysis of the Archimedes Palimpsest,” *Eur. Signal Process. Conf.*, no. Eusipco, pp. 1440–1444, 2011.
- [25] K. T. Knox, R. L. Easton, W. A. Christens-Barry and K. Boydston, “Recovery of handwritten text from the diaries and papers of David Livingstone,” *Proc. SPIE*, vol. 7869, no. 1, 2011.
- [26] M. Attas, E. Cloutis, C. Collins, D. Goltz, C. Majzels, J. R. Mansfield and H. Mantsch, “Near-infrared spectroscopic imaging in art conservation: Investigation of drawing constituents,” *J. Cult. Herit.*, vol. 4, no. 2, pp. 127–136, 2003.
- [27] E. Salerno, A. Tonazzini, E. Grifoni, G. Lorenzetti, S. Legnaioli, M. Lezzerini, L. Marras, S. Pagnotta and V. Palleschi, “Analysis of Multispectral Images in Cultural Heritage and Archaeology,” *J. Appl. Laser Spectrosc.*, vol. 1, no. 1, pp. 22–27, 2014.
- [28] A. Sparavigna, “Digital restoration of ancient papyri,” Torino, Italy, 2009.
- [29] E. Salerno, A. Tonazzini, and L. Bedini, “Digital image analysis to enhance underwritten text in the Archimedes palimpsest,” *Int. J. Doc. Anal. Recognit.*, vol. 9, no. 2–4, pp. 79–87, 2007.
- [30] J. Rodarmel and C. Shan, “Principal component analysis for hyperspectral image classification,” *Surv. L. Inf. Sci.*, vol. 62, no. 2, p. 115, 2002.

- [31] J. Mitra, R. Jolivot, P. Vabres, and F. S. Marzani, "Source separation on hyperspectral cube applied to dermatology," vol. 7624, no. 0, p. 76243I, 2010.
- [32] A. Hyvärinen, J. Karhunen and E. Oja, "Independent Component Analysis", *Applied and Computational Harmonic Analysis*, vol. 21, no. 1. 2001.
- [33] M. Bacci, A. Casini, C. Cucci, A. Muzzi, and S. Porcinai, "A study on a set of drawings by Parmigianino: Integration of art-historical analysis with imaging spectroscopy," *J. Cult. Herit.*, vol. 6, no. 4, pp. 329–336, 2005.
- [34] A. Alexopoulou, A. Kaminari, A. Panagopoulos, and E. Pohlmann, "Multispectral documentation and image processing analysis of the papyrus of tomb II at Daphne, Greece," *J. Archaeol. Sci.*, vol. 40, no. 2, pp. 1242–1249, 2013.
- [35] K. Bloechl, H. Hamlin, and R. Easton, "Text recovery from the ultraviolet-fluorescent spectrum for treatises of the Archimedes Palimpsest," *Appl. Opt.*, vol. 7531, p. 54, 2010.
- [36] A. Tonazzini, E. Salerno, M. Mochi, and L. Bedini, "Blind Source Separation Techniques for Detecting Hidden Texts and Textures in Document Images," pp. 241–248, 2004.
- [37] A. Tonazzini, L. Bedini, and E. Salerno, "Independent component analysis for document restoration," *Int. J. Doc. Anal. Recognit.*, vol. 7, no. 1, pp. 17–27, 2004.
- [38] K. Koonsanit, C. Jaruskulchai, and A. Eiumnoh, "Band Selection for Dimension Reduction in Hyper Spectral Image Using Integrated Information Gain and Principal Components Analysis Technique," *Int. J. Mach. Learn. Comput.*, vol. 2, no. 3, pp. 248–251, 2012.
- [39] F. Tsai, E. Lin, and K. Yoshino, "Spectrally segmented principal component analysis of hyperspectral imagery for mapping invasive plant species," *Int. J. Remote Sens.*, vol. 28, no. 5, pp. 1023–1039, 2007.
- [40] D. Wartenberg, "Multivariate spatial correlation: a method for exploratory geographical analysis," *Geogr. Anal.*, vol. 17, no. 4, pp. 263–283, 1985.
- [41] G. Lu and B. Fei, "Medical hyperspectral imaging: a review," *J. Biomed. Opt.*, vol. 19, no. 1, p. 10901, 2014.

- [42] J. K. Delaney, P. Ricciardi, L. Glinsman, M. Facini, M. Thoury, M. Palmer and E. R. de la Rie, “Use of imaging spectroscopy, fiber optic reflectance spectroscopy, and X-ray fluorescence to map and identify pigments in illuminated manuscripts,” *Stud. Conserv.*, vol. 59, no. 2, pp. 91–101, 2014.
- [43] J. K. Delaney, J. Zeibel, M. Thoury, R. Littleton, M. Palmer, K. M. Morales, E. R. de la Rie and A. Hoenigswald, “Visible and Infrared Imaging Spectroscopy of Picasso’s <I>Harlequin Musician</I>: Mapping and Identification of Artist Materials <I>in Situ</I>,” *Appl. Spectrosc.*, vol. 64, no. 6, pp. 584–594, 2010.
- [44] K. A. Dooley, S. Lomax, J. Zeibel, C. Miliani, P. Ricciardi, A. Hoenigswald, M. Loewb and J. K. Delaney, “Mapping of egg yolk and animal skin glue paint binders in Early Renaissance paintings using near infrared reflectance imaging spectroscopy,” *Analyst*, vol. 138, no. 17, p. 4838, 2013.
- [45] J. K. Delaney, P. Ricciardi, L. Glinsman, M. Palmer, and J. Burke, “Use of near infrared reflectance imaging spectroscopy to map wool and silk fibres in historic tapestries,” *Anal. Methods*, vol. 8, no. 44, pp. 7886–7890, 2016.
- [46] M. Bouchard, R. Rivenc, C. Menke, and T. Learner, “Micro-FTIR and micro-Raman study of paints used by Sam Francis,” *e-Preservation Sci.*, vol. 6, no. January, pp. 27–37, 2009.
- [47] F. Rosi, A. Burnstock, K. J. Van den Berg, C. Miliani, B. G. Brunetti, and A. Sgamellotti, “A non-invasive XRF study supported by multivariate statistical analysis and reflectance FTIR to assess the composition of modern painting materials,” *Spectrochim. Acta - Part A Mol. Biomol. Spectrosc.*, vol. 71, no. 5, pp. 1655–1662, 2009.
- [48] P. Westlake, P. Siozos, A. Philippidis, C. Apostolaki, B. Derham, A. Terlixi, V. Perdikatsis, R. Jones and D. Anglos, “Studying pigments on painted plaster in Minoan, Roman and Early Byzantine Crete. A multi-analytical technique approach,” *Anal. Bioanal. Chem.*, vol. 402, no. 4, pp. 1413–1432, 2012.
- [49] D. Melessanaki, K., Papadakis, V., Balas and D. Anglos, “Laser induced breakdown spectroscopy and hyper-spectral imaging analysis of pigments on an illuminated manuscript,” *Spectrochim. Acta Part B*, vol. 56, pp. 2337–2346, 2001.
- [50] S. Mosca, R. Alberti, T. Frizzi, A. Nevin, G. Valentini, and D. Comelli, “A

- whole spectroscopic mapping approach for studying the spatial distribution of pigments in paintings,” *Appl. Phys. A Mater. Sci. Process.*, vol. 122, no. 9, pp. 1–10, 2016.
- [51] M. Leona, “Microanalysis of organic pigments and glazes in polychrome works of art by surface-enhanced resonance Raman scattering,” *Proc. Natl. Acad. Sci. U. S. A.*, vol. 106, no. 35, pp. 14757–62, 2009.
- [52] A. V. Whitney, F. Casadio, and R. P. Van Duyne, “Identification and characterization of artists’ red dyes and their mixtures by surface-enhanced Raman spectroscopy,” *Appl. Spectrosc.*, vol. 61, no. 9, pp. 994–1000, 2007.
- [53] F. Casadio, M. Leona, J. R. Lombardi, and R. Van Duyne, “Identification of organic colorants in fibers, paints, and glazes by surface enhanced Raman spectroscopy,” *Acc. Chem. Res.*, vol. 43, no. 6, pp. 782–791, 2010.
- [54] M. Aceto, A. Agostino, G. Fenoglio, M. Gulmini, V. Bianco, and E. Pellizzi, “Non invasive analysis of miniature paintings: Proposal for an analytical protocol,” *Spectrochim. Acta - Part A Mol. Biomol. Spectrosc.*, vol. 91, pp. 352–359, 2012.
- [55] C. Sanchez, D. Renard, P. Robert, C. Schmitt, and J. Lefebvre, “Structure and rheological properties of acacia gum dispersions,” *Food Hydrocoll.*, vol. 16, no. 3, pp. 257–267, 2002.
- [56] G. Gautier and M. P. Colombini, “GC-MS identification of proteins in wall painting samples: A fast clean-up procedure to remove copper-based pigment interferences,” *Talanta*, vol. 73, no. 1, pp. 95–102, 2007.
- [57] Y. Dong, K. M. Sørensen, S. He, and S. Engelsen, “Gum Arabic authentication and mixture quantification by near infrared spectroscopy,” *Food Control*, vol. 78, no. February, pp. 144–149, 2017.
- [58] C. Marinach, M. C. Papillon, and C. Pepe, “Identification of binding media in works of art by gas chromatography–mass spectrometry,” *J. Cult. Herit.*, vol. 5, no. 2, pp. 231–240, 2004.
- [59] J.V. Gimeno-Adelantado, R. Mateo-Castro , M.T. Domenech-Carbo, F. Bosch-Reig, A. Domenech-Carbo, M. J. Casas-Catalan, L. Osete-Cortina, “Identification of lipid binders in paintings by gas chromatography: Influence of

- the pigments," *J. Chromatogr. A*, vol. 922, no. 1–2, pp. 385–390, 2001.
- [60] C. M. Grzywacz, "Identification of proteinaceous binding media in paintings by amino acid analysis using 9-fluorenylmethyl chloroformate derivatization and reversed-phase high-performance liquid chromatography," *J. Chromatogr. A*, vol. 676, no. 1, pp. 177–183, 1994.
- [61] I. Bonaduce, H. Brecoulaki, M. P. Colombini, A. Lluveras, V. Restivo, and E. Ribechini, "Gas chromatographic-mass spectrometric characterisation of plant gums in samples from painted works of art," *J. Chromatogr. A*, vol. 1175, no. 2, pp. 275–282, 2007.
- [62] C. Riedo, D. Scalarone, and O. Chiantore, "Multivariate analysis of pyrolysis-GC/MS data for identification of polysaccharide binding media," *Anal. Methods*, vol. 5, no. 16, p. 4060, 2013.
- [63] D. Bersani, G. Antonioli, P. P. Lottici, and A. Casoli, "Raman microspectrometric investigation of wall paintings in S. Giovanni Evangelista Abbey in Parma: A comparison between two artists of the 16th century," *Spectrochim. Acta - Part A Mol. Biomol. Spectrosc.*, vol. 59, no. 10, pp. 2409–2417, 2003.
- [64] C. D. Calvano, I. Van Der Werf, F. Palmisano and L. Sabbatini, "Fingerprinting of egg and oil binders in painted artworks by matrix-assisted laser desorption ionization time-of-flight mass spectrometry analysis of lipid oxidation by-products," *Anal. Bioanal. Chem.*, vol. 400, no. 7, pp. 2229–2240, 2011.
- [65] R. J. Meilunas, J. G. Bentsen and A. Steinberg, "Analysis of Aged Paint Binders by FTIR Spectroscopy", *St. in conservation*, vol. 35, no. 1, p.33-51, 1990.
- [66] L. Burgio and R. J. H. Clark, "Library of FT-Raman spectra of pigments, minerals, pigment media and varnishes, and supplement to existing library of Raman spectra of pigments with visible excitation", *Spectrochim. Acta - Part A Mol. Biomol. Spectrosc.*, vol. 57, no. 7. 2001.
- [67] P. Vandenabeele, K. Castro, M. Hargreaves, L. Moens, J. M. Madariaga, and H. G. M. Edwards, "Comparative study of mobile Raman instrumentation for art analysis," *Anal. Chim. Acta*, vol. 588, no. 1, pp. 108–116, 2007.
- [68] H. G. M. Edwards, P. Vandenabeele, J. Jehlicka, and T. J. Benoy, "An analytical

- Raman spectroscopic study of an important english oil painting of the 18th Century," *Spectrochim. Acta - Part A Mol. Biomol. Spectrosc.*, vol. 118, pp. 598–602, 2014.
- [69] P. Vandenabeele, B. Wehling, L. Moens, H. Edwards, M. De Reu, and G. Van Hooydonk, "Analysis with micro-Raman spectroscopy of natural organic binding media and varnishes used in art," *Anal. Chim. Acta*, vol. 407, no. 1–2, pp. 261–274, 2000.
- [70] P Ricciardi, J. K. Delaney, M. Facini, J. Zeibel, M. Picollo, S. Lomax and M. Loew, "Near infrared reflectance imaging spectroscopy to map paint binders in situ on illuminated manuscripts," *Angew. Chemie - Int. Ed.*, vol. 51, no. 23, pp. 5607–5610, 2012.
- [71] M. Vagnini, C. Miliani, L. Cartechini, P. Rocchi, B. G. Brunetti, and A. Sgamellotti, "FT-NIR spectroscopy for non-invasive identification of natural polymers and resins in easel paintings," *Anal. Bioanal. Chem.*, vol. 395, no. 7, pp. 2107–2118, 2009.
- [72] W. Vetter and M. Schreiner, "Characterization of pigment-binding media systems: comparison of non-invasive in-situ reflection FTIR with transmission FTIR microscopy," *e-Preservation Sci.*, vol. 8, pp. 10–22, 2011.
- [73] F. Rosi, C. Miliani, C. Clementi,K. Kahrim, F. Presciutti, M. Vagnini, V. Manuali, A. Daveri, L. Cartechini, B. Brunetti and A. Sgamellotti, "An integrated spectroscopic approach for the non-invasive study of modern art materials and techniques," *Appl. Phys. A Mater. Sci. Process.*, vol. 100, no. 3, pp. 613–624, 2010.
- [74] F. Rosi, A. Daveri, C. Miliani, G. Verri, P. Benedetti,F. Piqué,B. Brunetti and A. Sgamellotti, , "Non-invasive identification of organic materials in wall paintings by fiber optic reflectance infrared spectroscopy: A statistical multivariate approach," *Anal. Bioanal. Chem.*, vol. 395, no. 7, pp. 2097–2106, 2009.
- [75] W. A. Cote , "Papermaking Fibers: A Photomicrographic Atlas". Syracuse University Press, 1980.
- [76] E. Alarousu, L. Krehut, T. Prykäri, and R. Myllylä, "Study on the use of optical coherence tomography in measurements of paper properties," *Meas. Sci. Technol.*,

vol. 16, no. 5, pp. 1131–1137, 2005.

- [77] D. Wenjie, DUNHUANG ART: Through the eyes of Duan Wenjie. Abhinav Publications, 1994.
- [78] I. M. Bell, R. J. H. Clark, and P. J. Gibbs, “Raman spectroscopic library of natural and synthetic pigments (pre- approximately 1850 AD).,” *Spectrochim. Acta. A. Mol. Biomol. Spectrosc.*, vol. 53A, no. 12, pp. 2159–2179, 1997.
- [79] L. Burgio, R. J. H. Clark, and S. Firth, “Raman spectroscopy as a means for the identification of plattnerite ( $PbO_2$ ), of lead pigments and of their degradation products,” *Analyst*, vol. 126, no. 2, pp. 222–227, 2001.
- [80] S. Ghosal, J. M. Macher, and K. Ahmed, “Raman microspectroscopy-based identification of individual fungal spores as potential indicators of indoor contamination and moisture-related building damage,” *Environ. Sci. Technol.*, vol. 46, no. 11, pp. 6088–6095, 2012.
- [81] W. Anaf, K. Janssens, and K. De Wael, “Formation of metallic mercury during photodegradation/photodarkening of  $\alpha$ -HgS: Electrochemical evidence,” *Angew. Chemie - Int. Ed.*, vol. 52, no. 48, pp. 12568–12571, 2013.
- [82] Y. Zhao, Y. Tang, T. Tong, Z. Sun, Z. Yu, Y. Zhud and H. Tong, “Red lead degradation: monitoring of color change over time,” *New J. Chem.*, vol. 40, no. 4, pp. 3686–3692, 2016.
- [83] S. Švarcová, D. Hradil, J. Hradilová, E. Kočí, and P. Bezdička, “Micro-analytical evidence of origin and degradation of copper pigments found in Bohemian Gothic murals,” *Anal. Bioanal. Chem.*, vol. 395, no. 7, pp. 2037–2050, 2009.
- [84] K. Keune, J. Mass, A. Mehta, J. Church, and F. Meirer, “Analytical imaging studies of the migration of degraded orpiment, realgar, and emerald green pigments in historic paintings and related conservation issues,” *Herit. Sci.*, vol. 4, no. 1, p. 10, 2016.
- [85] M. Spring and R. Grout, “The blackening of Vermilion: an analytical study of the process in paintings,” *Natl. Gall. Tech. Bull.*, vol. 23, pp. 48–61, 2002.
- [86] M. Vermeulen, G. Nuyts, J. Sanyova, A. Vila, D. Buti, J. P. Suuronend and K. Janssensb, “Visualization of As(III) and As(V) distributions in degraded paint micro-samples from Baroque- and Rococo-era paintings,” *J. Anal. At. Spectrom.*,

vol. 31, no. 9, pp. 1913–1921, 2016.

- [87] K. L. Garg, K., K., Jain, K., A. K., Mishra, “Role of fungi in the deterioration of wall paintings,” *Sci. Total Environ.*, vol. 167, no. 1–3, pp. 255–271, 1995.
- [88] C. Miguel, A. Claro, A. P. Gonçalves, V. S. F. Muralha, and M. J. Melo, “A study on red lead degradation in a medieval manuscript Lorvão Apocalypse (1189),” *J. Raman Spectrosc.*, vol. 40, no. 12, pp. 1966–1973, 2009.
- [89] R. F. Kokaly, R. N. Clark, G. A. Swayze, K. E. , Livo, T. M. Hoefen, N. C. Pearson, R. A. Wise, W. M. Benzel, H. A. Lowers, R. L. Driscoll and A. J. Klein, “USGS Spectral Library Version 7: U.S. Geological Survey Data Series 1035,” 2017.
- [90] L. Yong and W. Shiwei, “Material analysis of the wall paintings in Xialu Temple, Tibet Autonomous Region, China,” *Stud. Conserv.*, vol. 59, no. 5, pp. 314–327, 2014.
- [91] L. Yong, “Copper trihydroxychlorides as pigments in China,” *Stud. Conserv.*, vol. 57, no. 2, pp. 106–111, 2012.
- [92] P. Holakooei, J. F. de Lapérouse, M. Rugiadi, and F. Carò, “Early Islamic pigments at Nishapur, north-eastern Iran: studies on the painted fragments preserved at The Metropolitan Museum of Art,” *Archaeol. Anthropol. Sci.*, 2016.
- [93] P. Ricciardi and A. Pallipurath, “The Five Colours of Art : Non-invasive Analysis of Pigments in Tibetan Prints and Manuscripts,” 2012.
- [94] S. Cotte, “Conservation of thangkas: a review of the literature since the 1970s,” *Stud. Conserv.*, vol. 56, no. 2, pp. 81–93, 2011.
- [95] S. Agnew, N. Maekawa and S. Wei, “Causes and Mechanisms of Deterioration and Damage in cave 85,” in *Conservation of Ancient Sites on the Silk Road*, 2004, pp. 412–420.
- [96] S. Neate and D. Howell, "The Technological Study of Books and Manuscripts as Artefacts: Research Questions and Analytical Solutions." Oxford: Archaeopress, 2011.
- [97] K. Bailey, “A note on Prussian blue in nineteenth-century Canton,” *Stud. Conserv.*, vol. 57, no. 2, pp. 116–121, 2012.

- [98] C. Clunas, *CHINESE EXPORT WATERCOLOURS*. London: The Victoria and Albert Museum, 1984.
- [99] H. Liang, L. Burgio, K. Bailey, A. Lucian, C. Dilley, S. Bellesia, C.S.Cheung and C. Brooks, “Culture and trade through the prism of technical art history: A study of Chinese export paintings,” *Stud. Conserv.*, vol. 59, no. S1, pp. S96–S99, 2014.
- [100] H. Liang, R. Lange, B. Peric and M. Spring, “Optimum spectral window for imaging of art with optical coherence tomography,” *Appl. Phys. B Lasers Opt.*, vol. 111, no. 4, pp. 589–602, 2013.
- [101] D. Saunders and J. Kirby, *National Gallery Technical Bulletin; Volume15*. London: National Gallery Publications Ltd, 1994.
- [102] C. Clementi, B. Doherty, P. L.Gentili, C. Miliani, A. Romani, B.Brunetti, A. Sgamellotti, “Vibrational and electronic properties of painting lakes,” *Appl. Phys. A Mater. Sci. Process.*, vol. 92, no. 1, pp. 25–33, 2008.
- [103] J. Winter, J. Giaccai and M. Leona, “East Asian Painting Pigments: Recent Progress and Remaining Problems,” in *Scientific Research in the Field of Asian Art: Proceedings of the First Forbes Symposium at the Freer Gallery of Art*, 2003, no. 1970, p. 157.
- [104] M. Leona and J. Winter, “Fiber Optics Reflectance Spectroscopy: A Unique Tool for the Investigation of Japanese Paintings” *Stud. Conserv.*, vol. 46, no. 3, pp. 153–162, 2001.
- [105] G. Favaro, C. Miliani, A. Romani, and M. Vagnini, “Role of protolytic interactions in photo-aging processes of carminic acid and carminic lake in solution and painted layers,” *J. Chem. Soc. Perkin Trans. 2*, no. 1, pp. 192–197, 2002.
- [106] C. Bisulca, M. Picollo, M. Bacci, and D. Kunzelman, “Uv-Vis-Nir Reflectance Spectroscopy of Red Lakes in Paintings,” *9th Int. Conf. NDT Art, Jerusalem, Isr. 25-30 May 2008*, no. May, pp. 1–7, 2008.
- [107] F. Yu, "Chinese Painting Colors: Studies of their Preparation and Application in Traditional and Modern Times", *J. Silbergeld and A. McNair, trans.* Hong Kong and London: Hong Kong University Press and University of Washington Press, 1988.

- [108] A. S. Whitney, R. P. Van Duyne and F. Casadio, “An innovative surface-enhanced Raman spectroscopy (SERS) method for the identification of six historical red lakes and dyestuffs,” *J. Raman Spectrosc.*, vol. 37, pp. 993–1002, 2006.
- [109] M. Canamares and M. Leona “Surface-enhanced Raman scattering study of the red dye laccaic acid,” *J. Raman Spectrosc.*, vol. 38, no. April, pp. 1259–1266, 2007.
- [110] T. Brook, *Mr Selden's Map of China: The spice trade, a lost chart and the South China sea*. London: Profile Books Ltd., 2013.
- [111] R. Batchelor, “The Selden Map Rediscovered : A Chinese Map of East Asian Shipping Routes , c . 1619,” *Imago Mundi Int. J. Hist. Cartogr.*, vol. 65, no. 1, pp. 37–63, 2013.
- [112] H. A. Nie, “The Selden Map of China: A New Understanding of the Ming Dynasty,” 2014.
- [113] S. Davies, “The International Journal for the History of Cartography The Construction of the Selden Map : Some Conjectures,” *Imago Mundi Int. J. Hist. Cartogr.*, vol. 65, no. 1, pp. 1479–7801, 2013.
- [114] P. Vandenabeele, H. G. M. Edwards, and J. Jehlička, “The role of mobile instrumentation in novel applications of Raman spectroscopy: archaeometry, geosciences, and forensics.,” *Chem. Soc. Rev.*, vol. 43, no. 8, pp. 2628–49, 2014.
- [115] C. S. Cheung, M. Spring, and H. Liang, “Ultra-high resolution Fourier domain optical coherence tomography for old master paintings,” *Opt. Express*, vol. 23, no. 8, p. 10145, 2015.
- [116] R. Minte, M. Stiglitz, K. Sugiyama, and M. Barnard, “From Quanzhou, China to Oxford, UK: An account of the Selden Map of China and its conservation,” *Stud. Conserv.*, vol. 59, no. sup1, pp. S115–S118, 2014.
- [117] A. Yu, F. Silbergeld and J. McNair, *Chinese Painting Colors: Studies of Their Preparation and Application in Traditional and Modern Times*, 1st ed. Hong Kong and London: Hong Kong University Press and University of Washington Press, 1988.
- [118] S. Kroustallis, “Binding media in medieval manuscript illumination: a source

- research," *Rev. História da Arte*, vol. W, no. 1, pp. 112–125, 2011.
- [119] A. Chowdry, "The studio practises of painters of the Mungal ateliers," in *Syposium on the Care and Conservation of Middle Eastern Manuscripts*, 2007, pp. 36–49.
- [120] M. Purinton, N., Watters, "A Study of the Materials Used by Medieval Persian Painters," *J. Am. Inst. Conserv.*, vol. 30, no. 2, pp. 125–144, 1991.
- [121] S. Kogou, S. Neate, C. Coveney, A. Miles, D. Boocock, L. Burgio,C. S. Cheung and H. Liang, "The origins of the Selden map of China : scientific analysis of the painting materials and techniques using a holistic approach," *Herit. Sci.*, vol. 4, no. 28, pp. 1–24, 2016.
- [122] C. Anselmi, P. Ricciardi, D. Buti, A. Romani, P. Moretti, K. R. Beers, B. Brunetti, C. Miliani and A. Sgamellotti, "MOLAB® meets Persia: Non-invasive study of a sixteenth-century illuminated manuscript," *Stud. Conserv.*, vol. 60, Supplement 1, pp. 185–192, 2015.
- [123] V. Tanevska, I. Nastova, B. Minceva-Sukarova, O. Grupce, M. Ozcatal, M. Kavcic and Z. Jakovlevska-Spirovsk, "Spectroscopic analysis of pigments and inks in manuscripts: II. Islamic illuminated manuscripts (16th-18th century)," *Vib. Spectrosc.*, vol. 73, pp. 127–137, 2014.
- [124] V. S. F. Muralha, L. Burgio, and R. J. H. Clark, "Raman spectroscopy analysis of pigments on 16-17th c. Persian manuscripts," *Spectrochim. Acta - Part A Mol. Biomol. Spectrosc.*, vol. 92, pp. 21–28, 2012.
- [125] G. Wang and S. Gai *The mustard seed garden manual of painting. Translation of Chieh Tzu Yuan Hua Chuan, 1679-1701*. New York and Princeton, N.J.: Bollingen Foundation and Princeton University Press, 1956.
- [126] K. Gibbs and P. Seddon, *Berberine and Huangbo: Ancient Colorants and Dyes*. London: The British Library, 1998.
- [127] E. Egel and S. Simon, "Investigation of the painting materials in Zhongshan Grottoes (Shaanxi, China)," *Herit. Sci.*, vol. 1, no. 1, p. 29, 2013.
- [128] D. A. Scott, "A Review of Copper Chlorides and Related Salts in Bronze Corrosion and as Painting Pigments", *Stud. Conserv.*, vol. 45, no. 1, pp . 39-53, 2000.

- [129] V. Daniels and B. Leach, “The occurrence and alteration of realgar on ancient Egyptian papyri,” *Stud. Conserv.*, vol. 49, no. 2, pp. 73–84, 2004.